NWC TP 6382

Blast Effects From Cylindrical Explosive Charges: Experimental Measurements

by
Myron N. Plooster
Denver Research Institute
for the
Ordnance Systems Department

NOVEMBER 1982

NAVAL WEAPONS CENTER
CHINA LAKE, CALIFORNIA 93555

Approved for public release; distribution unlimited.

Naval Weapons Center
AN ACTIVITY OF THE NAVAL MATERIAL COMMAND

FOREWORD

This report presents results of a test program, conducted between October 1979 and December 1981, to study the free-air blast wave properties for end-initiated cylindrical explosive charges. The work was sponsored by the Naval Weapons Center (NWC), China Lake, Calif., under Navy Contract N00123-79-C-0111 to the Denver Research Institute, University of Denver, Denver, Colo., and was supported by the Naval Air Systems Command (NAVAIR) under the Strike Warfare Weaponry Technology Block Program under Work Request 21104, AIRTASK A03W-03P2/008B/2F32-300-000 (appropriation 1721319.1901). This airtask provides for continued exploratory development in the air superiority and air-to-surface mission areas. Mr. H. Benefiel (AIR-350) was the cognizant NAVAIR Technology Administrator.

This report was reviewed for technical accuracy by Mr. T. R. Zulkoski (Technical Monitor) and by Mr. R. G. S. Sewell.

This report is released for information only and does not necessarily reflect the views of the Naval Weapons Center.

Approved by
C. L. SCHANIEL, *Head*
Ordnance Systems Department
2 August 1982

Under authority of
J. J. LAHR
Capt., U.S. Navy
Commander

Released for publication by
B. W. HAYS
Technical Director

NWC Technical Publication 6382

Published by ..... Technical Information Department
Collation ..... Cover, 113 leaves
First printing ..... 210 unnumbered copies

UNCLASSIFIED

SECURITY CLASSIFICATION OF THIS PAGE (When Data Entered)

REPORT DOCUMENTATION PAGE		READ INSTRUCTIONS BEFORE COMPLETING FORM
1. REPORT NUMBER NWC TP 6382	2. GOVT ACCESSION NO. AD-A121 263	3. RECIPIENT'S CATALOG NUMBER
4. TITLE (and Subtitle) BLAST EFFECTS FROM CYLINDRICAL EXPLOSIVE CHARGES: EXPERIMENTAL MEASUREMENTS		5. TYPE OF REPORT & PERIOD COVERED Final Report October 1979—December 1981 6. PERFORMING ORG. REPORT NUMBER
7. AUTHOR(s) Myron N. Plooster		8. CONTRACT OR GRANT NUMBER(s) N00123-79-C-0111
9. PERFORMING ORGANIZATION NAME AND ADDRESS Denver Research Institute University of Denver Denver, Colorado		10. PROGRAM ELEMENT, PROJECT, TASK AREA & WORK UNIT NUMBERS A03W-03P2/008B/2F32-300-000 Appropriation 1721319.1901
11. CONTROLLING OFFICE NAME AND ADDRESS Naval Weapons Center China Lake, California 93555		12. REPORT DATE November 1982 13. NUMBER OF PAGES 224
14. MONITORING AGENCY NAME & ADDRESS (if different from Controlling Office)		15. SECURITY CLASS. (of this report) UNCLASSIFIED 15a. DECLASSIFICATION/DOWNGRADING SCHEDULE

16. DISTRIBUTION STATEMENT (of this Report)

Approved for public release; distribution unlimited.

17. DISTRIBUTION STATEMENT (of the abstract entered in Block 20, if different from Report)

18. SUPPLEMENTARY NOTES

19. KEY WORDS (Continue on reverse side if necessary and identify by block number)

Blast Parameter Models
Cylindrical Charges
Explosive Performance
Free-air Blast Waves
High Explosives

20. ABSTRACT (Continue on reverse side if necessary and identify by block number)

See reverse side of this form.

DD FORM 1 JAN 73 1473 EDITION OF 1 NOV 65 IS OBSOLETE
S/N 0102-LF-014-6601

UNCLASSIFIED

SECURITY CLASSIFICATION OF THIS PAGE (When Data Entered)

(U) *Blast Effects From Cylindrical Explosive Charges: Experimental Measurements*, by Myron N. Plooster. China Lake, Calif., Naval Weapons Center, November 1982. 224 pp. (NWC TP 6382, publication UNCLASSIFIED.)

(U) This report presents results of an experimental study of free-air blast wave properties for end-initiated cylindrical explosive charges. The study was motivated by the need for data on positive impulse from cylindrical charges, as a function of charge length/diameter (L/D) ratio, distance, and angle from the charge axis. Cast cylindrical charges of Pentolite were used, with L/D ratios of 1/4, 1/2, 1/1, 2/1, 3/1, 4/1, and 6/1. In all, 64 charges were fired: 54 8-pound cylinders, 4 16-pound cylinders, and 6 7/8-pound spheres (used for internal calibration purposes). For each shot, blast parameters were measured at two angles, 90-degrees apart, using six pressure gauges at each angle. Gauge arrays extended from 7 feet to 31 feet from the charge, covering a nominal pressure range of 100 psi down to 3 psi.

(U) Pressure-time plots from all gauges on all shots are presented, together with measured values of peak pressure, positive impulse, positive duration, and time of arrival. Graphs of the variation of peak pressure and impulse with L/D ratio and angle are presented together with a comparison with spherical charge data. Substantial differences between blast waves from cylindrical and spherical charges are observed. Also presented are the results of scaling tests, an error analysis, and recommendations for further work.

CONTENTS

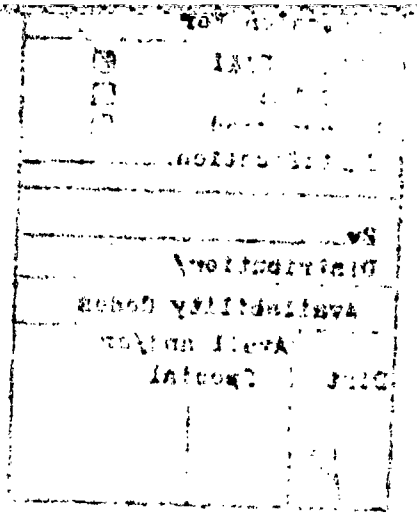

ACKNOWLEDGMENT

The author gratefully acknowledges the contributions of the following DRI staff to the successful execution of this study: C. B. Adams, R. Bjarnason, L. L. Brown, C. R. Hoggatt, J. H. Robinson, L. W. Smith, W. H. Snyer and J. Whitfield.

OBJECTIVES

The objectives of this work were to measure the properties of free-air blast waves from cylindrical charges of high explosives (as a function of the length/diameter (L/D) ratio of the charge, the angle from the cylindrical axis, and the distance) to develop a model of the positive impulse from such charges.

INTRODUCTION

MOTIVATION

This work was motivated by the dearth of data on blast wave properties other than those for center-initiated spherical charges. Many ordnance devices are more nearly cylindrical than spherical in geometry, and the data that are available for cylindrical charges indicate large variations in blast wave properties as a function of the angle from the charge axis. Adequate data are available to characterize the variation of the blast front pressure (the peak pressure of the first shock wave to arrive at a given point in space) with respect to charge geom try, angle, and distance. However, the available data on other blast parameters, including the positive impulse, are insufficient for this purpose.

BACKGROUND

The work reported here is the fourth phase of a program begun in 1976 to characterize the properties of free-air blast waves from cylindrical high explosive charges. The initial phase was a search of the literature from the Defense Technical Information Center (DTIC), to determine what information was already available, either in the form of experimental data or models. This search revealed that DTIC had no records of models for prediction of properties of blast waves from cylindrical charges. The only experimental data suitable for development of blast parameter models were those from a previous study carried out at the Denver Research Institute (DRI) and reported by Wisotski and Snyer.[1] This study determined the blast front pressure (the peak pressure of the leading shock wave) from time-of-arrival measurements. Blast front pressures from end-initiated cylindrical charges with L/D ratios ranging from 1/4 to 10/1 were obtained as a function of angle and distance. Some positive impulse data were also obtained, but with far less thorough coverage in terms of angle and distance.

The second phase of the program was the development of a model of the blast front pressure as a function of L/D, angle, and distance,

[1]Denver Research Institute. *Characteristics of Blast Waves Obtained from Cylindrical High Explosive Charges*, by J. Wisotski and W.H. Snyer. Denver, Colo., DRI, November 1965. (DRI 2286, publication UNCLASSIFIED.)

from the data of Wisotski and Snyer. This model was a multi-parameter curve fit to the experimental data and is described in the report by Plooster.[2]

The third phase was an attempt to use the blast front pressure vs. distance data to estimate the positive impulse, based on the theoretical work of Brinkley and Kirkwood.[3] This attempt was not uniformly successful. Satisfactory estimates were obtained for cases in which "classical" blast wave pressure-time profiles were observed (a smooth decay of pressure behind the leading shock front). However, impulse estimates were poor when the pressure-time profiles were complex (multiple shock waves, etc.). Complex pressure-time profiles are commonly encountered when using cylindrical charges. The results of this phase were described in 1979 in an interim report by Plooster and Yatteau, which is included as Appendix B to this report.

Since the positive impulse is generally a more useful indicator of blast damage potential than the peak pressure, and since insufficient data were available to characterize the positive impulse from cylindrical charges, it was decided to carry out an experimental program to obtain the required data. The remainder of this report describes this experimental program and the results obtained.

PROGRAM PLAN

The original program plan comprised the following six phases:

1. Program design
2. Explosive charge procurement
3. Test arena set-up
4. Firing of charges
5. Data reduction and analysis
6. Impulse model development

This report covers the work done on the first five phases.

PROGRAM DESIGN

The goal of the program design phase was to plan an experimental program that would characterize blast parameters from a range of cylindrical charge geometries with a minimum number of charge firings. A

[2]Naval Weapons Center. *Blast Front Pressure from Cylindrical Charges of High Explosives*, by M.N. Plooster, Denver Research Institute. China Lake, Calif. NWC, September 1978. (NWC TM 3631, publication UNCLASSIFIED.)

[3]S.R. Brinkley and J.G. Kirkwood. "Theory of the Propagation of Shock Waves," *Physical Review*, May 1947, pp. 606-611.

test arena was laid out with two lines of pressure gauges (six gauges per line) placed 90° apart. Thus each shot generated pressure-time data at two angles. Charge-to-gauge distances ranged from 7 to 31 feet, covering a nominal pressure range from about 100 psi down to 3 psi for 8-pound Pentolite spheres. Eight-pound cylindrical charges of Pentolite with seven L/D ratios (1/4, 1/2, 1/1, 2/1, 3/1, 4/1, and 6/1) were used. Charges with L/D = 1/4, 1/1, and 4/1 were investigated in detail. Charge orientations were varied in 22.5° increments, with duplicate runs at each angle for L/D = 1/4 and 4/1, and triplicate runs for L/D = 1/1. For the other L/D ratios, charge orientations were varied in 45° increments, with single runs at most orientations. In addition, two 16-pound charges were fired at 90° angular increments for each of the L/D ratios 1/1 and 1/4, for scaling tests. Eight-pound Pentolite spheres were fired at intervals throughout the program for internal calibration purposes.

Pressure-time data were recorded on magnetic tape. A preliminary determination of peak pressure and impulse was made in the field immediately following each shot, using a Norland Model 3001 Waveform Analyzer, primarily for purposes of quality control. Final data reduction and analysis was carried out in the laboratory following the field program, using the Norland Model 3001 and a Hewlett-Packard Model 9845 Desktop Computer.

EXPLOSIVE CHARGES

In the program design phase, the possibility of using pressed explosive charges was investigated in connection with the desire to minimize the shot-to-shot variability in explosive performance and thus reduce the total number of shots required. It was felt that pressed charges would be more uniform in explosive density, grain size, etc. In addition, use of TNT-based explosives could be avoided. However, it was found infeasible to use pressed charges because of cost and procurement time limitations. In addition, one explosive fabricator advised that it might not be possible to press long charges (L/D of 2/1 or greater) because of mold release problems, etc.

It was therefore decided to use cast Pentolite charges, because of the availability of Pentolite and the relative ease of charge fabrication, and also because Pentolite has been extensively used in the past as a standard for blast measurements. The charges were cast at the DRI casting facility. Precision molds were fabricated to give 8-pound charges for each L/D ratio, assuming an explosive density of 1.64 gm/cm^3. A total of 58 8-pound cylinders, 6 16-pound cylinders, and 8 7.8-pound spheres were cast. The average explosive density in these charges, obtained from finished length, diameter, and charge weight measurements, was 1.641 gm/cm^3, with a standard deviation of 0.010 gm/cm^3 (0.60%).

TEST ARENA LAYOUT

Figure 1 is a plan view of the test arena, showing the two gauge lines oriented 90° apart. In each line, the gauge distances were 7, 11, 16, 21, 26, and 31 feet (except for the first two shots, for which the distances were 7, 12, 17, 22, 27, and 32 feet). Cylindrical charges were mounted with their axes horizontal and 12 feet above ground level; pressure gauges were mounted at the same height. The charge support was a 6-foot long cardboard tube, 4 inches in diameter, placed atop a metal stand. The metal stand, shown in Figure 2, was pointed on the end to deflect any reflected shocks below the horizontal. Figure 3 shows a charge supported by the cardboard tube on the stand. The charge stand/tube assembly was carefully plumbed vertical for each shot. Distances from the charge center to each gauge were measured, and adjusted if necessary, to maintain gauge distances within 1/8 inch of the desired values for each shot.

Vee-shaped notches were cut into the top of the cardboard tube to provide a positive horizontal support for the charge, which was secured to the tube by a single layer of tape.

Charge orientation with respect to the gauge lines was accomplished by aligning the charge axis with a set of alignment stakes (shown in Figure 1) which were located at 22.5° intervals from the gauge lines. Alignment was achieved by placing a telescopic sight on the top of the charge, as shown in Figure 4, and then rotating the cardboard tube until the cross-hairs were centered on the appropriate alignment stake.

The charge initiation system comprised an XM-70 initiator and a Detasheet booster. A 3/8-inch diameter hole was bored in a 9/16-inch length of 1-inch diameter hardwood dowel. Two circular plugs of 1/4-inch thick Detasheet were packed into this hole, and the outer plug was bored to accept the XM-70 initiator. This assembly was centered on one end face of the charge, and attached with double-surface adhesive tape. The initiator system is shown on Figure 5.

Spherical charges were center-initiated using a No. 8 Vibrodet initiator.

PRESSURE MEASUREMENT SYSTEM

The pressure gauges were Susquehanna Instruments Model ST-7 pencil gauges. All pressure gauges were calibrated in the laboratory immediately before and after the firing program; in addition, a field calibration was carried out on the set of pressure gauges installed at the beginning of the firing program. A quasi-static gauge calibration system was used (100 psi step function with 20 msec rise time). Pressure gauges were replaced whenever obvious defects or questionable signals were observed. Pressure signals were transmitted to the data acquisition system through approximately 400' of buried RG-62U coaxial

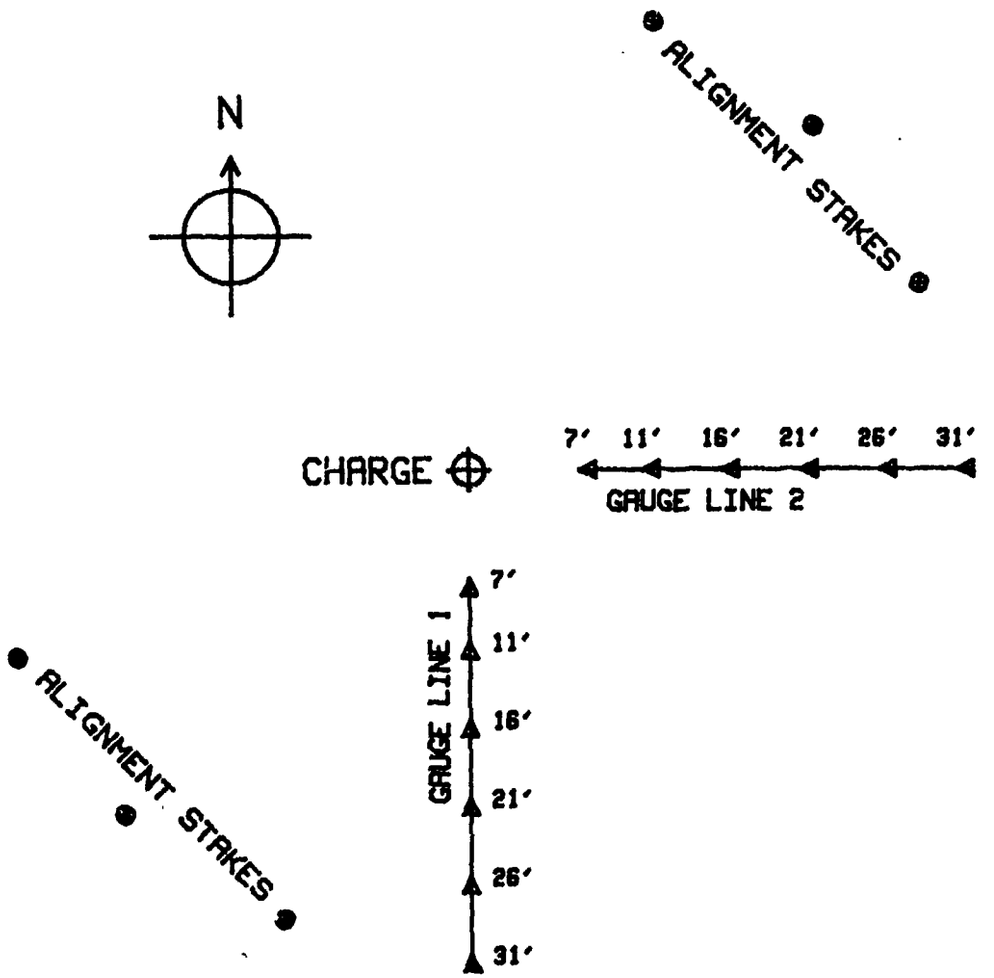

FIGURE 1. Plan View of Test Arena, Showing Locations of Charge, Pressure Gauges, and Alignment Stakes.

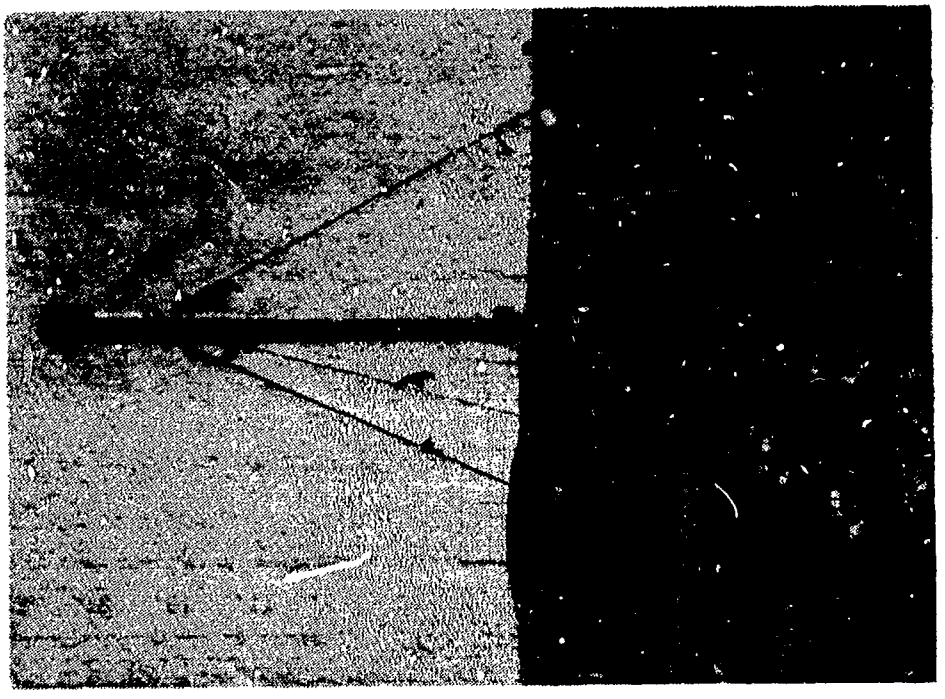

FIGURE 3. Explosive Charge Supported on Cardboard Tube on Charge Stand.

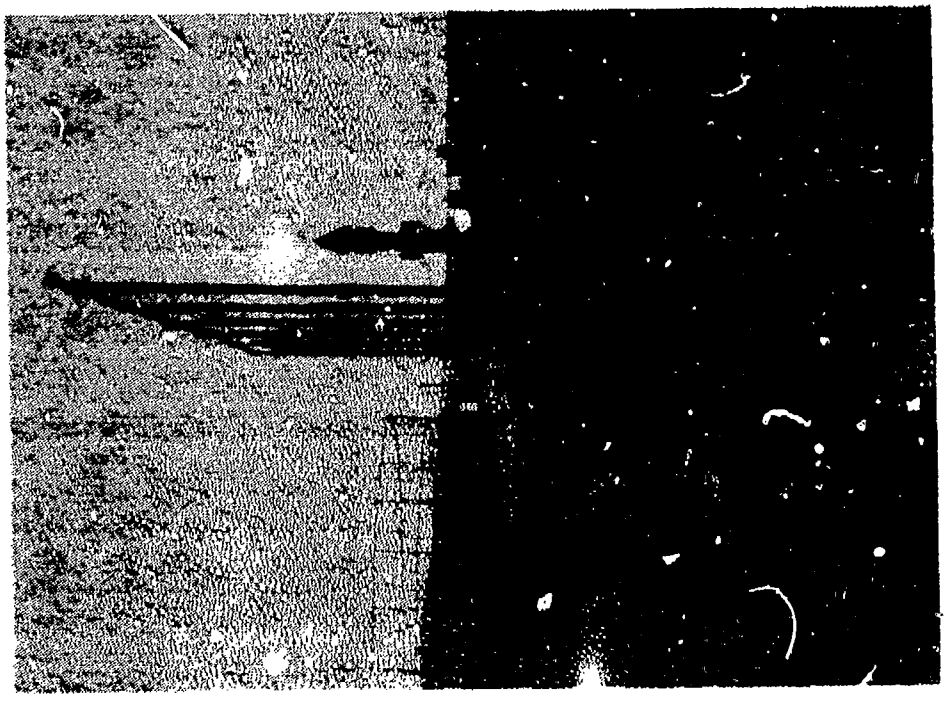

FIGURE 2. Metal Charge Stand.

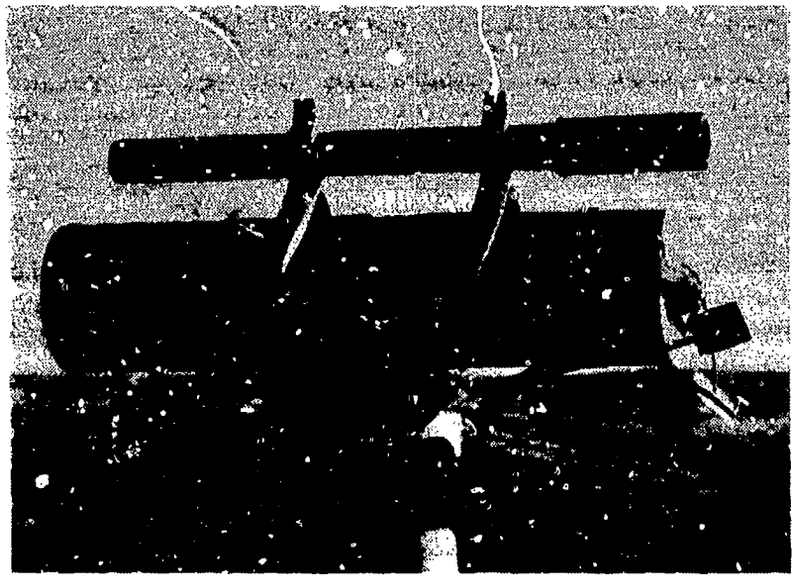

FIGURE 4. Close-up View of Charge on Support with Alignment Scope in Place.

FIGURE 5. Close-up View of Charge with Initiator in Place.

cable. Each cable was terminated at the pressure gauge connection by a matching line resistor, which was adjusted for optimum frequency response in the line.

A "solar cell" photometer was used to detect the light output from each charge, to verify the time of detonation.

Meteorological data (temperature, barometric pressure, and wind speed and direction) were recorded just prior to each shot.

DATA ACQUISITION SYSTEM

The pressure gauge signals were recorded on magnetic tape, using a Honeywell Model 101 14-channel tape recorder. Twelve channels were used for the pressure-time data; the other two channels recorded the solar cell light output and the firing pulse to the XM-70 initiator. A 16-channel amplifier was used to supply gain or attenuation, as needed, to the signals prior to recording on tape. The amplifier also generated a stairstep voltage calibration waveform, which was recorded on each pressure-time data channel on tape just prior to shot time.

A Norland Model 3001 Waveform Analyzer was used to read the pressure gauge and calibration waveforms from tape; store them on flexible disks; and measure peak pressure, positive impulse and duration, and time of arrival. The Norland system combines analog-to-digital converters, a microcomputer and digital data memory, and a display oscilloscope. Reading the data from tape, storing it on disks, and getting a first estimate of peak pressure and positive impulse were accomplished within about an hour after completion of each shot. This capability was most valuable for detection of instrumentation problems, such as pressure gauge malfunctions, because it made it possible to take remedial action before the next shot. It also served to detect abnormal explosive behavior, so that shots giving questionable data could be identified immediately and repeated using spare charges.

FIRING PROGRAM

Table 1 presents the firing program design: the number of sets of pressure-time data planned for each L/D ratio and at each angle with respect to the charge axis. A "pressure-time data set" here refers to the set of data from one line of six gauges, from one shot. Since there were two gauge lines, each shot generated two sets of pressure-time data.

The convention used here to define the angle of observation (illustrated in Figure 6) is that initiation takes place at the 180° end of the charge. Thus the detonation wave propagates through the charge along the 0° radial, and the 90° radial is at right angles to the charge axis. This is the same convention used in the previous DRI study.[1]

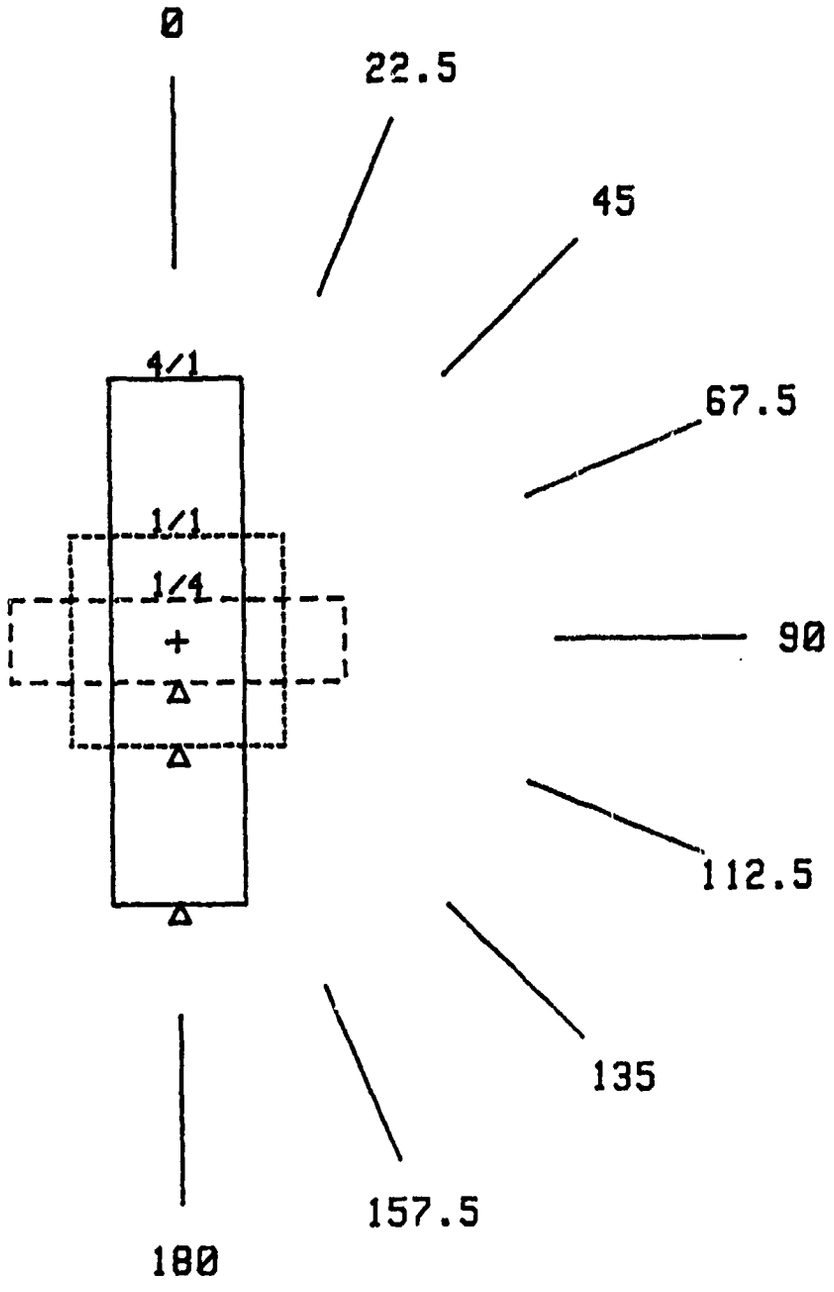

FIGURE 6. Charge Observation Angle Defined for Cylindrical Charges with L/D = 1/4, 1/1, and 4/1. Triangles mark point of initiation.

The use of two gauge lines spaced 90° apart allows measurement of pressure signals at all angles from 0° to 180° in five shots, when data are taken at 22.5° intervals. Three shots suffice when the interval is 45°, and two when the interval is 90°. Each such group of shots gives duplicate data sets at 90° and a single data set at each of the other angles. As can be seen from Table 1, two groups of five shots each were planned for charges with L/D ratios of 1/4 and 4/1, and three groups for charges with an L/D ratio of 1/1, to enable estimation of the statistical shot-to-shot variability in blast wave parameters for charges with disk-like, equidimensional, and rod-like geometries. (One of the three 1/1 ratio groups was fired at a different point in the firing schedule than the other two, to see if there were any variations in system behavior with time.) The plan called for a single group of three shots for each of the other L/D ratios. As can be seen from Table 1, the matrix of data sets thus has no large gaps in either L/D ratio or angle, so that no long interpolations or extrapolations will be needed when the experimental data are eventually used to develop blast parameter models covering the entire range of geometries and angles.

The number of charges at each L/D ratio required to complete this firing program is shown just below the matrix of data sets in Table 1. To allow for the possibility that some shots would have to be repeated, due to either instrumentation or charge malfunctions, the number of charges needed at each L/D ratio was increased by a minimum of 20 percent (the "contingency allowance" in Table 1), and the actual number of charges cast is given in the bottom line of the table.

Table 2 is a summary of the data for the shots as actually fired, giving charge characteristics (L/D ratio, dimensions, and weights), gauge line angles, and meteorological data. There were 64 shots in the test series: 54 8-pound cylinders, 4 16-pound cylinders, and 6 7.8-pound spheres. (Shots numbered 1 and 16 were fired for purposes of instrumentation check-out, and are not shown in Table 2.)

RESULTS

PRESSURE-TIME DATA

Plots of pressure vs time from all the charges fired in this program are given in Appendix A. Each page in the Appendix displays one data set, i.e., the data from the six gauges in one gauge line. The data are presented in the order in which the shots were fired, i.e., in the order given in Table 2. Table A-1 indentifies the data sets obtained at each combination of L/D ratio and angle; the entries in the table give the shot number first, followed by the gauge line number.

TABLE 1. Firing Program Design. Number of Data Sets Planned at Each Combination of Charge L/D and Angle, and Number of Charges Required at each L/D.

Angle, degrees	L/D ratio									Sphere
	1/4	1/2	1/1	2/1	3/1	4/1	6/1	1/1	4/1	
	8-pound charge							16-pound charge		8-pound charge
	Number of data sets required									
0	2	1	3	1	1	2	1	1	1	
22.5	2		3			2				
45	2	1	3	1	1	2	1			
67.5	2		3			2				
90	4	2	6	2	2	4	2	2	2	
112.5	2		3			2				
135	2	1	3	1	1	2	1			
157.5	2		3			2				
180	2	1	3	1	1	2	1	1	1	
No. of charges	10	3	15	3	3	10	3	2	2	8
Contingency allowance	2	1	3	1	1	2	1	1	1	
Total No. of charges cast	12	4	18	4	4	12	4	3	3	8

TABLE 2. Firing Program Summary.

SHOT No.	L/D	CHARGE WEIGHT (lb)	LENGTH (in)	DIAM (in)	LINE 1 ANGLE (deg)	LINE 2 ANGLE (deg)	METEOROLOGICAL DATA Temp (degC)	Press (mm)	W/S (m/s)	W/D
2	1/1	8.04	5.595	5.550	0.0	90.0	17.0	619.8	1.5	NE
3	1/1	8.03	5.595	5.517	0.0	90.0	20.3	623.3	4.5	SSW
4	1/1	7.96	5.592	5.565	22.5	112.5	.3	628.1	4.3	NNE
5	1/1	8.04	5.592	5.540	45.0	135.0	4.9	627.0	1.5	NE
6	1/1	7.99	5.590	5.539	67.5	157.5	4.6	626.2	3.7	SE
7	1/1	8.06	5.593	5.545	90.0	180.0	16.2	613.7	.2	W
8	1/1	7.92	5.583	5.542	90.0	0.0	16.7	614.4	2.4	W
9	1/1	8.01	5.594	5.549	180.0	90.0	16.5	614.7	4.2	S
10	1/1	8.01	5.595	5.544	157.5	67.5	16.8	616.4	1.5	S
11	1/1	7.94	5.583	5.553	135.0	45.0	16.6	618.6	4.0	SW
12	1/1	8.00	5.567	5.529	112.5	22.5	13.7	619.0	2.7	NW
13	SPHERE	7.84					15.8	620.7	2.1	SSE
14	SPHERE	7.78					3.0	611.0	5.0	NNW
15	1/2	8.10	3.550	7.029	90.0	180.0	3.4	610.7	5.3	NNE
17	1/2	8.13	3.548	7.019	45.0	135.0	10.2	609.2	1.0	SE
18	1/2	8.13	3.544	7.020	0.0	90.0	13.0	611.0	1.5	NW
19	1/4	8.04	2.223	8.810	90.0	180.0	11.5	610.7	1.5	NNE
20	1/4	8.00	2.227	8.812	45.0	135.0	13.7	611.0	2.5	ESE
21	1/4	7.97	2.218	8.809	0.0	90.0	15.4	609.4	1.9	ESE
22	1/4	7.98	2.219	8.810	67.5	157.5	15.7	610.1	4.5	ESE
23	1/4	8.00	2.217	8.811	22.5	112.5	19.9	611.4	2.3	W
24	1/4	8.00	2.221	8.814	157.5	67.5	19.5	612.6	2.9	NW
25	1/4	8.02	2.220	8.812	135.0	45.0	19.9	613.6	.4	N
26	1/4	7.95	2.212	8.809	112.5	22.5	19.7	613.1	1.3	NNW
27	1/4	7.94	2.211	8.813	45.0	135.0	12.5	611.2	3.7	ESE
28	1/4	8.03	2.221	8.810	180.0	90.0	14.6	613.1	2.8	SE
29	1/4	7.96	2.222	8.811	90.0	0.0	11.8	613.1	4.7	NE
30	SPHERE	7.84					16.9	609.0	3.0	WSW
31	1/1	7.99	5.595	5.552	157.5	67.5	16.4	610.9	0.0	-
32	1/1	8.03	5.592	5.551	112.5	22.5	16.6	611.8	1.6	Var
33	1/1	8.05	5.587	5.550	135.0	45.0	19.6	613.7	.2	NE
34	1/1	7.93	5.580	5.544	180.0	90.0	20.9	613.9	.6	SW

TABLE 2. (Contd.)

SHOT No.	L/D	CHARGE WEIGHT (lb)	LENGTH (in)	DIAM (in)	LINE 1 ANGLE (deg)	LINE 2 ANGLE (deg)	METEOROLOGICAL DATA Temp (degC)	Press (mm)	W/S (m/s)	W/D
35	1/1	7.94	5.582	5.547	90.0	0.0	19.7	612.9	1.4	E
36	2/1	7.94	8.820	4.405	135.0	45.0	21.2	617.8	3.2	NW
37	2/1	7.92	8.821	4.406	180.0	90.0	19.9	620.8	.1	NW
38	2/1	7.86	8.832	4.407	90.0	0.0	16.9	619.0	.4	Var
39	3/1	7.90	11.550	3.844	135.0	45.0	20.0	619.4	2.8	N
40	3/1	7.89	11.559	3.845	180.0	90.0	21.3	619.7	4.6	NNE
41	3/1	7.89	11.563	3.844	90.0	0.0	21.5	621.1	1.5	ESE
42	4/1	7.90	14.006	3.493	135.0	45.0	17.1	617.7	2.4	ESE
43	4/1	7.97	14.023	3.495	157.5	67.5	17.8	616.6	4.6	ESE
44	4/1	8.00	14.009	3.495	112.5	22.5	16.7	617.3	3.0	S
45	4/1	7.99	14.011	3.497	180.0	90.0	15.3	617.3	1.4	SE
46	4/1	7.99	14.009	3.497	90.0	0.0	16.6	615.9	2.9	ESE
47	4/1	8.02	14.014	3.497	45.0	135.0	15.3	617.8	2.4	SE
48	4/1	7.99	14.013	3.497	67.5	157.5	18.2	621.4	5.2	N
49	4/1	8.07	14.013	3.498	22.5	112.5	20.6	622.0	4.9	W
50	4/1	8.03	14.012	3.498	0.0	90.0	20.5	622.0	2.6	W
51	4/1	7.99	14.015	3.498	90.0	180.0	18.2	621.0	3.7	W
52	SPHERE	7.84					1.1	610.7	1.2	SW
53	6/1	7.94	18.361	3.058	135.0	45.0	.6	613.1	.5	SW
54	6/1	8.02	18.360	3.059	180.0	90.0	-2.1	613.5	.3	SSW
55	6/1	8.06	18.365	3.060	90.0	0.0	1.7	610.4	1.3	N
56	1/1	8.14	5.587	5.548	0.0	90.0	2.6	609.8	2.2	N
57	1/2	8.15	3.544	7.018	90.0	180.0	2.8	611.7	.3	W
58	4/1	8.04	14.013	3.496	112.5	22.5	2.8	613.0	2.6	S
59	4/1	8.02	14.009	3.498	90.0	180.0	3.5	613.1	2.6	S
60	3/1	7.95	11.570	3.845	180.0	90.0	3.4	613.9	2.5	SW
61	2/1	7.93	8.841	4.406	0.0	90.0	1.4	613.8	1.3	SE
62	1/1	15.90	7.010	6.995	180.0	90.0	1.5	607.9	1.8	S
63	1/1	16.01	7.004	6.994	90.0	0.0	2.8	608.0	2.2	SE
64	4/1	15.92	17.635	4.405	180.0	90.0	4.1	608.4	2.0	S
65	4/1	15.86	17.650	4.405	90.0	0.0	3.1	608.0	1.4	SE
66	SPHERE	7.79					8.1	612.2	3.5	WSW

The procedure followed in preparing these plots was as follows. The data were stored on the magnetic tape in the form of voltage vs. time. The tape data were digitized using the Norland Waveform Analyzer; data from the gauges closest to the charge were digitized at a rate of one data point every 2 microseconds, while those from the more distant gauges were digitized at 5 or 10 microseconds per point. There is a certain amount of random, very high-frequency noise in the tape signals, which was filtered out by applying a 5-point moving average. (On a few shots, for example shot 15, sporadic noise bursts of much larger amplitude were present; a 15-point moving average was required to smooth out such traces.) The voltage level of the pre-shock signal (the flat base line preceding the first shock wave) was then determined by averaging over at least 100 data points, and this voltage was subtracted from the entire trace to correct for any base line voltage drift. The resulting voltage signal was converted to units of pressure (in psi) by multiplying by the pressure gauge calibration factor and the tape gain factor (determined from the stairstep calibration signal recorded on each pressure-time channel on the tape.) 2048 data points were used to store each trace in the Norland Waveform Analyzer. From this, 100 points of base line data and 1000 points of post-shock data were transmitted to a Hewlett-Packard Model 9845 Desktop computer, which then was used to generate the plots shown in Appendix A. Thus these plots show 2, 5, or 10 milliseconds of pressure-time data following the shock wave at each pressure gauge, depending on the digitizing rate used for the waveform analyzer.

The time bases of the tape deck and waveform analyzer were checked periodically and found to be accurate to within 0.5% in every case. The standard deviation of the tape gain factors was also less than 1%. The largest source of error in the pressure-time plots is the pressure gauge calibration. As mentioned earlier, pressure gauges were calibrated in the laboratory both before and after the firing program, and some gauges were also calibrated in the field. Furthermore, a complete log has been kept of gauge calibrations from programs both prior to and subsequent to this one. The pressure gauge calibrations appear to change with time in a random manner, sometimes increasing and sometimes decreasing. The relative standard deviation in gauge calibration factors, averaged over all the gauges used in the program, was 2.9%. Since it was not possible to determine the variations in gauge calibration factors for each shot, the averages of the individual determinations for each gauge were used to reduce the data for this report.

PEAK PRESSURE

Determination of peak pressure in blast waves from cylindrical charges is more difficult than for spherical charges, because the pressure-time traces are often more complex. For spherical charges, the pressure at the close-in gauges generally falls smoothly and nearly exponentially with time after passage of the shock wave, so that an extrapolation to the peak at the shock front is easily made. A wide variety of pressure-time waveforms is evident in the plots shown in

Appendix A. Cylindrical charges often generate secondary shock waves which are comparable or even greater in amplitude than the leading shock, and which sometimes overtake it. Also, there are instances in which short-duration pressure pulses of large amplitude are observed. It is questionable whether the pressure gauges are capable of accurately following such rapidly changing signals, because the pressure decays in times comparable to the transit time of the wave over the gauge.

For these reasons it was often not possible to use an extrapolation technique in a consistent manner to determine peak pressures. For consistency in the data, most peak pressures reported here were determined by measuring the highest point on the pressure trace at each shock, after using the 5-point smoothing process to remove the high-frequency noise. It is realized that this smoothing produces some rounding of the peaks and thus leads to a slight underestimate of the peak pressures. This is especially true for those traces with short-duration pressure pulses; the peak pressure in these traces can be determined only approximately in any case. Peak pressure was determined by extrapolation only when there was clear evidence of ringing or overshoot at the peak. (Ringing signals were relatively infrequent; this is probably a result of using the matching line resistors to optimize the frequency response of the coaxial cables.) In the case of strong secondary shocks, two peak pressures were measured.

The peak pressure data are listed in Table 3. Missing data in this table indicate either that there was evidence of gauge failure, or that a close-in gauge was removed because peak pressures high enough to damage the gauges were expected. (The gauges at 7 ft from the charge were removed for the 16-lb charges, shots 62-65, and for the spherical charge shot immediately following.) An asterisk following a table entry denotes a questionable value, either because of a suspicious-looking pressure-time trace or because the value is clearly inconsistent with data from neighboring gauges or from other shots at the same L/D ratio and angle. Peak pressures from secondary shocks are preceeded by the letter "S" in the table.

Figures 7 through 15 show peak pressures plotted vs. the L/D ratio, at each of the angles used in this study. The pressures and distances in these figures have been scaled to a charge weight of one pound and to sea-level ambient pressure (using an ambient pressure of 615 mm Hg, the average of the barometric pressure data for all the shots fired here). The average spherical charge peak pressures measured in this program are shown at the right in each figure. Where secondary shock pressures exceeded the pressures at the leading shocks, the lower leading shock pressures are connected by dashed lines.

Figures 16, 17, and 18 show peak pressure vs. angle (again scaled to one pound and sea level) for L/D ratios of 1/4, 1/1, and 4/1, respectively. The scaled spherical charge pressures are again shown for comparison.

TABLE 3. Peak Shock Pressure (psi).

Note: * denotes questionable value
S denotes peak pressure of secondary shock

L/D=1/4 Charge Weight= 8 lb

Angle	Shot	Distance (ft) 7	11	16	21	26	31
0.0	21-1	387.66	124.51	16.20	8.56	5.30	3.69
	29-2	572.64	100.64	24.77	6.51*	5.83	3.68
22.5	23-1	89.26	49.15	15.72	9.63	5.29	3.66
	26-2	145.50	46.66	16.34	6.53	5.34	3.71
45.0	20-1	43.95	18.83	8.11	5.86	3.86	3.25
			S 10.64	S 8.89	S 4.95		
	25-2	40.80	16.77	9.35	5.36	3.91	2.94
		S 26.24	S 9.94	S 6.40	S 4.41	S 3.56	
	27-1	40.35	19.42	8.32	5.62	3.81	3.50
		S 27.17	S 12.82	S 7.38	S 5.15	S 3.85	
67.5	22-1	27.45	19.76	8.62	6.58	4.24	3.53
		S 30.03					
	24-2	27.80	18.04	10.32	6.18	4.36	3.26
		S 34.89					
90.0	19-1	29.42	10.22	5.16	5.87	4.12	3.47
				S 6.87			
	21-2	48.60	10.62	5.45	4.93	3.95	3.12
				S 6.31			
	28-2	45.77	11.11	5.52	3.14	3.86	2.98
				S 5.69	S 4.37		
	29-1	34.80	12.06	5.47	6.14	4.09	3.46
				S 6.76			
112.5	23-2	25.83	18.74	10.47	6.22	4.35	3.35
		S 29.24					
	26-1	26.71	19.41	8.90	6.50	4.10	3.21
		S 29.23					
135.0	20-2	49.04	18.83	8.25	5.35	3.85	2.84
			S 10.45	S 7.52	S 4.54	S 3.49	S 2.92
	25-1	40.73	19.05	8.14	6.14	3.94	3.11
						S 4.02	S 3.18
	27-2	42.35	17.15	9.55	4.36*	3.72	2.88
		S 33.33	S 11.85	S 7.60	S 4.06*	S 3.80	
157.5	22-2	147.15	46.34	15.70	8.09	4.96	3.58
	24-1	141.47	54.04	13.93	9.20	5.28	3.54
180.0	19-2	458.08	45.06	23.35	10.52	4.72	3.30
	28-1	286.16	151.02	12.75	6.70	1.87	3.68
				S 24.37	S 9.56	S 4.67	

TABLE 3. (Contd.)

For shots 2 and 3, gauges are at 7, 12, 17, 22, 27, and 32 ft
L/D=1/1 Charge Weight= 8 lb

Angle	Shot	Distance (ft) 7	11	16	21	26	31
0.0	2-1	333.93	48.39	7.90	5.07	2.86	2.30
							S 2.81
	3-1	-.--	61.54	13.13	6.97	3.42	2.33
						S 2.02	S 2.50
	8-2	283.27	73.68	13.52	4.94	3.65	2.34
					S 6.08		
	35-2	251.22	63.85	16.15	6.41	3.81	2.43
	56-1	285.56	62.18	14.28	7.32	3.63	2.44
						S 3.01	S 2.93
22.5	4-1	50.08	29.11	9.74	3.23*	3.29	2.30
				S 5.15	S 2.27*	S 2.99	S 2.27
	12-2	84.20	30.24	12.46	6.42	3.78	2.49
				S 5.59	S 4.31	S 2.97	S 2.18
	32-2	71.51	25.86	11.49	4.86	3.68	2.33
				S 4.89	S 2.89	S 2.25	S 1.76
45.0	5-1	61.23	27.33	10.90*	8.83	5.42	4.01
	11-2	80.04	25.22	14.42	7.86	5.33	3.71
	33-2	64.83	24.87	14.59	9.21	5.95	4.02
67.5	6-1	47.78	19.04	8.27	6.80	4.37	3.20
	10-2	98.19	19.40	9.96	6.40	4.45	3.39
			S 8.02	S 8.71			
	31-2	94.15	18.98	8.99	5.46	4.31	3.17
90.0	2-2	90.73	21.09	9.46	4.95	3.42	2.53
	3-2	79.94	18.63	8.16	4.52	3.05	2.41
	7-1	82.46	22.95	8.68	6.18	3.47	2.91
	8-1	78.79	25.14	8.58	6.43	3.57	2.72
	9-2	230.51*	33.50	9.64	5.31	3.53	2.63
	34-2	79.43	20.79	9.42	5.60	3.63	2.53
	35-1	89.76	24.12	8.43	5.99	3.61	2.87
	56-2	75.95	21.48	9.44	5.00	3.90	2.67
112.5	4-2	62.74	20.05	11.57	8.21	4.37	3.66
	12-1	64.58	19.93	11.18	7.73	4.13	3.66
		S 26.47	S 19.53				
	32-1	49.33	22.65	10.53	7.27	4.51	3.72
135.0	5-2	59.36	23.81	11.91	6.81	4.87	3.66
	11-1	74.47	27.50	13.22	7.78	4.50	3.64
	33-1	61.12	26.48	10.53	7.87	4.69	3.78
157.5	6-2	83.25	22.81	8.53	4.67	3.57	3.04
				S 6.33	S 5.30		
	10-1	118.77	24.40	10.26	5.40	3.01	2.33
				S 5.41	S 5.35	S 3.32	S 2.93
	31-1	49.73	20.56	8.33	5.44	3.94	3.23
		S 57.62		S 6.39	S 5.40		
180.0	7-2	132.23	36.00	11.17	5.34	3.29	2.16
					S 2.73	S 3.32	S 2.97
	9-1	153.15	12.42	3.56	5.77	3.25	2.30
			S 49.54	S 11.09	S 5.22*	S 2.90	S 3.23
	34-1	128.42	31.53	11.87	6.03	3.17	2.28
					S 3.33	S 3.02	S 3.04

TABLE 3. (Contd.)

L/D=4/1 Charge Weight= 8 lb

Angle	Shot	Distance (ft) 7	11	16	21	26	31
0.0	46-2	88.91	15.07	5.36	2.64	1.73	1.17
				S 10.14	S 8.82	S 6.12	S 4.33
	50-1	96.81	14.53	4.17	2.63	2.01	1.40
				S 8.59	S 8.61	S 6.74	S 4.99
22.5	44-2	30.69	12.12	4.46	4.04	4.13	3.08
		S 13.23	S 11.12	S 7.38			
	49-1	34.45	10.75	3.86	5.93	4.13	3.36
		S 12.68	S 12.41	S 7.12			
	58-2	34.53	9.98	8.35	5.62	4.58	3.29
		S 10.48	S 12.60				
45.0	42-2	45.15	19.05	11.33	7.21	4.78	3.76
	47-1	40.37	22.37	11.30	7.88	4.94	3.95
		S 43.31					
67.5	43-2	72.31	24.11	11.58	5.78	3.94	2.82
	48-1	71.13	24.12	10.12	6.25	3.75	3.06
90.0	45-2	165.78	32.82	12.06	6.69	4.08	3.00
	46-1	108.08	36.77	10.97	7.16	4.09	3.22
	50-2	136.64	30.07	12.21	6.26	4.17	3.03
	51-1	169.17	34.75	10.82	6.68	4.20	3.23
	59-1	147.52	33.72	11.03	6.71	4.09	2.87
112.5	44-1	67.98	24.01	10.50	6.36	3.91	3.25
	49-2	68.23	20.44	11.83	6.55	4.15	3.08
	58-1	65.53	21.16	10.22	6.43	4.00	2.97
135.0	42-1	41.98	20.19	9.42	6.55	4.44	3.47
	47-2	40.38	18.48	11.32	5.66	4.74	3.35
157.5	43-1	23.60	8.47	7.68	5.78	3.98	3.30
			S 14.57				
	48-2	17.46	14.72	9.34	5.49	4.39	3.25
180.0	45-1	35.63	9.49	3.87	2.58	5.90	4.21
			S 8.05	S 11.09	S 9.04		
	51-2	27.98	10.52	4.20	2.17	6.46	3.84
			S 6.89	S 11.48	S 7.25		
	59-2	13.99	8.85	4.18	2.48	6.06	3.79
		S 26.68	S 6.87	S 10.37	S 8.23		

TABLE 3. (Contd.)

L/D=1/2 Charge Weight= 8 lb

Angle	Shot	Distance (ft) 7	11	16	21	26	31
0.0	18-1	-.--	86.44	16.97	9.94	4.93	3.60
45.0	17-1	54.84	23.18	12.11	8.27	5.26	4.08
90.0	15-1	58.43*	20.07*	6.46*	5.91*	3.71*	3.49*
	18-2	85.09	15.45	7.41	3.97	3.04	2.50
					S 3.70	S 3.29	S 2.71
	57-1	83.01	17.80	6.56	4.46	3.08	2.50
				S 4.51	S 3.93	S 3.44	S 2.78
135.0	17-2	68.37	22.15	12.09	6.98	4.96	3.71
180.0	15-2	68.01*	9.20*	3.55*	2.46*	1.31*	1.50*
				S 2.96*	S 3.27*	S 2.17*	S 2.69*
	57-2	150.61*	33.82*	18.73*	3.64*	3.64*	3.34*
			S 44.54*		S 5.95*	S 4.91*	S 3.67*

L/D=2/3 Charge Weight= 8 lb

Angle	Shot	Distance (ft) 7	11	16	21	26	31
0.0	38-2	142.00	31.84	9.46	4.00	2.68	1.72
					S 3.47	S 4.54	S 3.73
	61-1	120.87*	46.46	10.34	5.17	2.59	1.63
					S 3.64	S 3.52	S 3.19
45.0	36-2	49.41	26.86	14.11	7.76	5.47	3.56
90.0	37-2	110.19	27.11	10.98	5.81	4.00	2.67
	38-1	114.24	28.27	9.69	6.68	3.93	3.34
	61-2	151.18*	28.55	4.18	5.64	4.23	2.74
				S 10.34			S 5.24
135.0	36-1	50.35	22.49	10.09	7.50	4.69	3.57
180.0	37-1	68.93	17.66	6.20	3.96	2.20	1.76
			S 18.49	S 6.63	S 7.60	S 5.01	S 4.52

TABLE 3. (Cont'd.)

L/D=3/1 Charge Weight= 8 lb

Angle	Shot	Distance (ft) 7	11	16	21	26	31
0.0	41-2	158.04	67.40	8.99	3.58	1.96	1.33
					S 4.30	S 4.19	S 4.17
45.0	39-2	43.90	23.08	13.37	7.99	5.24	3.94
90.0	40-2	60.99*	19.16*	10.26	7.08	4.34	3.18
	41-1	124.84	33.38	9.67	6.93	4.15	3.33
	60-2	152.19	28.11	11.39	6.06	4.47	2.91
135.0	39-1	46.11	19.66	9.54	7.04	4.46	3.50
180.0	40-1	49.29	14.59	4.65	3.19	1.89	1.49
				S 6.37	S 8.23	S 5.89	S 4.81
	60-1	45.97	11.81	4.54	3.06	1.93	4.00
			S 5.52	S 8.77	S 8.50	S 5.58	

L/D=6/1 Charge Weight= 8 lb

Angle	Shot	Distance (ft) 7	11	16	21	26	31
0.0	55-2	59.26	8.64	3.99	2.13	6.33	3.88
			S 6.35	S 12.96	S 8.26		
45.0	53-2	39.48	18.94	10.88	6.08	4.69	3.21
		S 30.17					
90.0	54-2	145.51	35.50	11.30	6.15	4.55	.90
	55-1	75.06*	34.33	11.92	7.39	4.10	2.61
135.0	53-1	37.70	17.50	9.26	6.30	4.11	3.02
180.0	54-1	24.64	6.92	3.02	8.68	4.82	3.29
			S 9.84	S 10.17			

TABLE 3. (Contd.)

L/D=1/1 Charge Weight= 16 lb

Angle	Shot	Distance (ft) 7	11	16	21	26	31
0.0	63-2	-.--	115.28	42.55	13.73	7.60	4.14
90.0	62-2	-.--	50.10	14.98	7.73	5.78	3.77
	63-1	-.--	45.95	14.22	8.80	4.97	3.50
180.0	62-1	-.--	66.10	20.91	9.18	4.89	3.08
						S 3.09	S 2.87

L/D=4/1 Charge Weight= 16 lb

Angle	Shot	Distance (ft) 7	11	16	21	26	31
0.0	65-2	-.--	27.91	9.31	4.66	2.43	2.05
				S 4.67	S 8.21	S 6.50	S 5.05
90.0	64-2	-.--	49.84	17.22	9.61	7.08	4.45
	65-1	-.--	67.20	20.23	11.75	6.40	3.63
180.0	64-1	-.--	18.98	6.50	3.86	2.33	1.58
				S 10.11	S 12.77	S 8.41	S 5.83

SPHERES Charge Weight= 7.8 lb

Shot	Distance (ft) 7	11	16	21	26	31
13-1	69.71	22.67	8.82	6.73	3.84	3.11
13-2	83.29	-.--	10.44	5.75	4.03	2.34
14-1	10.69*	24.41	9.68	6.29	3.87	3.15
14-2	98.72	19.79	10.20	6.18	3.92	2.98
30-1	52.80*	22.75	8.83	6.41	3.96	3.27
30-2	113.76*	20.71	10.38	6.01	4.06	3.03
52-1	61.49	21.05	9.53	6.09	3.78	2.50
52-2	64.82	19.62	9.76	4.18*	4.19	2.83
66-1	-.--	20.24	9.13	6.23	3.68	2.64
66-2	-.--	17.98	9.79	5.59	4.18	2.92

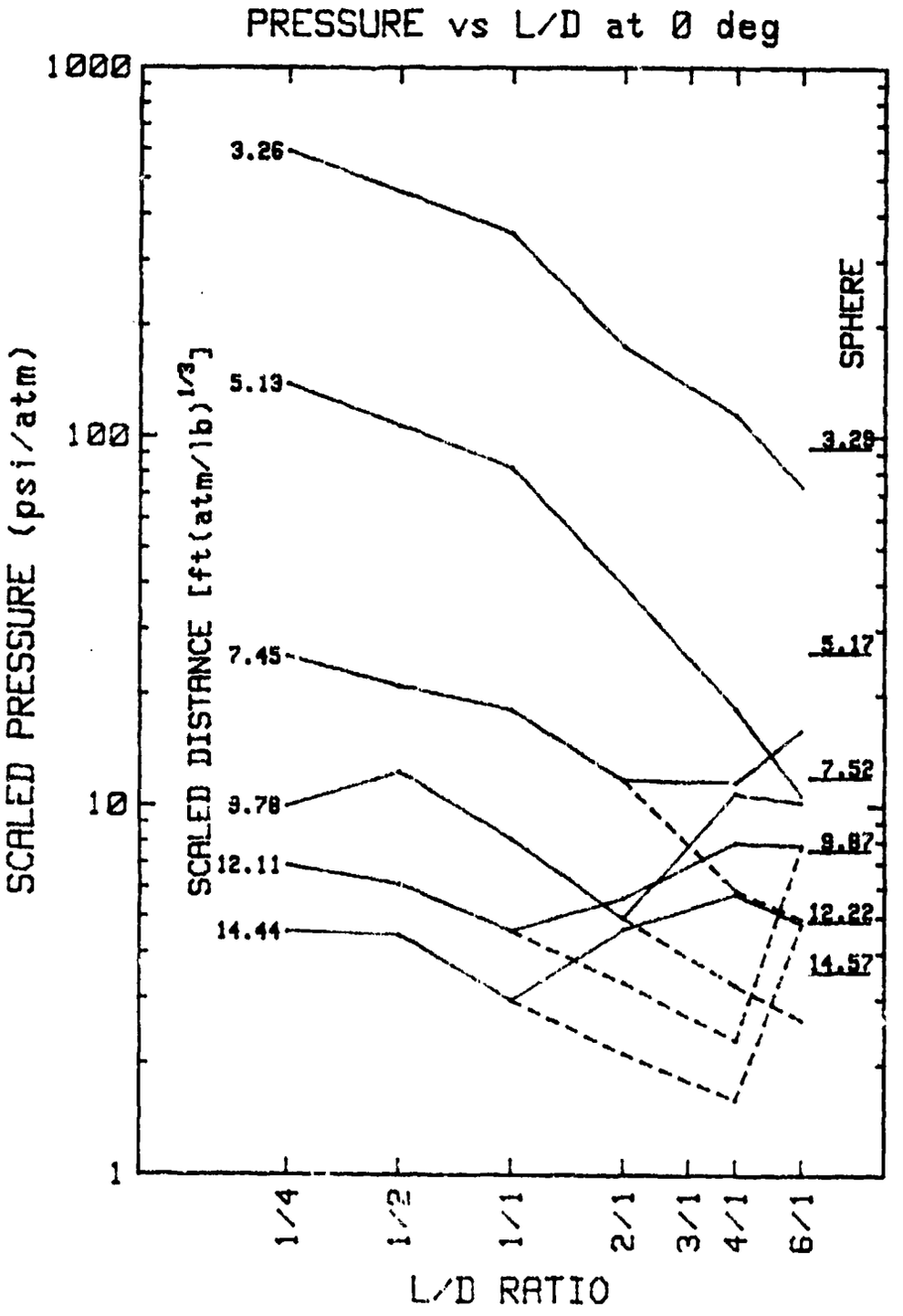

FIGURE 7. Peak Pressure vs. L/D at 0-Degree Angle, Scaled to 1-Pound Charge at Sea Level; Spherical Charge Data at Right. Dashed lines connect first shock pressures when peak occurs at later shock.

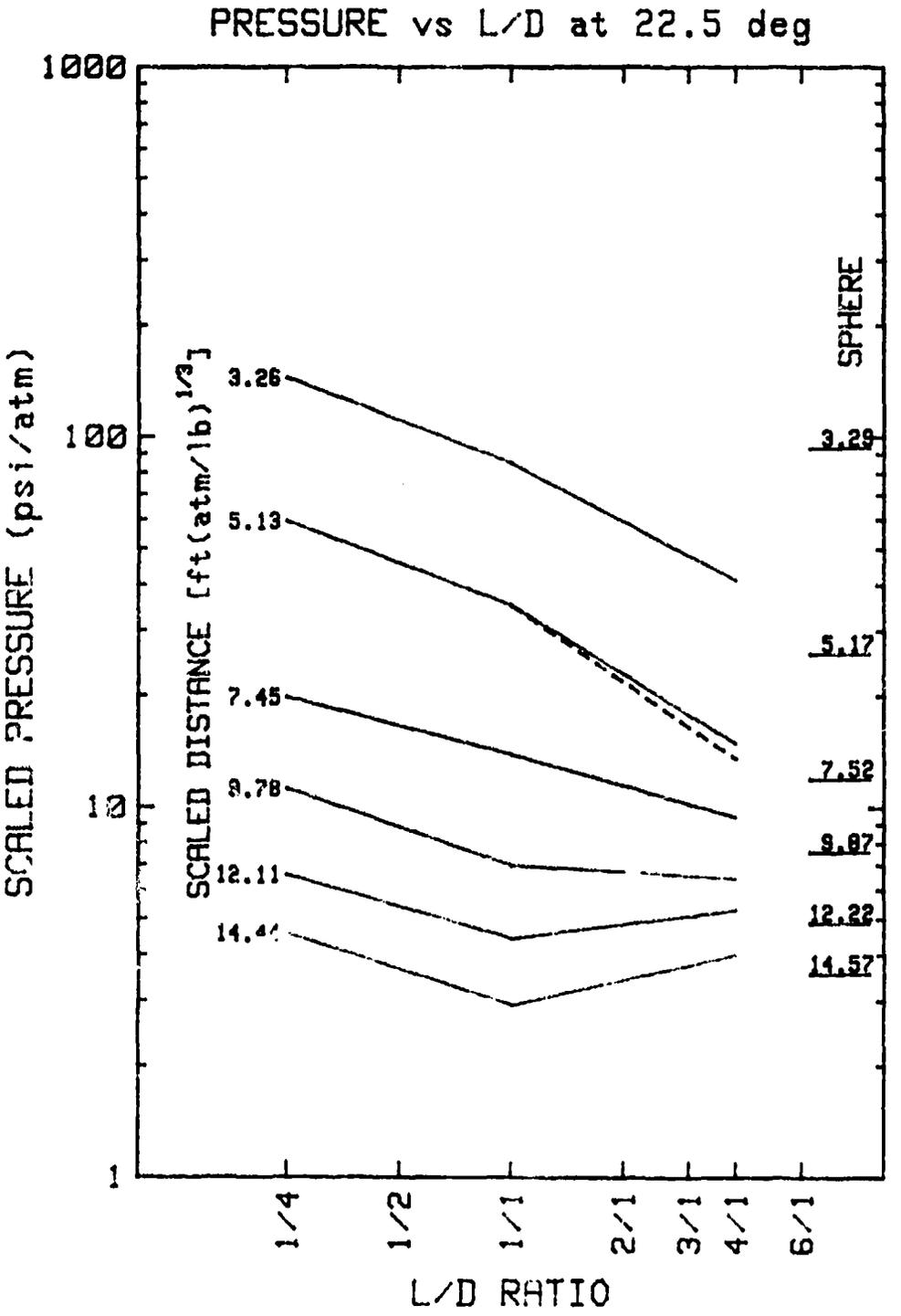

FIGURE 8. Peak Pressure vs. L/D at 22.5-Degree Angle, as in Figure 7.

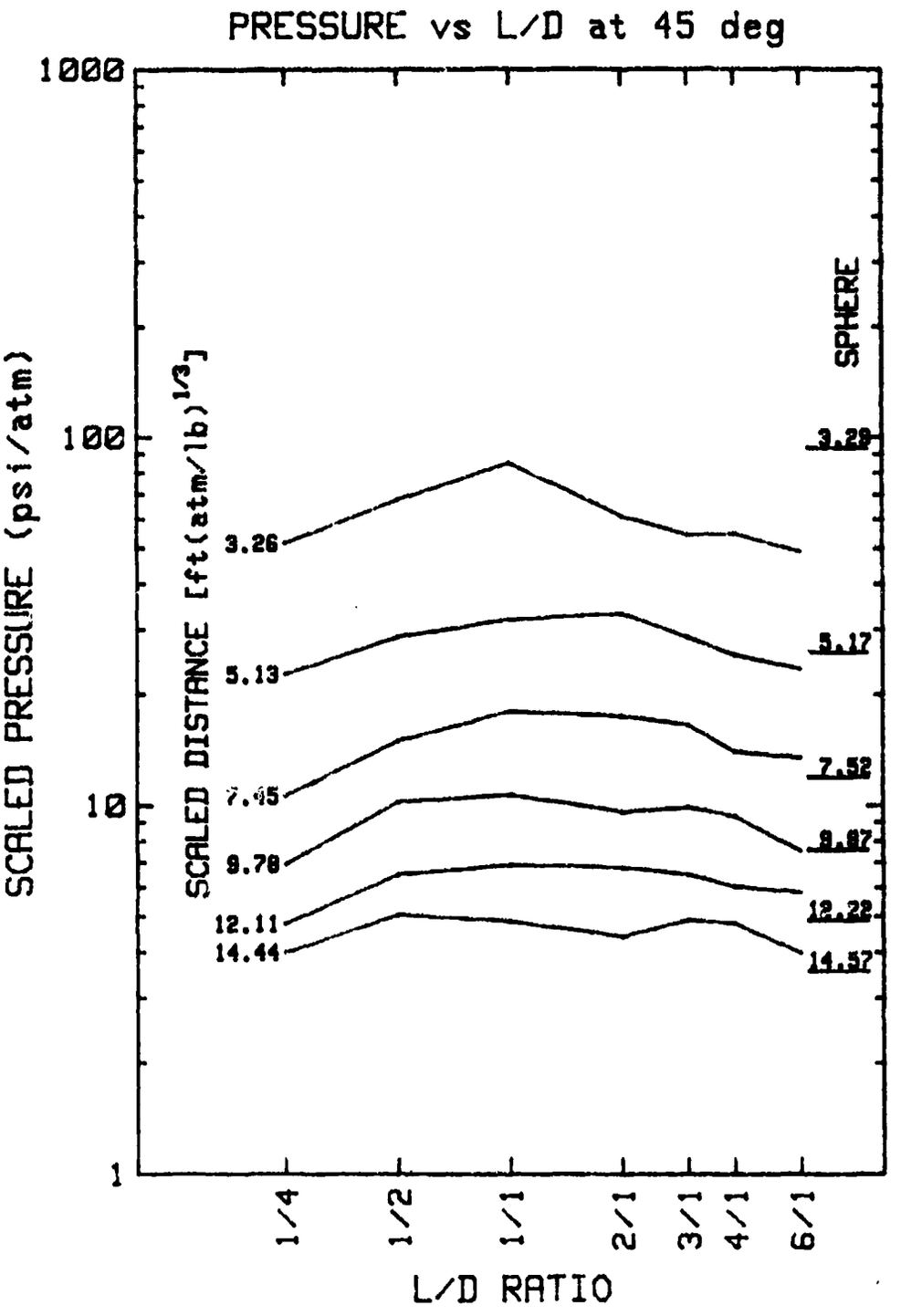

FIGURE 9. Peak Pressure vs. L/D at 45-Degree Angle, as in FIGURE 7.

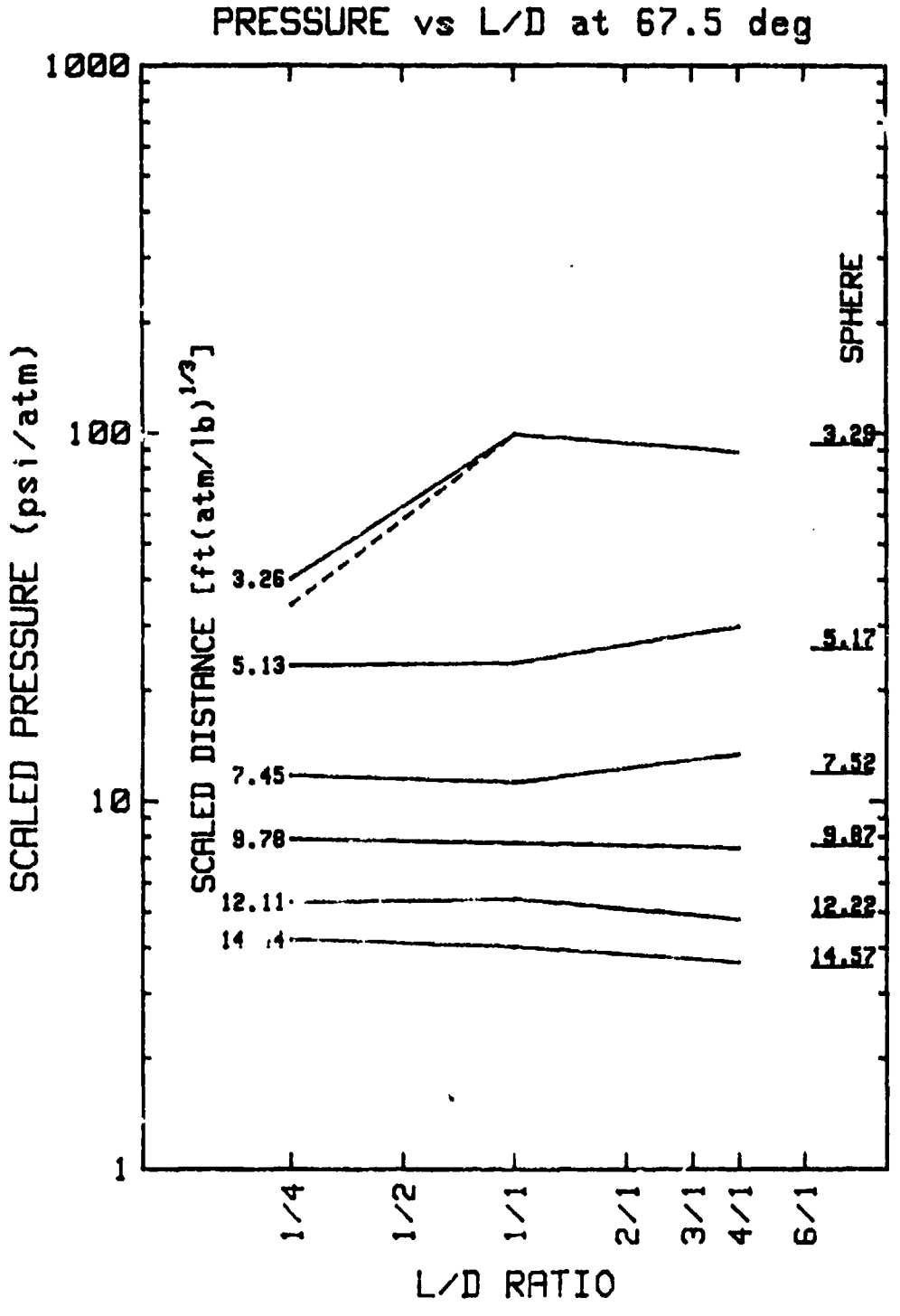

FIGURE 10. Peak Pressure vs. L/D at 67.5-Degree Angle, as in FIGURE 7.

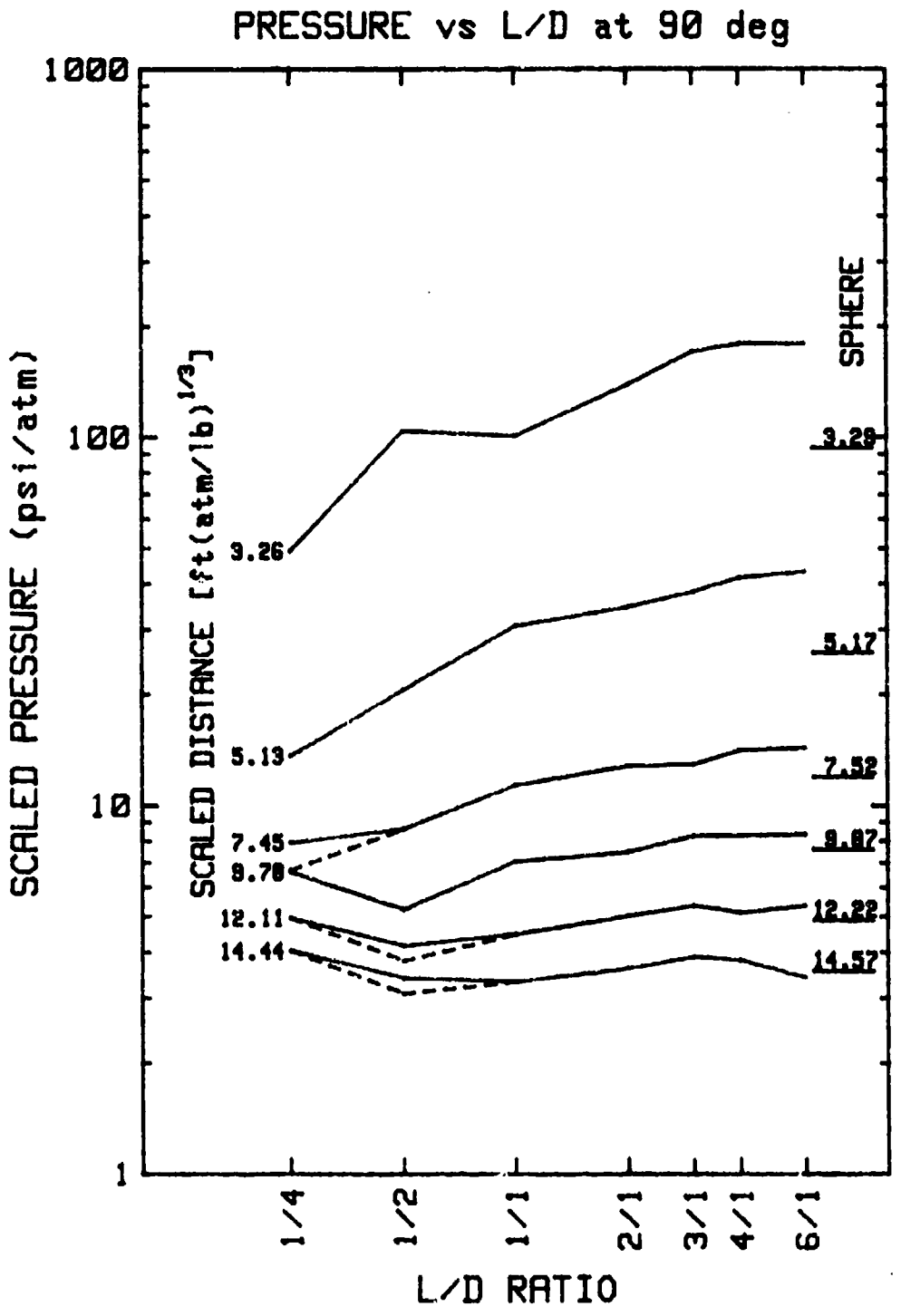

FIGURE 11. Peak Pressure vs. L/D at 90-Degree Angle, as in FIGURE 7.

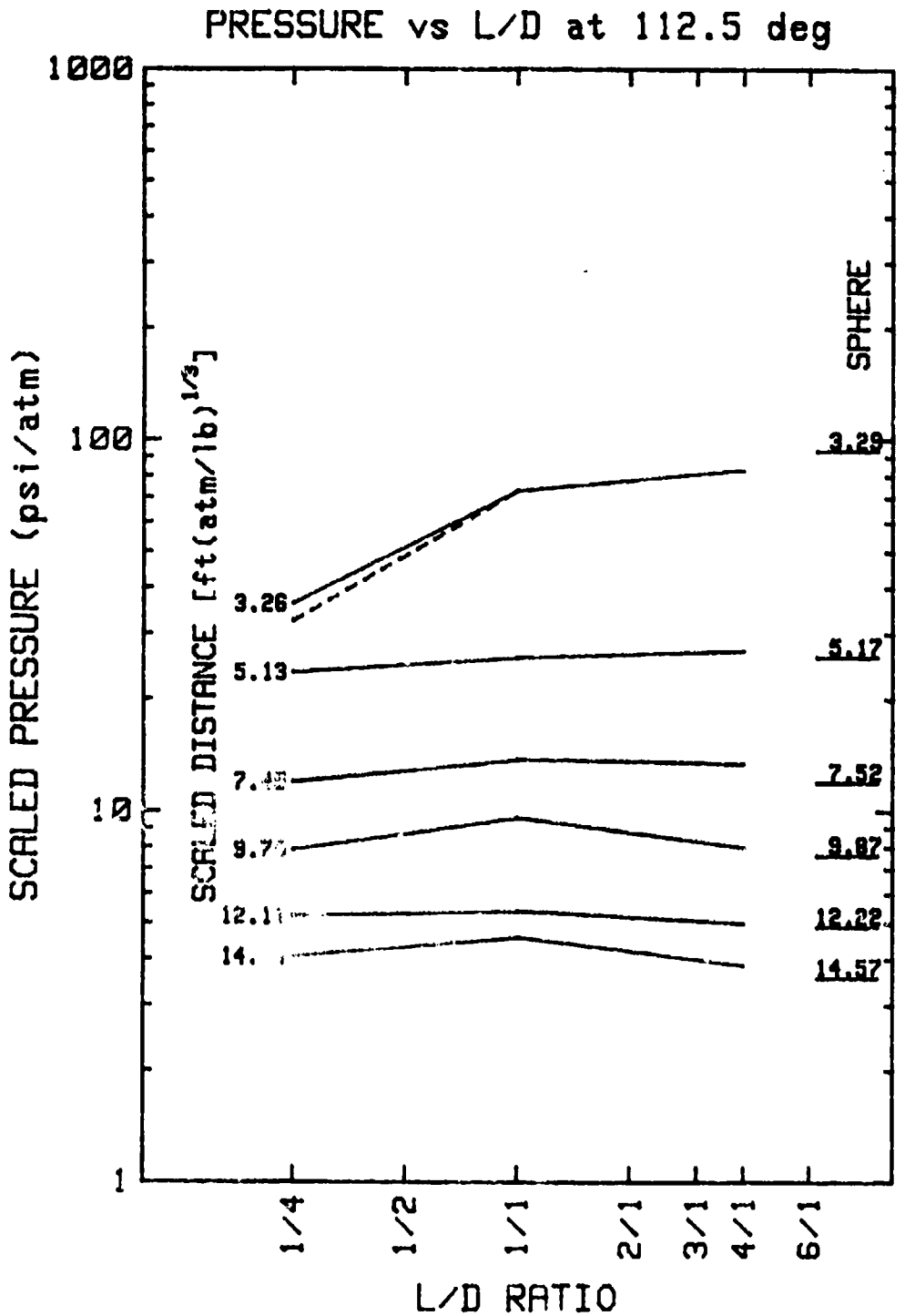

FIGURE 12. Peak Pressure vs. L/D at 112.5-Degree Angle, as in FIGURE 7.

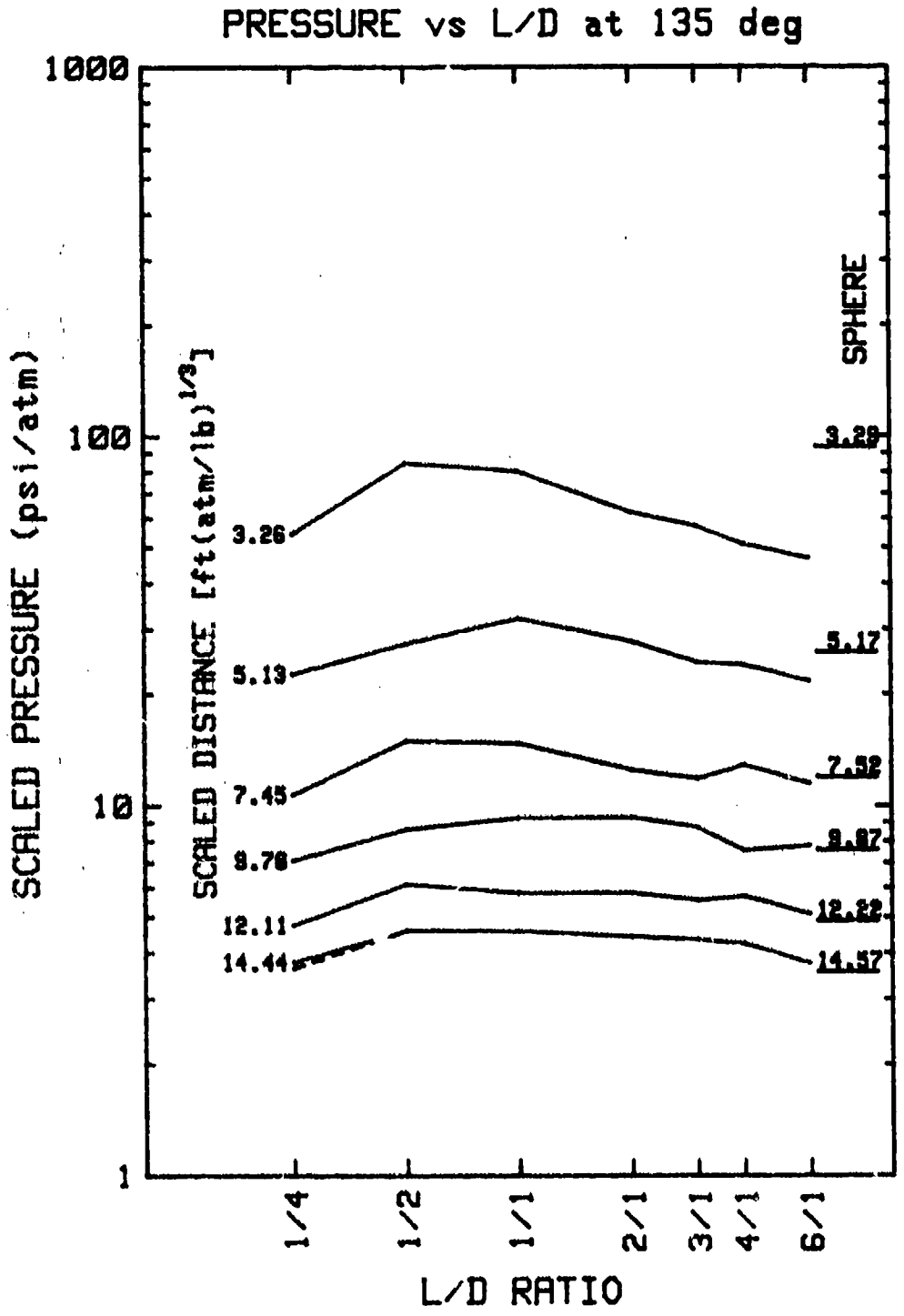

FIGURE 13. Peak Pressure vs. L/D at 135-Degree Angle, as in FIGURE 7.

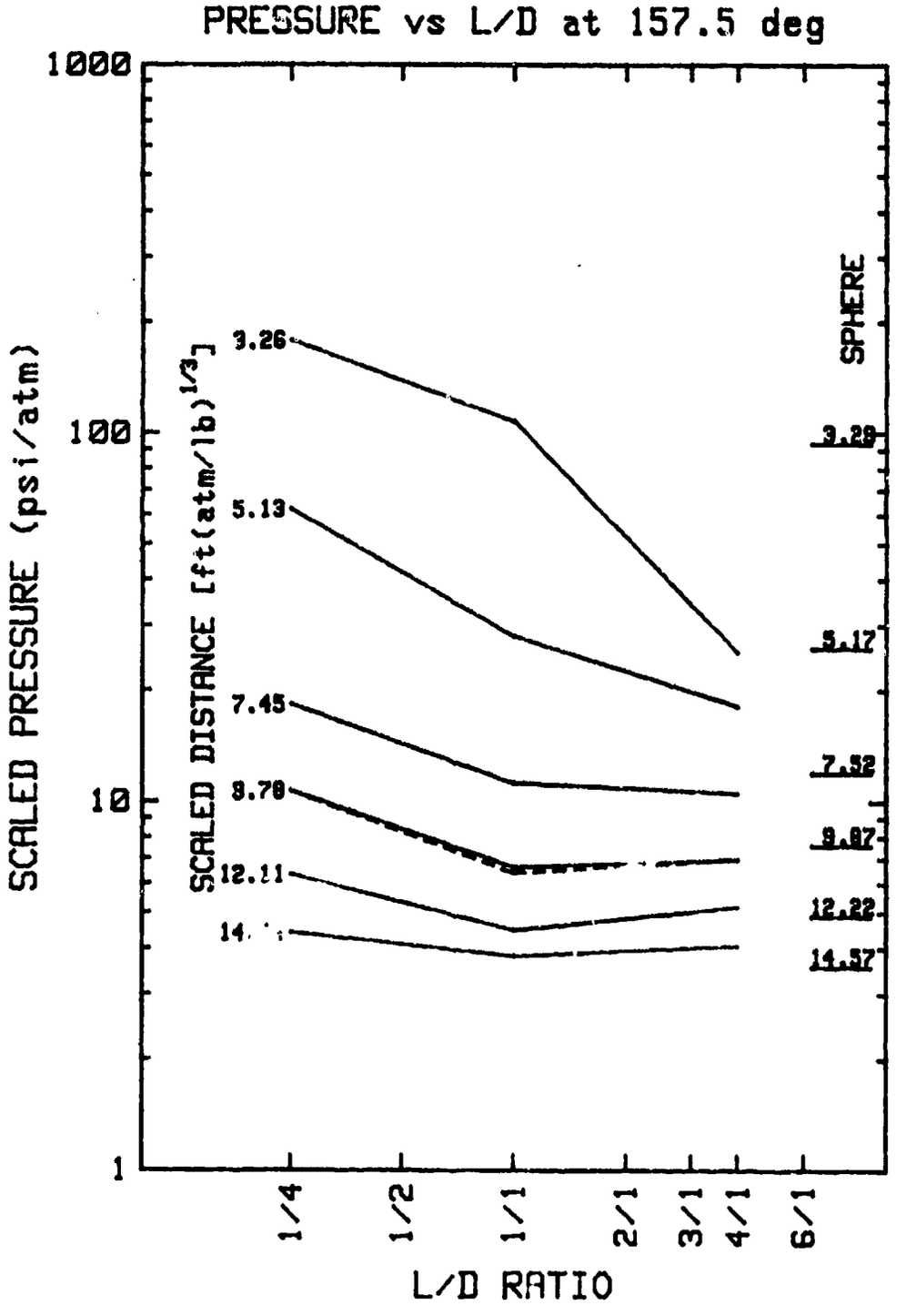

FIGURE 14. Peak Pressure vs. L/D at 157.5-Degree Angle, as in FIGURE 7.

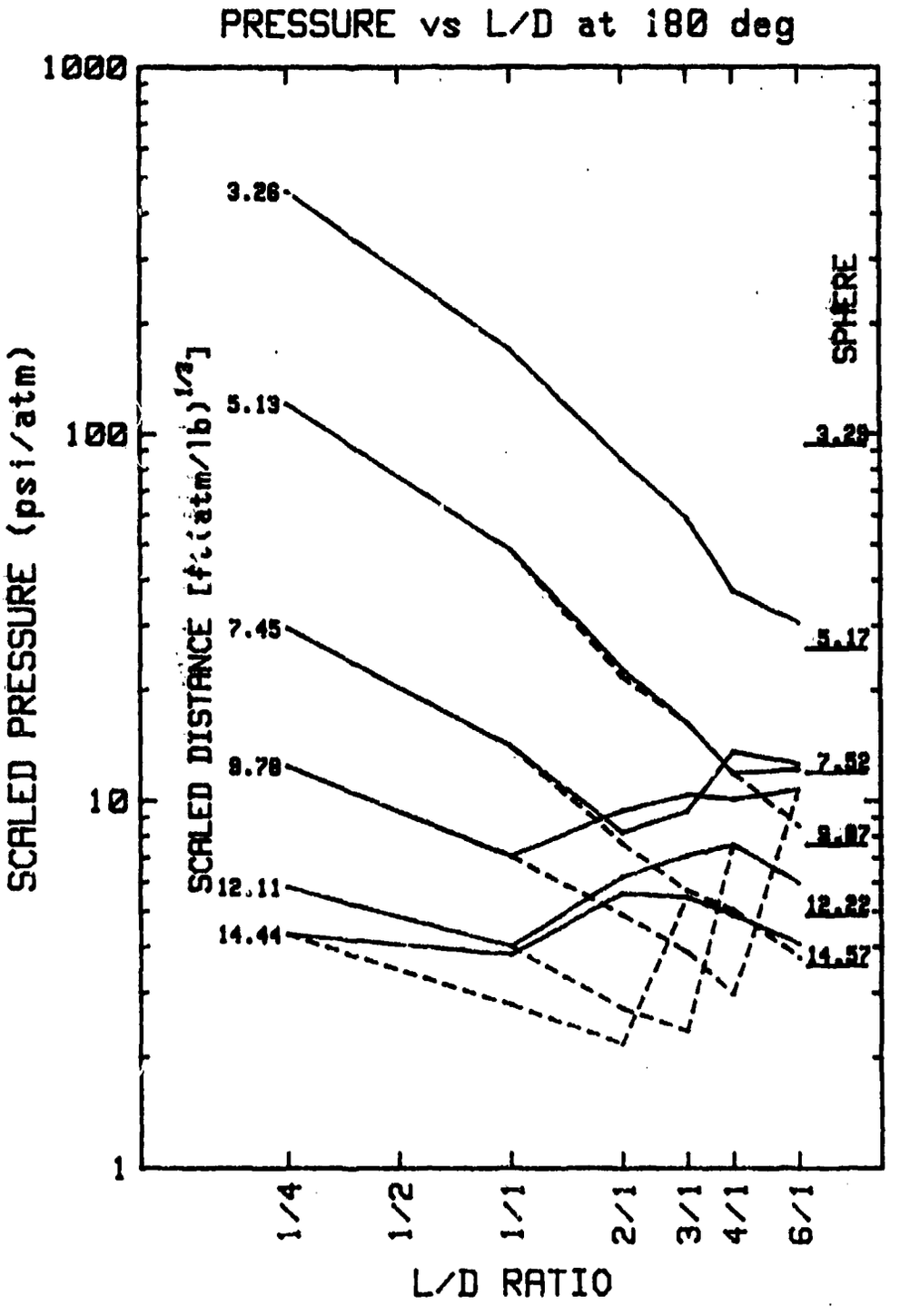

FIGURE 15. Peak Pressure vs. L/D at 180-Degree Angle, as in FIGURE 7.

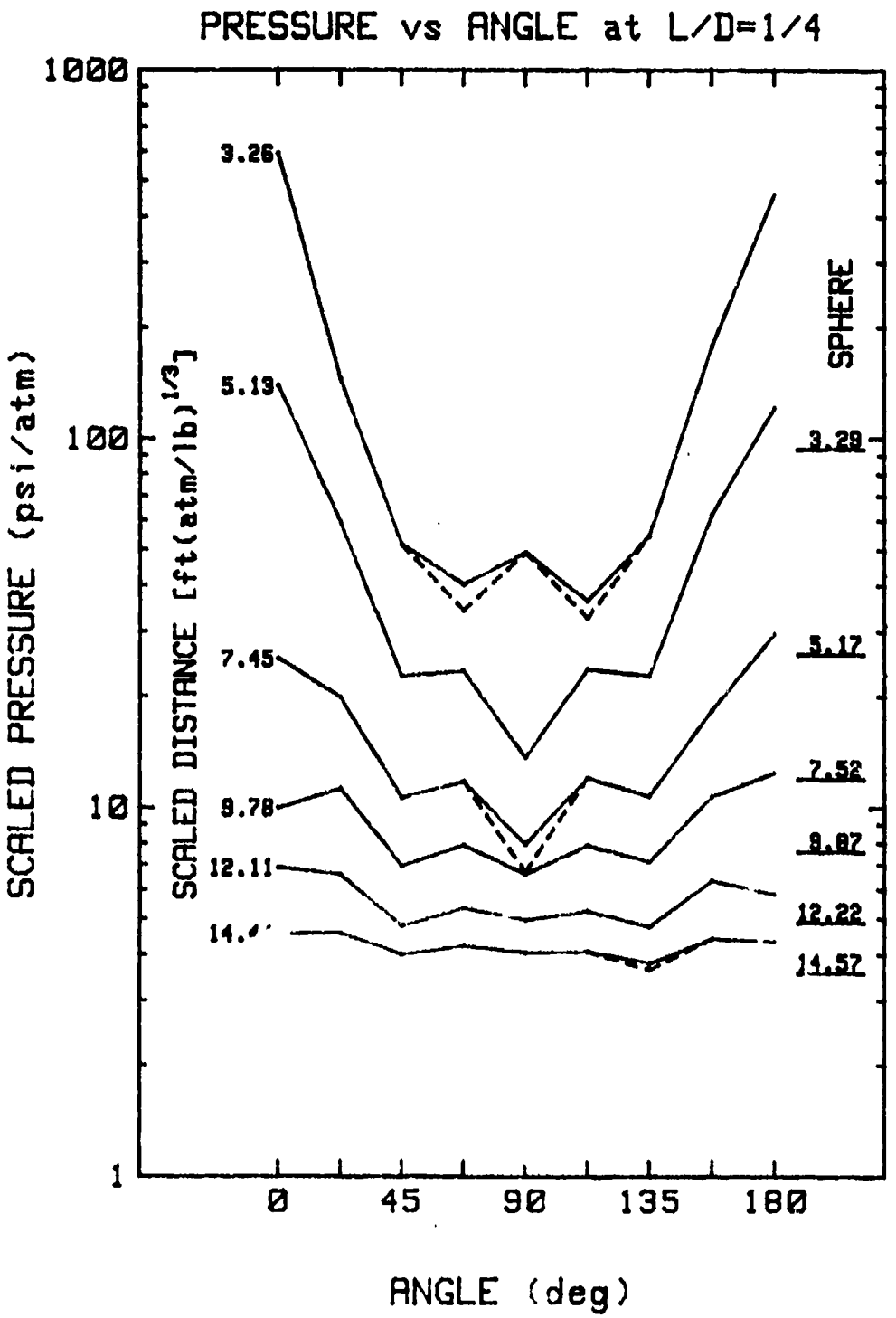

FIGURE 16. Peak Pressure vs. Angle for L/D = 1/4, Scaled to 1-Pound Charge at Sea Level; Spherical Charge Data at Right. Dashed lines connect first shock pressures when peak is at second shock.

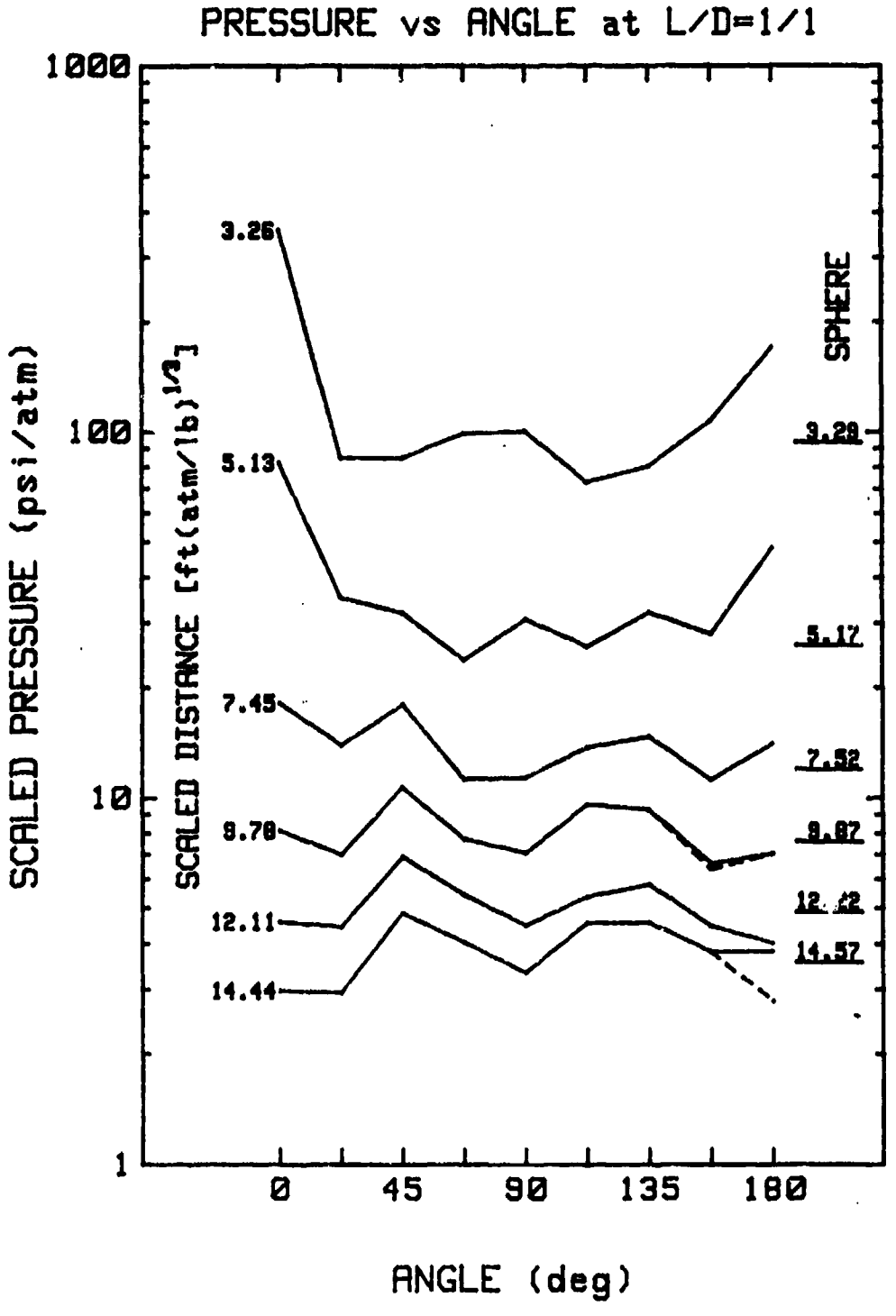

FIGURE 17. Peak Pressure vs. Angle at L/D = 1/1, as in FIGURE 16.

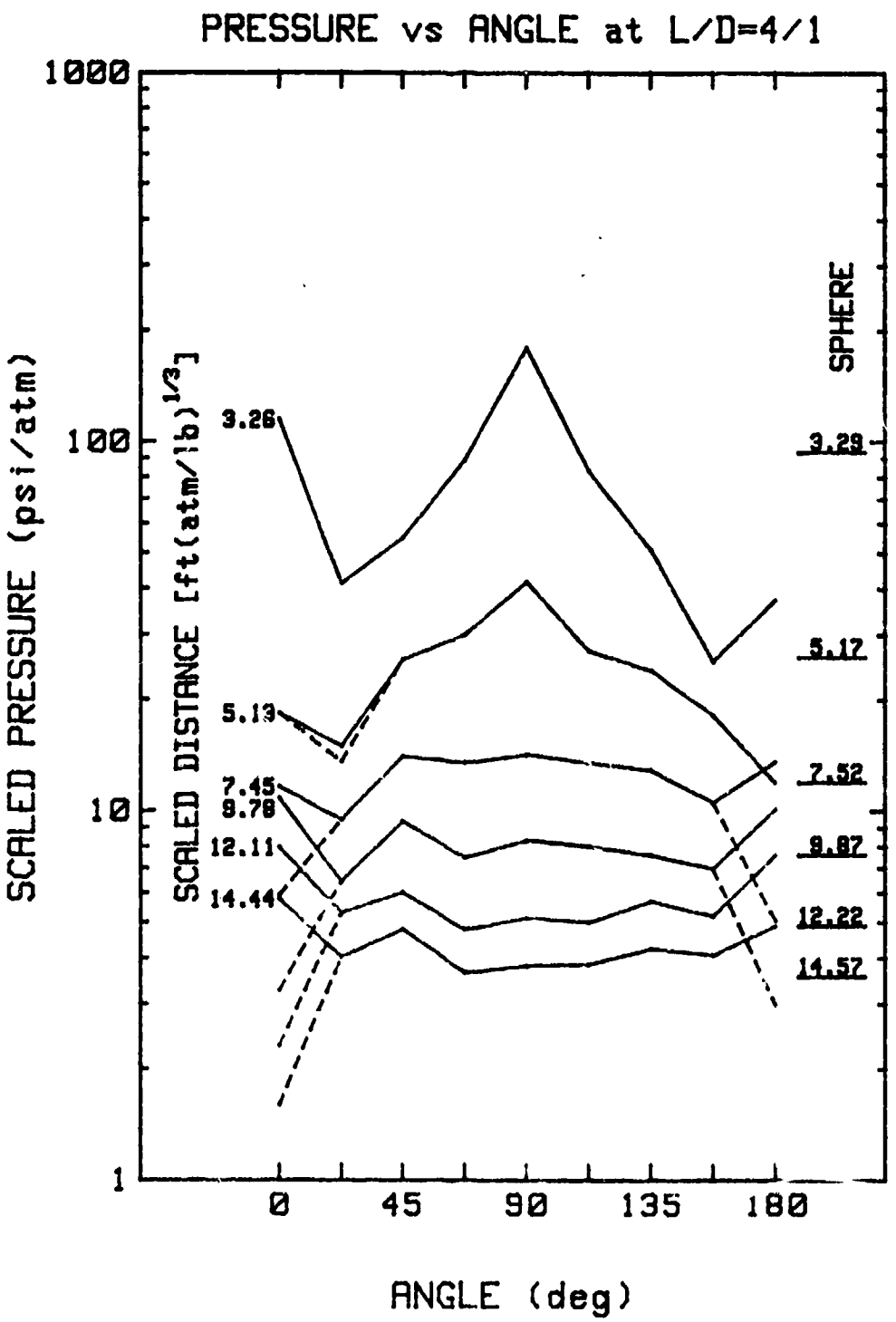

FIGURE 18. Peak Pressure vs. Angle at L/D = 4/1, as in FIGURE 16.

POSITIVE IMPULSE AND DURATION

The positive impulse and duration data reported here include all secondary shocks which arrive before the overpressure returns to zero. In some shots, a ground reflection arrived at the more distant gauges before the overpressure had returned to zero. In such cases, the impulse and positive duration were determined by extrapolating the tail of the trace to zero. A number of pressure-time traces exhibited long positive tails, as is seen in the plots in Appendix A. In most such cases, the zero crossing is simply off the scale of the plots shown here. However, some traces never returned to zero, presumably because of a shift in the baseline after shock passage. The choice of the end point for the impulse integration on these traces was an educated guess. The effect on the accuracy of the impulse is small (less than the shot-to-shot variability in most cases) because the tails are always very close to zero and contribute little to the impulse. Clearly, however, the positive duration cannot be determined in these cases.

The positive impulse data are listed in Table 4. As for the peak pressure data, missing data indicate gauge absence or malfunction, and questionable values are followed by an asterisk.

Figures 19 through 27 show positive impulse vs. L/D ratio at each of the angles used in this study, and Figures 28, 29, and 30 show impulse vs. angle for L/D ratios of 1/4, 1/1, and 4/1. All data are scaled to one pound and sea level, and the spherical charge impulse data are shown on the right side of each figure.

The positive duration data are listed in Table 5. No values are given for traces without zero crossings.

TIME OF ARRIVAL

The arrival times reported here represent the time interval from the leading edge of the electrical firing pulse to the XM-70 initiator, to the arrival of the leading shockwave. Table 6 lists the time of arrival data for each gauge on each shot.

DISCUSSION

ERROR ANALYSIS

Sources of Error

There are three main types of errors in a program such as this: random, or statistical, errors; systematic errors, or bias; and human errors, such as writing down the wrong number.

A substantial portion of the effort expended in data reduction and analysis was devoted to ensuring accuracy. The firing program generated

TABLE 4. Positive Impulse (psi-ms).

Note: * denotes questionable value

L/D=1/4 Charge Weight= 8 lb

Angle	Shot	Distance (ft) 7	11	16	21	26	31
0.0	21-1	109.05	44.67	15.78	11.15	8.87	7.53
	29-2	103.94	44.35	15.81	6.72*	8.85	6.98
22.5	23-1	26.69	20.13	14.29	10.90	8.19	6.93
	26-2	31.52	18.03	13.87	9.77	8.23	6.64
45.0	20-1	17.96	15.81	15.63	11.58	9.27	8.34
	25-2	18.19	16.87	14.81	11.11	9.19	7.64
	27-1	17.64	17.73	14.91	11.35	9.04	8.15
67.5	22-1	18.62	15.00	11.90	10.39	8.68	7.86
	24-2	19.29	15.25	12.30	9.64	8.46	7.33
90.0	19-1	17.54	12.42	12.10	9.76	8.22	7.73
	21-2	19.48	12.74	10.75	9.13	8.03	6.88
	28-2	20.74	13.15	11.55	8.34	8.27	7.24
	29-1	16.03	13.75	12.73	10.63	8.38	7.78
112.5	23-2	19.70	15.73	12.36	9.39	8.45	7.37
	26-1	18.59	15.96	10.95	9.48	8.10	7.41
135.0	20-2	23.20	14.36	14.62	11.02	9.04	7.98
	25-1	19.41	20.65	14.11	11.87	9.40	8.06
	27-2	21.30	17.65	14.43	8.60*	8.99	7.44
157.5	22-2	36.11	21.76	13.58	10.69	8.31	6.86
	24-1	31.33	21.33	13.33	10.73	8.19	6.55
180.0	19-2	128.[illegible]	35.25	17.51	11.87	8.65	7.16
	28-1	76.[illegible]4	33.62	19.29	13.27	9.38	8.00

TABLE 4. (Contd.)

For shots 2 and 3, gauges are at 7, 12, 17, 22, 27, and 32 ft

L/D=1/1 Charge Weight= 8 lb

Angle	Shot	Distance (ft) 7	11	16	21	26	31
0.0	2-1	58.62	26.17	13.61	12.49	9.38	8.42
	3-1	-.--	30.57	14.40	11.76	9.08	8.05
	8-2	60.38	33.72	14.28	10.96	9.30	8.14
	35-2	38.24*	30.60	14.60	10.23	9.36	7.64
	56-1	70.27	28.25	17.73	11.61	9.73	8.30
22.5	4-1	14.80	15.59	14.41	6.95*	10.24	8.35
	12-2	20.52	14.97	14.22	11.85	9.35	8.19
	32-2	15.01	15.40	13.96	9.56	9.51	7.64
45.0	5-1	27.50	21.67	12.90*	10.78	10.31	8.61
	11-2	22.43	19.93	17.04	12.22	9.80	8.12
	33-2	26.62	21.14	17.53	13.11	10.38	8.09
67.5	6-1	23.98	18.14	13.18	7.29*	9.41	7.64
	10-2	24.30	16.10	14.78	10.89	9.05	7.38
	31-2	24.43	17.27	13.42	9.73	8.67	7.12
90.0	2-2	32.07	18.38	13.78	9.30	7.76	6.66
	3-2	27.09	14.03	10.89	8.61	7.39	6.82
	7-1	33.55	18.64	11.44	11.19	7.97	7.57
	8-1	29.77	17.14	11.31	10.87	8.21	7.20
	9-2	94.70*	18.02	12.41	9.49	8.01	7.60
	34-2	28.27	15.27	12.50	10.03	8.37	6.79
	35-1	30.90	15.67	12.35	10.02	8.27	7.32
	56-2	28.67	15.82	12.59	10.07	9.20	7.29
112.5	4-2	34.79*	19.00	11.84	14.82*	8.69	8.41
	12-1	22.52	18.06	12.13	9.91	8.57	7.73
	32-1	22.51	17.39	13.88	10.97	8.84	7.72
135.0	5-2	22.09	18.67	14.28	11.12	9.61	8.09
	11-1	27.56	18.56	13.56	11.70	9.11	7.95
	33-1	23.67	20.69	13.53	11.11	8.88	7.76
157.5	6-2	42.49*	19.76	11.43	12.14	8.73	8.72
	10-1	21.95	15.57	13.42	11.51	9.37	8.13
	31-1	24.81	14.01	11.78	11.02	9.24	8.53
180.0	7-2	42.66	19.24	15.92	11.17	9.24	8.20
	9-1	41.21	17.62	11.56	11.01	9.48	8.44
	34-1	38.03	18.08	12.62	11.03	9.58	8.25

TABLE 4. (Contd.)

L/D=4/1 Charge Weight= 8 lb

Angle	Shot	Distance (ft) 7	11	16	21	26	31
0.0	46-2	24.63	13.36*	15.00	11.23	10.20	8.43
	50-1	29.82	17.22	13.02	10.98	10.61	8.84
22.5	44-2	13.72	14.72	13.24	8.13*	9.64	7.82
	49-1	15.68	15.40	12.49	10.37	9.64	8.62
	58-2	14.21	16.08	13.62	11.77	10.53	8.46
45.0	42-2	22.26	18.93	16.62	12.33	9.09	8.12
	47-1	21.57	18.96	15.17	11.54	9.55	8.45
67.5	43-2	23.32	19.13	13.98	10.00	8.60	7.17
	48-1	24.07	18.82	13.51	10.86	8.62	7.71
90.0	45-2	42.27	16.59	13.60	9.72	7.35	6.40
	46-1	41.06	17.93	12.74	9.78	7.75	6.94
	50-2	32.70	17.84	13.36	8.93	7.79	7.31
	51-1	37.61	17.84	13.11	9.68	7.69	6.59
	59-1	37.05	19.12	13.50	10.26	7.76	6.47
112.5	44-1	21.24	16.88	13.76	10.19	8.19	7.47
	49-2	20.21	17.25	13.70	9.85	8.33	7.14
	58-1	20.75	16.94	13.82	10.61	8.57	7.10
135.0	42-1	20.66	17.23	13.09	10.44	8.80	7.61
	47-2	19.76	17.80	13.78	8.90*	9.24	7.62
157.5	43-1	15.30	17.24	13.10	10.97	9.59	8.76
	48-2	13.76	17.09	13.95	10.26	10.09	8.36
180.0	45-1	18.12	18.18	13.89	11.98	10.35	9.40
	51-2	15.68	16.72	14.15	9.72*	10.76	8.47
	59-2	18.07	17.84	16.00	13.56	11.04	9.34

L/D=1/2 Charge Weight= 8 lb

Angle	Shot	Distance (ft) 7	11	16	21	26	31
0.0	18-1	-	32.29	15.64	10.83	7.38	6.65
45.0	17-1	27.16	20.19	16.08	12.41	9.95	8.57
90.0	15-1	21.21	14.61	9.09*	9.78	7.27	6.89
	18-2	36.21	14.10	11.79	9.42	8.29	6.87
	57-1	47.37*	27.83*	25.06*	20.06*	17.09*	14.03*
135.0	17-2	25.41	19.44	15.50	11.39	9.32	7.91
180.0	15-2	26.29*	5.93*	5.75*	6.30*	4.11*	5.44*
	57-2	149.21*	50.08*	25.35*	20.46*	15.96*	18.49*

L/D=2/1 Charge Weight= 8 lb

Angle	Shot	Distance (ft) 7	11	16	21	26	31
0.0	38-2	36.77	20.09	15.49	9.49*	9.46	7.73
	61-1	20.23*	17.41	15.80	13.29	10.21	5.46
45.0	36-2	24.98	22.27	16.03	11.45	9.54	7.48
90.0	37-2	29.61	16.92	12.65	8.85	7.90	6.24
	38-1	32.83	16.37	12.30	9.77	7.35	7.10
	61-2	50.13*	10.73*	11.33	11.15	8.90	6.88
135.0	36-1	21.63	18.51	13.27	10.82	8.93	8.05
180.0	37-1	27.58	13.60	12.81	11.09	9.25	8.49

TABLE 4. (Contd.)

L/D=3/1 Charge Weight= 8 lb

Angle	Shot	Distance (ft) 7	11	16	21	26	31
0.0	41-2	20.94	17.25	11.36	10.66	9.56	8.12
45.0	39-2	22.87	20.47	16.05	11.69	9.64	7.99
90.0	40-2	27.12	17.44	13.12	9.82	7.75	6.47
	41-1	34.04	17.92	11.98	9.33	7.47	6.80
	60-2	57.69*	17.49	12.35	10.38	8.34	7.16
135.0	39-1	20.96	16.79	12.92	10.56	8.81	7.67
180.0	40-1	20.23	12.36*	12.88	11.25	9.46	8.60
	60-1	19.18	16.75	14.46	11.68	10.17	7.45

L/D=6/1 Charge Weight= 8 lb

Angle	Shot	Distance (ft) 7	11	16	21	26	31
0.0	55-2	24.95	16.84	14.24	11.72	10.63	8.50
45.0	53-2	25.52	18.01	13.00	11.35	9.98	7.60
90.0	54-2	54.63	19.19	10.95*	11.15	8.89	6.58
	55-1	33.07	17.17	13.88	9.91	7.89	5.85
135.0	53-1	19.83	15.75	13.25	10.29	8.48	6.70
180.0	54-1	18.04	17.46	16.38	13.06	10.72	7.35

L/D=1/1 Charge Weight= 16 lb

Angle	Shot	Distance (ft) 7	11	16	21	26	31
0.0	63-2	-.--	66.57	27.62	21.65	18.99	14.10
90.0	62-2	-.--	24.17	17.47	15.62	13.80	11.04
	63-1	-.--	23.53	18.54	15.03	12.72	9.62
180.0	62-1	-.--	32.38	18.40	17.78	15.04	10.60

L/D=4/1 Charge Weight= 16 lb

Angle	Shot	Distance (ft) 7	11	16	21	26	31
0.0	65-2	-.--	25.03	18.36	18.85	15.62	12.14
90.0	64-2	-.--	34.14	17.88	16.78	13.44	10.19
	65-1	-.--	31.93	21.52	16.85	12.74	7.61
180.0	64-1	-.--	25.33	21.38	16.96	14.86	10.11

SPHERES Charge Weight= 7.8 lb

Shot	Distance (ft) 7	11	16	21	26	31
13-1	23.01	16.45	11.83	9.81	7.73	6.88
13-2	29.10	17.42*	12.82	9.07	7.61	6.68
14-1	-.--	15.46	14.30	7.45	8.06	6.81
14-2	32.49	16.58	10.57	10.19	7.55	6.60
30-1	20.71*	16.54	12.00	9.14	7.58	6.77
30-2	31.65*	16.12	12.62	9.02	7.63	6.20
52-1	21.34	15.73	12.97	9.49	7.77	5.60
52-2	24.45	16.74	11.69	6.11*	8.30	6.35
66-1	-.--	15.79	12.32	9.16	7.37	5.52
66-2	-.--	16.41	11.86	9.40	7.86	6.19

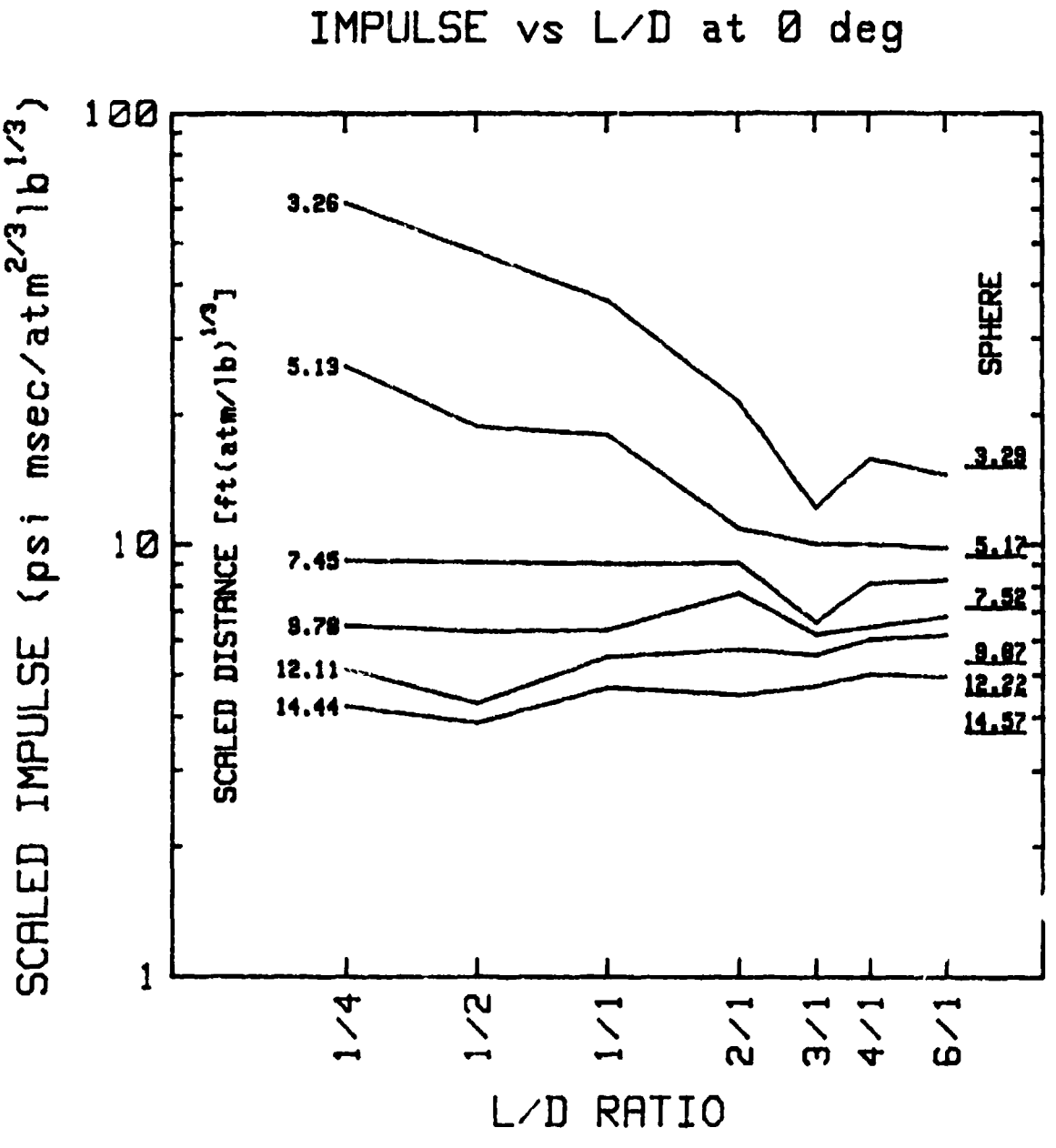

FIGURE 19. Positive Impulse vs. L/D at 0-Degree Angle, Scaled to 1-Pound Charge at Sea Level; Spherical Charge Data at Right.

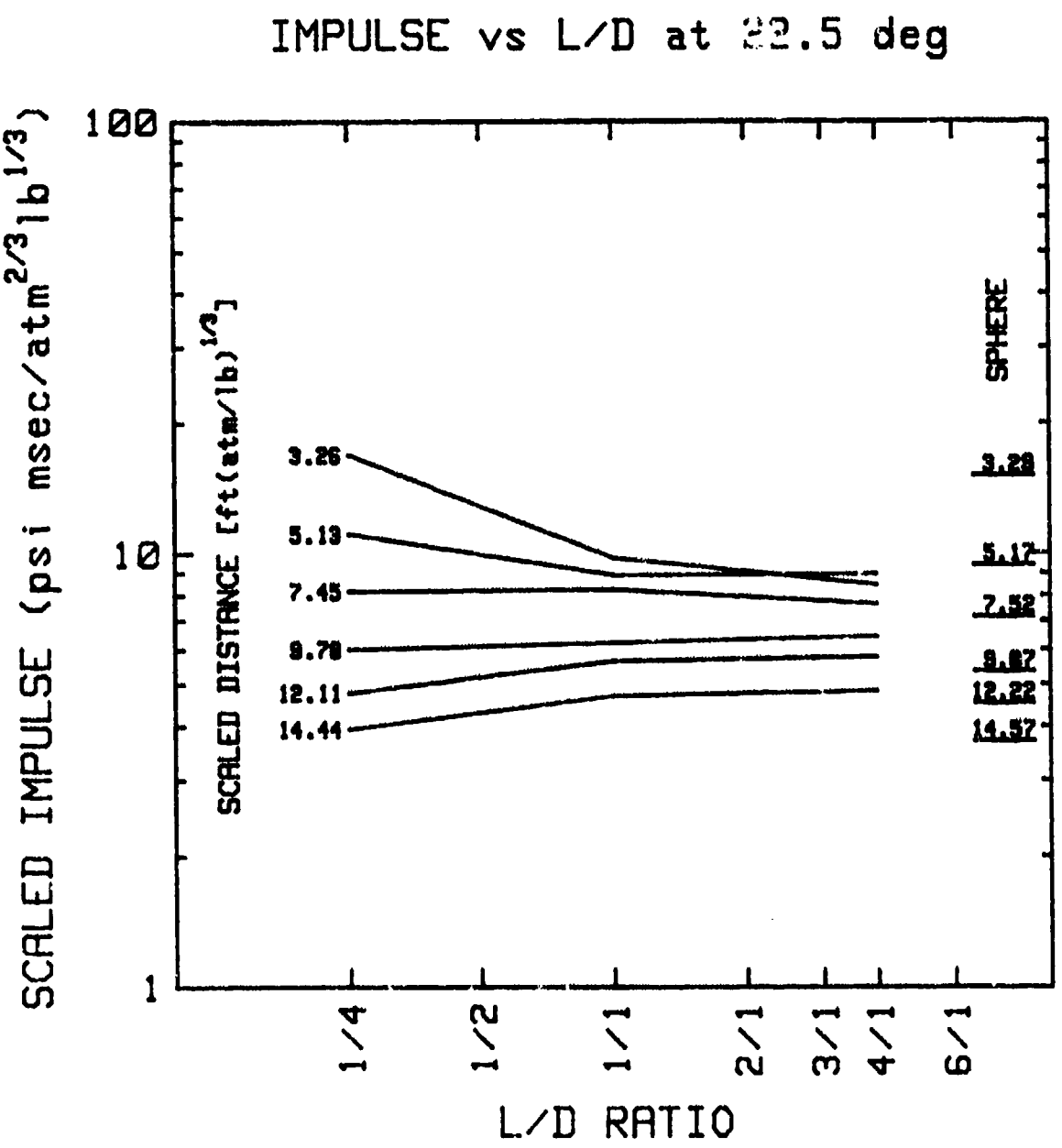

FIGURE 20. Positive Impulse vs. L/D at 22.5-Degree Angle, as in FIGURE 19.

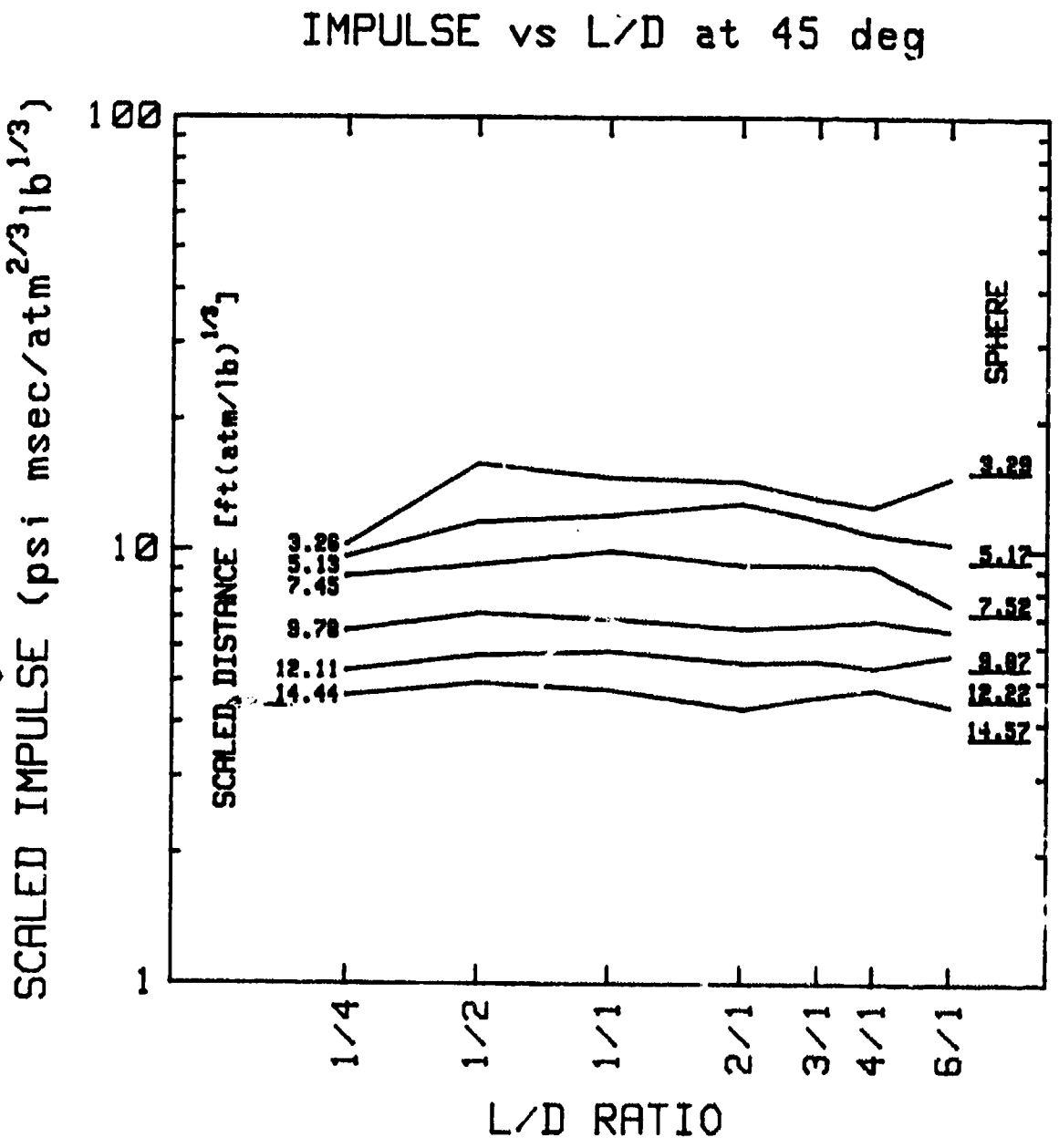

FIGURE 21. Positive Impulse vs. L/D at 45-Degree Angle, as in FIGURE 19.

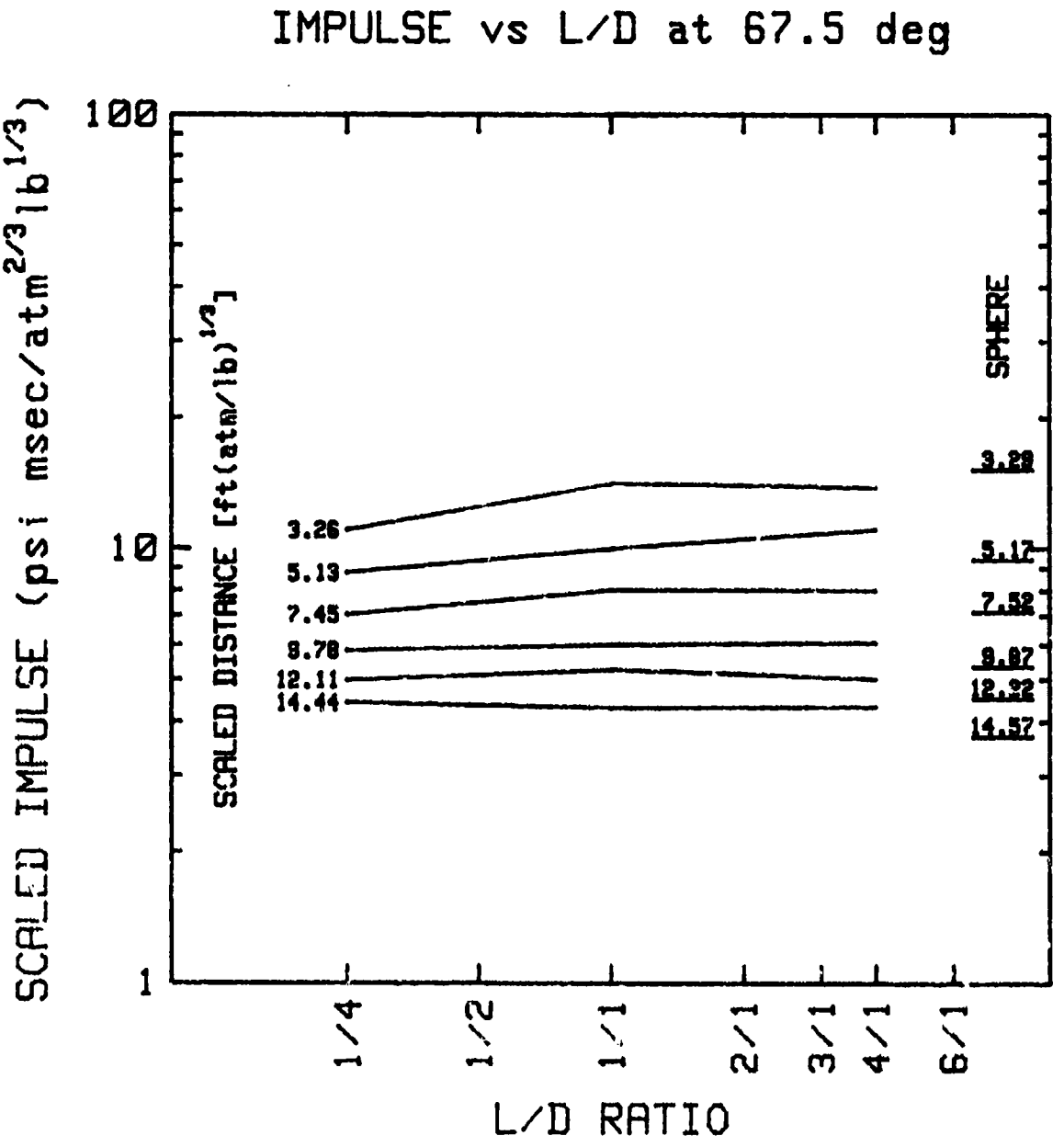

FIGURE 22. Positive Impulse vs. L/D at 67.5-Degree Angle, as in FIGURE 19.

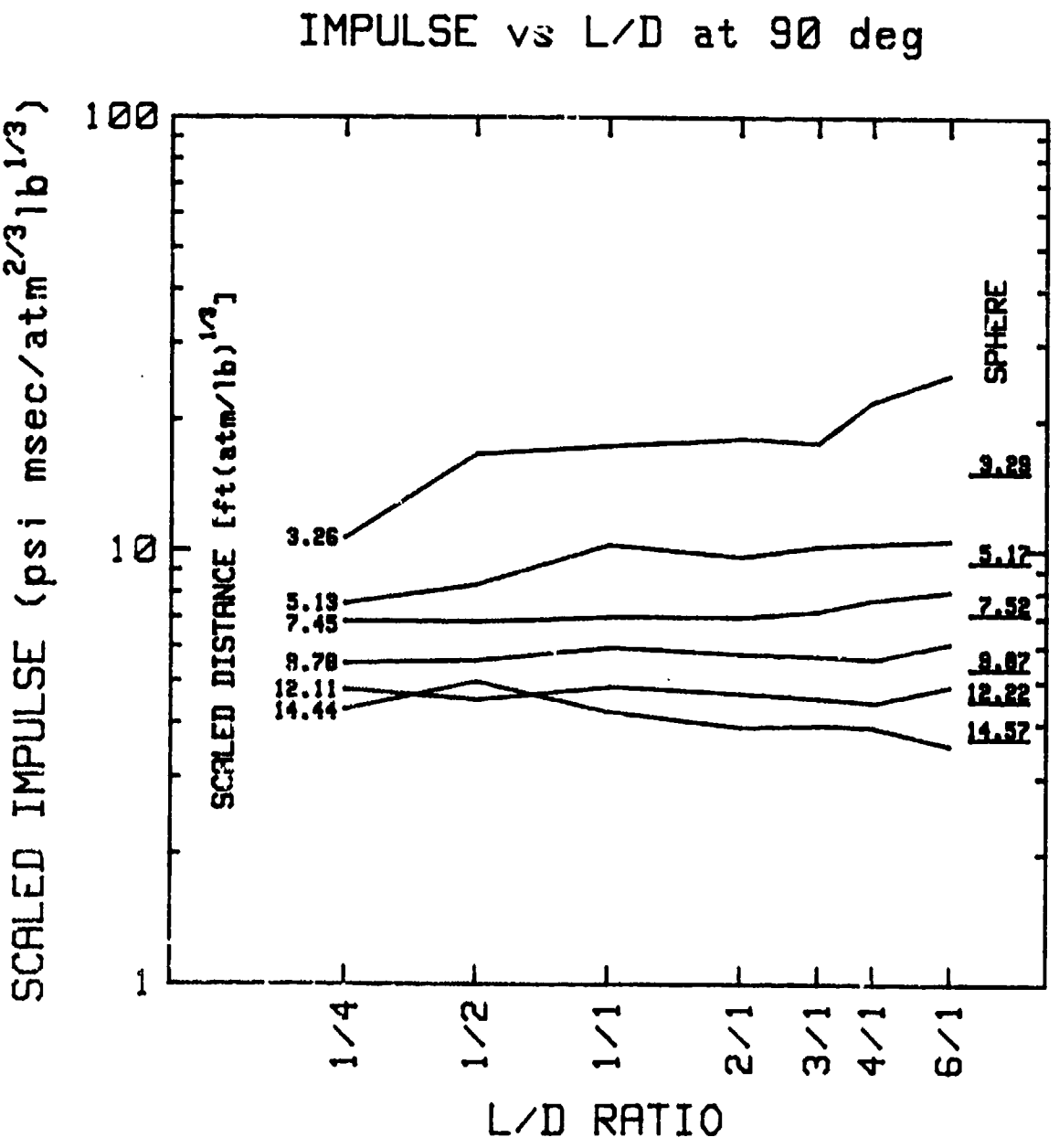

FIGURE 23. Positive Impulse vs. L/D at 90-Degree Angle, as in FIGURE 19.

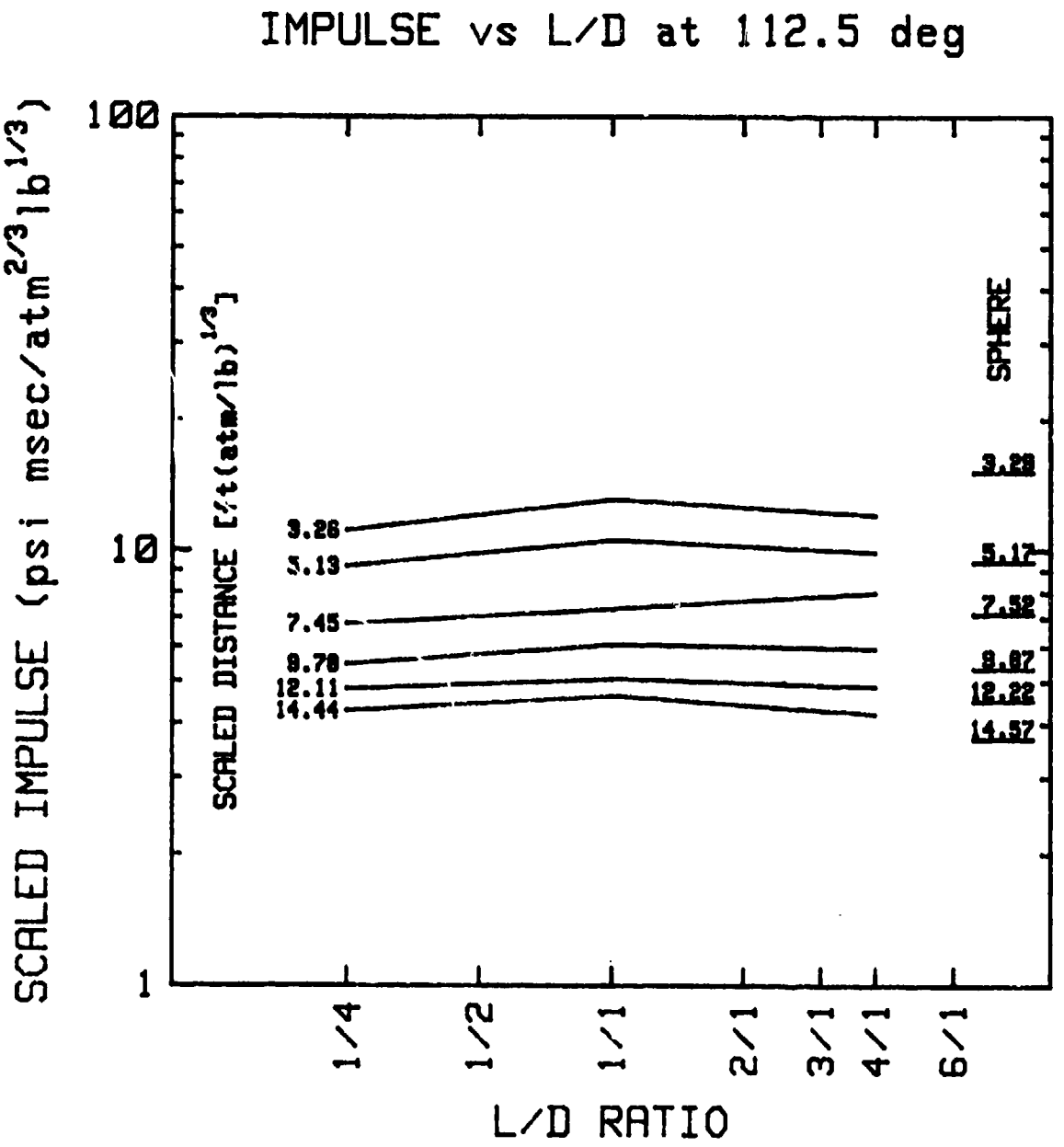

FIGURE 24. Positive Impulse vs. L/D at 112.5-Degree Angle, as in FIGURE 19.

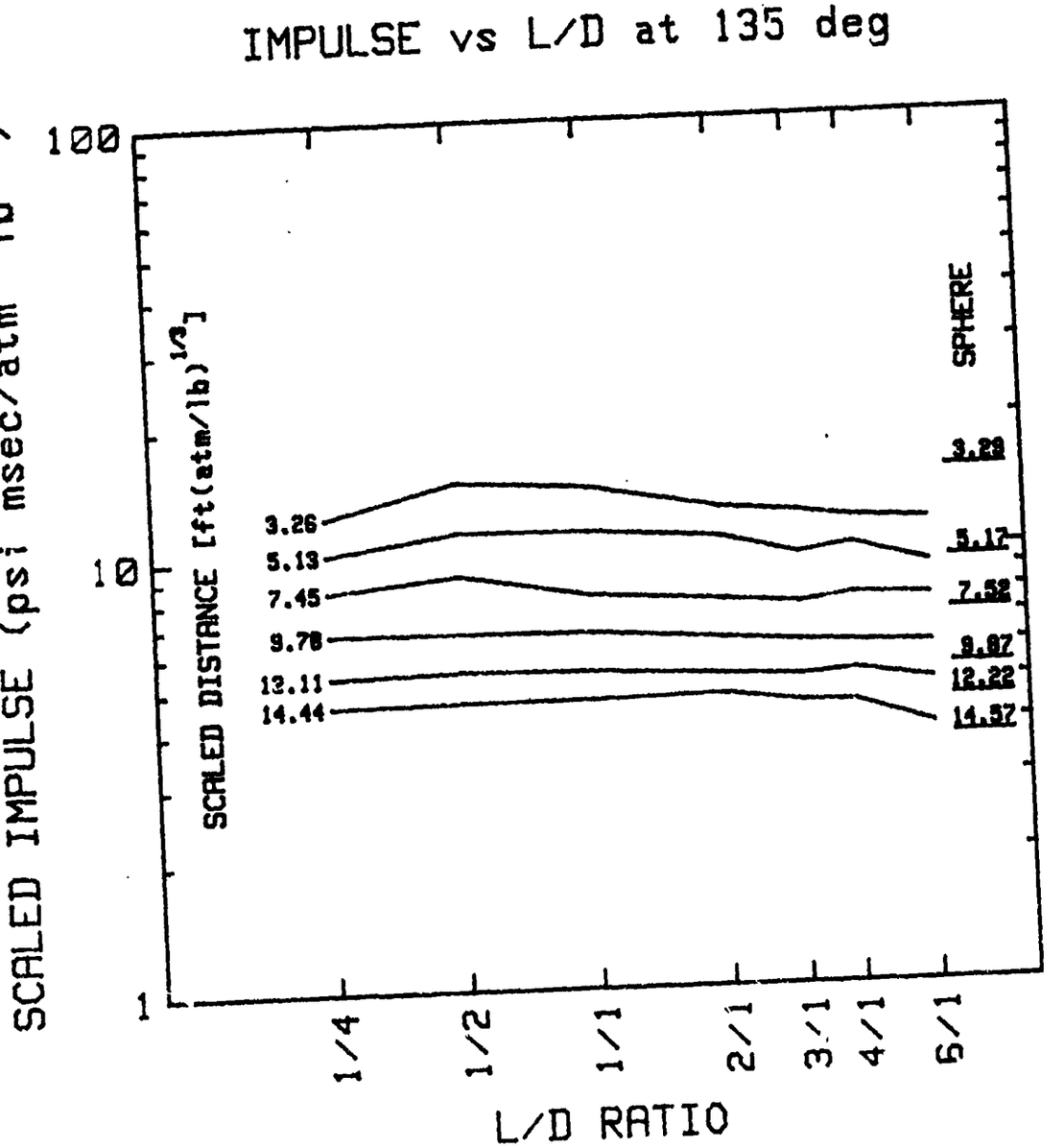

FIGURE 25. Positive Impulse vs. L/D at 135-Degree Angle, as in FIGURE 19.

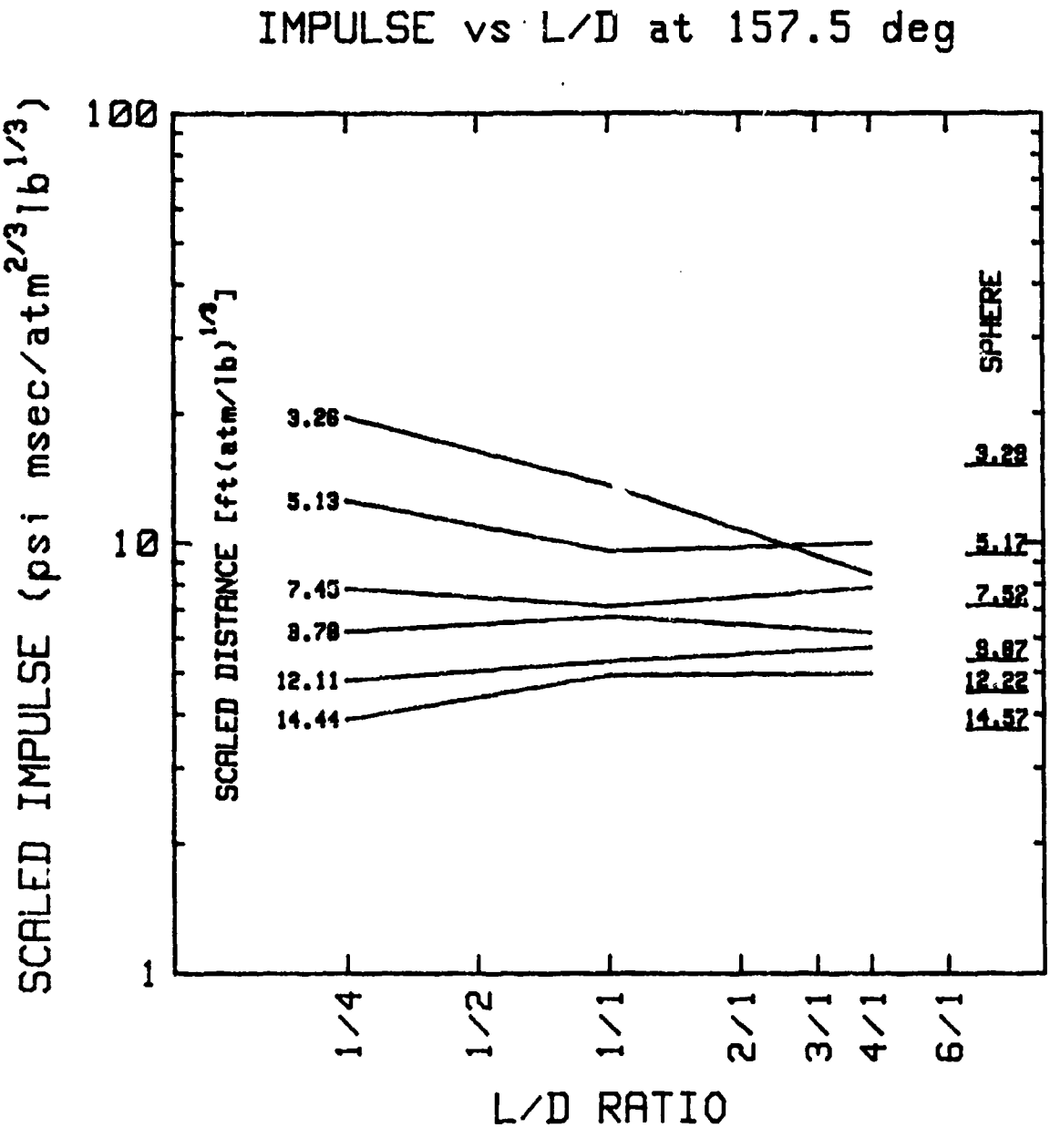

FIGURE 26. Positive Impulse vs. L/D at 157.5-Degree Angle, as in FIGURE 19.

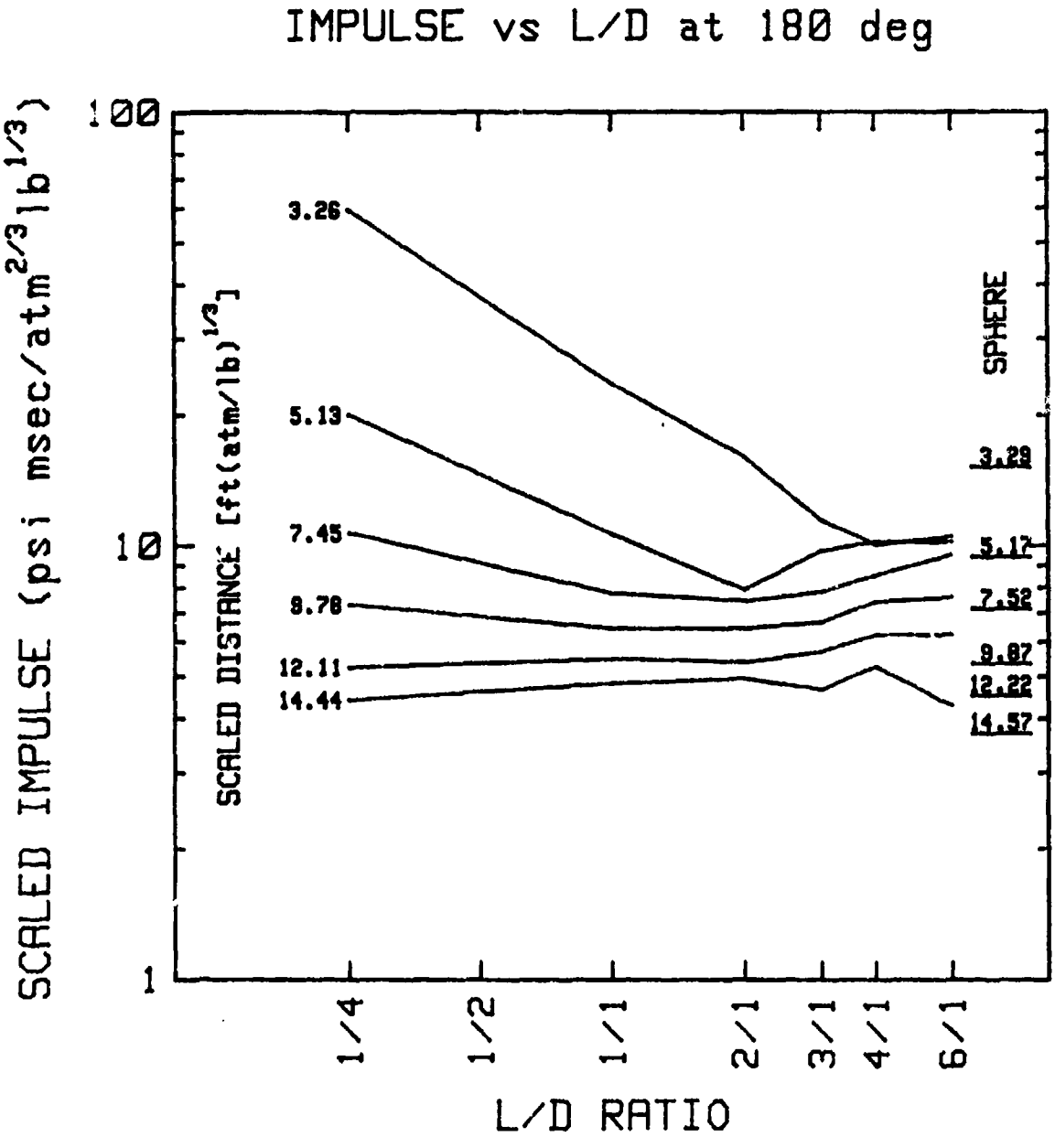

FIGURE 27. Positive Impulse vs. L/D at 180-Degree Angle, as in FIGURE 19.

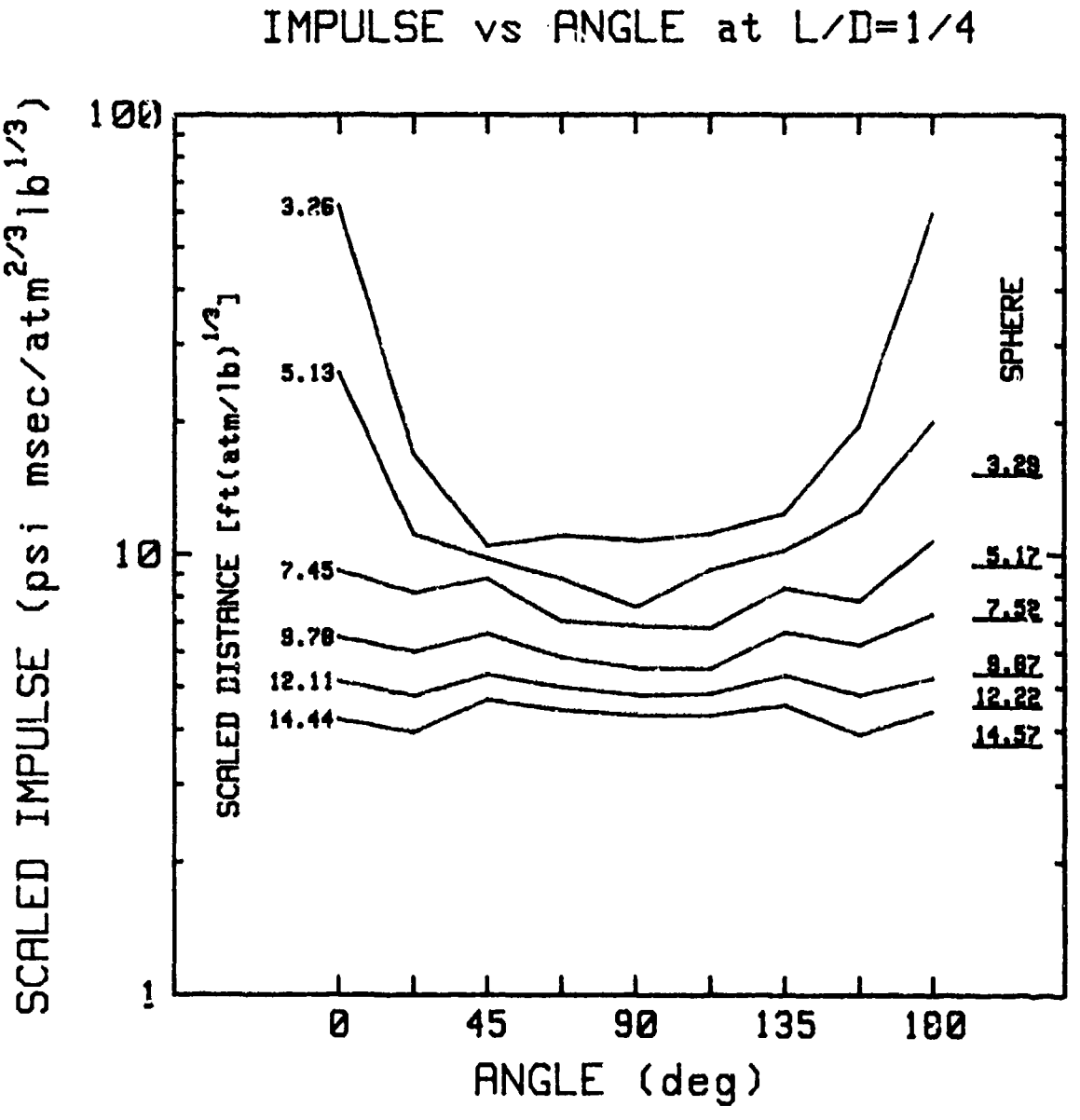

FIGURE 28. Positive Impulse vs. Angle at L/D = 1/4, Scaled to 1-Pound Charge at Sea Level; Spherical Charge Data at Right.

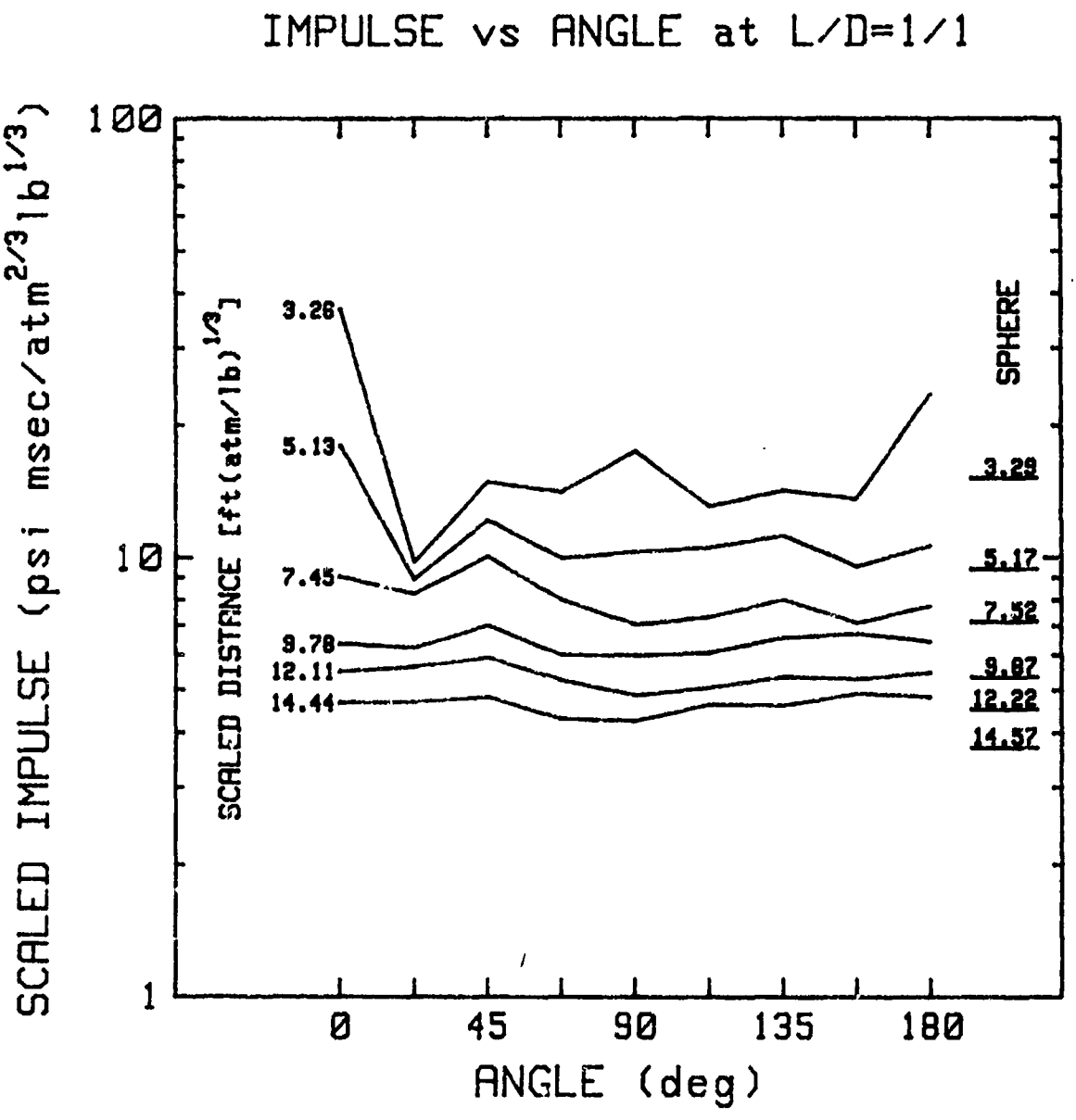

FIGURE 29. Positive Impulse vs. Angle at L/D = 1/1, as in FIGURE 28.

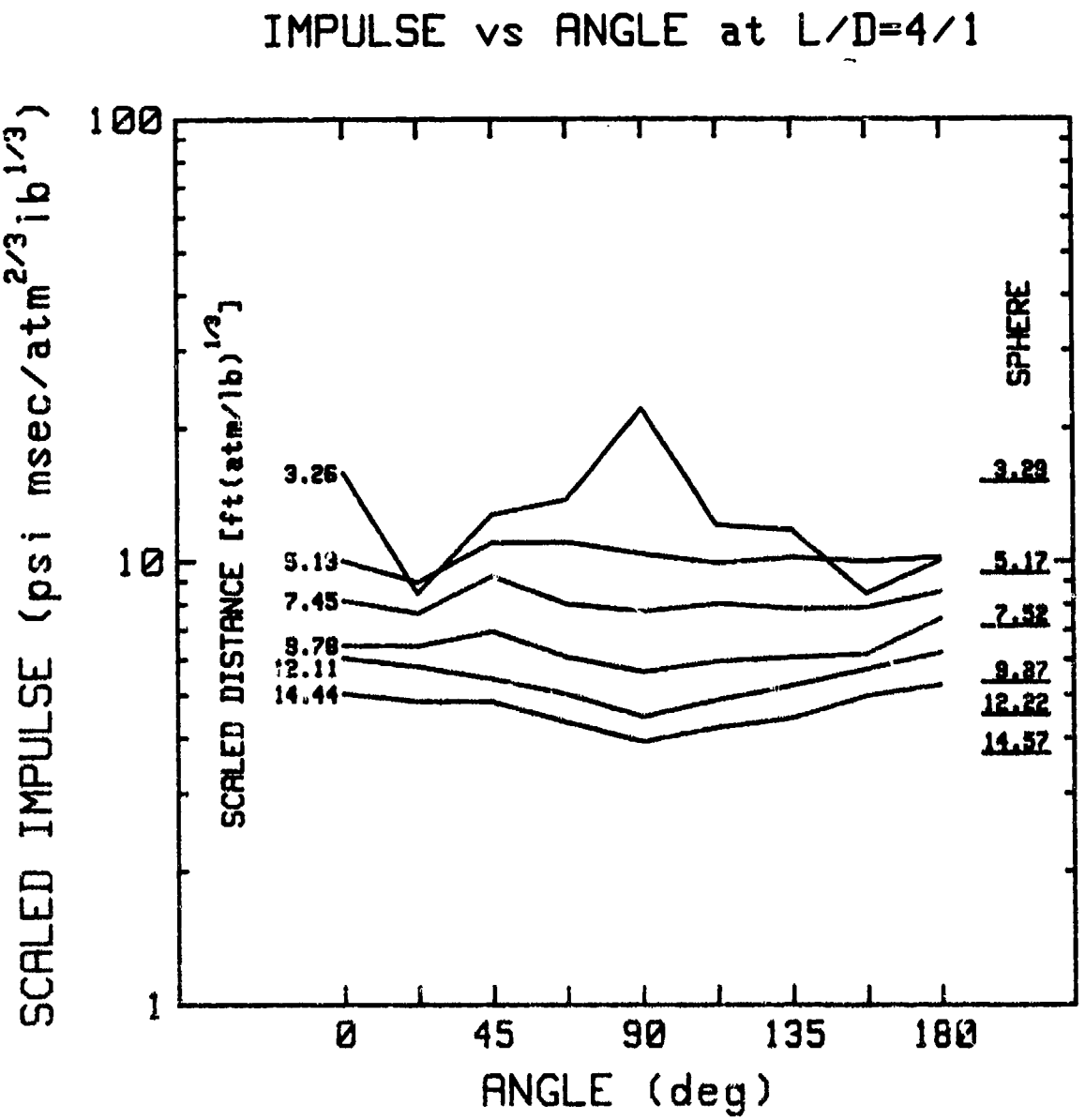

FIGURE 30. Positive Impulse vs. Angle at L/D = 4/1, as in FIGURE 28.

TABLE 5. Positive Duration (ms).

L/D=1/4 Charge Weight= 8 lb

Angle	Shot	Distance (ft) 7	11	16	21	26	31
0.0	21-1	1.46	2.90	2.50	2.96	3.86	4.38
	29-2	1.71	2.26	1.90	3.30	3.84	4.40
22.5	23-1	2.22	1.86	2.44	3.16	3.75	4.59
	26-2	1.27	1.53	2.36	3.10	3.91	4.40
45.0	20-1	1.68	-.--	3.53	4.31	4.67	4.77
	25-2	1.73	2.92	3.56	4.34	4.62	4.99
	27-1	1.75	2.68	3.53	4.43	4.50	4.75
67.5	22-1	1.76	2.31	3.85	4.71	5.29	5.43
	24-2	1.51	2.23	3.49	4.12	5.12	5.27
90.0	19-1	1.96	3.39	3.93	3.99	4.79	5.23
	21-2	1.82	-.--	3.73	4.47	4.73	5.02
	28-2	2.29	3.37	3.84	4.60	5.15	5.75
	29-1	1.99	3.33	4.08	4.37	4.62	5.37
112.5	23-2	1.71	2.27	3.38	3.97	5.11	5.55
	26-1	1.64	2.35	3.36	3.98	5.36	5.48
135.0	20-2	1.52	2.59	3.50	4.54	4.71	5.34
	25-1	1.84	2.91	3.62	4.45	4.91	5.35
	27-2	1.64	2.97	3.55	4.41	4.88	5.71
157.5	22-2	.87	2.08	2.48	3.42	4.04	4.43
	24-1	1.15	1.44	2.53	3.23	3.73	3.95
180.0	19-2	1.88	1.97	2.06	3.36	4.07	4.54
	28-1	1.71	1.66	2.48	3.48	4.17	4.44

For shots 2 and 3, gauges are at 7, 12, 17, 22, 27, and 32 ft

L/D=1/1 Charge Weight= 8 lb

Angle	Shot	Distance (ft) 7	11	16	21	26	31
0.0	2-1	.85	2.38	-.--	8.20	8.50	8.75
	3-1	-.--	2.61	6.73	8.39	9.54	9.23
	8-2	1.65	3.60	5.45	7.92	-.--	-.--
	35-2	1.75	2.46	5.00	7.90	8.00	8.18
	56-1	1.15	2.03	5.66	7.94	8.83	8.94
22.5	4-1	2.03	2.93	5.22	6.27	7.03	7.69
	12-2	2.14	2.88	4.28	5.90	6.38	7.66
	32-2	1.70	-.--	4.20	5.57	6.42	6.88
45.0	5-1	1.60	2.59	3.11	4.66	4.55	5.22
	11-2	1.26	2.77	3.61	4.10	4.47	5.24
	33-2	1.48	2.61	3.32	3.90	4.51	4.92
67.5	6-1	2.36	2.93	3.69	4.56	4.72	5.24
	10-2	2.40	2.68	3.78	4.49	4.84	5.19
	31-2	2.89	2.83	3.56	4.43	4.81	5.02
90.0	2-2	1.10	3.21	2.44	4.76	5.31	5.82
	3-2	2.14	3.18	4.54	5.28	5.69	5.88
	7-1	2.72	2.98	4.00	4.85	5.26	-.--
	8-1	2.16	2.94	4.16	4.84	5.24	5.43
	9-2	-.--	-.--	4.01	4.93	5.39	5.92
	34-2	1.94	2.90	3.99	4.76	5.40	5.94
	35-1	2.22	-.--	4.44	4.70	5.23	5.23
	56-2	1.89	2.94	4.19	4.92	5.47	5.87
112.5	4-2	2.58	2.57	3.02	4.76	4.89	5.41
	12-1	1.65	-.--	4.62	4.40	4.68	4.95
	32-1	1.95	2.23	3.56	4.37	4.52	4.75
135.0	5-2	1.52	2.60	3.30	3.99	4.95	5.20
	11-1	1.52	-.--	4.73	3.67	4.45	5.11
	33-1	1.50	2.53	3.24	3.70	4.33	4.82
157.5	6-2	-.--	4.49	5.64	6.29	6.40	7.04
	10-1	1.88	3.05	6.85	5.14	5.65	6.80
	31-1	2.03	2.14	3.62	6.37	6.71	7.41
180.0	7-2	2.58	2.64	6.76	7.17	7.42	7.74
	9-1	1.56	1.66	6.51	-.--	7.51	7.55
	34-1	1.68	1.73	6.53	7.05	7.56	-.--

TABLE 5. (Contd.)

L/D=4/1 Charge Weight= 8 lb

Angle	Shot	Distance (ft) 7	11	16	21	26	31
0.0	46-2	-.--	-.--	6.08	6.05	6.37	6.54
	50-1	-.--	6.05	5.47	5.18	5.50	5.61
22.5	44-2	2.18	2.96	4.81	4.93	5.51	6.01
	49-1	2.09	3.41	4.61	4.72	5.54	5.79
	58-2	2.42	3.27	5.12	5.67	5.77	5.95
45.0	42-2	2.39	2.88	3.48	4.36	4.57	4.98
	47-1	2.33	2.74	3.49	3.97	4.57	4.90
67.5	43-2	2.16	2.58	3.89	4.55	5.07	5.67
	48-1	2.45	2.64	3.95	4.55	5.01	5.57
90.0	45-2	1.89	1.94	3.54	4.36	4.70	5.24
	46-1	1.86	1.95	3.73	4.45	4.75	5.82
	50-2	1.66	2.15	3.59	4.18	4.72	7.83
	51-1	2.04	1.78	3.42	4.08	4.53	5.20
	59-1	2.21	2.15	3.57	4.56	5.00	5.58
112.5	44-1	2.43	2.53	3.76	4.34	4.86	5.82
	49-2	2.16	2.71	3.78	4.49	4.80	5.83
	58-1	2.24	2.72	3.94	4.57	4.97	5.78
135.0	42-1	2.04	2.57	3.82	4.47	4.54	5.10
	47-2	1.78	2.94	3.36	4.48	4.76	5.45
157.5	43-1	2.19	4.95	5.36	5.45	5.89	6.42
	48-2	2.16	4.83	5.38	5.74	6.02	7.06
180.0	45-1	2.61	4.91	4.94	5.42	5.42	5.74
	51-2	2.04	5.11	5.89	5.89	5.63	5.79
	59-2	-.--	5.05	5.96	6.05	5.72	7.26

L/D=1/2 Charge Weight= 8 lb

Angle	Shot	Distance (ft) 7	11	16	21	26	31
0.0	18-1	-.--	1.58	2.69	3.30	3.88	4.54
45.0	17-1	1.65	2.46	3.17	4.07	4.61	4.73
90.0	15-1	1.72	-.--	4.04	4.18	4.25	4.87
	18-2	2.11	-.--	4.04	4.64	4.96	5.42
	57-1	-.--	6.49	8.73	9.68	9.41	10.37
135.0	17-2	1.46	2.52	3.27	3.94	4.45	4.97
180.0	15-2	1.20	1.96	5.60	5.61	5.94	6.02
	57-2	3.82	3.94	5.39	8.02	8.05	9.90

TABLE 5. (Contd.)

L/D=2/1 Charge Weight= 8 lb

Angle	Shot	Distance (ft) 7	11	16	21	26	31
0.0	38-2	.73	2.77	6.74	6.61	6.78	7.51
	61-1	.42	1.77	6.60	7.77	8.10	6.87
45.0	36-2	1.91	2.43	3.04	3.76	4.41	4.80
90.0	37-2	1.81	2.34	3.26	5.01	5.59	6.22
	38-1	1.81	2.52	3.78	4.84	5.55	6.01
	61-2	2.86	1.77	3.73	5.12	5.63	6.11
135.0	36-1	1.56	2.63	3.31	4.01	4.62	5.36
180.0	37-1	2.49	-.--	6.01	5.91	6.16	5.83

L/D=3/1 Charge Weight= 8 lb

Angle	Shot	Distance (ft) 7	11	16	21	26	31
0.0	41-2	.69	1.59	5.26	7.63	6.07	5.86
45.0	39-2	2.28	2.63	3.32	3.82	4.54	5.00
90.0	40-2	1.98	2.47	3.42	3.93	4.54	5.41
	41-1	1.99	-.--	3.39	3.84	4.58	5.89
	60-2	-.--	2.27	3.06	4.56	4.87	8.07
135.0	39-1	1.73	2.56	3.31	4.44	4.67	4.73
180.0	40-1	2.63	-.--	5.46	5.61	5.44	5.13
	60-1	2.16	5.29	5.52	5.70	6.59	4.94

L/D=6/1 Charge Weight= 8 lb

Angle	Shot	Distance (ft) 7	11	16	21	26	31
0.0	55-2	-.--	4.87	4.77	5.09	5.02	5.57
45.0	53-2	2.61	2.69	3.32	4.61	4.89	5.34
90.0	54-2	1.76	2.21	3.14	4.66	5.01	4.89
	55-1	1.25	1.95	3.41	3.94	5.38	5.32
135.0	53-1	1.95	2.61	3.69	4.60	5.04	5.09
180.0	54-1	-.--	4.68	5.23	4.88	5.44	5.63

TABLE 5. (Contd.)

L/D=1/1 Charge Weight= 16 lb

Angle	Shot	Distance (ft) 7	11	16	21	26	31
0.0	63-2	-.--	-.--	3.42	7.76	11.89	11.65
90.0	62-2	-.--	2.68	3.84	5.51	6.20	6.78
	63-1	-.--	2.53	4.35	5.27	5.98	6.70
180.0	62-1	-.--	1.93	4.25	8.55	9.33	10.21

L/D=4/1 Charge Weight= 16 lb

Angle	Shot	Distance (ft) 7	11	16	21	26	31
0.0	65-2	-.--	-.--	6.54	-.--	8.14	7.46
90.0	64-2	-.--	3.51	2.97	4.58	4.80	5.75
	65-1	-.--	2.37	3.71	4.59	5.16	4.84
180.0	64-1	-.--	6.48	6.30	5.62	5.75	5.46

SPHERES Charge Weight= 7.8 lb

Shot	Distance (ft) 7	11	16	21	26	31
13-1	1.69	2.40	3.39	3.64	4.65	4.83
13-2	1.71	2.84	3.37	4.07	4.46	5.66
14-1	-.--	2.36	3.48	3.42	4.77	4.64
14-2	1.60	2.38	3.00	4.57	4.75	4.95
30-1	1.91	2.47	3.36	3.89	4.31	4.80
30-2	2.06	2.37	3.29	3.77	4.52	4.66
52-1	1.71	2.36	3.50	4.15	4.72	-.--
52-2	1.81	2.47	3.08	3.80	4.71	5.11
66-1	-.--	2.32	3.51	3.97	4.60	4.86
66-2	-.--	2.37	3.27	4.07	4.59	4.92

TABLE 6. Time of Arrival (ms).

Note: * denotes questionable value

L/D=1/4 Charge Weight= 8 lb

Angle	Shot	Distance (ft) 7	11	16	21	26	31
0.0	21-1	.71	1.56	3.47	6.49	10.08	13.97
	29-2	.67	1.49	3.62	6.67	10.22	14.09
22.5	23-1	.81	1.92	4.11	7.09	10.57	14.34
	26-2	1.05	2.13	4.33	7.38	10.87	14.63
45.0	20-1	1.39	2.98	5.73	9.02	12.63	16.51
	25-2	1.38	2.96	5.63	8.94	12.55	16.39
	27-1	1.42	3.03	5.79	9.16	12.82	16.71
67.5	22-1	1.56	3.65	6.75	10.25	14.02	17.92
	24-2	1.56	3.59	6.63	10.09	13.78	17.76
90.0	19-1	1.30	3.53	7.11	11.04	14.88	18.84
	21-2	1.38	3.63	7.21	11.15	15.02	19.02
	28-2	1.33	3.57	7.13	10.07*	15.00	19.02
	29-1	1.38	3.64	7.21	11.11	14.95	18.95
112.5	23-2	1.65	3.69	6.69	10.13	13.80	17.64
	26-1	1.85	3.93	6.99	10.44	14.16	18.07
135.0	20-2	1.53	2.92	5.70	9.06	12.71	16.58
	25-1	1.52	3.14	5.74	8.95	12.50	16.32
	27-2	1.51	3.09	5.82	9.15	12.86	16.77
157.5	22-2	.87	1.84	4.22	7.34	10.91	14.73
	24-1	.84	1.93	4.21	7.27	10.76	14.54
180.0	19-2	.79	1.47	3.53	6.56	10.15	14.12
	28-1	.77	1.68	3.41	5.91	9.61	13.82

TABLE 6. (Contd.)

For shots 2 and 3, gauges are at 7, 12, 17, 22, 27, and 32 ft

L/D=1/1 Charge Weight= 8 lb

Angle	Shot	Distance (ft) 7	11	16	21	26	31
0.0	2-1	.65	1.95	4.08	7.80	11.68	15.71
	3-1	.60	1.84	4.25	7.68	11.53	15.61
	8-2	.61	1.47*	3.92	7.46	11.29	15.39
	35-2	.68	1.72	4.12	7.48	11.26	15.28
	56-1	.66	1.68	4.09	7.53	11.40	15.50
22.5	4-1	.98	2.30	4.92	8.37	12.18	16.27
	12-2	.94	2.26	4.77	8.01	11.64	15.55
	32-2	.94	2.34	4.84	8.06	11.75	15.70
45.0	5-1	1.59	3.37	6.26	9.64	13.28	17.99*
	11-2	1.54	3.30	6.19	9.54	13.18	17.08
	33-2	1.51	3.29	6.03	9.27	12.80	16.55
67.5	6-1	1.27	3.10	6.20	9.79	13.61	17.65
	10-2	1.20	2.92	6.01	9.60	13.35	17.30
	31-2	1.24	2.94	5.97	9.59	13.38	17.31
90.0	2-2	1.11	3.24	6.30	9.91	13.97	17.84
	3-2	1.07	3.28	6.42	10.04	13.88	17.89
	7-1	1.07	2.73	5.81	9.41	13.25	17.30
	8-1	1.09	2.75	5.81	9.38	13.19	17.19
	9-2	1.07	2.76	5.84	9.94	13.32	17.39
	34-2	1.71	3.41	6.48	10.08	12.64	17.93
	35-1	1.02	2.75	5.79	9.35	13.15	17.13
	56-2	1.08	2.78	5.93	9.63	13.56	17.64
112.5	4-2	1.41	3.37	6.34	9.90	13.73	17.79
	12-1	1.39	3.22	6.21	9.66	13.37	17.27
	32-1	1.40	3.21	6.14	9.61	13.33	17.23
135.0	5-2	1.56	3.41	6.42	9.94	13.69	17.65
	11-1	1.54	3.35	6.31	9.78	13.49	17.39
	33-1	1.56	3.36	6.26	9.65	13.33	17.20
157.5	6-2	1.19	2.95	6.07	9.79	13.79	17.90
	10-1	1.15	2.59	5.64	9.23	13.10	17.14
	31-1	1.14	2.89	5.94	9.47	13.29	17.24
180.0	7-2	.95	2.36	5.03	8.61	12.48	16.58
	9-1	.98	2.38	4.78	8.50	12.38	16.46
	34-1	1.63	3.02	5.73	9.17	11.75	17.07

TABLE 6. (Contd.)

L/D=4/1 Charge Weight= 8 lb

Angle	Shot	Distance (ft) 7	11	16	21	26	31
0.0	46-2	.88	2.74	6.20	10.21	14.34	18.61
	50-1	.98	2.78	6.23	10.18	14.30	18.51
22.5	44-2	1.31	3.16	6.46	10.31	14.15	18.12
	49-1	1.19	3.11	6.51	10.24	14.02	17.97
	58-2	1.27	3.29	6.84	10.50	14.35	18.34
45.0	42-2	1.58	3.46	6.44	9.88	13.57	17.44
	47-1	1.58	3.47	6.37	9.75	13.40	17.27
67.5	43-2	1.13	2.66	5.45	8.91	12.67	16.66
	48-1	1.15	2.73	5.55	9.07	12.87	16.92
90.0	45-2	.93	2.31	5.20	8.69	12.46	16.44
	46-1	.97	2.45	5.22	8.66	12.40	16.35
	50-2	.99	2.36	5.04	8.48	12.18	16.10
	51-1	.95	2.32	5.15	8.63	12.40	16.34
	59-1	.98	2.43	5.32	8.87	12.76	16.82
112.5	44-1	1.35	2.93	5.74	9.19	12.94	16.88
	49-2	1.25	2.81	5.55	8.89	12.54	16.41
	58-1	1.31	2.96	5.90	9.41	13.25	17.34
135.0	42-1	1.77	3.65	6.60	10.02	13.74	17.64
	47-2	1.76	3.65	6.64	10.10	13.82	17.77
157.5	43-1	1.64	4.03	7.32	10.91	14.71	18.47
	48-2	1.59	4.11	7.23	10.73	14.40	18.31
180.0	45-1	1.42	3.63	7.30	11.29	15.37	19.17
	51-2	1.38	3.66	7.24	11.21	15.29	19.05
	59-2	1.39	3.75	7.50	11.60	15.74	19.63

L/D=1/2 Charge Weight= 8 lb

Angle	Shot	Distance (ft) 7	11	16	21	26	31
0.0	18-1	-.--	1.65	3.76	6.90	10.48	14.35
45.0	17-1	1.49	3.19	5.99	9.31	12.94	16.77
90.0	15-1	1.37	3.53	7.01	10.93	15.06	19.30
	18-2	1.18	3.12	6.44	10.24	14.25	18.33
	57-1	-.--	-.--	-.--	-.--	-.--	-.--
135.0	17-2	1.54	3.27	6.14	9.55	13.26	17.16
180.0	15-2	1.40	3.43	6.94	11.02	15.21	19.52
	57-2	-.--	-.--	-.--	-.--	-.--	-.--

TABLE 6. (Contd.)

L/D=2/1 Charge Weight= 8 lb

Angle	Shot	Distance (ft) 7	11	16	21	26	31
0.0	38-2	.79	2.17	5.08	8.75	12.68	16.80
	61-1	.70	1.82	4.60	8.31	12.36	16.63
45.0	36-2	1.57	3.32	6.07	9.37	12.95	16.73
90.0	37-2	1.00	2.51	5.39	8.88	12.64	16.59
	38-1	1.04	2.61	5.57	9.07	12.85	16.82
	61-2	1.07	2.33	5.46	9.27	13.21	17.29
135.0	36-1	1.65	3.51	6.46	9.86	13.52	17.36
180.0	37-1	1.19	2.98	6.18	9.65	13.32	18.08

L/D=3/1 Charge Weight= 8 lb

Angle	Shot	Distance (ft) 7	11	16	21	26	31
0.0	41-2	.56	1.43	4.07	7.75	11.76	15.94
45.0	39-2	1.56	3.42	6.25	9.56	13.14	16.95
90.0	40-2	.95	2.17	5.14	8.58	12.27	16.15
	41-1	.95	2.38	5.20	8.64	12.37	16.28
	60-2	.96	2.48	5.42	9.00	12.86	16.89
135.0	39-1	1.72	3.62	6.57	9.98	13.64	17.49
180.0	40-1	1.25	3.38	6.83	10.70	14.73	18.89
	60-1	1.36	3.45	7.11	11.14	15.36	19.60

L/D=6/1 Charge Weight= 8 lb

Angle	Shot	Distance (ft) 7	11	16	21	26	31
0.0	55-2	1.03	3.32	7.09	11.21	15.36	19.25
45.0	53-2	1.61	4.86	6.62	10.19	14.01	18.04
90.0	54-2	1.04	2.50	5.18	8.97	12.87	16.95
	55-1	1.02	2.46	5.27	8.75	12.57	16.61
135.0	53-1	1.89	3.86	6.95	10.54	14.41	18.47
180.0	54-1	1.13	4.20	8.14	12.37	16.15	20.14

TABLE 6. (Contd.)

L/D=1/1 Charge Weight= 16 lb

Angle	Shot	Distance (ft) 7	11	16	21	26	31
0.0	63-2	-.--	1.34	3.04	5.74	9.17	13.00
90.0	62-2	-.--	2.06	4.83	8.23	11.95	15.89
	63-1	-.--	2.14	4.76	8.11	11.83	15.78
180.0	62-1	-.--	1.68	3.85	7.04	10.85	14.86

L/D=4/1 Charge Weight= 16 lb

Angle	Shot	Distance (ft) 7	11	16	21	26	31
0.0	65-2	-.--	1.93	4.81	8.54	12.58	16.76
90.0	64-2	-.--	1.81	4.14	7.39	10.98	14.81
	65-1	-.--	1.91	4.26	7.43	11.00	14.85
180.0	64-1	-.--	2.85	6.15	10.06	14.19	18.48

SPHERES Charge Weight= 7.8 lb

Shot	Distance (ft) 7	11	16	21	26	31
13-1	1.45	3.29	6.36	9.95	13.72	17.70
13-2	1.46	3.21	6.39	9.97	13.76	17.79
14-1	1.49	3.37	6.48	10.11	13.97	17.98
14-2	1.50	3.40	6.60	10.30	14.21	18.31
30-1	1.46	3.32	6.42	9.97	13.75	17.72
30-2	1.50	3.33	6.36	9.89	13.65	17.61
52-1	1.49	3.41	6.59	10.27	14.22	18.36
52-2	1.51	3.38	6.57	10.24	14.16	18.23
66-1	-.--	3.39	6.51	10.14	14.02	18.06
66-2	-.--	3.34	6.46	10.04	13.88	17.87

757 pressure-time traces and calibration waveforms, and many operations were required to derive the blast parameters from each trace. Each derived number has been double-checked, and questionable values checked again, to minimize the incidence of human error in the results presented here.

One source of systematic error, or bias, in the results has been noted in the section entitled Peak Pressure. The process of smoothing the digitized pressure-time waveforms to filter out high-frequency noise may result in a systematic underestimate of peak pressures. The magnitude of this bias cannot be quantitatively defined, but it is probably small, of the order of a few percent at most. It can be shown that the smoothing process introduces no error in the integration of the traces to obtain the positive impulse.

The firing program was designed to minimize another possible source of systematic error. Whenever duplicate runs were made at a given L/D ratio and angle, the charge orientation was such that the pressure gauge lines were interchanged between runs, so that different pressure gauges were used in each "matched pair" of data points. This reduces the effect on the final results of any systematic error in the calibration of a pressure gauge.

There are three main sources of random errors in the results presented here: shot-to-shot variability in explosive performance, uncertainties in pressure gauge calibrations, and data acquisition system variations (changes in amplifier gains, time bases, etc.) Acquisition system variability has been found to be small, well under one percent in all cases. It is not possible to separate the contributions from gauge calibrations and explosive performance unambiguously, but the results obtained here are consistent with the hypothesis that explosive variability is the largest source of scatter in the data.

Variability of Blast Parameters

Relative standard deviations (standard deviations divided by the means) in peak pressure and impulse were computed at each angle and distance for the data at L/D ratios of 1/4, 1/1, and 4/1. The average of all these values was 8.4% for the peak pressures and 4.9% for the positive impulse. (The questionable data points, marked with asterisks, in Tables 3 and 4 were not included here.) Figures 31 and 32 show the relative deviations as a function of gauge distance and angle, respectively. From Figure 31, it is clear that the deviations are largest at the close-in gauges, and decrease with distance. Figure 32 shows a tendency toward higher deviations off the ends and sides of the charges. An analysis of variance study of the deviations shows that both the distance and angle dependencies are statistically significant.

A similar analysis has not been carried out for the time of arrival and positive duration data.

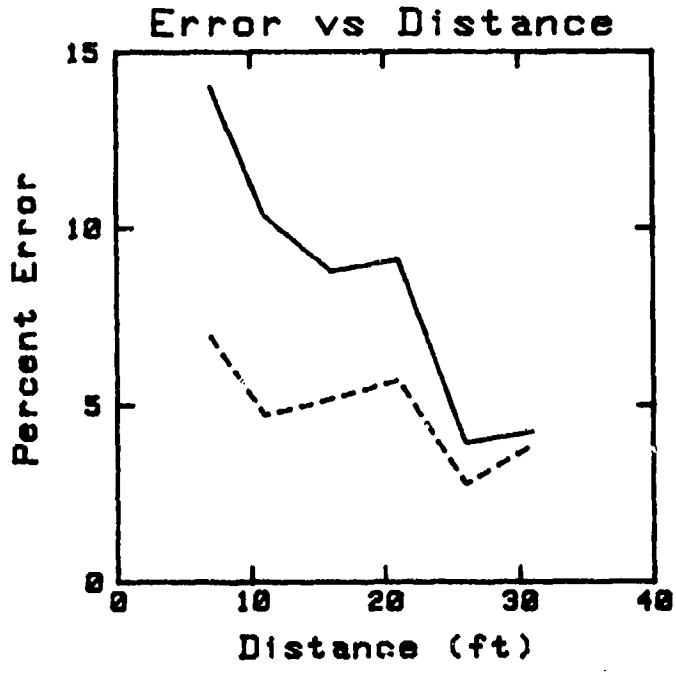

FIGURE 31. Relative Standard Deviation vs. Distance from Charge. Solid line--peak pressure; dashed line--impulse.

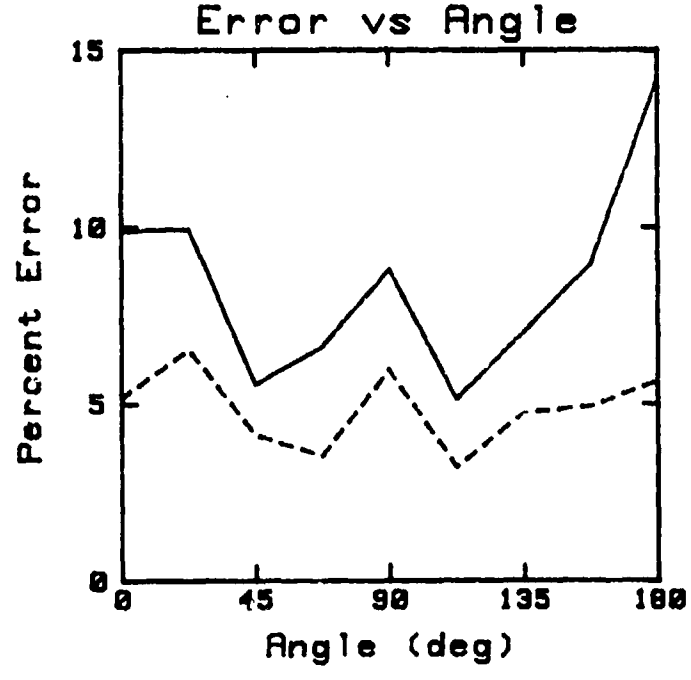

FIGURE 32. Relative Standard Deviation vs. Angle. Solid line--peak pressure; dashed line--impulse.

Gauge Calibration Errors

As described earlier, the average relative deviation in pressure gauge calibrations is 2.9% for all the gauges used in this program. Inspection of the data showed that 2 out of the 27 gauges used sporadically gave pressures and impulses that were clearly out of line with other gauges or shots. (The suspect data points marked with an asterisk in the tables include these points.)

In another program at DRI, pressures and impulses from three explosives (cast Pentolite spheres and pressed spheres of two HMX-based explosives, LX-10 and PBX-9501) were compared. The HMX-based explosives consistently gave peak pressures and impulses varying by 2% or less from shot to shot at distances comparable to those used in this investigation. It is thus reasonable to conclude that the observed variability of 2.9% in gauge calibrations is a conservative value to use in estimating the errors attributable to the pressure gauges in this study.

Explosive Variability

The pressure-time plots in Appendix A clearly show the shot-to-shot variability for Pentolite charges. In the other program just mentioned, the spheres of HMX-based explosives gave very smooth pressure-time traces; Pentolite spheres fired in the same series showed the same "bumps and wiggles" observed in this study. High-resolution laser photography of the blast waves from the Pentolite spheres showed many density fluctuations in the flow behind the shock fronts, while almost none were detected from the HMX spheres. This clearly indicates that the variations in the pressure-time waveforms presented here are real, and not artifacts of the measurement system.

Both peak pressure and impulse measurements are affected to the same extent by gauge calibration errors. The fact that the scatter in peak pressures is greater than for impulse can also be attributed to the explosive. Peak pressure determination is sensitive to local variations in the shape of the pressure-time traces, which are smoothed out in the integration used to obtain the impulse. The plots in Appendix A clearly show that the variation in waveform shape is greatest at the close-in gauges. It is also significant that the scatter in the impulse at the more distant gauges is comparable to the observed 2.9% variation in gauge calibrations, suggesting that 2.9% may be too high a value to use for gauge calibration variations over the duration of the firing program.

Assuming that the total deviation in peak pressure and impulse is the root-mean-square sum of the deviations due to explosive variability, gauge calibration uncertainties, and acquisition system variations, and assigning relative deviations of 2.9% and 1% for the latter two sources of error, respectively, the deviations attributable to explosive variability are found to be 7.8% for the peak pressures and 3.8% for the positive impulse.

The plots in Appendix A show that the greatest variability in pressure-time waveforms is observed off the ends and sides of the charges, at angles of 0°, 90°, and 180°. The "raggedness" of the traces at 180°, the end at which the charges are initiated, is especially marked. In the previous DRI study[1], it was also noted that the pressure waves off the ends of the charges, especially the long charges, were quite variable. By contrast, the waveforms and the pressure and impulse at the intermediate angles are usually quite consistent from shot to shot.

In general, the pressure-time traces from repeated runs at the same L/D and angle show a strong family resemblance. One group of shots for which this is not true is the group at L/D = 1/2. There are substantial differences between "duplicate" shots in this group, which are reflected in the tables of blast parameters. Moreover, the parameter values often diverge strongly from a smooth curve drawn through the data at other L/D ratios. It is interesting again to note that in reference 1, data at L/D = 1/2 did not seem to fit into the patterns established at other L/D ratios. The data obtained here at L/D = 1/2 should probably be omitted in any attempt to develop blast parameter models.

BLAST SCALING

Figures 33 through 38 show peak pressures from both 8- and 16-pound charges, all scaled to a charge weight of one pound at sea level. These plots show peak pressures from secondary shocks as well as the leading shocks, whenever the secondary shock pressures are higher; this accounts for the two branches in the data at 0° and 180° for L/D = 4/1. The corresponding scaled impulse plots are shown in Figures 39 through 44. In general, the data scale satisfactorily. There is somewhat more scatter in the impulse plots, especially at angles of 0° and 180° where there was only one data point at each distance for the 16-pound charges.

VARIATION OF BLAST PARAMETERS WITH L/D AND ANGLE

Figures 7 through 30 show the variation of peak pressure and impulse with L/D and angle. In all cases, the peak pressure and impulse close to the charge are largest in the direction of largest presented area. Pressures and impulses are highest off the end faces of the disk-shaped charges (L/D<1) and off the sides of the long charges (L/D>1). The direction of propagation of the detonation wave in the charge also has an effect: pressure and impulse are higher at 0° than at 180°. These close-in effects are highly directional, the pressure and impulse often fall off very rapidly with angle from the peaks. At the intermediate angles, 45° and 135°, there is very little variation with L/D, although both pressures and impulses show a weak maximum near L/D = 1/1.

As distance increases, the peaks and valleys in the plots of both pressure and impulse vs. angle flatten out, and often even become inverted.

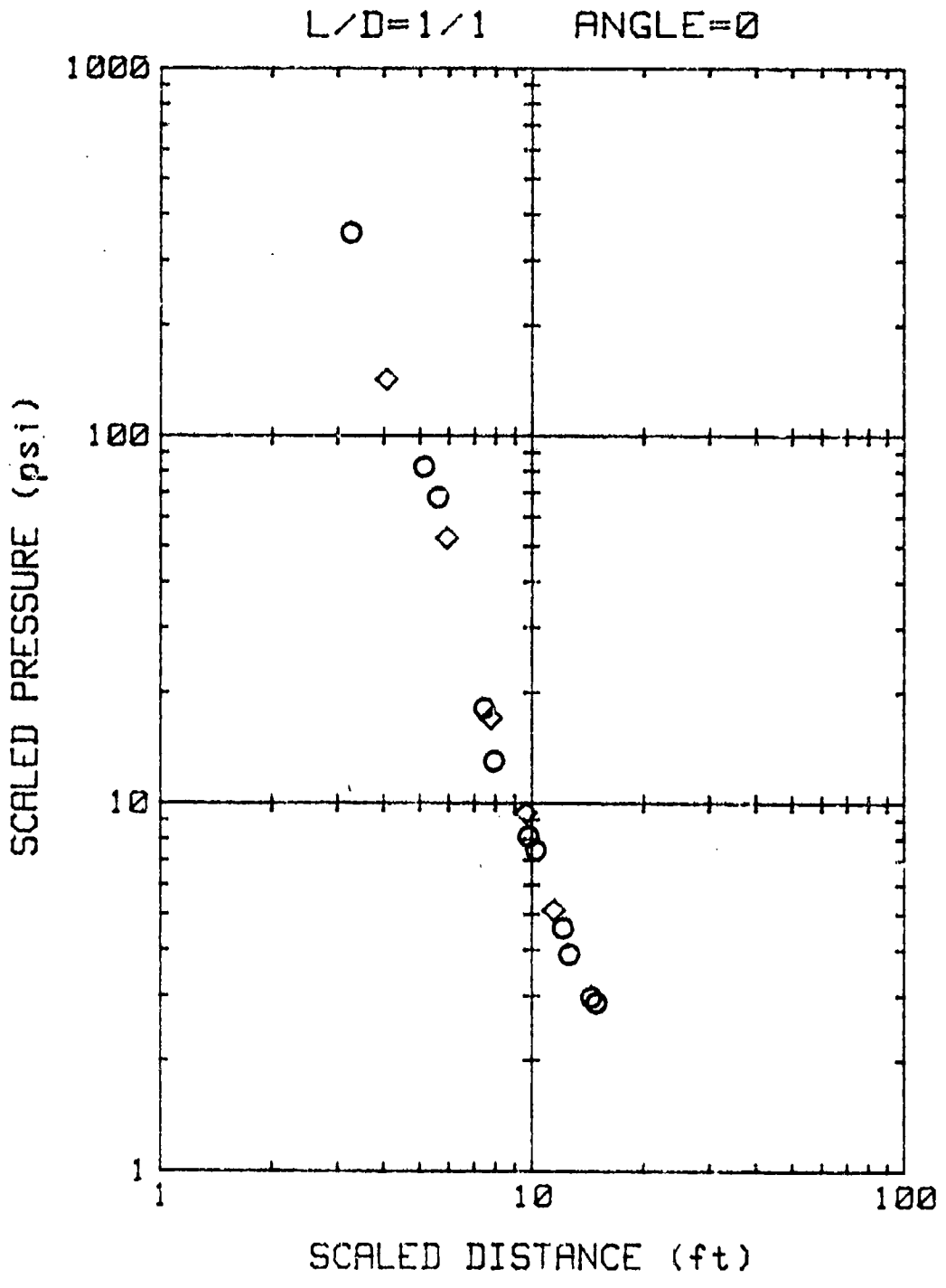

FIGURE 33. Peak Pressure vs. Distance for 8-Pound Charges (Circles) and 16-Pound Charges (Diamonds), Scaled to 1-Pound Charge at Sea Level, for L/D = 1/1 at 0-Degree Angle.

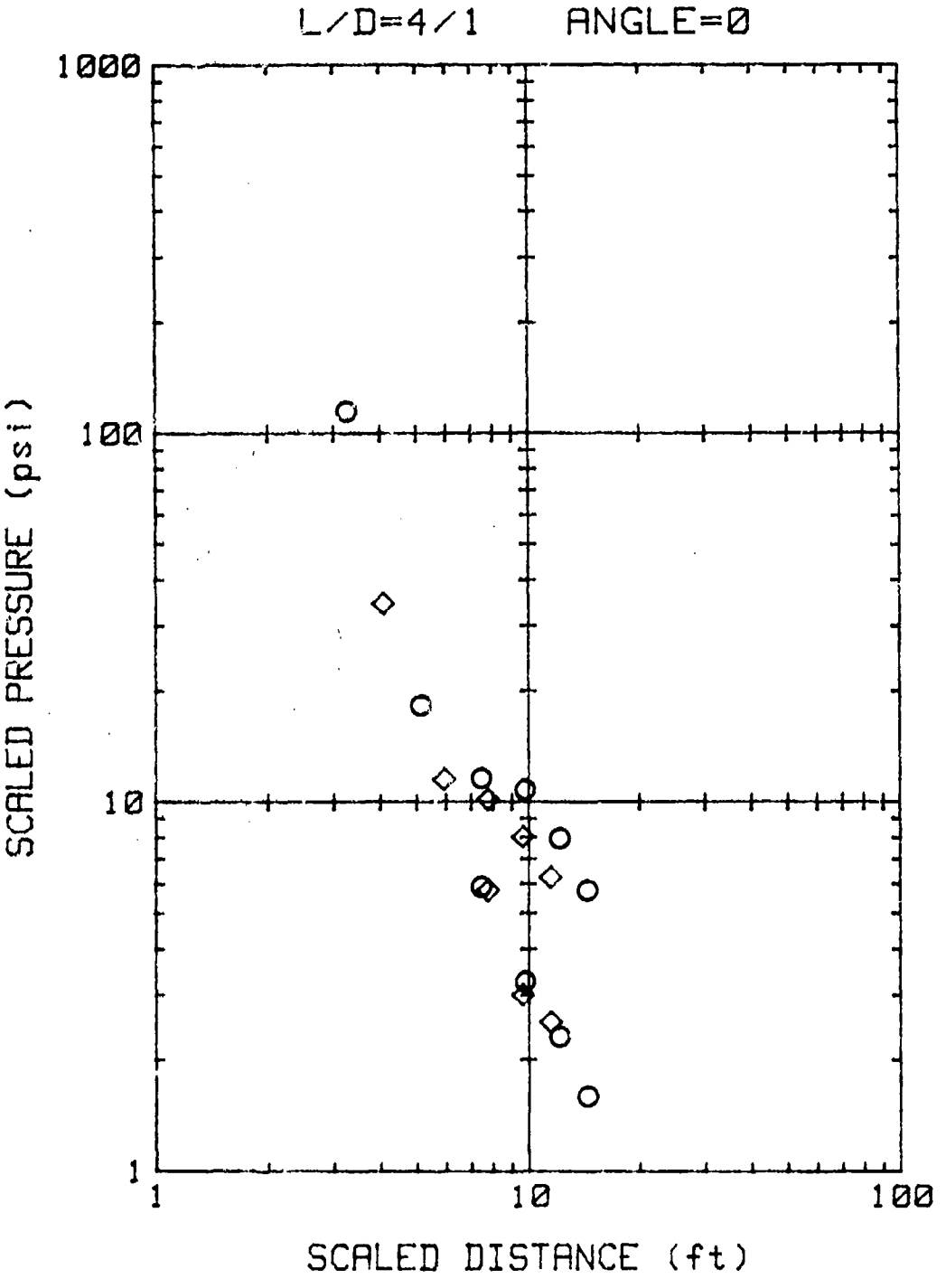

FIGURE 34. Scaled Pressure vs. Distance as in FIGURE 33, for L/D = 4/1 at 0-Degree Angle.

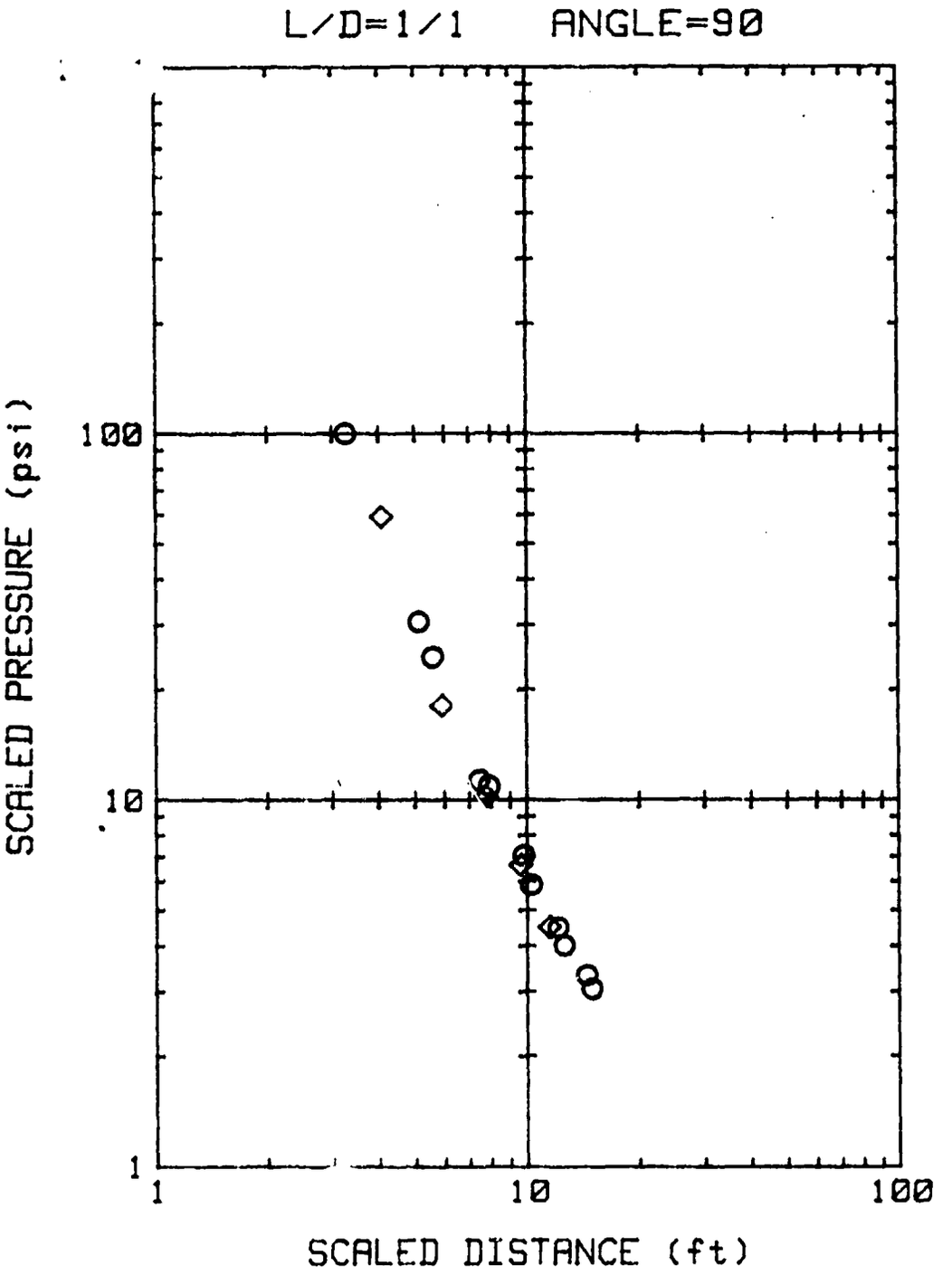

FIGURE 35. Scaled Pressure vs. Distance, as in FIGURE 33, for L/D = 1/1 at 90-Degree Angle.

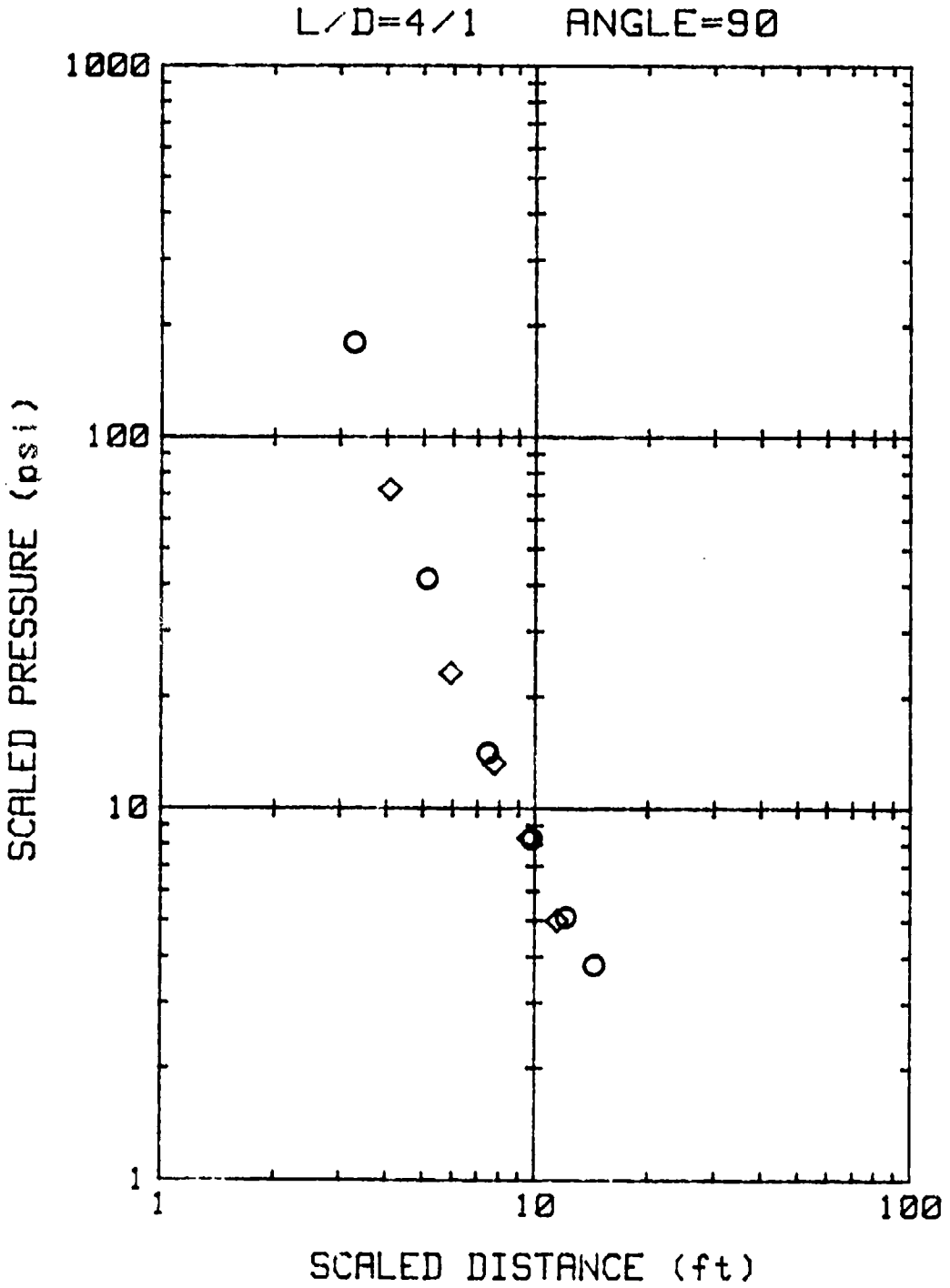

FIGURE 36. Scaled Pressure vs. Distance, as in FIGURE 33, for L/D = 4/1 at 90-Degree Angle.

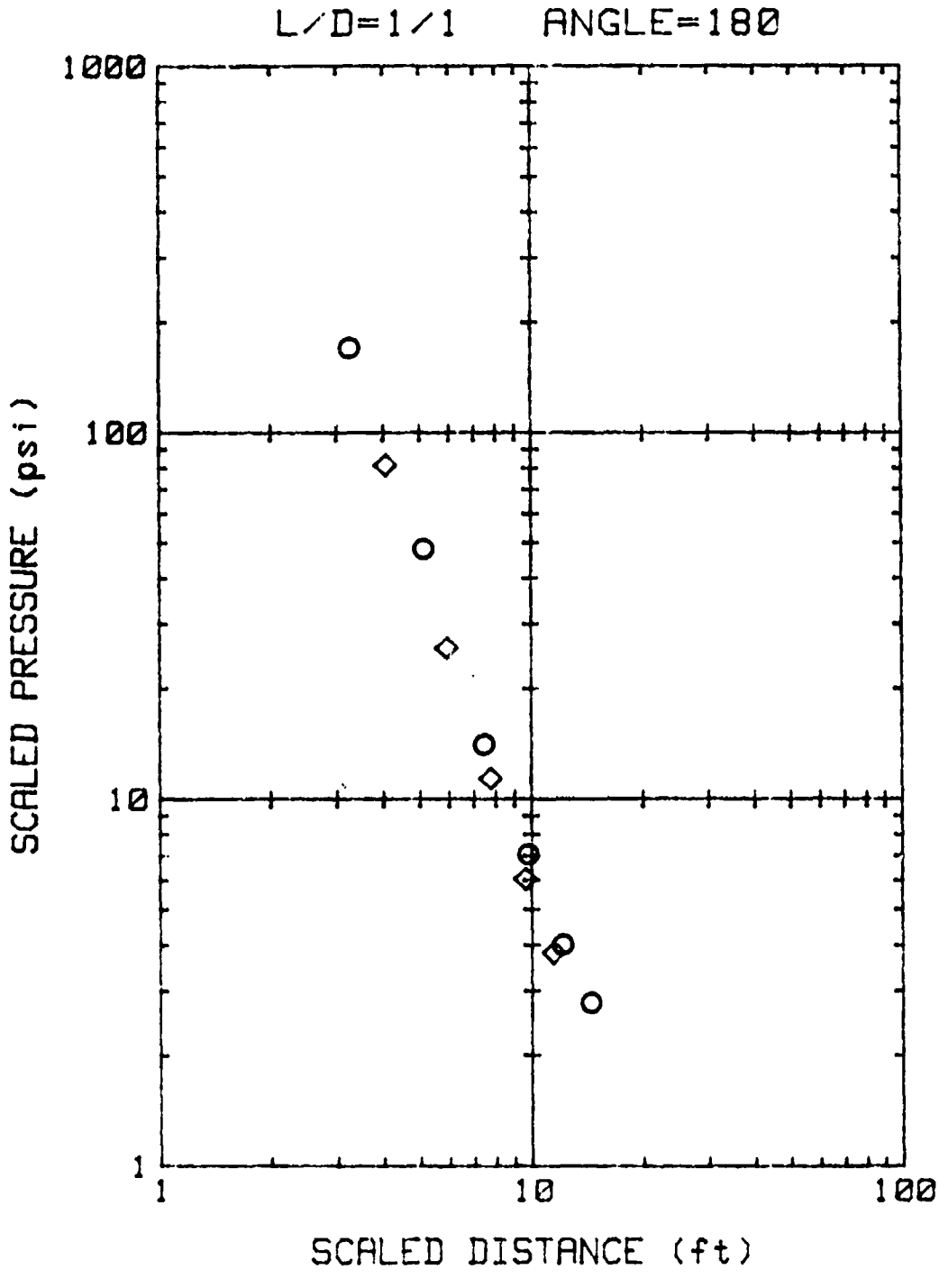

FIGURE 37. Scaled Pressure vs. Distance, as in FIGURE 33, for L/D = 1/1 at 180-Degree Angle.

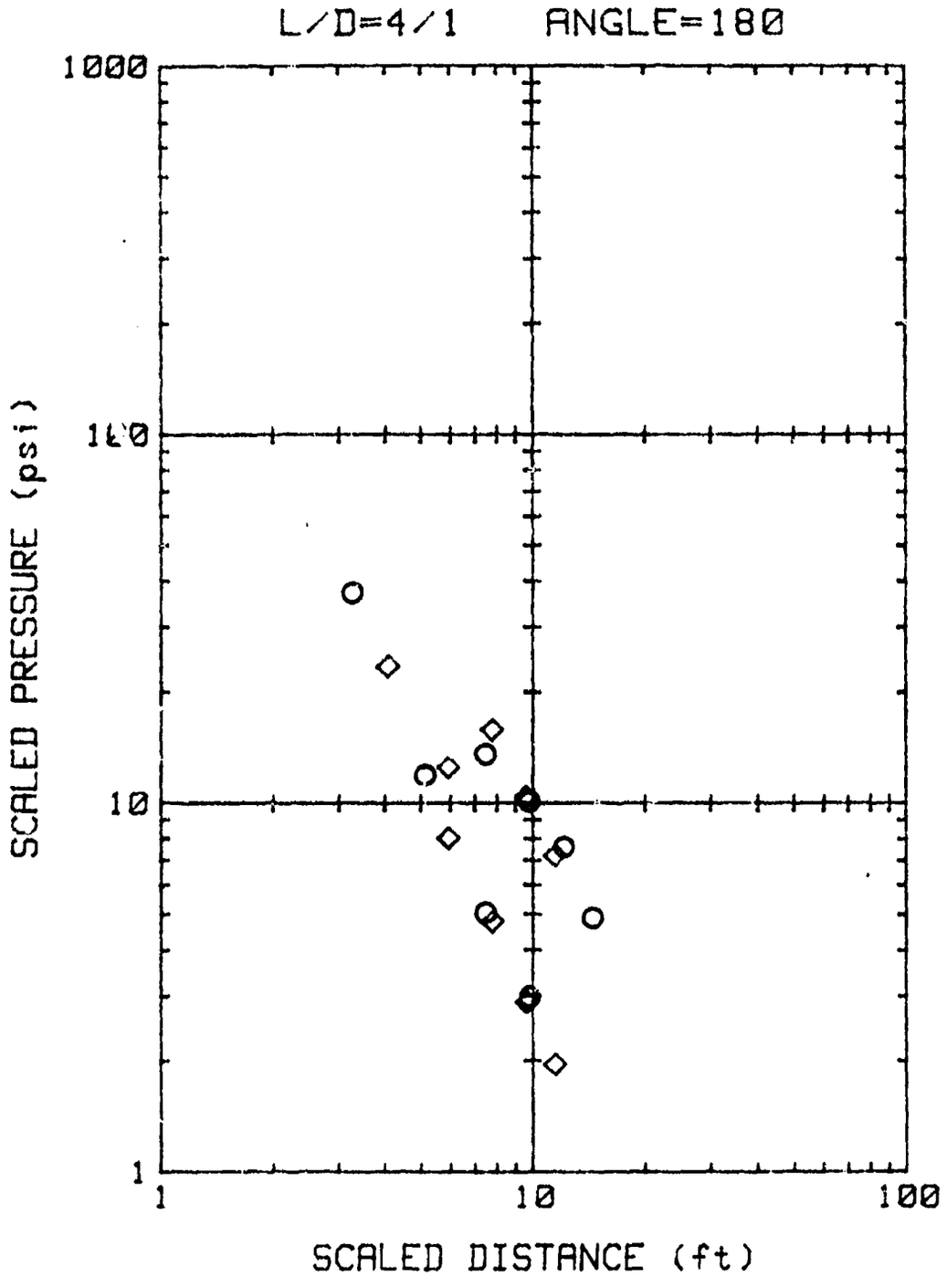

FIGURE 38. Scaled Pressure vs. Distance, as in FIGURE 33, for L/D = 4/1 at 180-Degree Angle.

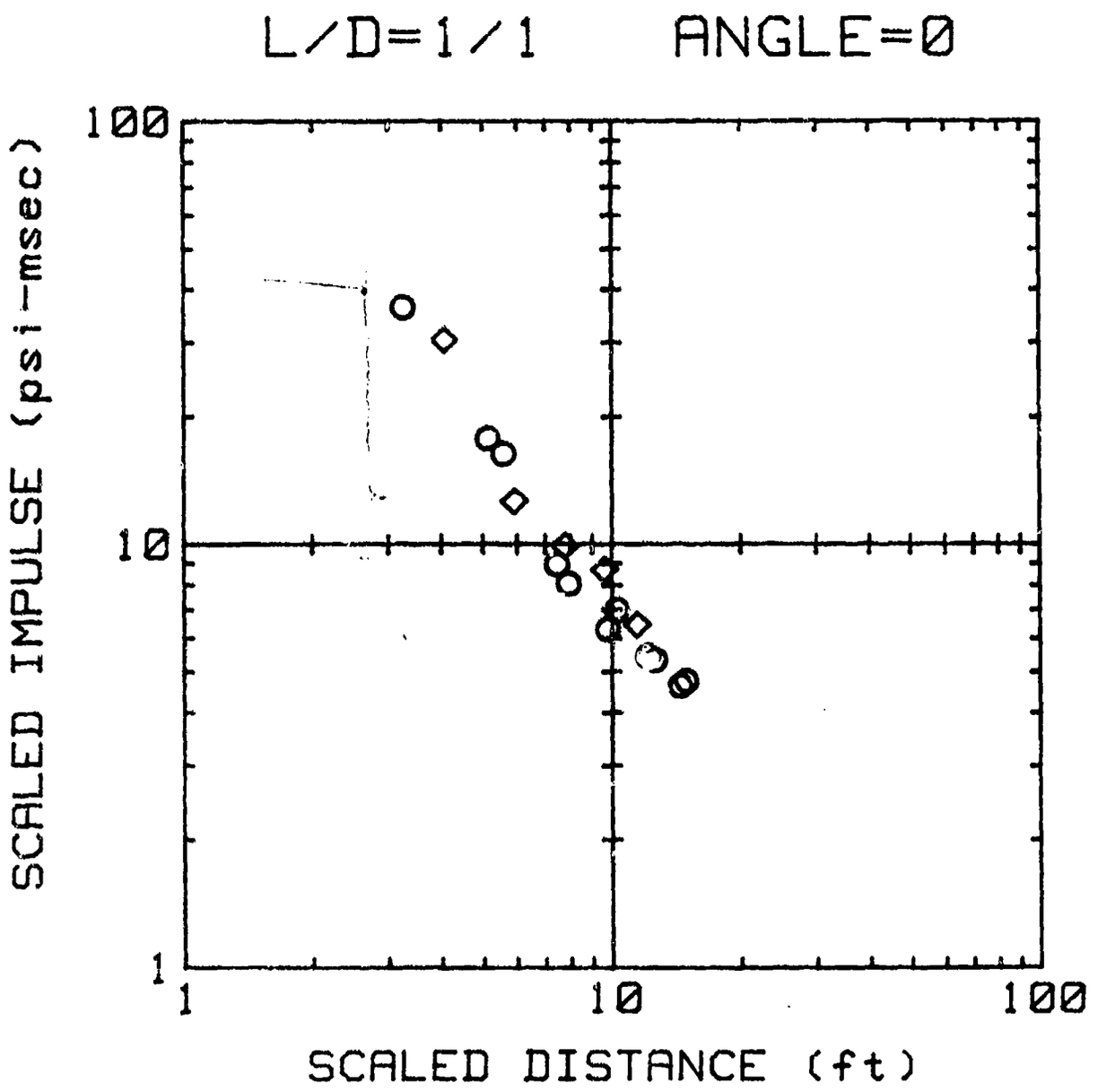

FIGURE 39. Positive Impulse vs. Distance for 8-Pound Charges (Circles) and 16-Pound Charges (Diamonds), Scaled to 1-Pound Charge at Sea Level, for L/D = 1/1 at 0-Degree Angle.

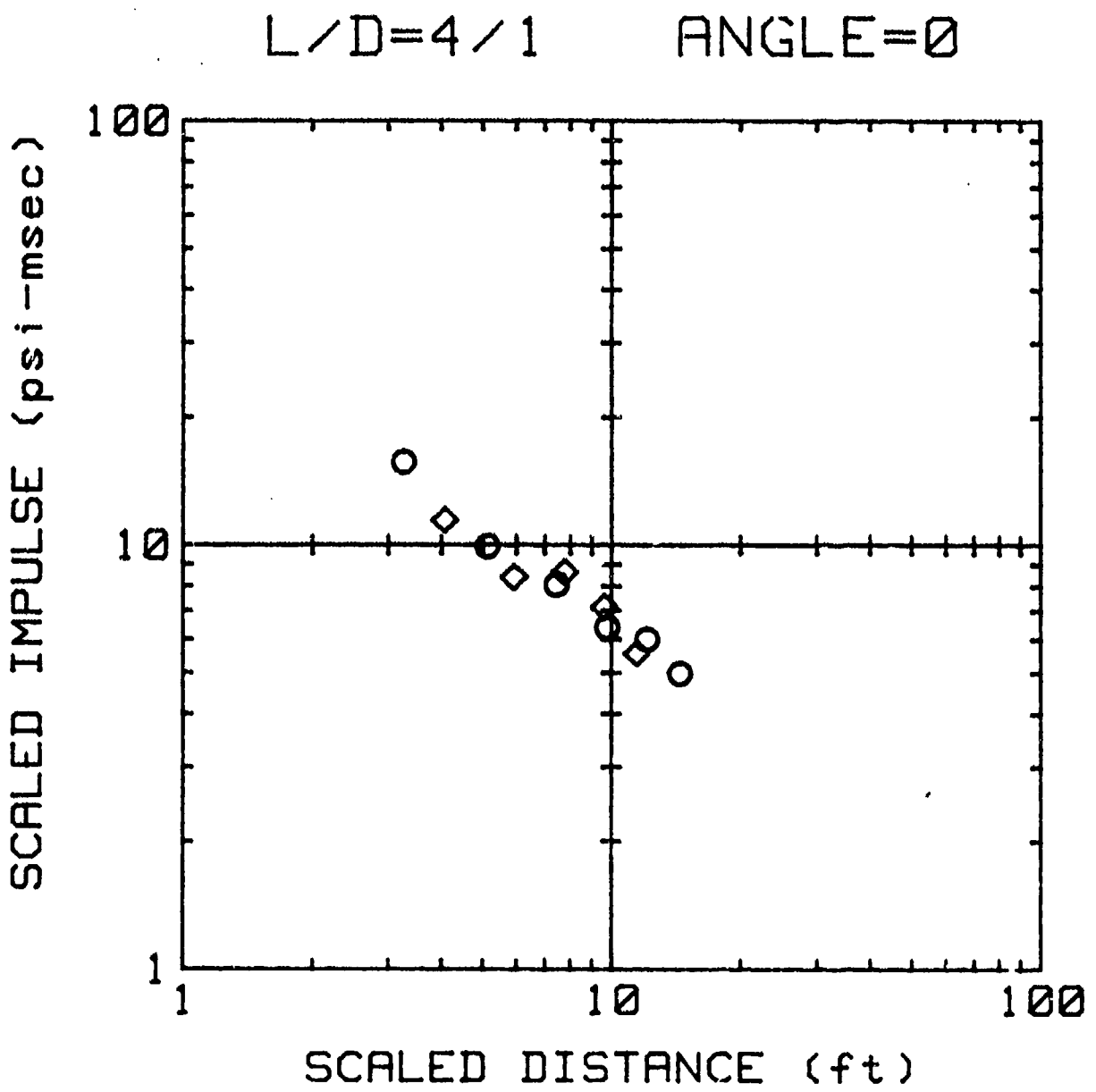

FIGURE 40. Scaled Impulse vs. Distance, as in FIGURE 39, for L/D = 4/1 at 0-Degree Angle.

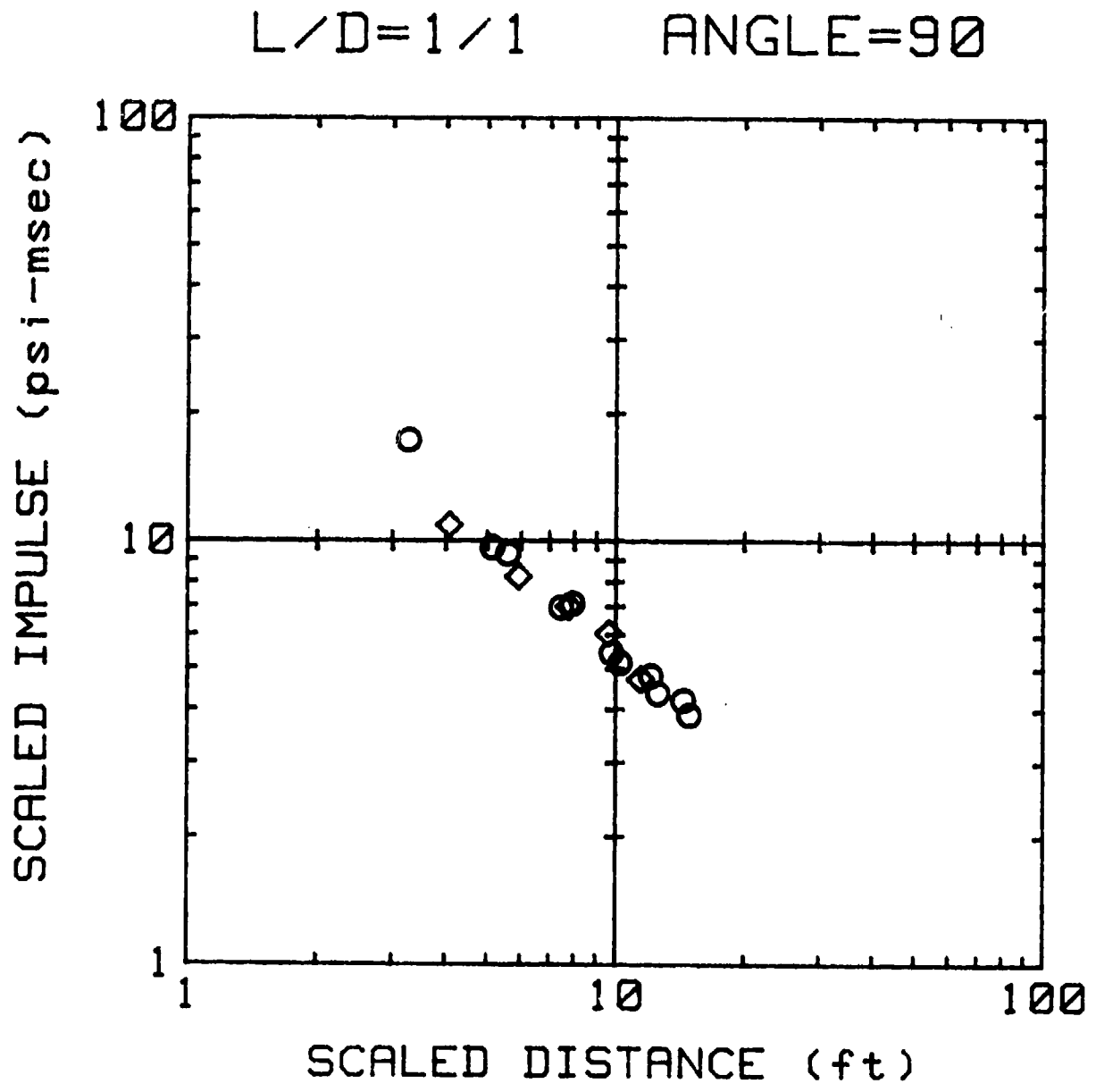

FIGURE 41. Scaled Impulse vs. Distance, as in FIGURE 39, for L/D = 1/1 at 90-Degree Angle.

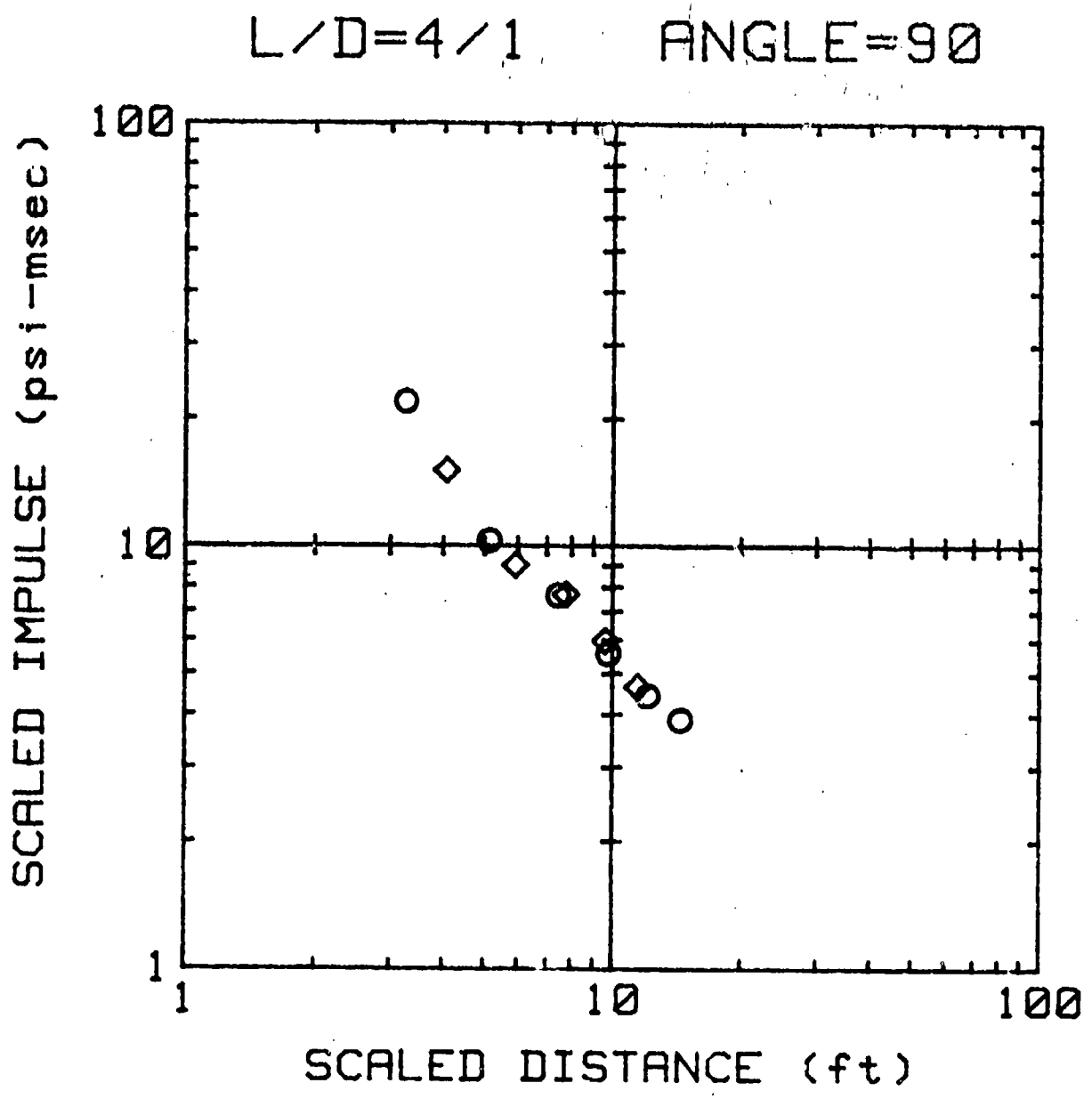

FIGURE 42. Scaled Impulse vs. Distance, as in FIGURE 39, for L/D = 4/1 at 90-Degree Angle.

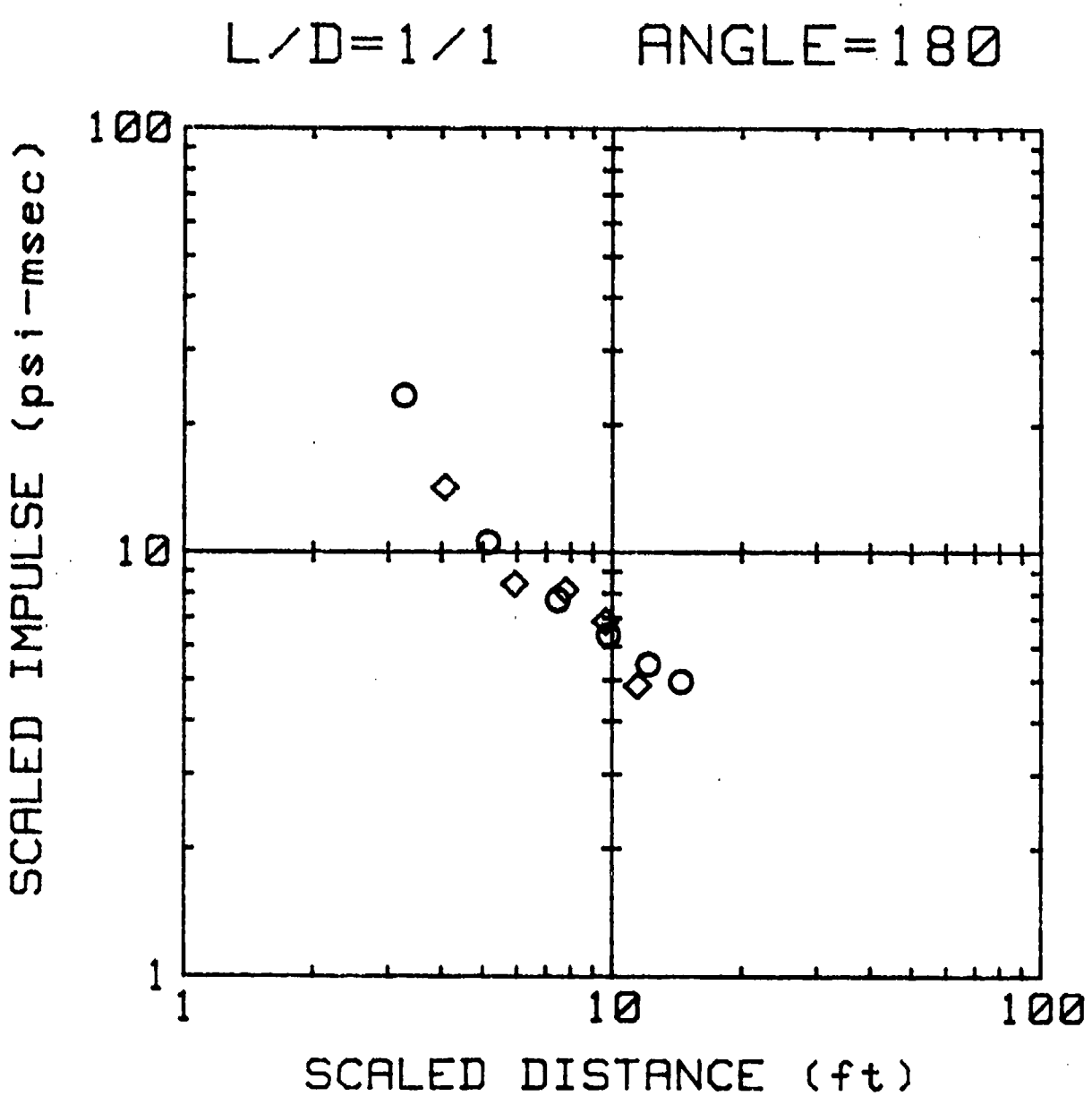

FIGURE 43. Scaled Impulse vs. Distance, as in FIGURE 39, for L/D = 1/1 at 180-Degree Angle.

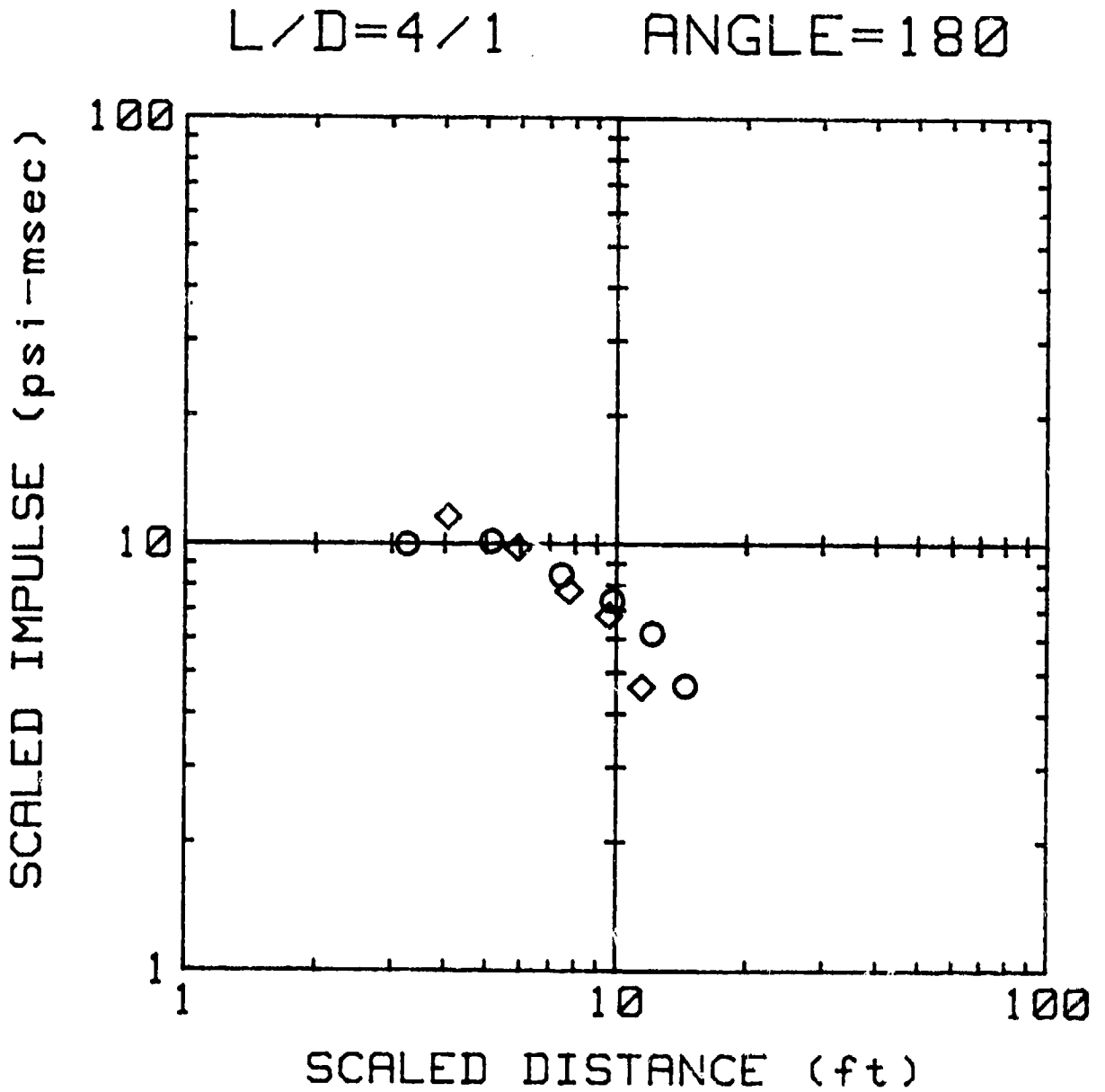

FIGURE 44. Scaled Impulse vs. Distance, as in FIGURE 39, for L/D = 4/1 at 180-Degree Angle.

As a general rule, the pressures and impulses at the closer gauges exceed the values for spherical charges only in the vicinity of the peak values. At the more distant gauges, on the other hand, they exceed the spherical charge values almost everywhere.

The blast waves from cylindrical charges are obviously far from spherical. This is evident from the time of arrival data as well as from the pressure and impulse plots. The tables of time of arrival show that the blast wave envelope is initially elongated in the directions of highest initial pressures, and remains so for the duration of the experiment.

RECOMMENDATIONS FOR FURTHER WORK

FURTHER DATA ANALYSIS

Further analysis of the data reported here is in order. First, the time of arrival data should be used to get an independent estimate of the peak pressure from the leading shock waves. This would be valuable as an internal check on the pressure gauge data. Second, an error analysis on the time of arrival data itself would be useful as another tool for studying explosive variability and for identifying questionable data sets. Third, it would be useful to "invert" the time of arrival data, to give shock positions at fixed times. This would allow tracing the envelope of the blast waves as it expands, along with the positions of the secondary shocks, and would give, in effect, a frame-by-frame picture of the blast wave on a polar plot.

It would also be useful to do an error analysis of the positive duration data, since this is the first study to measure this parameter for cylindrical charges, to our knowledge.

MODELING

Both peak pressure and positive impulse models should be developed from the data reported here. The blast front pressure model[2] developed from the results of the previous DRI study[1] could not include the pressures from secondary shocks with pressures higher than the leading shocks, because those pressures were not determined in the previous study. In effect, the pressures used in the existing blast front pressure model were equivalent to the pressures shown by the dashed lines in Figures 7 through 18. It is clear from these figures that the actual peak pressures, including those from strong secondary shocks, are often substantially higher than the leading shock pressures.

Finally, the positive impulse model should be developed, since this was the primary motivation for the present study.

FURTHER EXPERIMENTAL STUDIES

The primary limitation of this study is that it applies only to

end-initiated cylindrical charges. The asymmetries in the data about the 90° angle indicate that the point of initiation has a strong effect on blast properties for long charges. It would be advantageous to study center-initiated charges as well. Even more interesting would be the effects of simultaneous initiation from both ends.

Charge case effects should also be studied, since the results would be directly applicable to design of ordnance devices. Considerable work has been done on case effects in the 90° direction, but little if any data are available at other angles.

It is clear that it would be advantageous to use an explosive other than Pentolite for future work. From the results of this and the previous DNA study[1] (which used charges of Composition B) it appears that TNT-based explosives should be avoided if possible, because of the shot-to-shot variability in explosive performance. The reason, simply stated, is that the number of shots required to give results of a given accuracy can be most easily reduced by decreasing the statistical variability of each data point, as is shown in any text on statistics: the number of data points required is proportional to the square of the error in each point. If the use of TNT-based explosives cannot be avoided, then every data point should be duplicated at the very minimum. Most of the wiggles in the plots of pressure or impulse vs L/D or angle presented here can be attributed to combinations of L/D and angle at which only a single experimental measurement was made.

The obvious approach to higher-quality charges is to use pressed charges. If pressing long charges is indeed a problem, as indicated above, such charges could be built up by joining shorter cylinders end to end. A less obvious approach which should be investigated is the use of liquid explosives. Here, uniformity of the explosive can be guaranteed. Liquid explosives have the disadvantage of requiring a container, with the consequent introduction of cased-charge effects. However, this could be minimized by using thin-walled containers of a frangible material which shatters into fine particles on detonation of the explosive.

In any further work in this area, it would be very desirable to have high-speed camera coverage of each shot, preferably using one camera viewing each pressure gauge line. High-speed shock photography would provide a record of any abnormalities in explosive performance. It would give an independent set of data on arrival times, and also display secondary shocks and ground reflections.

APPENDIX A

PRESSURE-TIME PLOTS

This appendix presents the plots of pressure vs. time for every gauge on every shot fired for this program. Each page displays the pressure-time traces in our data set: the data from one gauge line (6 gauges) for one shot.

Table A-1 identifies each data set by charge weight, L/D ratio, and angle. The entries in the table give the shot number first, followed by the gauge line number.

TABLE A-1. Catalog of Data Sets by L/D and Angle

	Angle	L/D 1/4	1/2	1/1	2/1	3/1	4/1	6/1	Sphere
8-lb. Cylinders	0°	21-1 29-2	18-1	2-1 3-1 8-2 35-2 56-1	38-2 61-1	41-2	46-2 50-1	55-2	13-1 13-2 14-1
	22.5°	23-1 26-2		4-1 12-2 32-2			44-2 49-1 58-2		14-2 30-1 30-2
	45°	20-1 25-2 27-1	17-1	5-1 11-2 33-2	36-2	39-2	42-2 47-1	53.2	52-1 52-2 66-1
	67.5°	22-1 24-2		6-1 10-2 31-2			43-2 48-1		66-2
	90°	19-1 21-2 28-2 29-1	15-1 18-2 57-1	2-2 3-2 7-1 8-1 9-2 34-2 35-1 56-2	37-2 38-1 61-2	40-2 41-1 60-2	45-2 46-1 50-2 51-1 59-1	54-2 55-1	
	112.5°	23-2 26-1		4-2 12-1 32-1			44-1 49-2 58-1		
	135°	20-2 25-1 27-2	17-2	5-2 11-1 33-1	36-1	39-1	42-1 47-2	53-1	
	157.5°	22-2 24-1		6-2 10-1 31-1			43-1 48-2		
	180°	19-2 28-1	15-2 57-2	7-2 9-1 34-1	37-1	40-1 60-1	45-1 51-2 59-2	54-1	
16 lb.	0°			63-2			65-2		
	90°			62-2 63-1			64-2 65-1		
	180°			62-1			64-1		

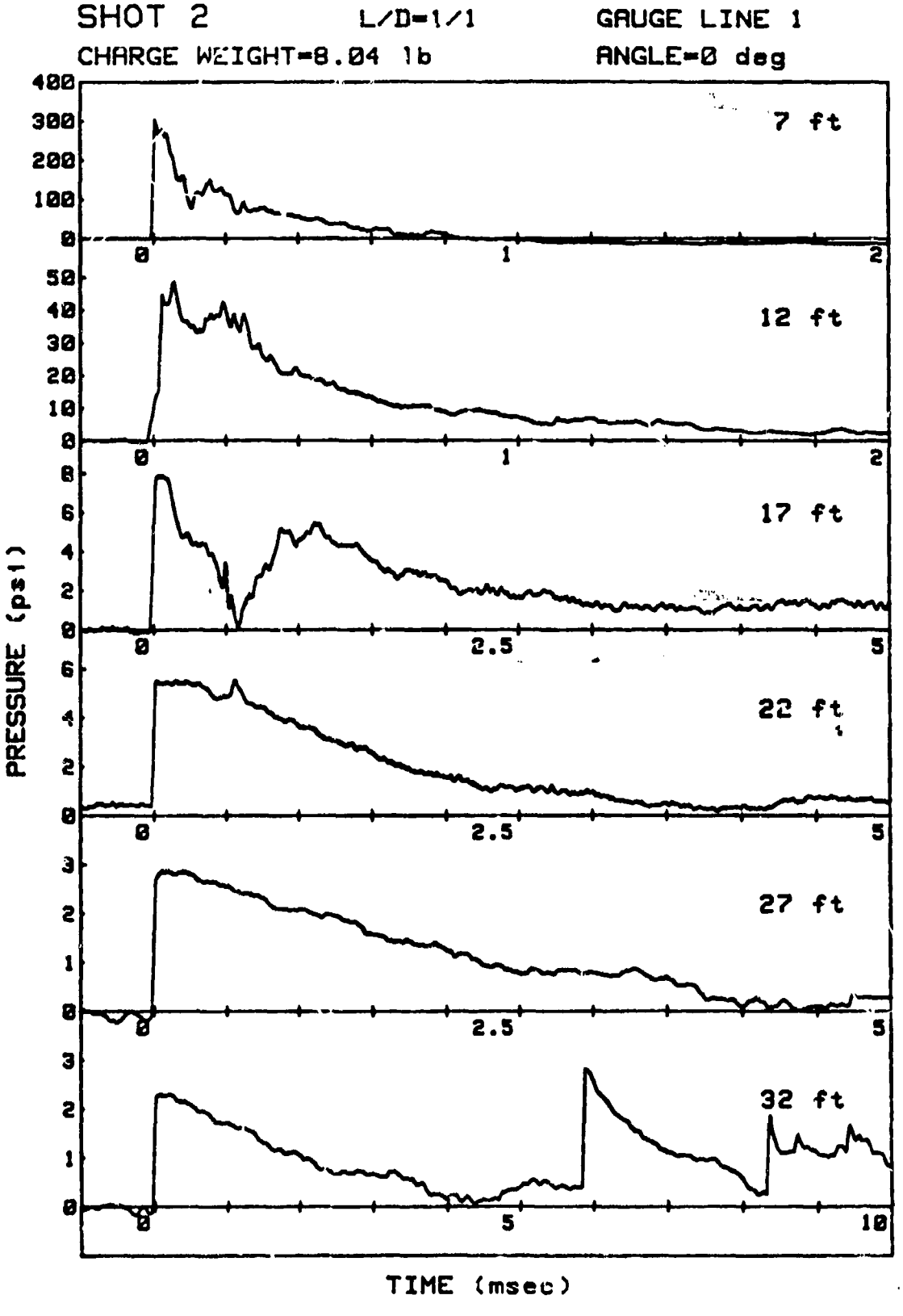
SHOT 2
L/D=1/1
GAUGE LINE 1
CHARGE WEIGHT=8.04 lb
ANGLE=0 deg
7 ft
12 ft
17 ft
22 ft
27 ft
32 ft
PRESSURE (psi)
TIME (msec)

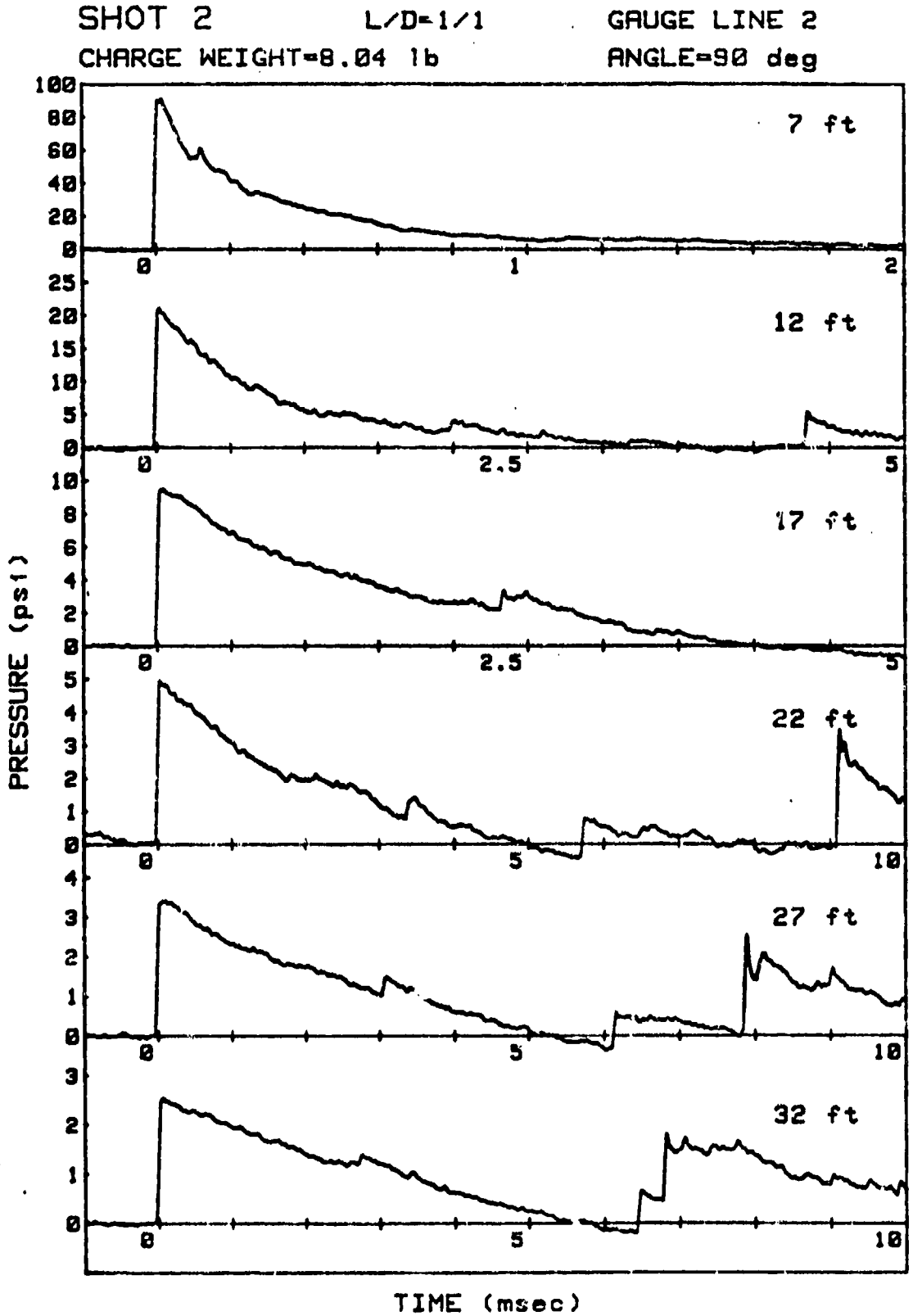
SHOT 2
L/D=1/1
GAUGE LINE 2
CHARGE WEIGHT=8.04 lb
ANGLE=90 deg
7 ft
12 ft
17 ft
22 ft
27 ft
32 ft
PRESSURE (psi)
TIME (msec)

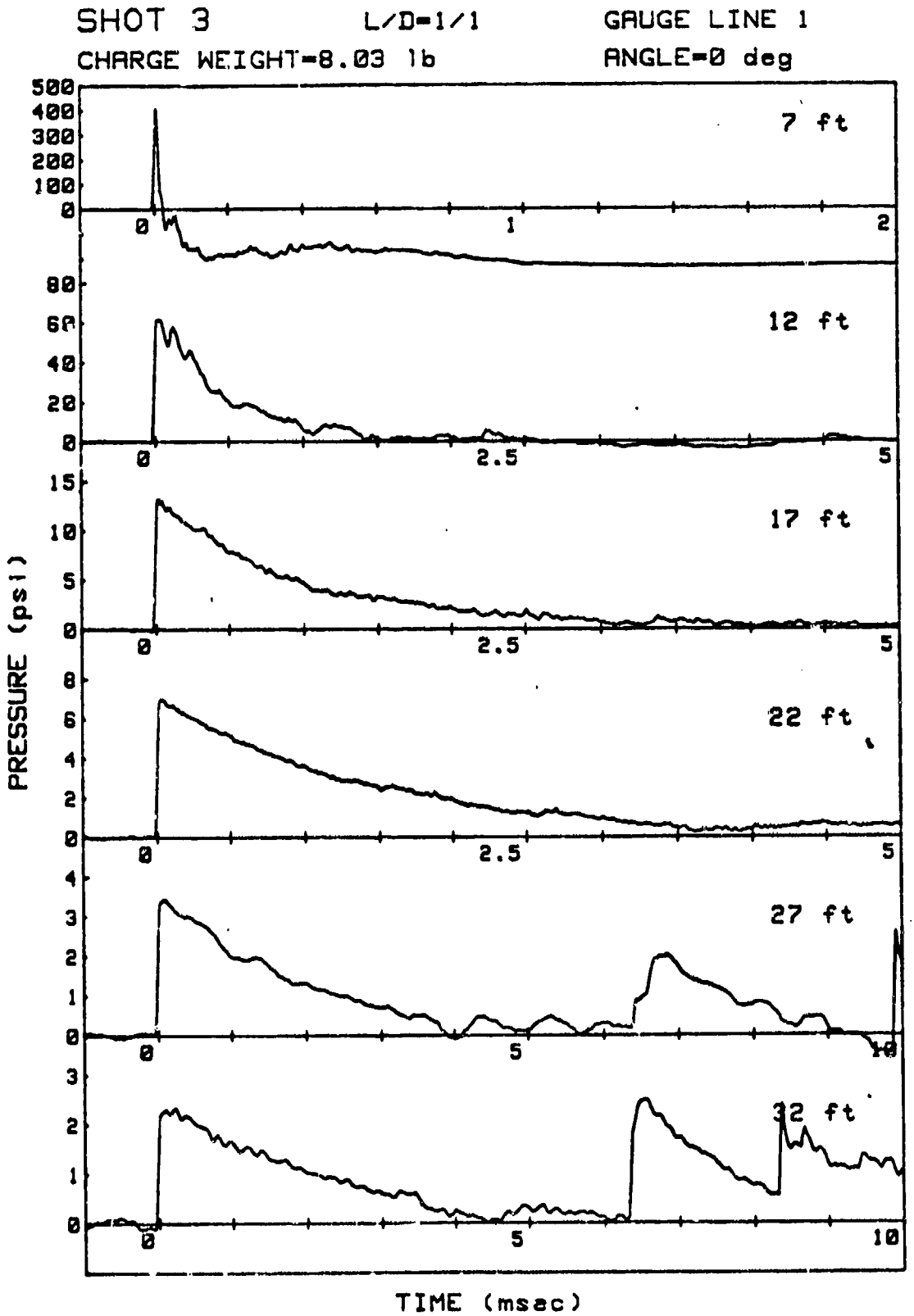
SHOT 3
L/D=1/1
GAUGE LINE 1
CHARGE WEIGHT=8.03 lb
ANGLE=0 deg
7 ft
12 ft
17 ft
22 ft
27 ft
32 ft
PRESSURE (psi)
TIME (msec)

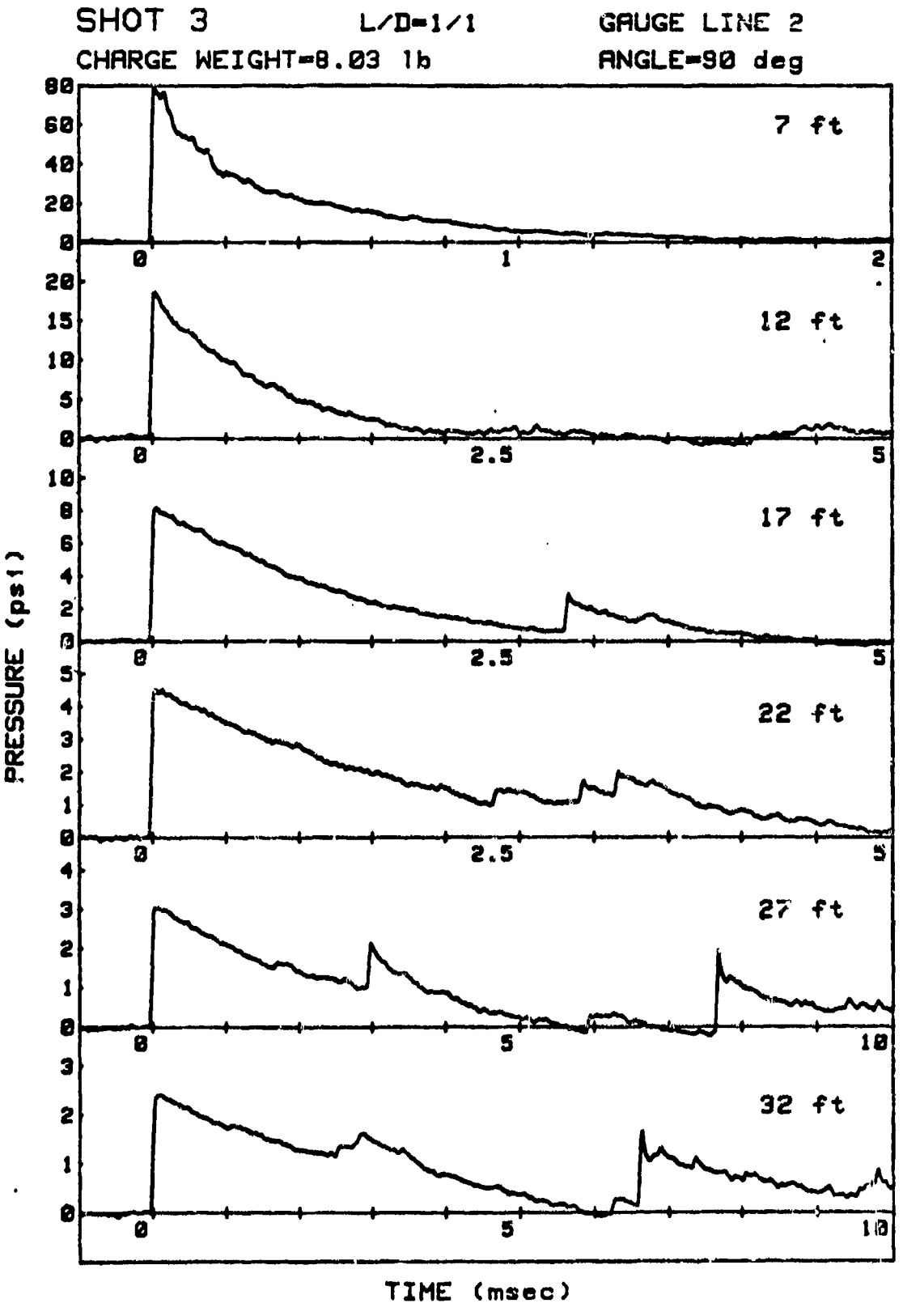
SHOT 3
L/D=1/1
GAUGE LINE 2
CHARGE WEIGHT=8.03 lb
ANGLE=90 deg
7 ft
12 ft
17 ft
22 ft
27 ft
32 ft
PRESSURE (psi)
TIME (msec)

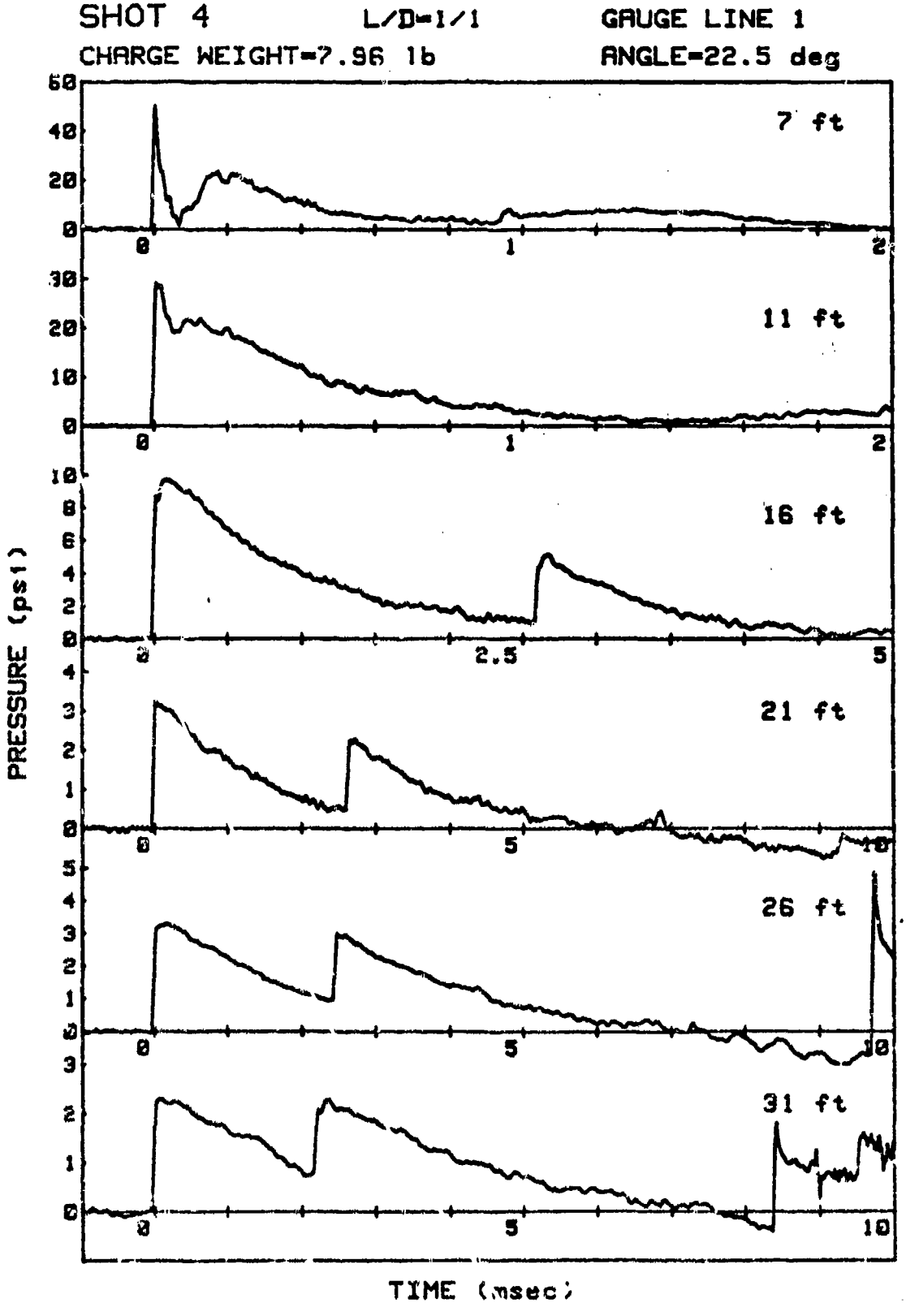
SHOT 4
L/D=1/1
GAUGE LINE 1
CHARGE WEIGHT=7.96 lb
ANGLE=22.5 deg
7 ft
11 ft
16 ft
21 ft
26 ft
31 ft
PRESSURE (psi)
TIME (msec)

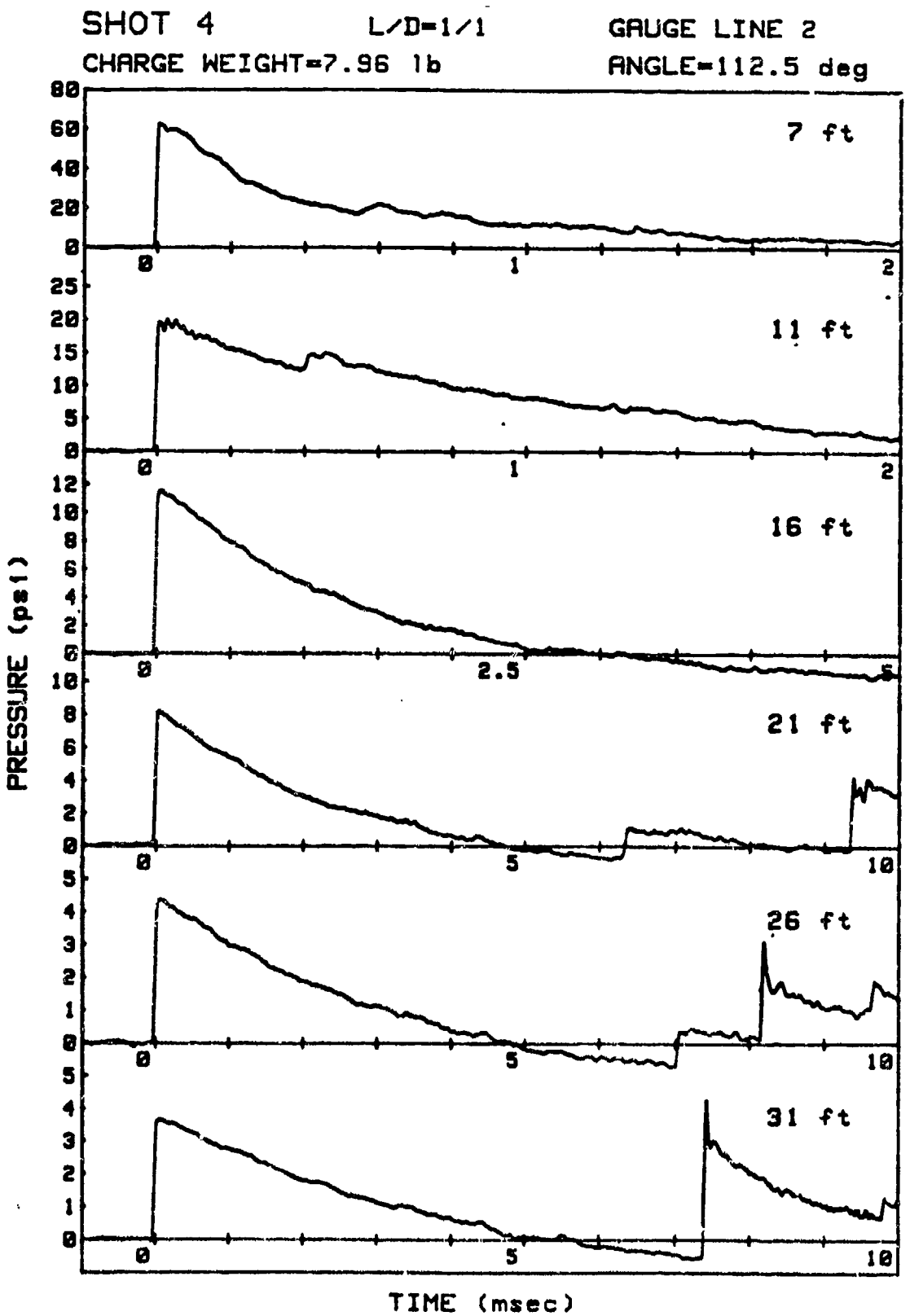
SHOT 4
L/D=1/1
GAUGE LINE 2
CHARGE WEIGHT=7.96 lb
ANGLE=112.5 deg
7 ft
11 ft
16 ft
21 ft
26 ft
31 ft
PRESSURE (psi)
TIME (msec)

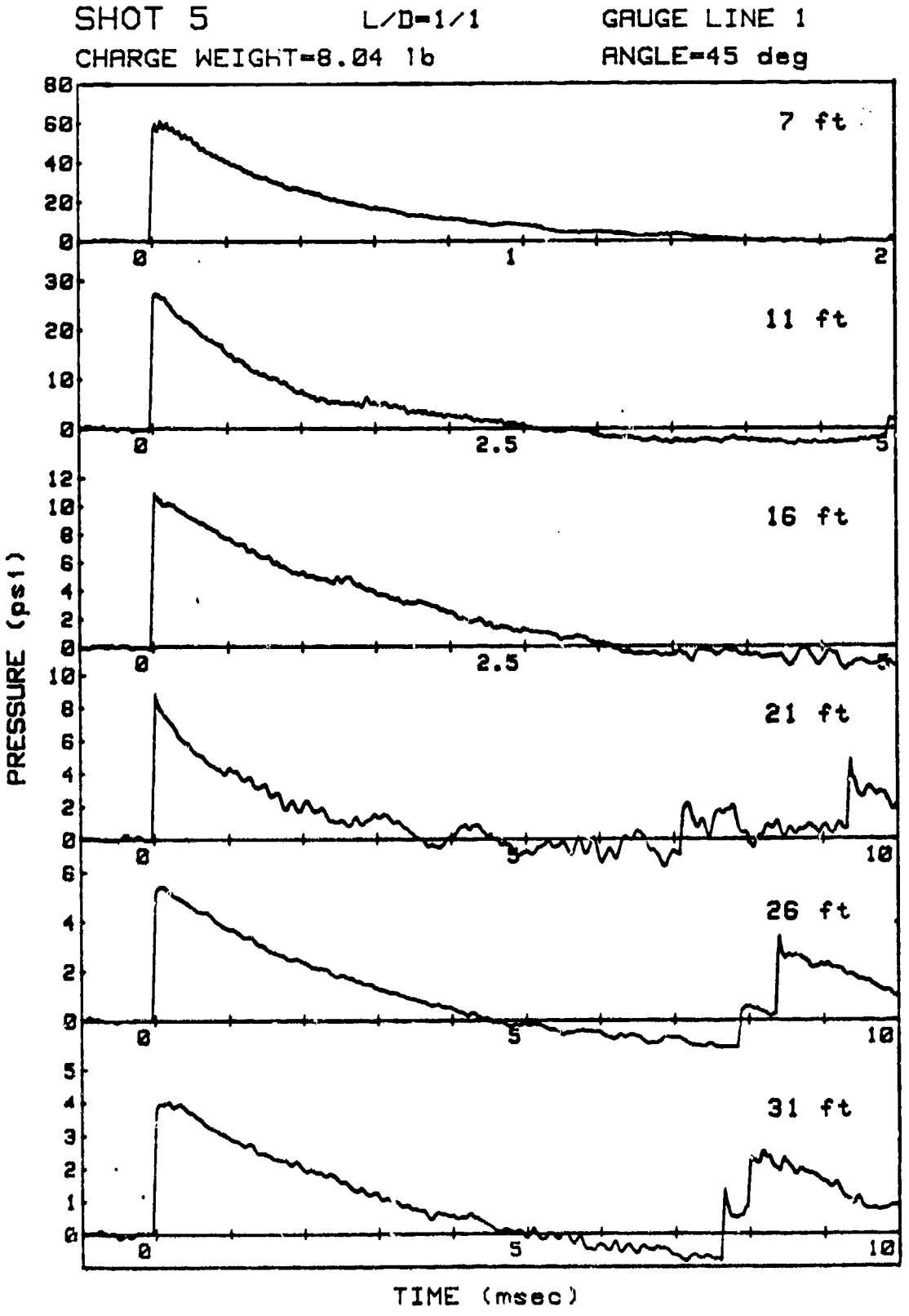
SHOT 5
L/D=1/1
GAUGE LINE 1
CHARGE WEIGHT=8.04 lb
ANGLE=45 deg
7 ft
11 ft
16 ft
21 ft
26 ft
31 ft
PRESSURE (psi)
TIME (msec)

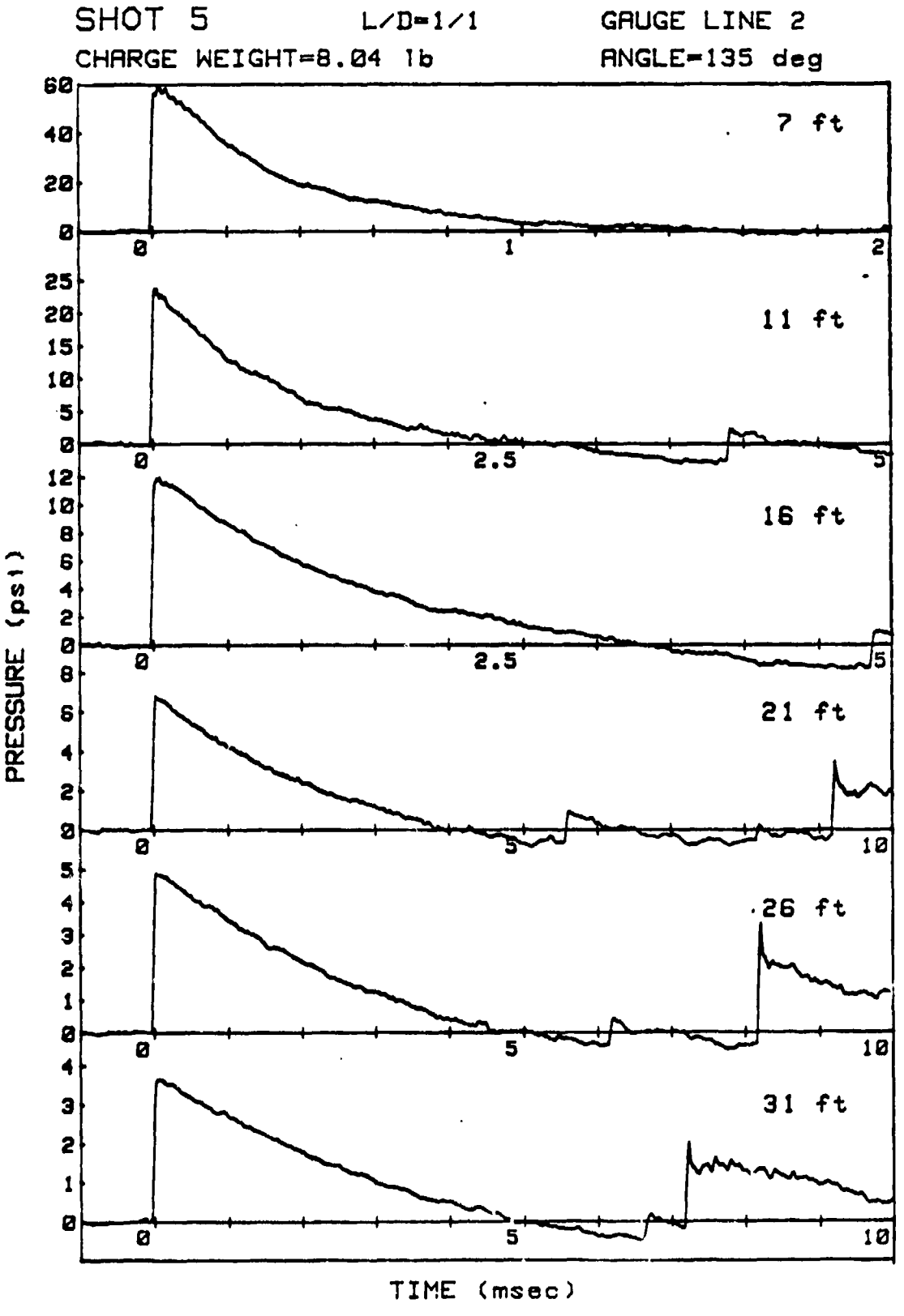
SHOT 5
L/D=1/1
GAUGE LINE 2
CHARGE WEIGHT=8.04 lb
ANGLE=135 deg
7 ft
11 ft
16 ft
21 ft
26 ft
31 ft
PRESSURE (psi)
TIME (msec)

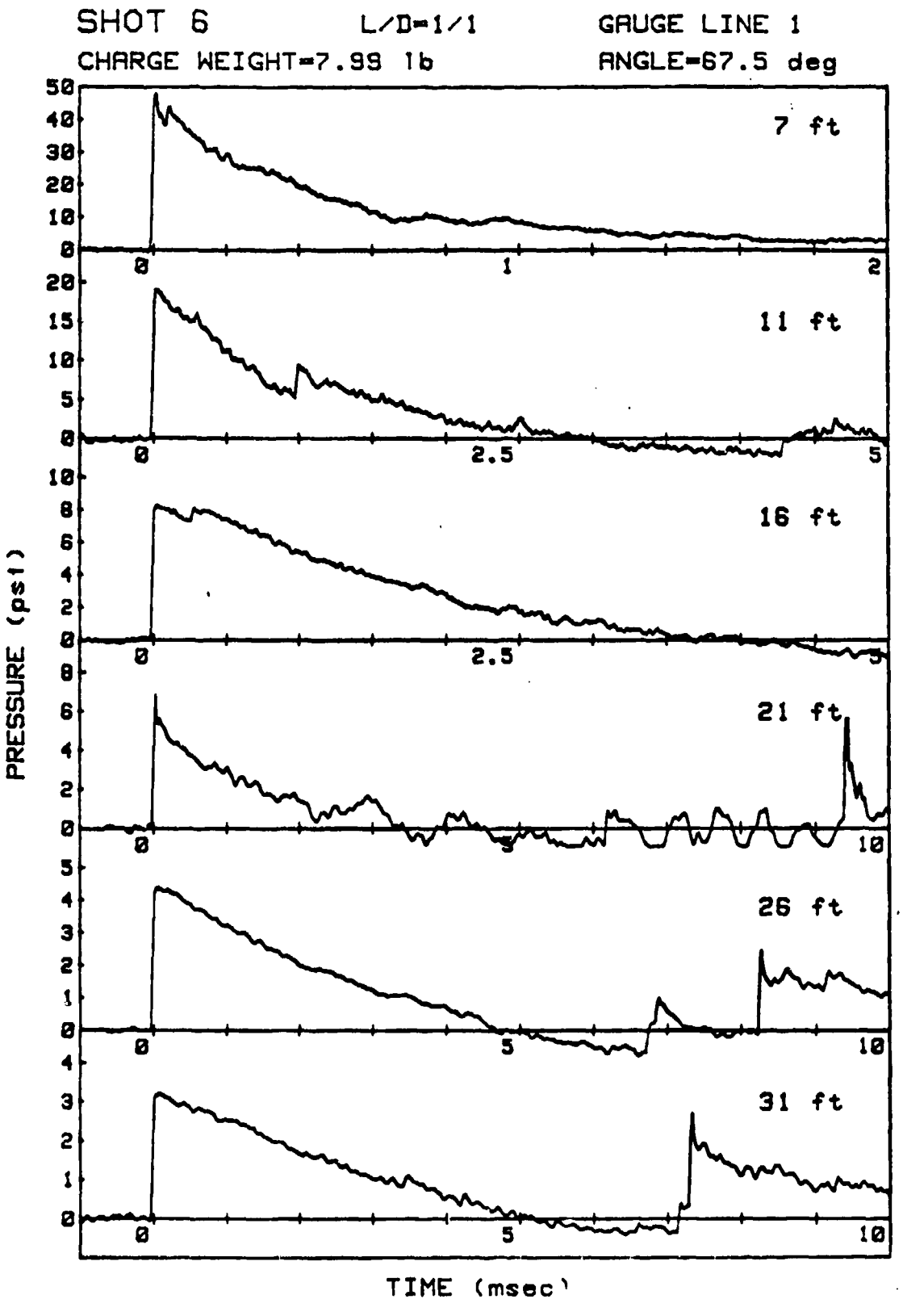
SHOT 6
L/D=1/1
GAUGE LINE 1
CHARGE WEIGHT=7.99 lb
ANGLE=67.5 deg
7 ft
11 ft
16 ft
21 ft
26 ft
31 ft
PRESSURE (psi)
TIME (msec)

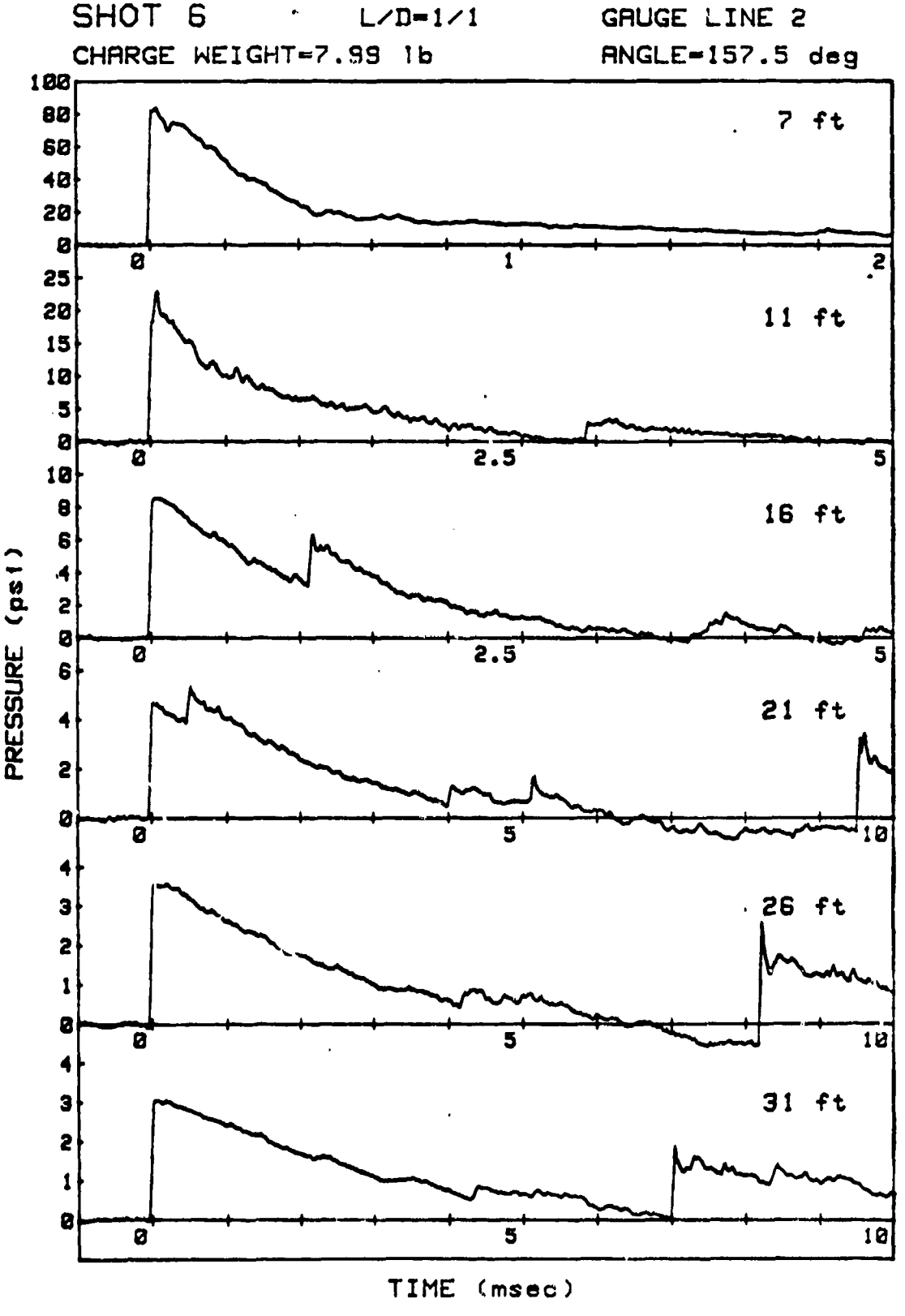
SHOT 6
L/D=1/1
GAUGE LINE 2
CHARGE WEIGHT=7.99 lb
ANGLE=157.5 deg
7 ft
11 ft
16 ft
21 ft
26 ft
31 ft
PRESSURE (psi)
TIME (msec)

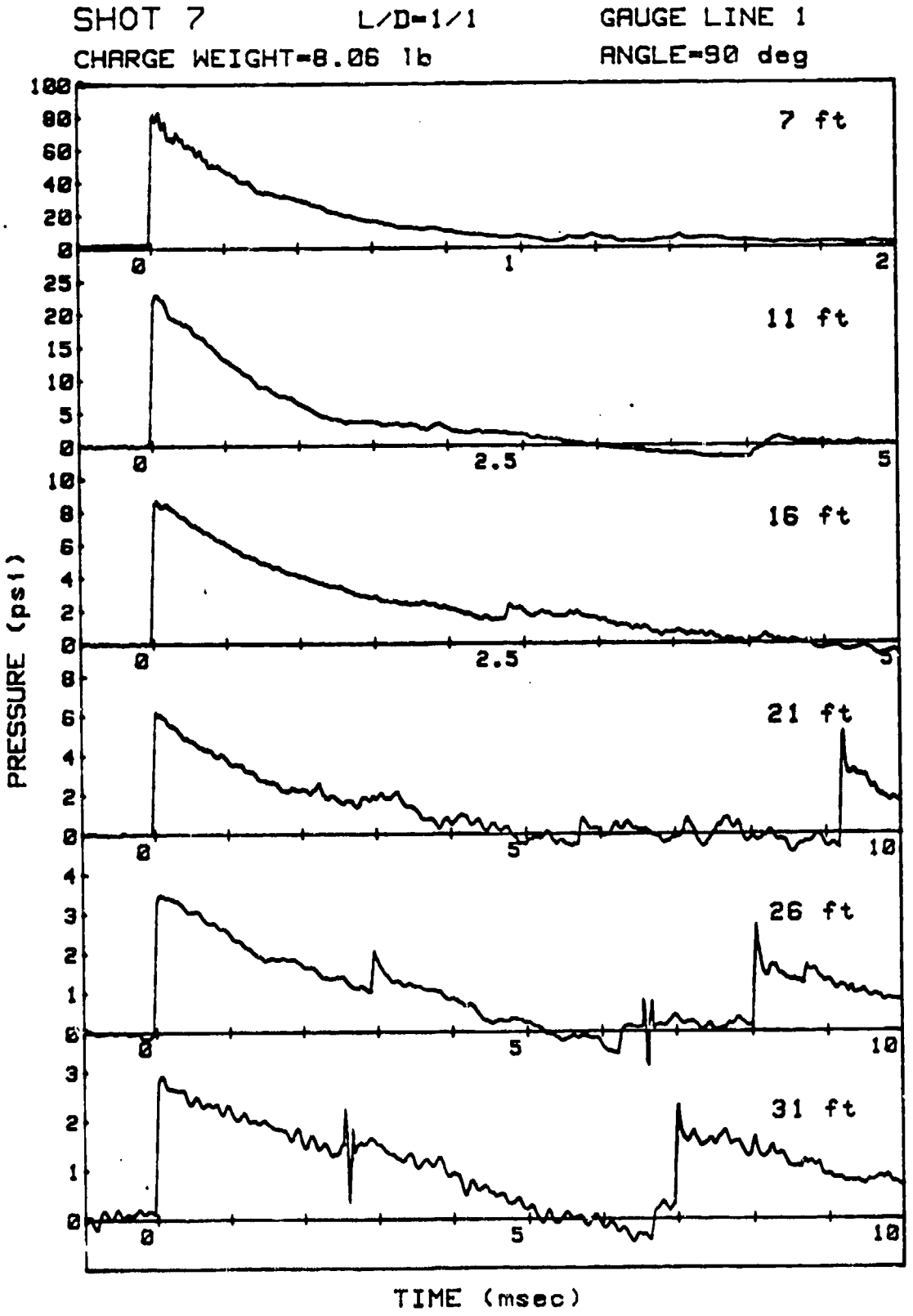
SHOT 7
L/D=1/1
GAUGE LINE 1
CHARGE WEIGHT=8.06 lb
ANGLE=90 deg
7 ft
11 ft
16 ft
21 ft
26 ft
31 ft
PRESSURE (psi)
TIME (msec)

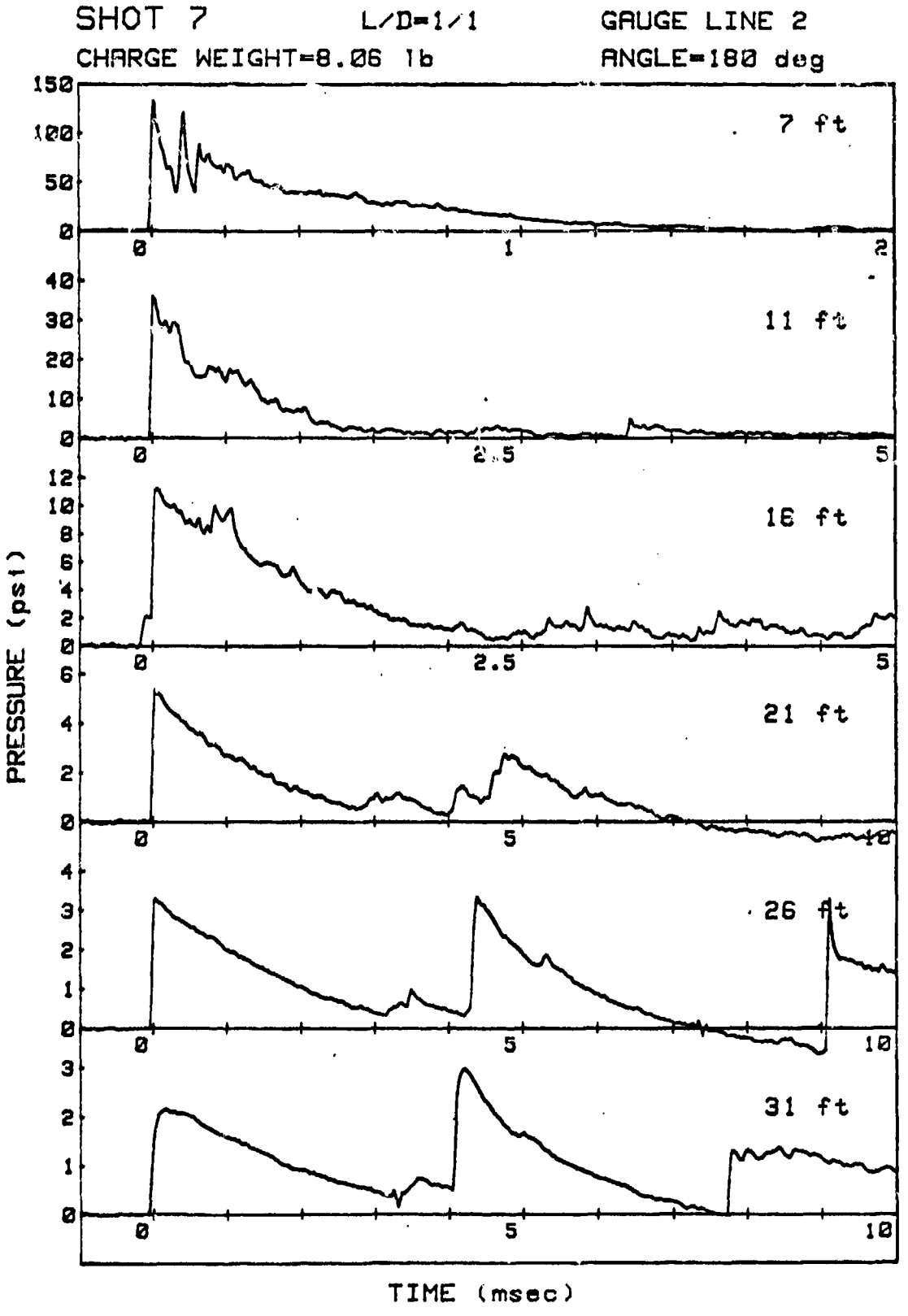
SHOT 7
L/D=1/1
GAUGE LINE 2
CHARGE WEIGHT=8.06 lb
ANGLE=180 deg
7 ft
11 ft
16 ft
21 ft
26 ft
31 ft
PRESSURE (psi)
TIME (msec)

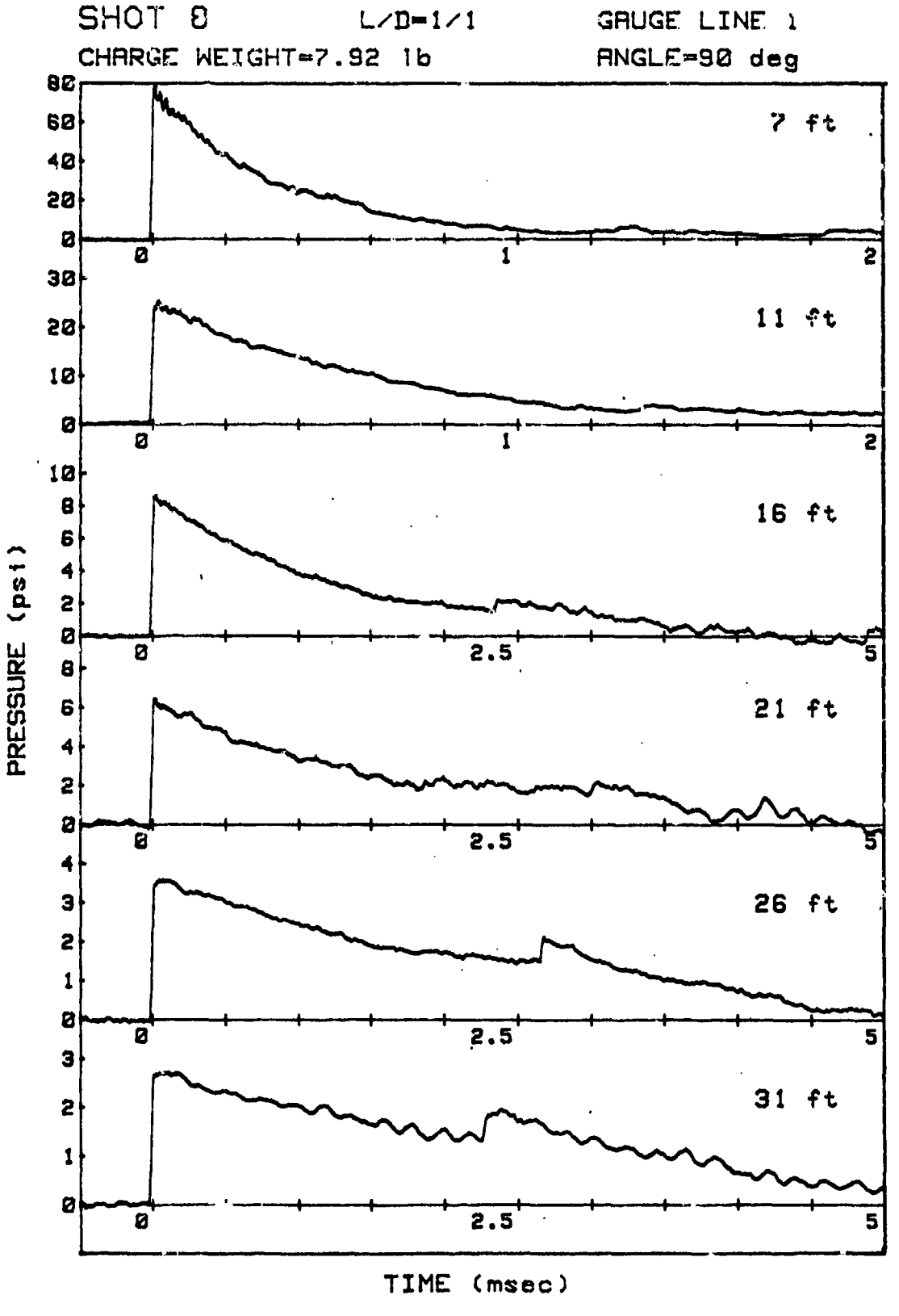
SHOT 8
L/D=1/1
GAUGE LINE 1
CHARGE WEIGHT=7.92 lb
ANGLE=90 deg
7 ft
11 ft
16 ft
21 ft
26 ft
31 ft
PRESSURE (psi)
TIME (msec)

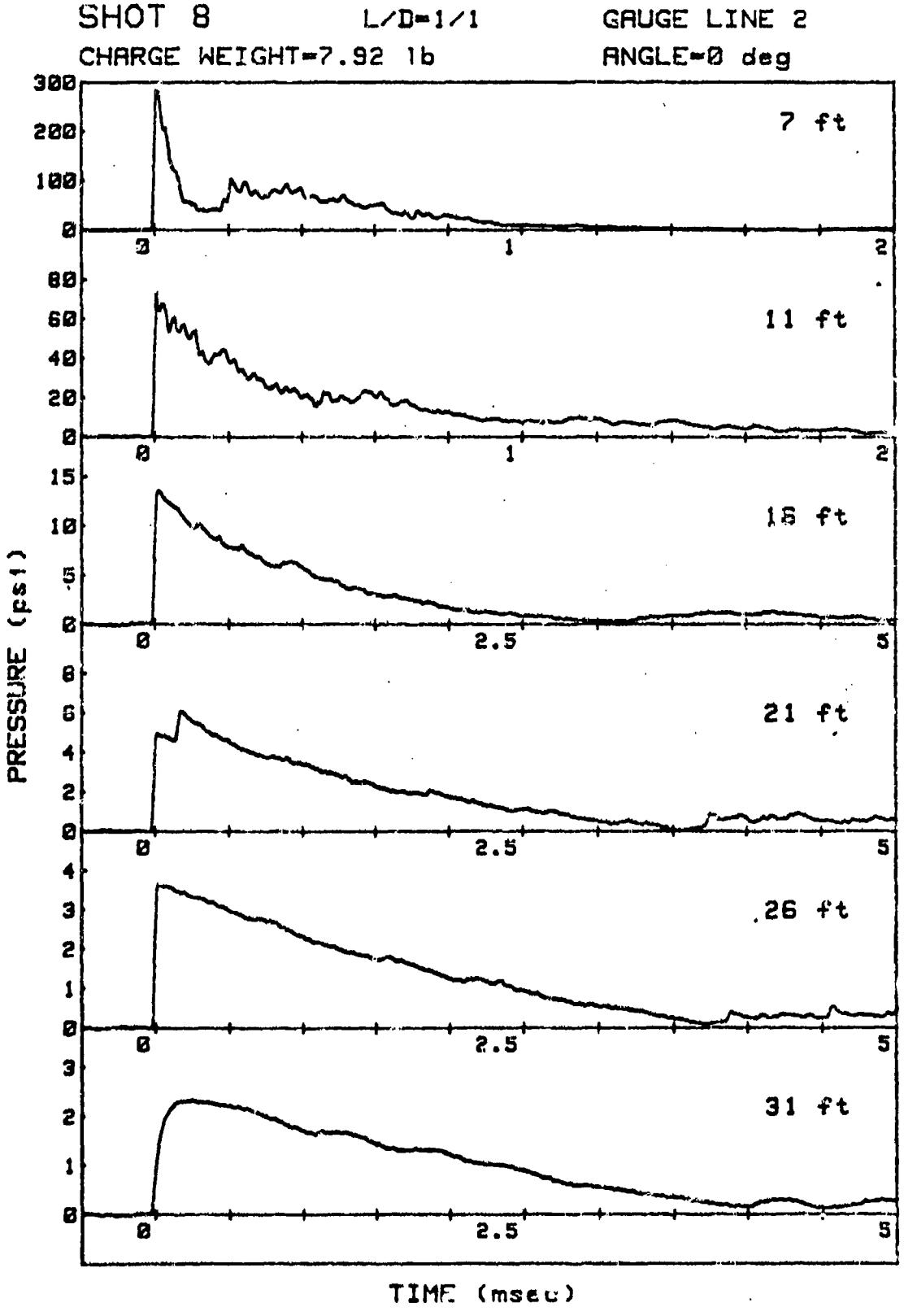
SHOT 8
L/D=1/1
GAUGE LINE 2
CHARGE WEIGHT=7.92 lb
ANGLE=0 deg
7 ft
11 ft
16 ft
21 ft
26 ft
31 ft
PRESSURE (psi)
TIME (msec)

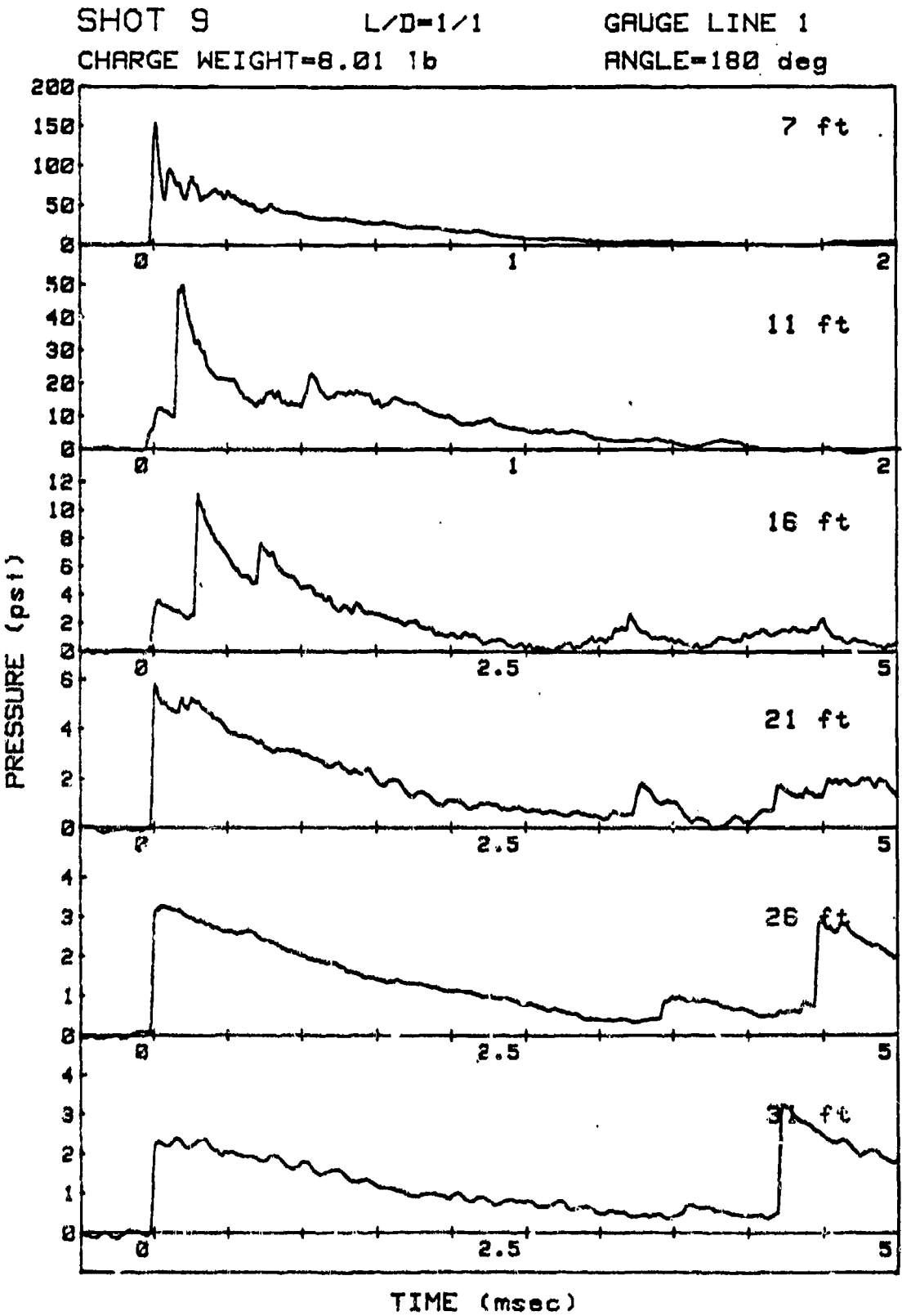
SHOT 9
L/D=1/1
GAUGE LINE 1
CHARGE WEIGHT=8.01 lb
ANGLE=180 deg
7 ft
11 ft
16 ft
21 ft
26 ft
31 ft
PRESSURE (psi)
TIME (msec)

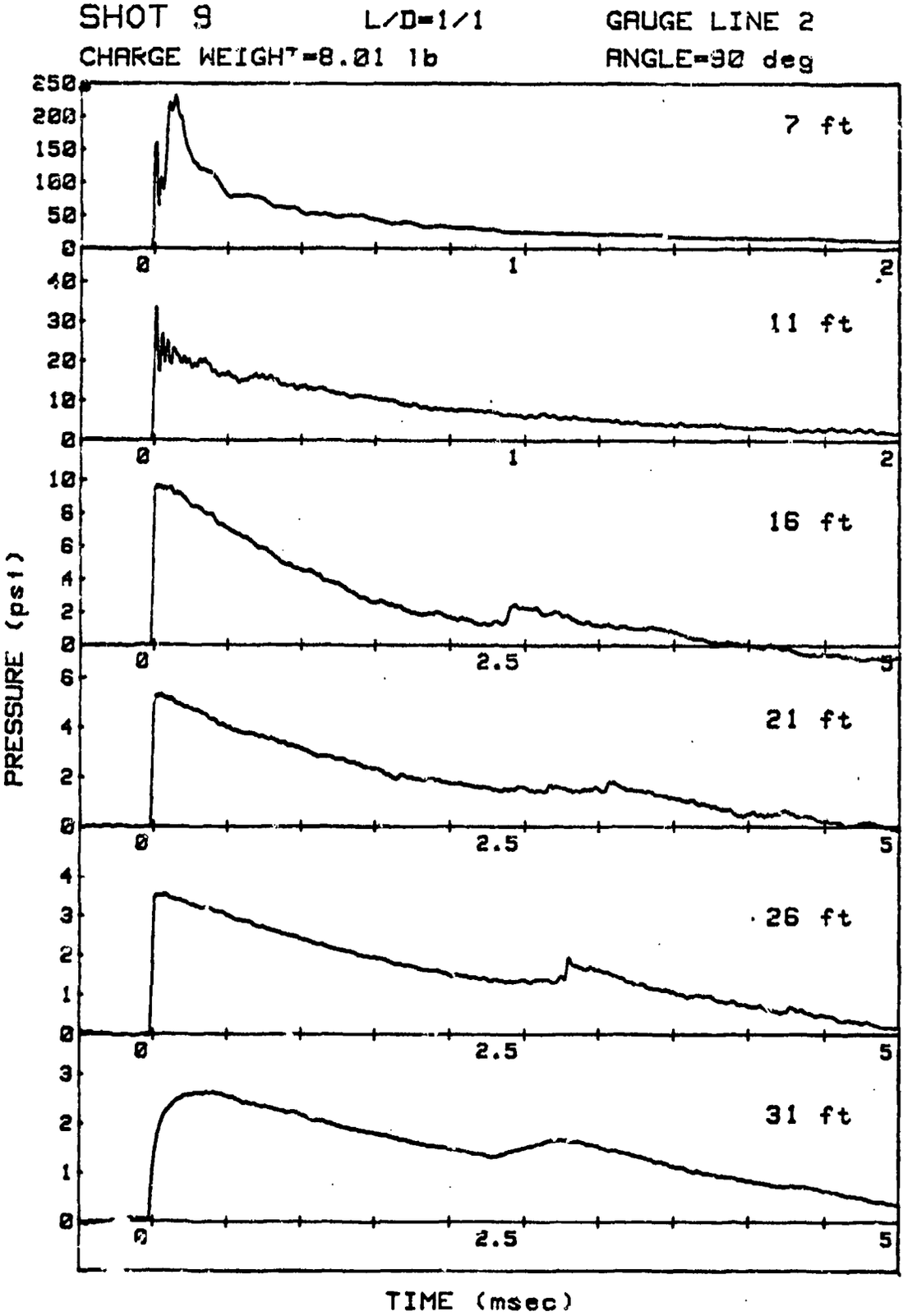
SHOT 9
L/D=1/1
GAUGE LINE 2
CHARGE WEIGHT=8.01 lb
ANGLE=90 deg
7 ft
11 ft
16 ft
21 ft
26 ft
31 ft
PRESSURE (psi)
TIME (msec)

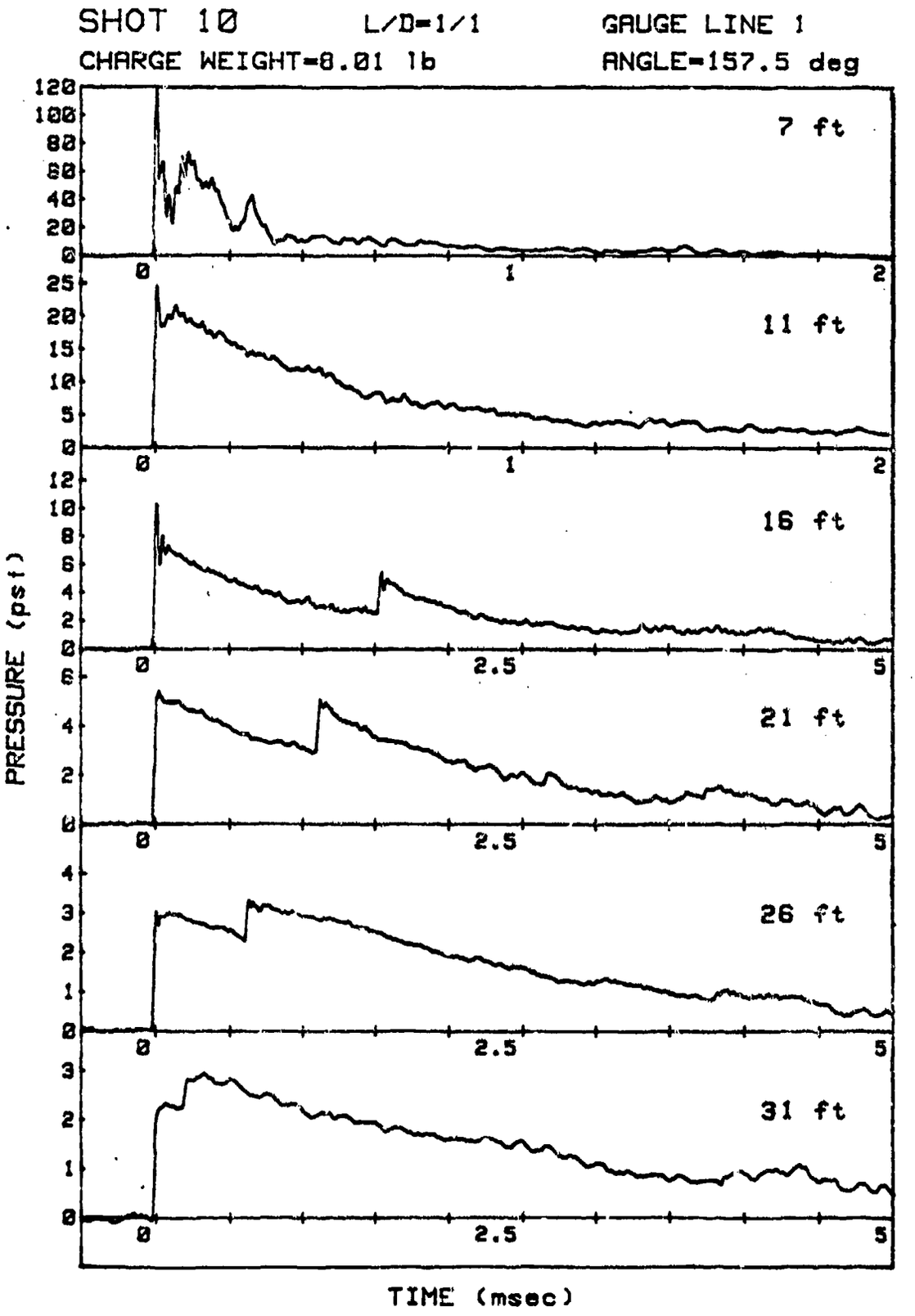
SHOT 10
L/D=1/1
GAUGE LINE 1
CHARGE WEIGHT=8.01 lb
ANGLE=157.5 deg
7 ft
11 ft
16 ft
21 ft
26 ft
31 ft
PRESSURE (psi)
TIME (msec)

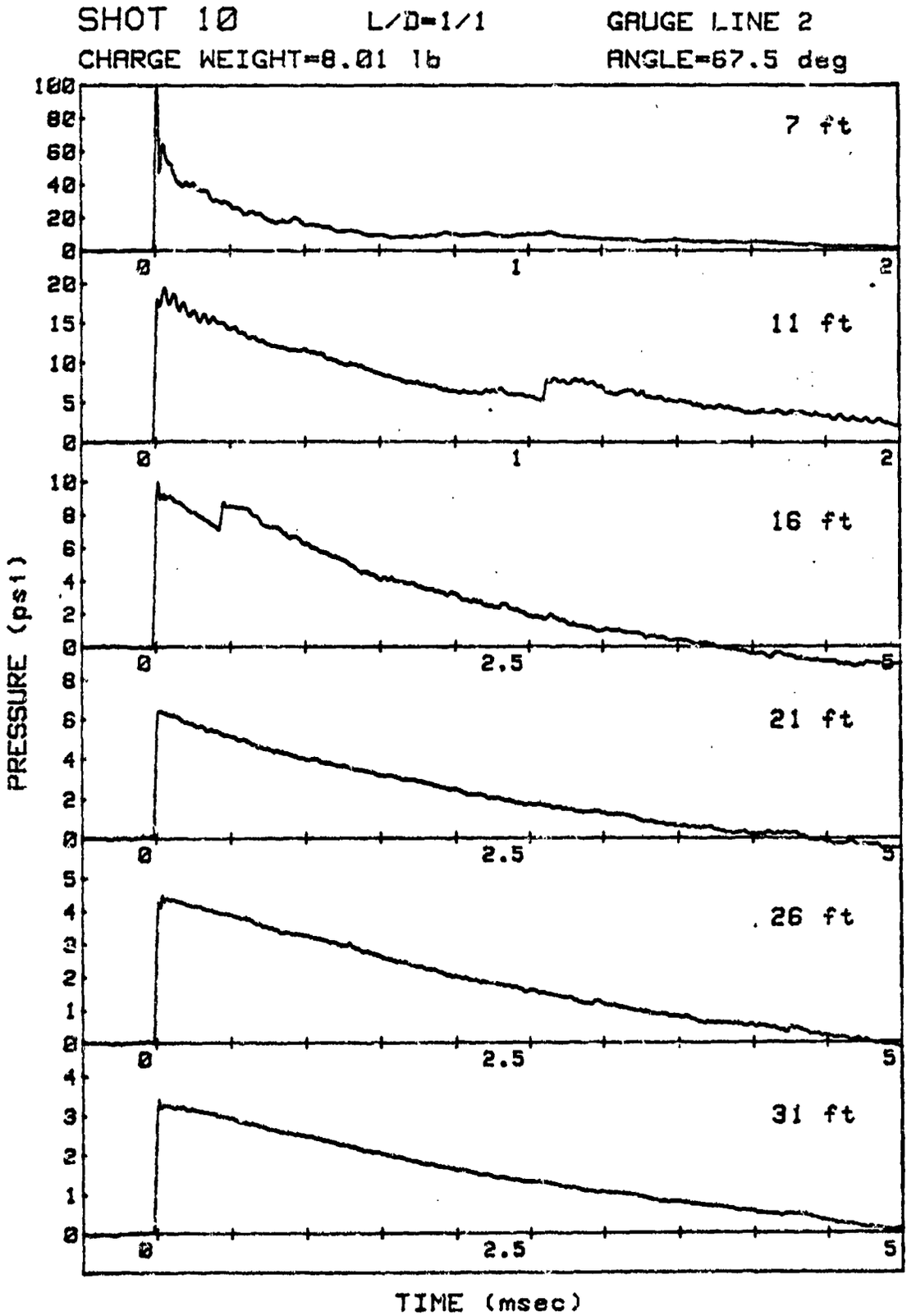
SHOT 10
L/D=1/1
GAUGE LINE 2
CHARGE WEIGHT=8.01 lb
ANGLE=67.5 deg
7 ft
11 ft
16 ft
21 ft
26 ft
31 ft
PRESSURE (psi)
TIME (msec)

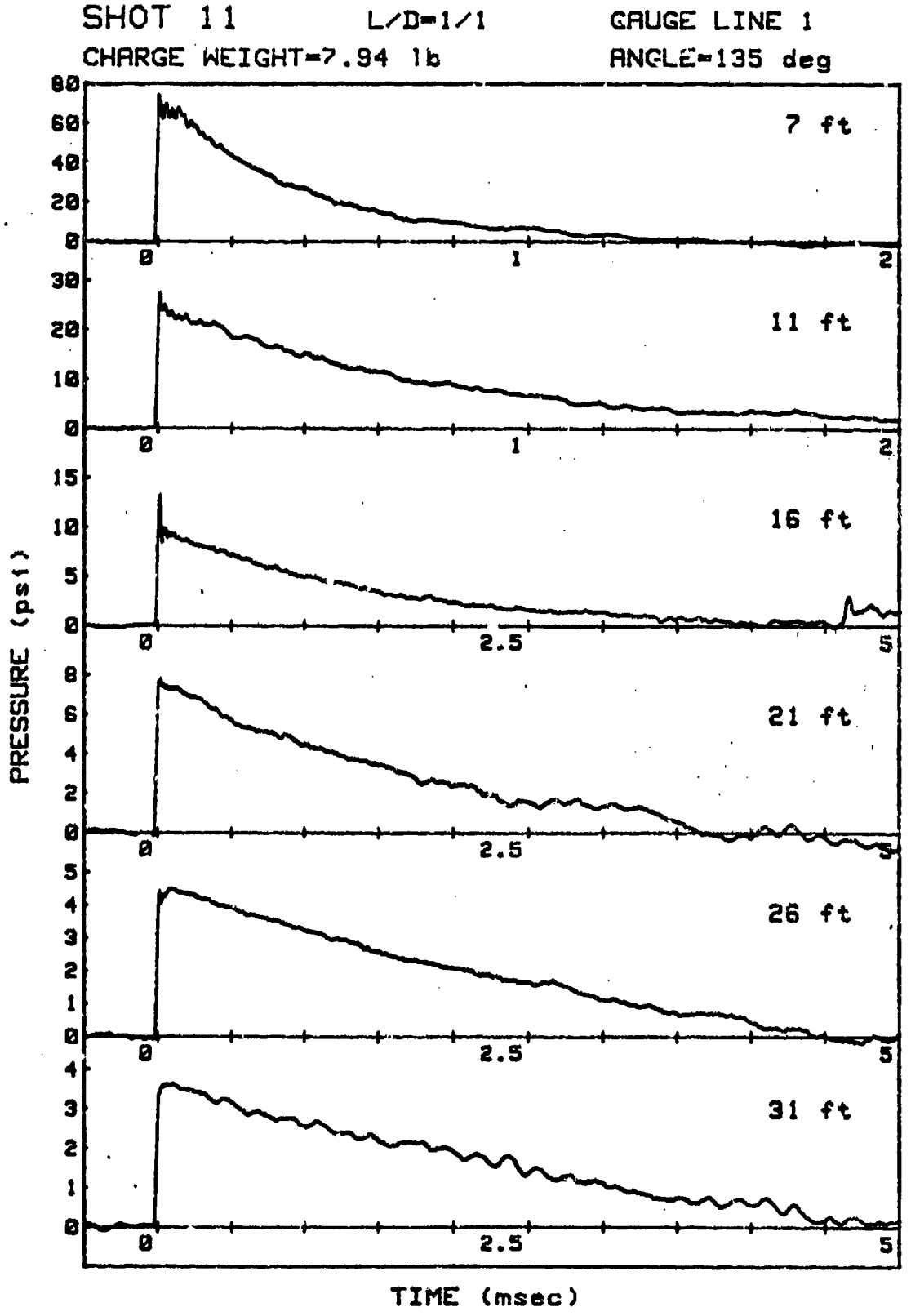
SHOT 11
L/D=1/1
GAUGE LINE 1
CHARGE WEIGHT=7.94 lb
ANGLE=135 deg
7 ft
11 ft
16 ft
21 ft
26 ft
31 ft
PRESSURE (psi)
TIME (msec)

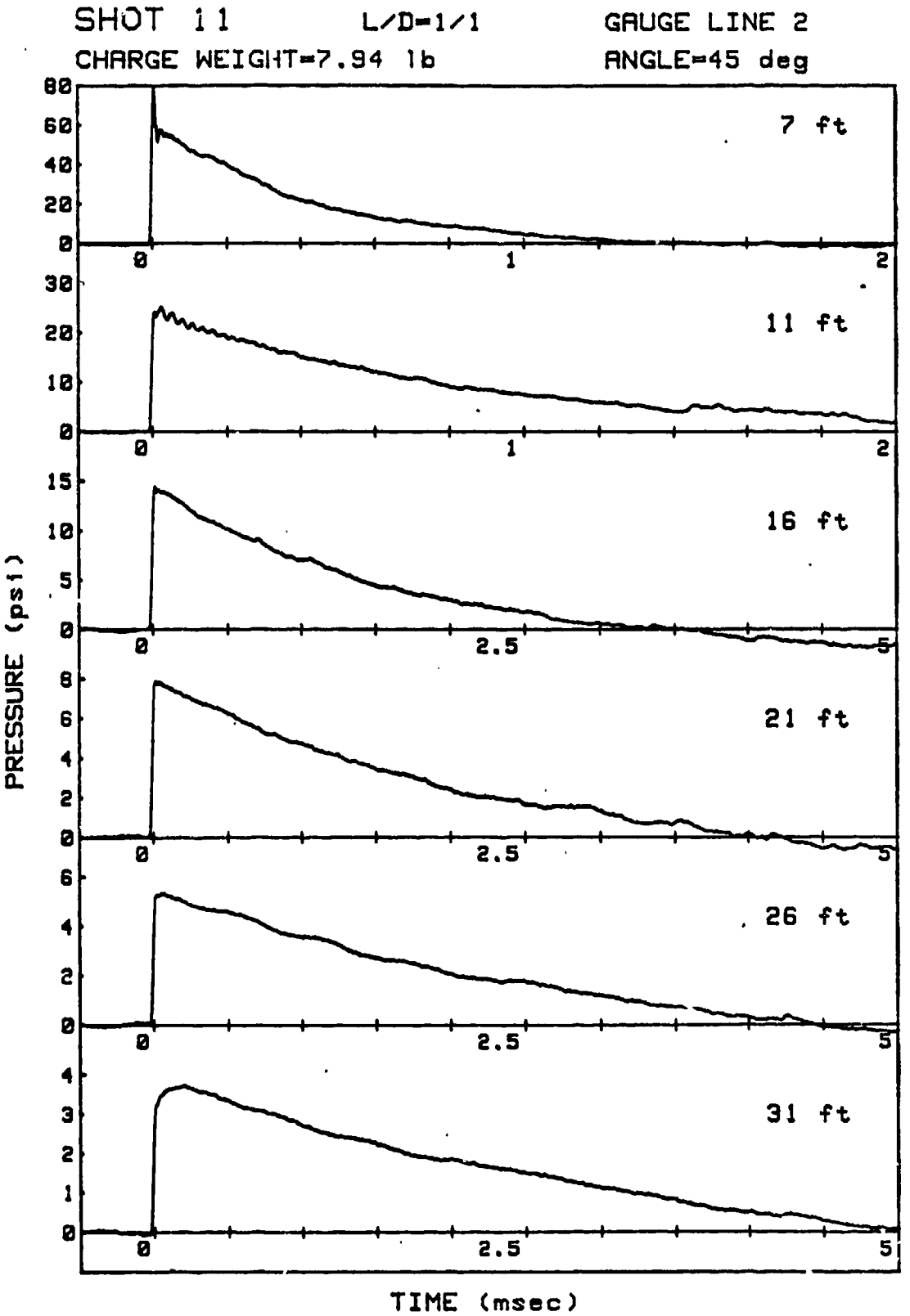
SHOT 11
L/D=1/1
GAUGE LINE 2
CHARGE WEIGHT=7.94 lb
ANGLE=45 deg
7 ft
11 ft
16 ft
21 ft
26 ft
31 ft
PRESSURE (psi)
TIME (msec)

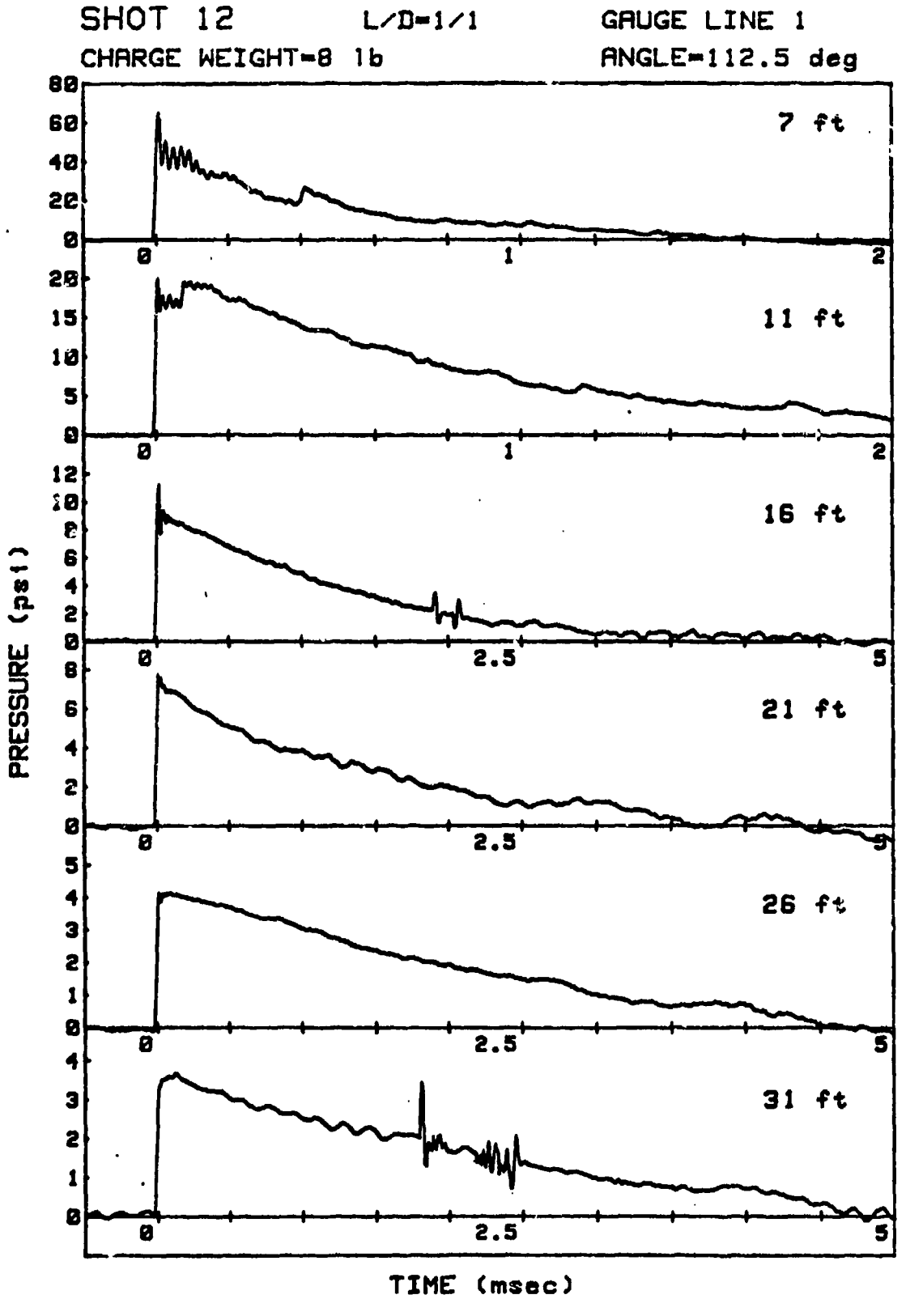
SHOT 12
L/D=1/1
GAUGE LINE 1
CHARGE WEIGHT=8 lb
ANGLE=112.5 deg
7 ft
11 ft
16 ft
21 ft
26 ft
31 ft
PRESSURE (psi)
TIME (msec)

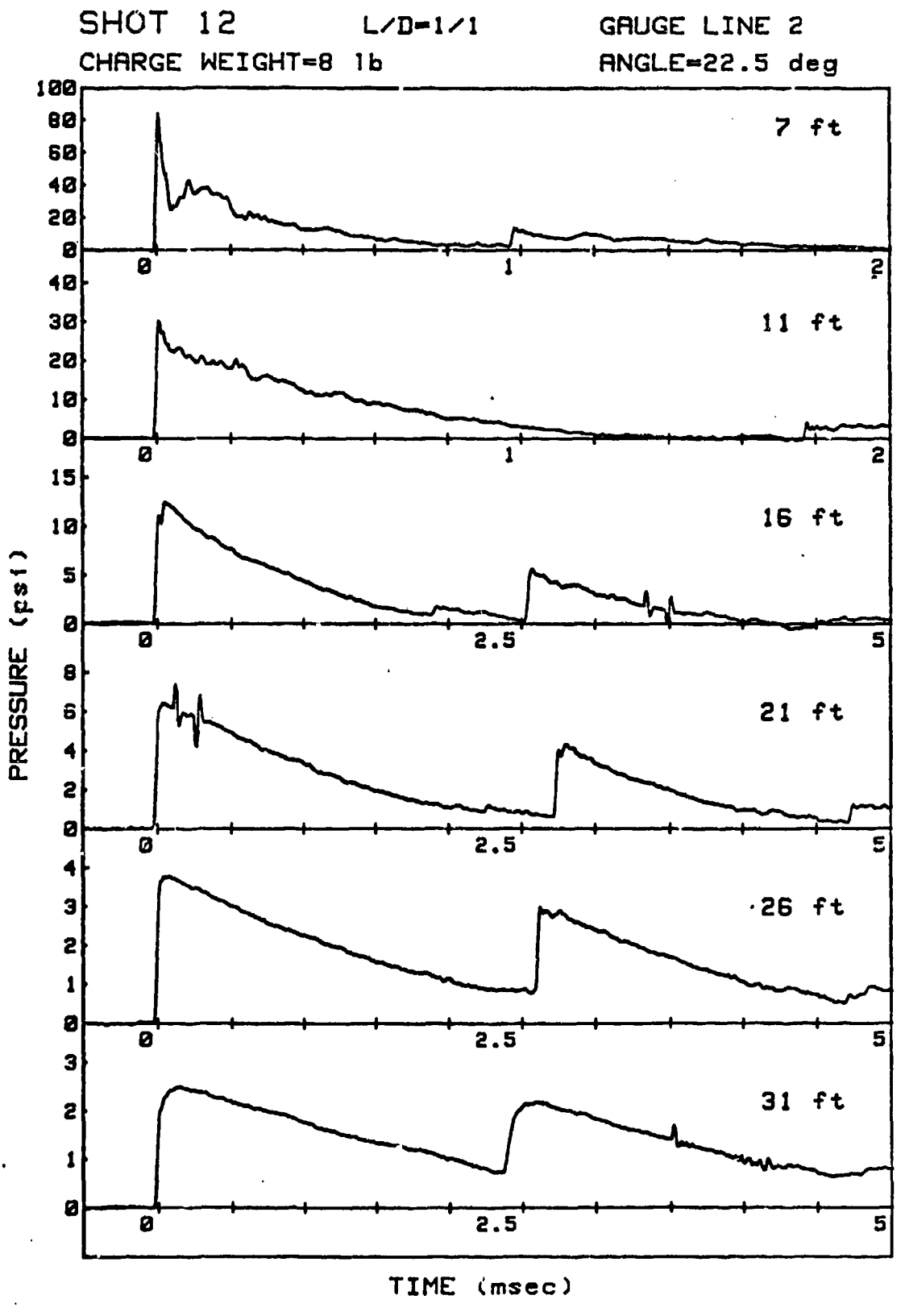
SHOT 12
L/D=1/1
GAUGE LINE 2
CHARGE WEIGHT=8 lb
ANGLE=22.5 deg
7 ft
11 ft
16 ft
21 ft
26 ft
31 ft
PRESSURE (psi)
TIME (msec)

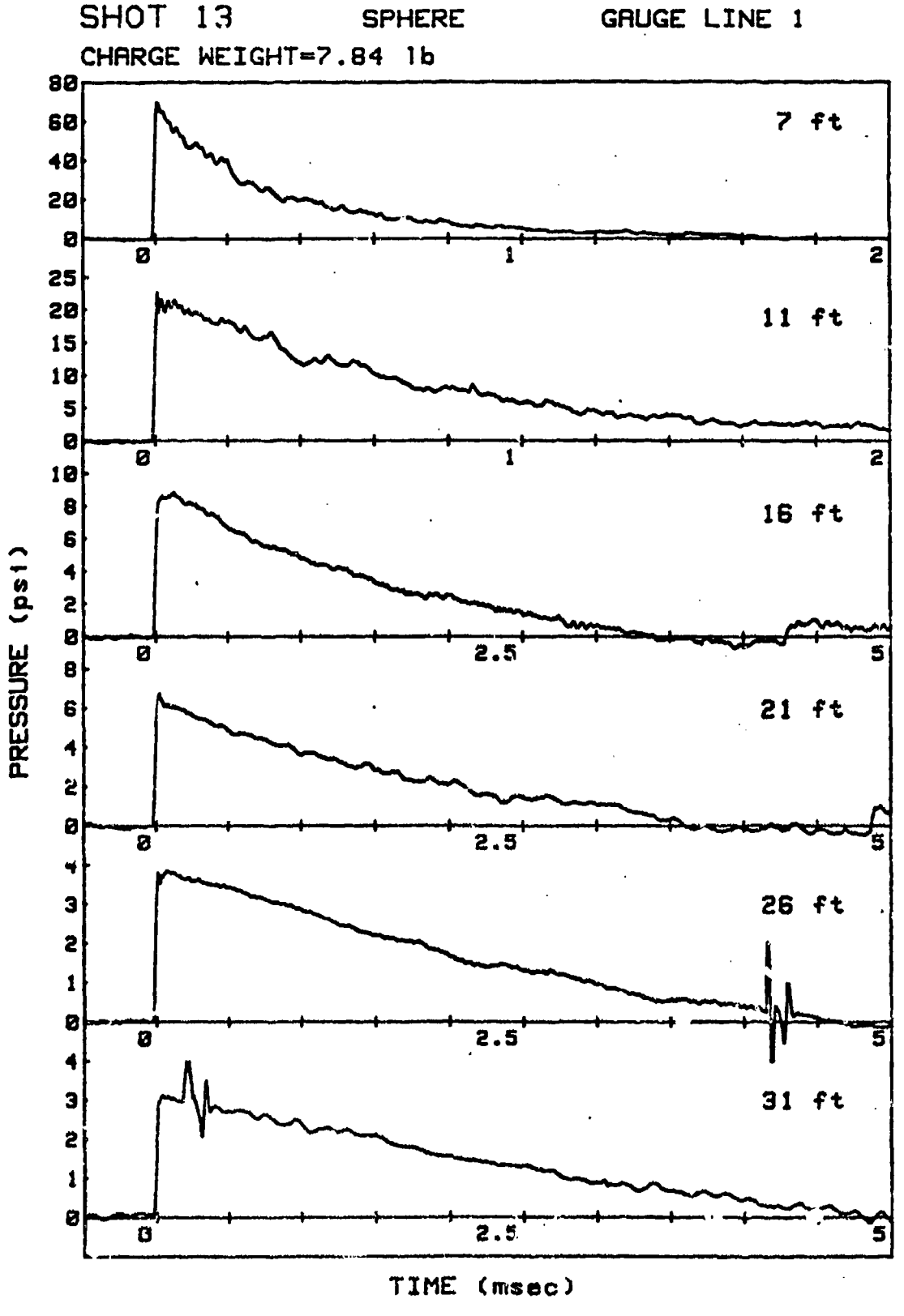
SHOT 13
SPHERE
GAUGE LINE 1
CHARGE WEIGHT=7.84 lb
7 ft
11 ft
16 ft
21 ft
26 ft
31 ft
PRESSURE (psi)
TIME (msec)

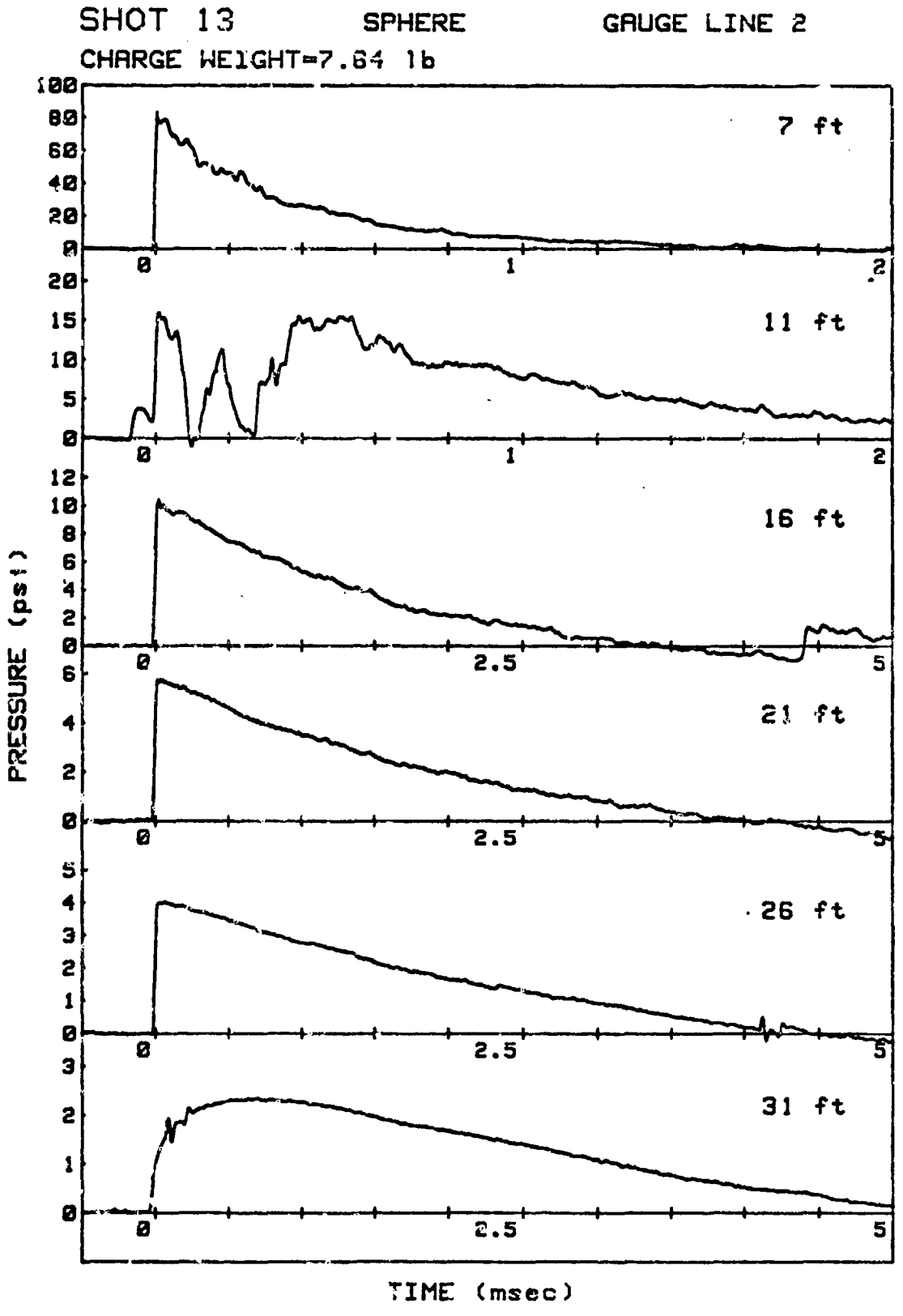
SHOT 13
SPHERE
GAUGE LINE 2
CHARGE WEIGHT=7.64 lb
7 ft
11 ft
16 ft
21 ft
26 ft
31 ft
PRESSURE (psi)
TIME (msec)

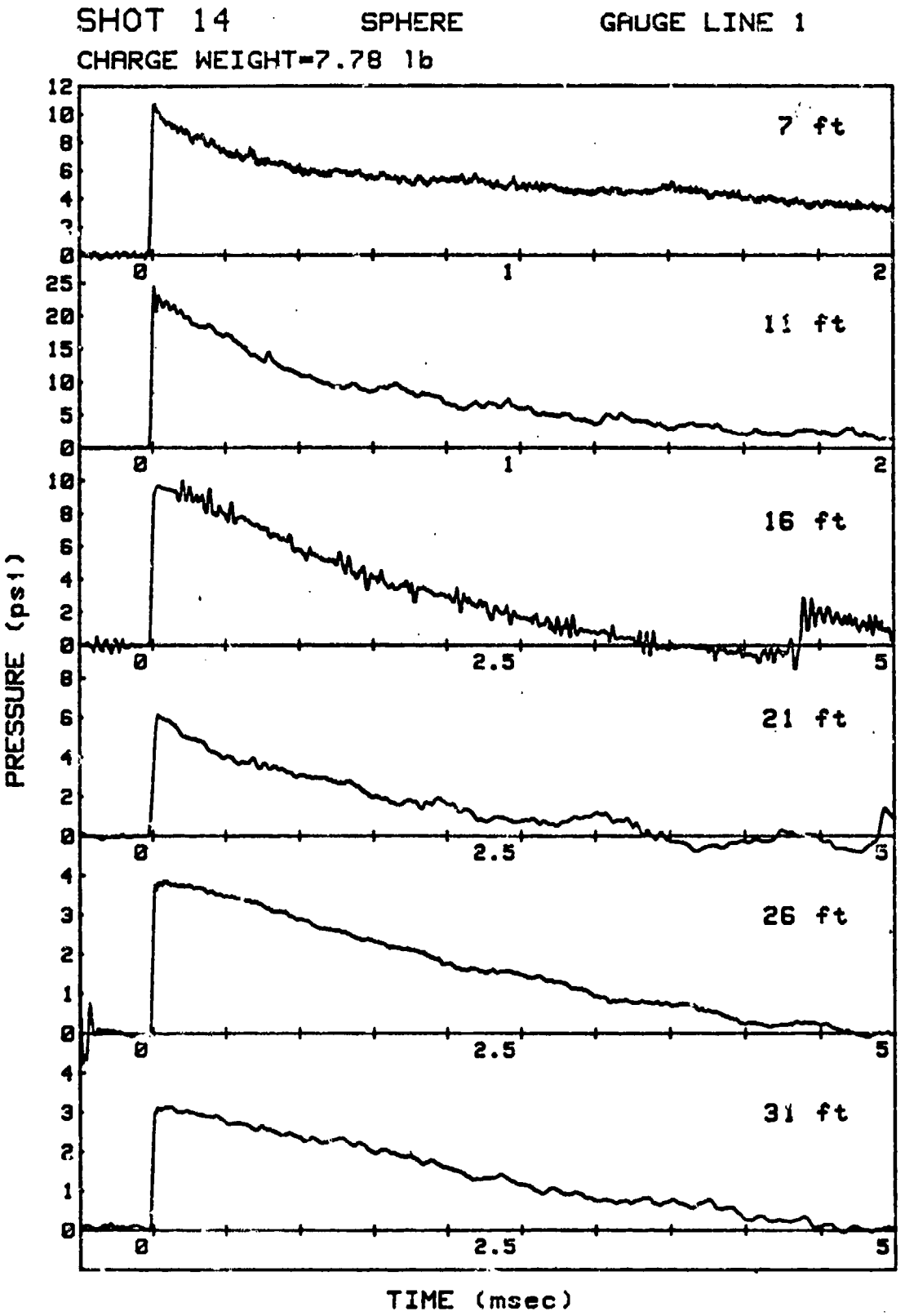
SHOT 14
SPHERE
GAUGE LINE 1
CHARGE WEIGHT=7.78 lb
7 ft
11 ft
16 ft
21 ft
26 ft
31 ft
PRESSURE (psi)
TIME (msec)

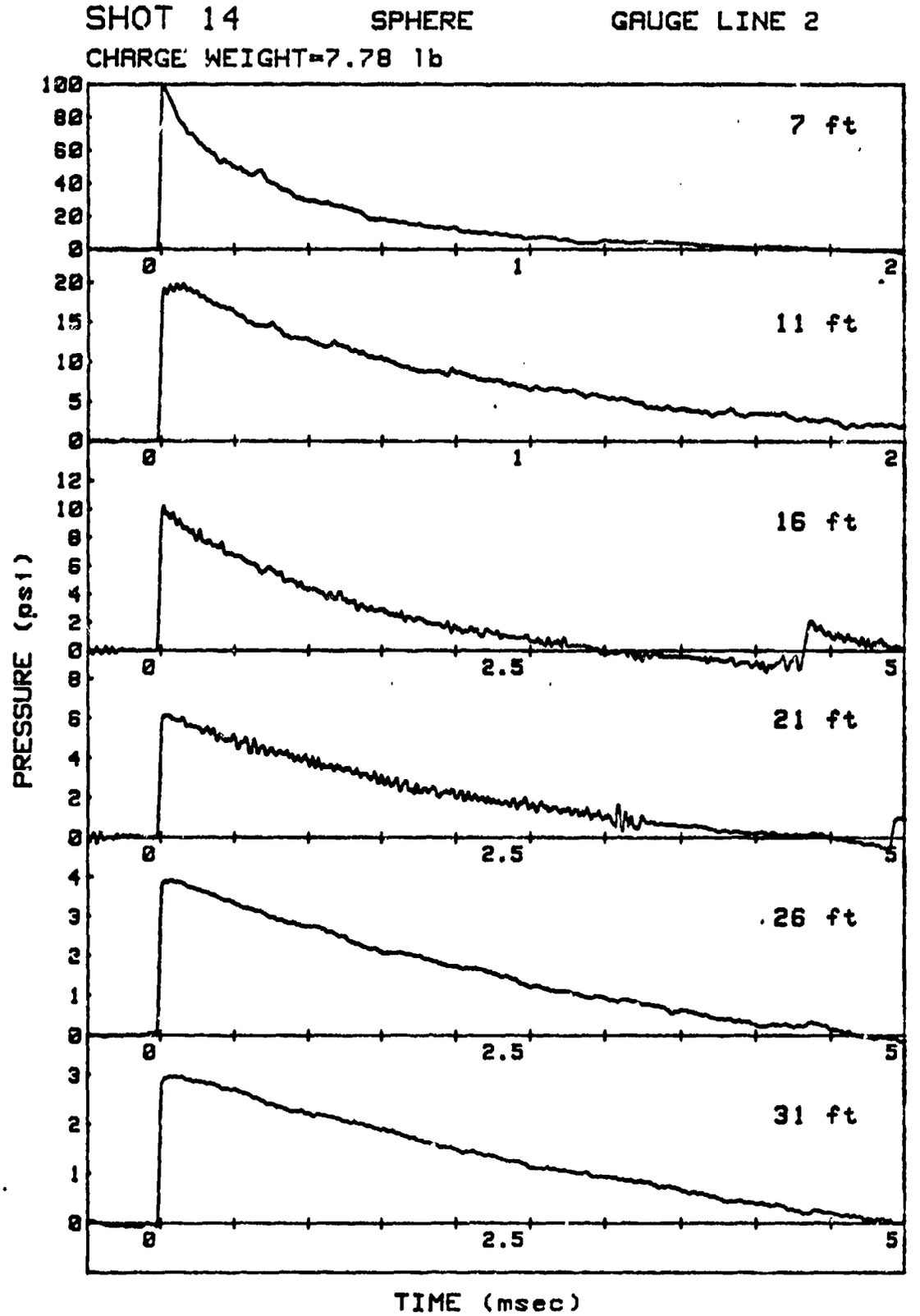
SHOT 14 SPHERE GAUGE LINE 2
CHARGE WEIGHT=7.78 lb
7 ft
11 ft
16 ft
21 ft
26 ft
31 ft
PRESSURE (psi)
TIME (msec)

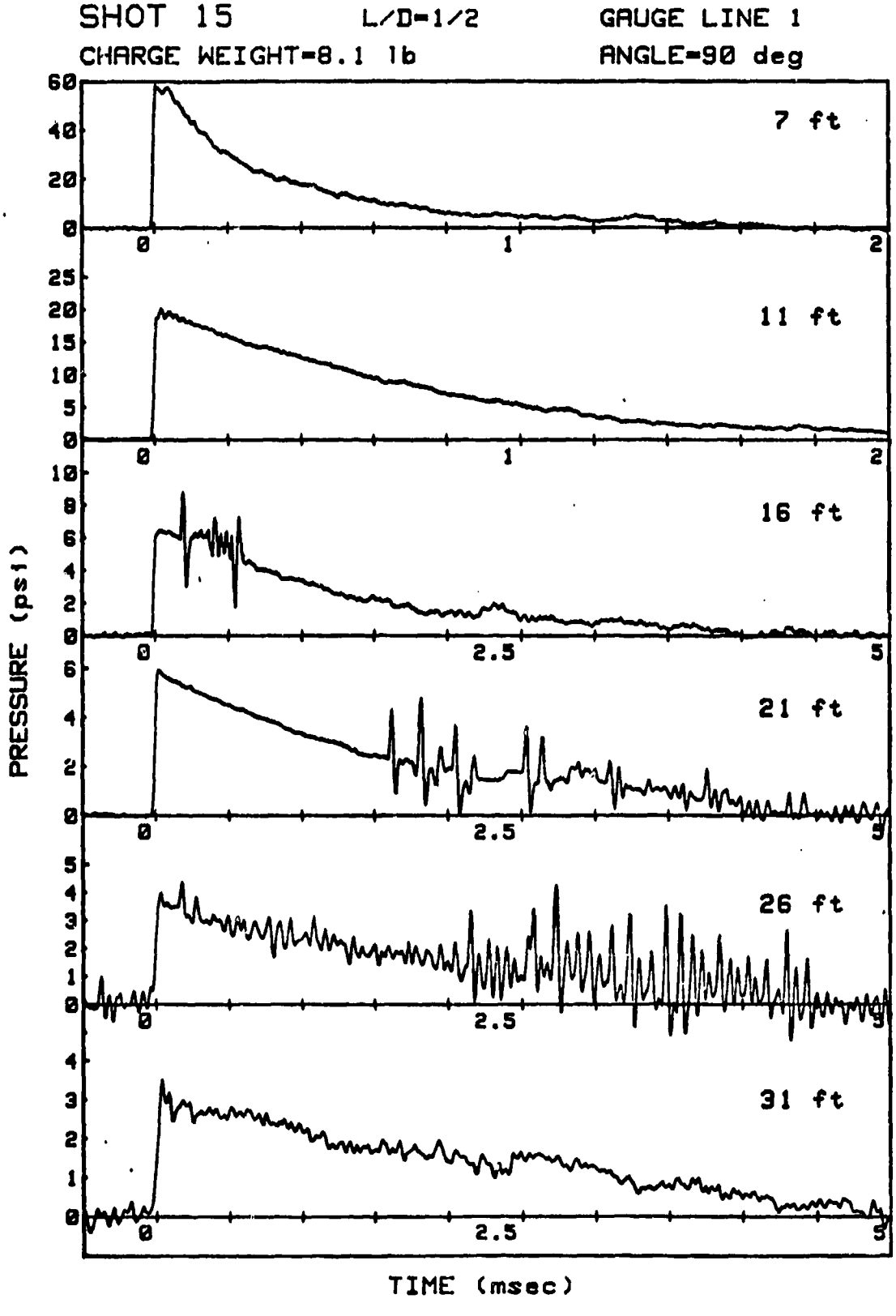
SHOT 15
L/D=1/2
GAUGE LINE 1
CHARGE WEIGHT=8.1 lb
ANGLE=90 deg
7 ft
11 ft
16 ft
21 ft
26 ft
31 ft
PRESSURE (psi)
TIME (msec)

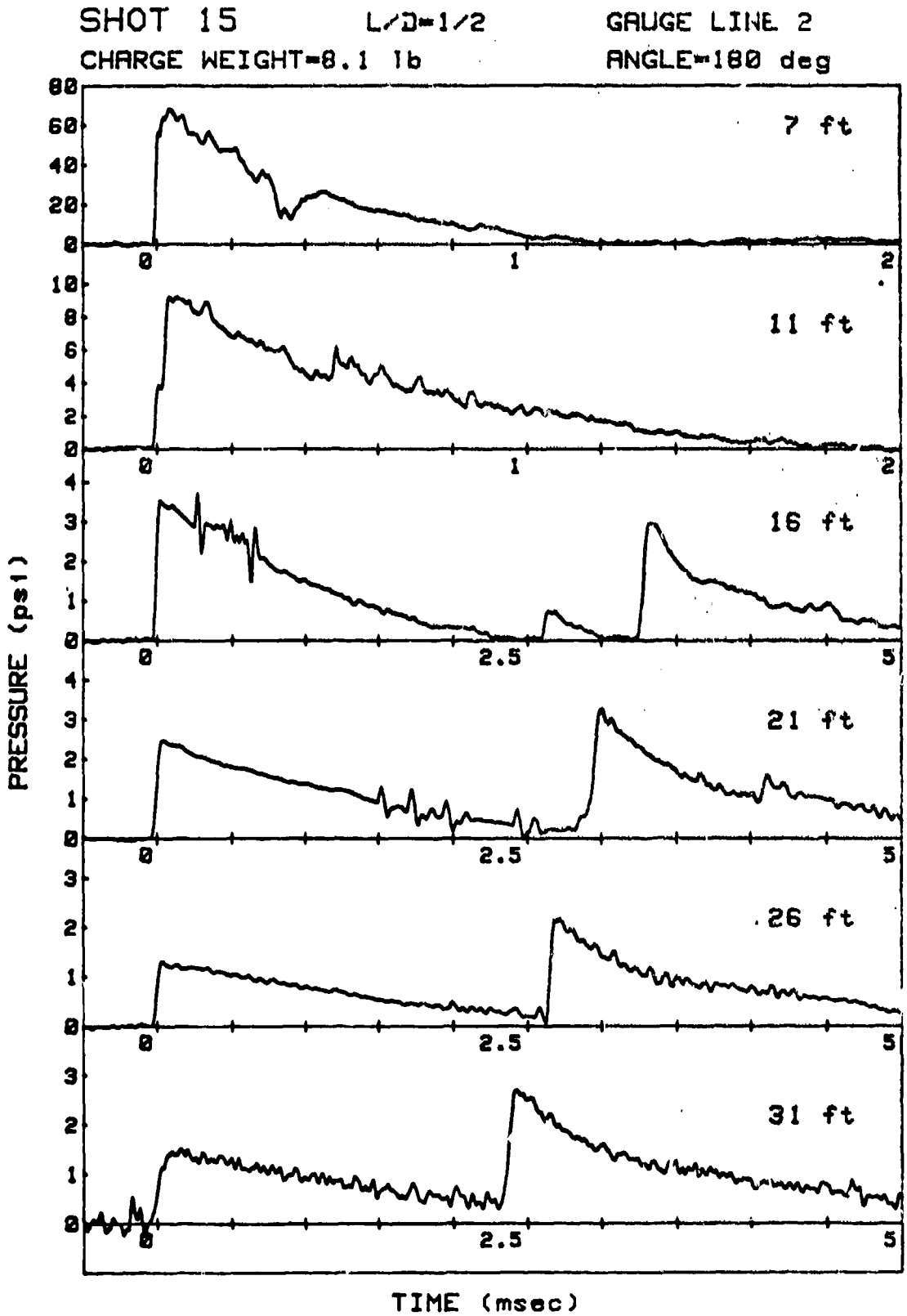
SHOT 15
L/D=1/2
GAUGE LINE 2
CHARGE WEIGHT=8.1 lb
ANGLE=180 deg
7 ft
11 ft
16 ft
21 ft
26 ft
31 ft
PRESSURE (psi)
TIME (msec)

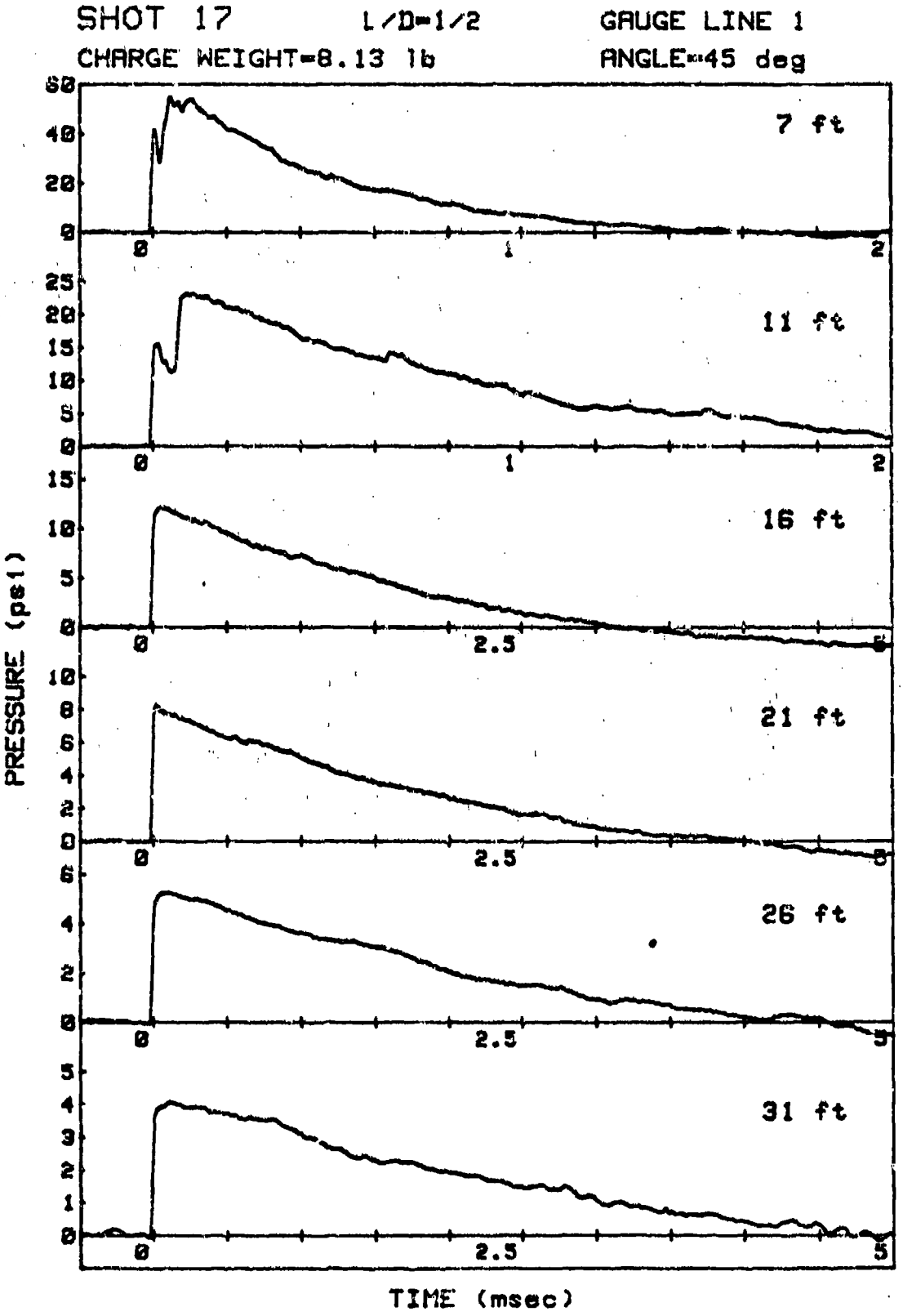
SHOT 17
L/D=1/2
GAUGE LINE 1
CHARGE WEIGHT=8.13 lb
ANGLE=45 deg
7 ft
11 ft
16 ft
21 ft
26 ft
31 ft
PRESSURE (psi)
TIME (msec)

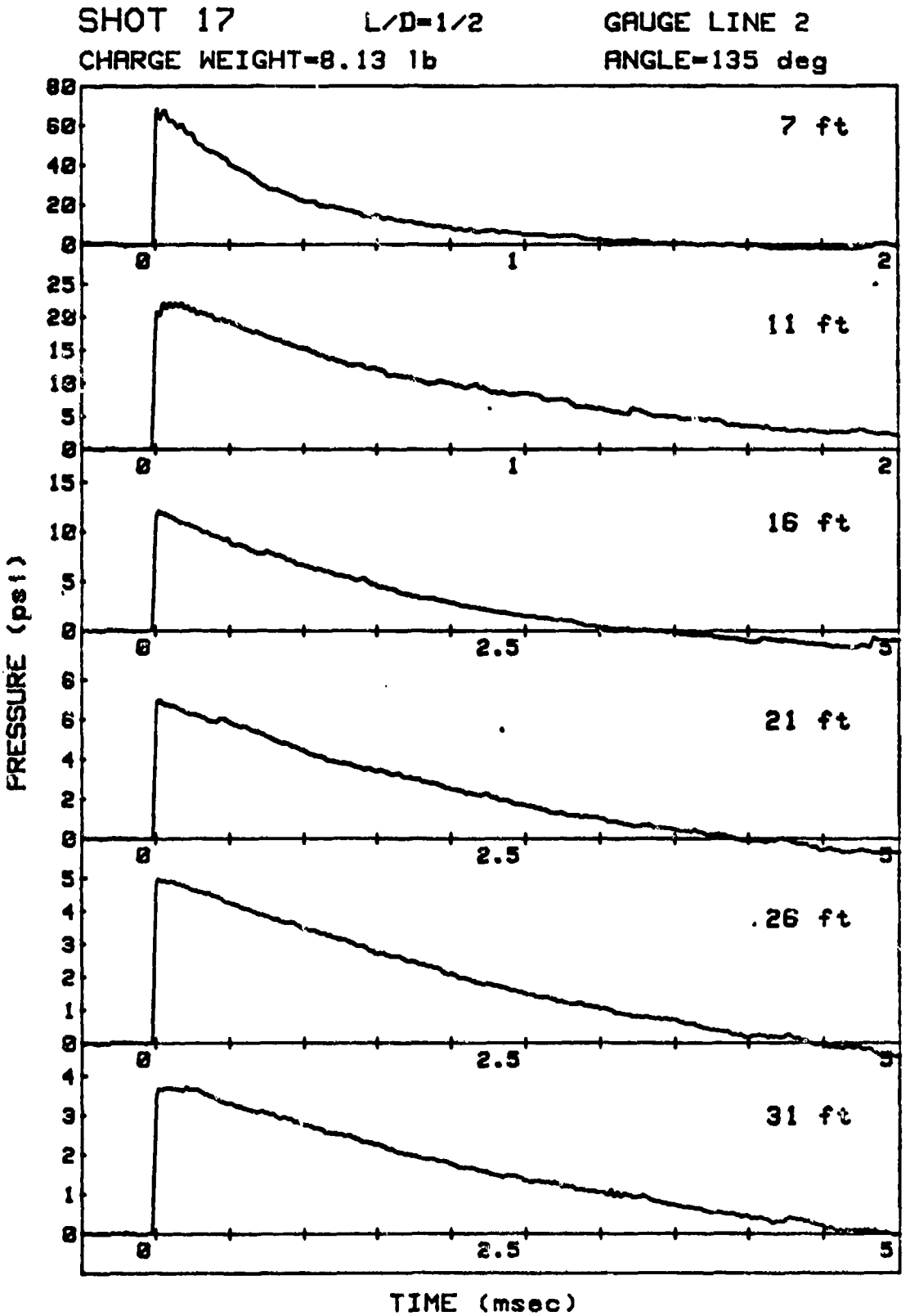
SHOT 17
L/D=1/2
GAUGE LINE 2
CHARGE WEIGHT=8.13 lb
ANGLE=135 deg
7 ft
11 ft
16 ft
21 ft
.26 ft
31 ft
PRESSURE (psi)
TIME (msec)

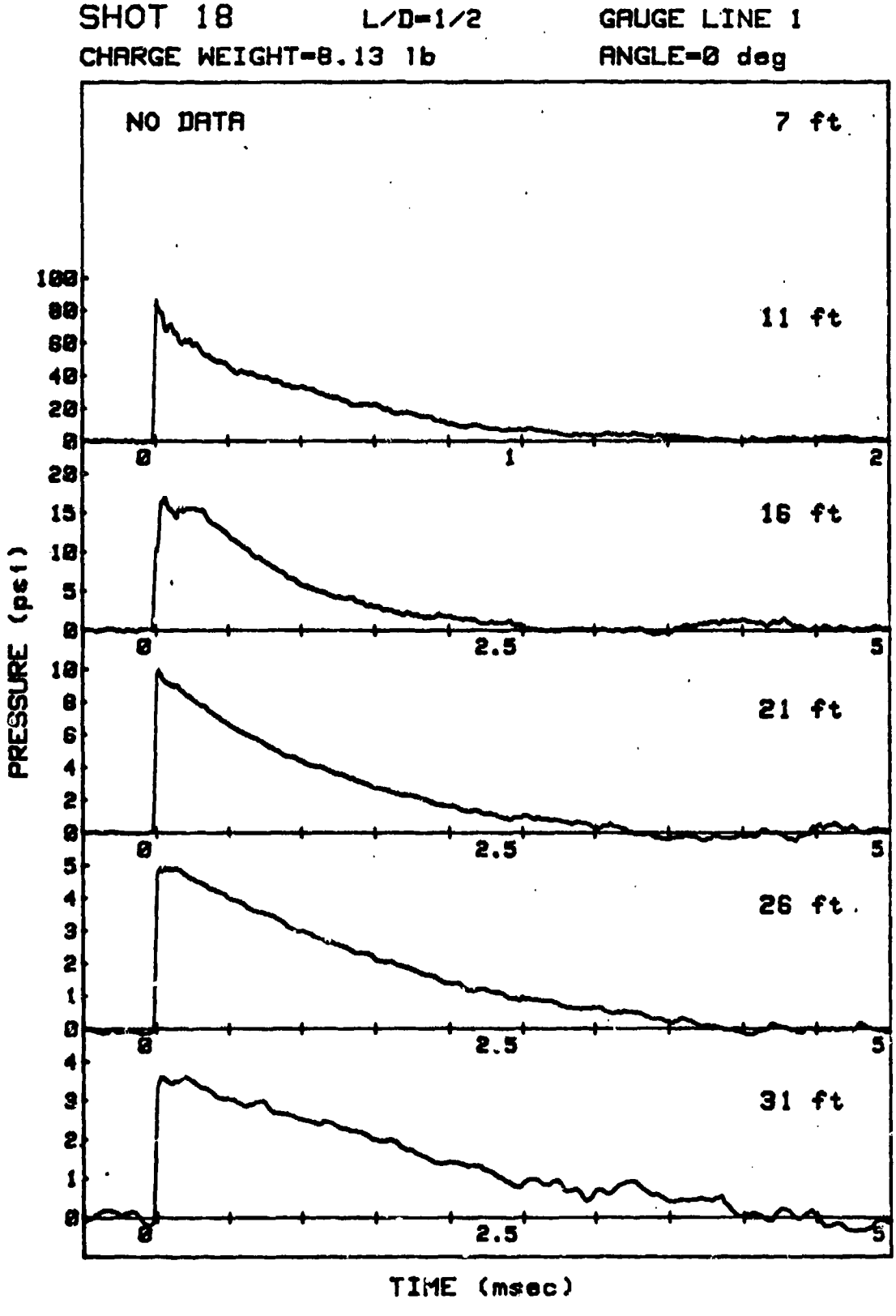
SHOT 18
L/D=1/2
GAUGE LINE 1
CHARGE WEIGHT=8.13 lb
ANGLE=0 deg
NO DATA
7 ft
11 ft
16 ft
21 ft
26 ft
31 ft
PRESSURE (psi)
TIME (msec)

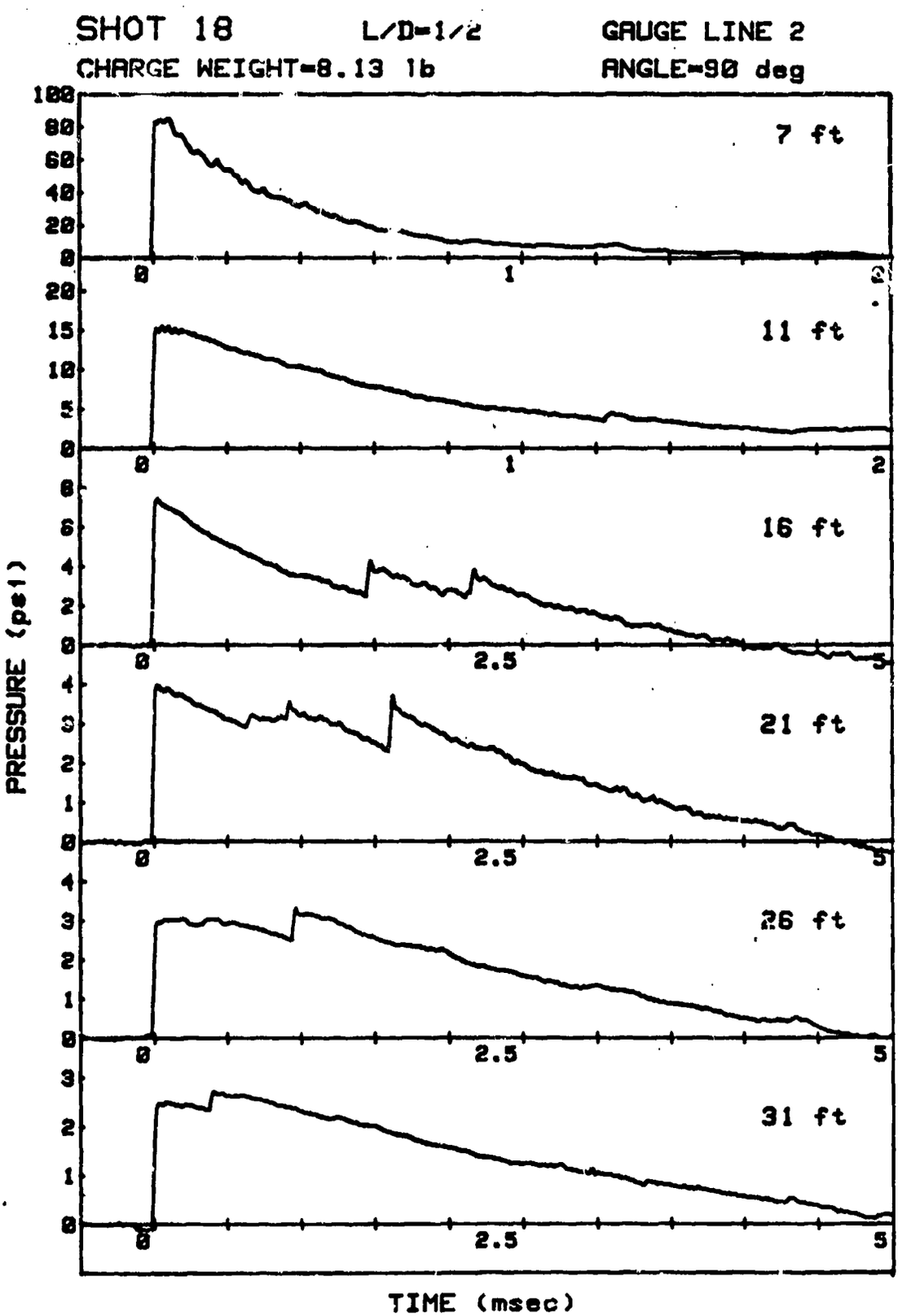
SHOT 18
L/D=1/2
GAUGE LINE 2
CHARGE WEIGHT=8.13 lb
ANGLE=90 deg
7 ft
11 ft
16 ft
21 ft
26 ft
31 ft
PRESSURE (psi)
TIME (msec)

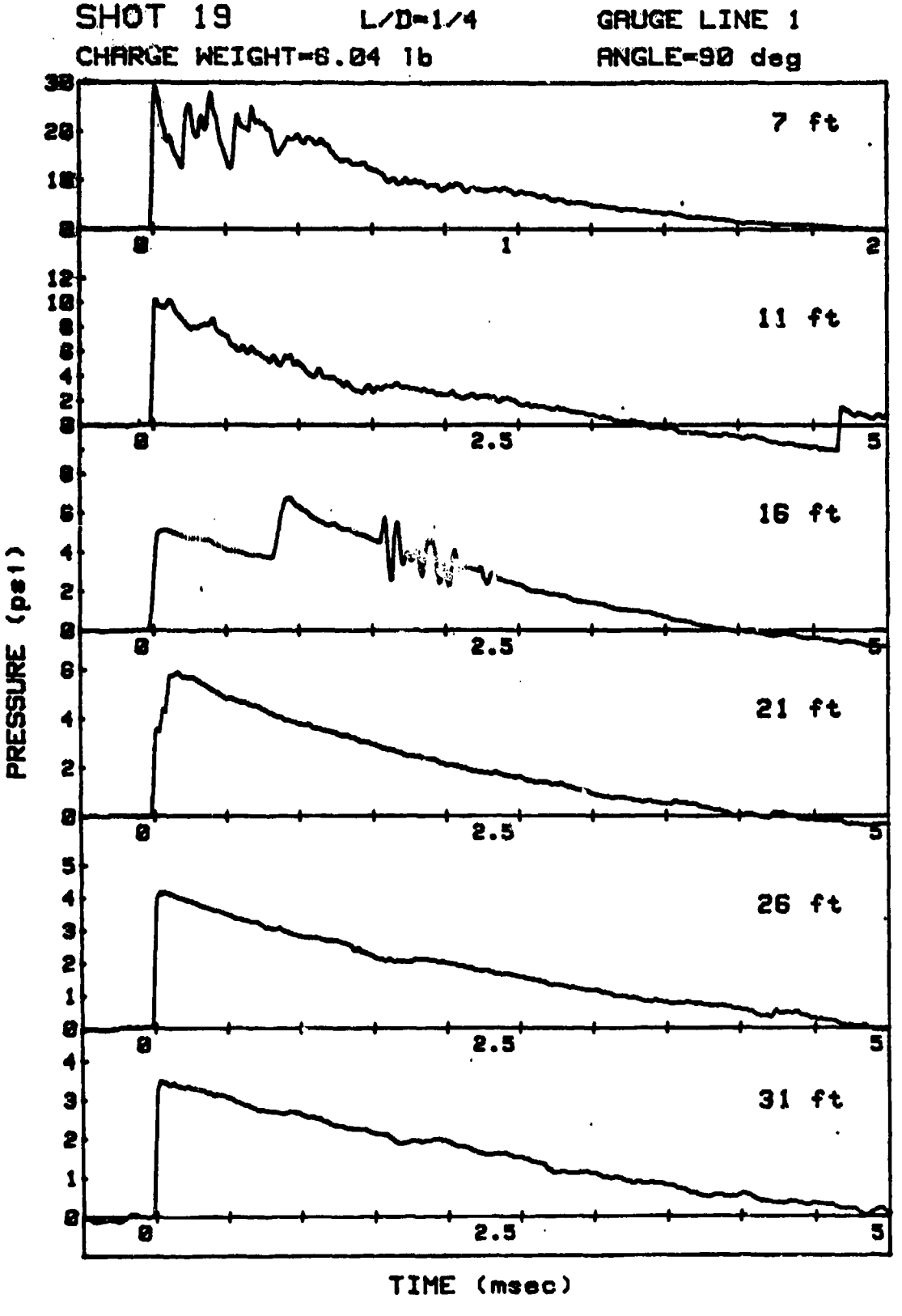
SHOT 19
L/D=1/4
GAUGE LINE 1
CHARGE WEIGHT=8.04 lb
ANGLE=90 deg
7 ft
11 ft
16 ft
21 ft
26 ft
31 ft
PRESSURE (psi)
TIME (msec)

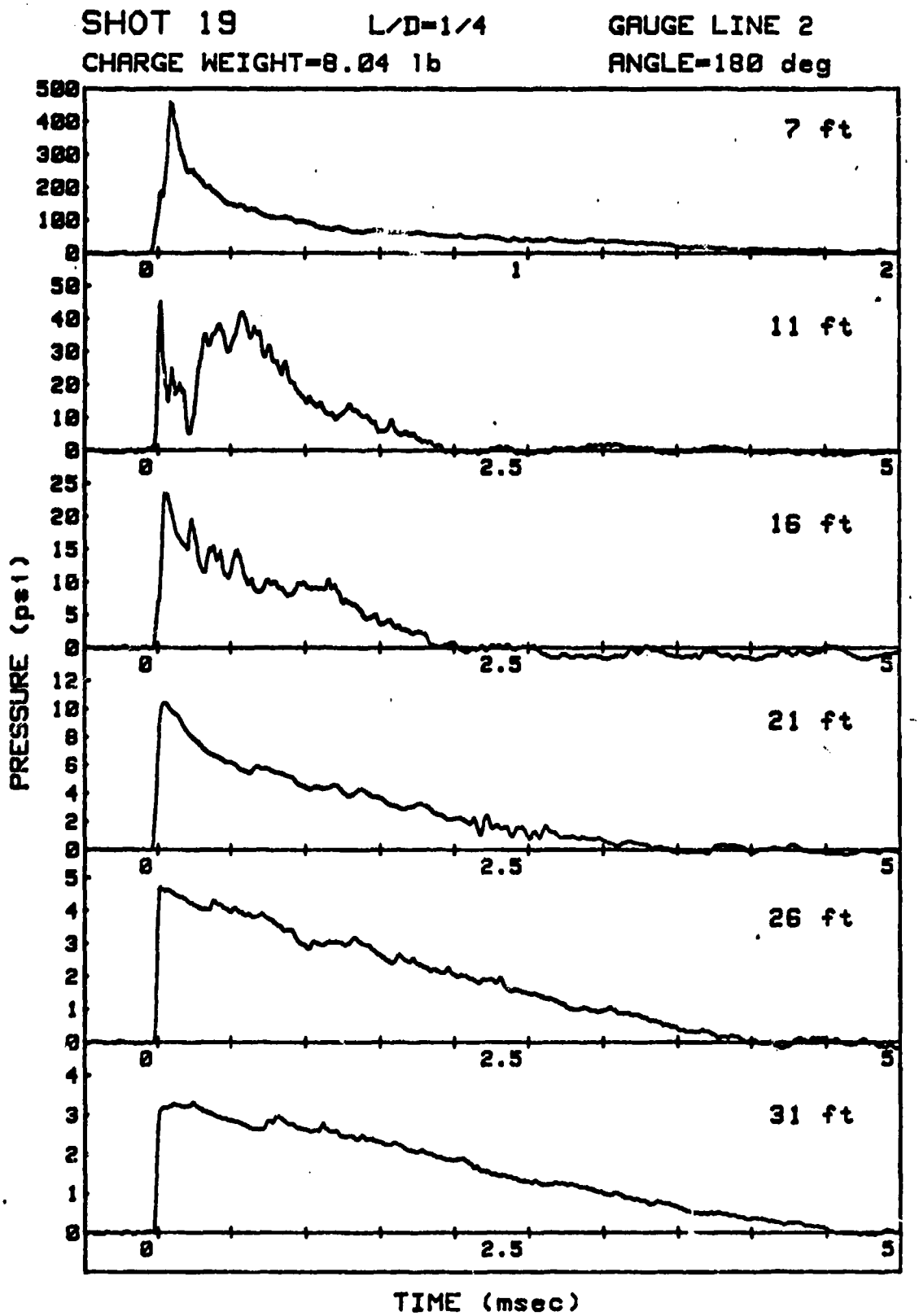
SHOT 19
L/D=1/4
GAUGE LINE 2
CHARGE WEIGHT=8.04 lb
ANGLE=180 deg
7 ft
11 ft
16 ft
21 ft
26 ft
31 ft
PRESSURE (psi)
TIME (msec)

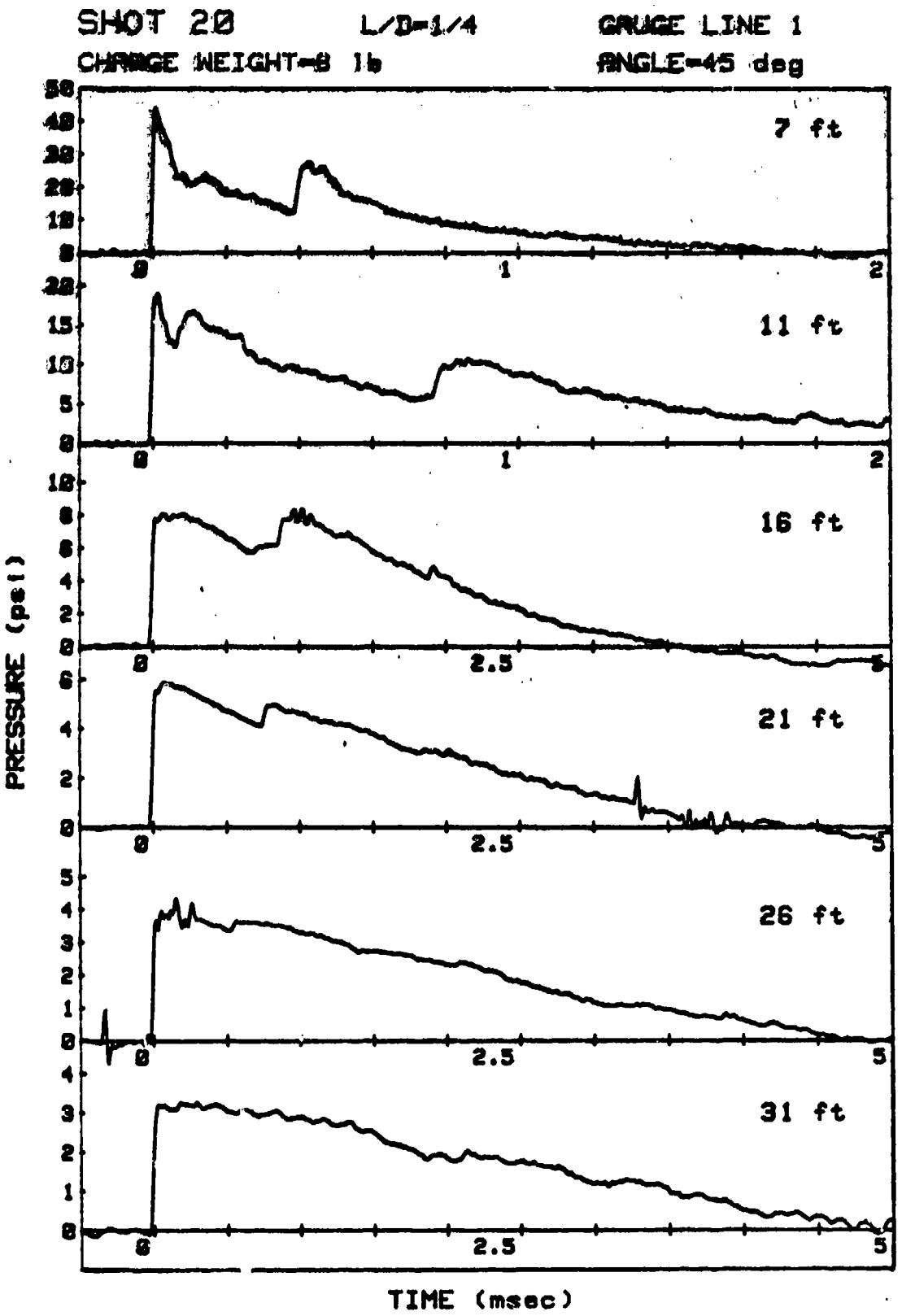
SHOT 20
L/D=1/4
GAUGE LINE 1
CHARGE WEIGHT=8 lb
ANGLE=45 deg
7 ft
11 ft
16 ft
21 ft
26 ft
31 ft
PRESSURE (psi)
TIME (msec)

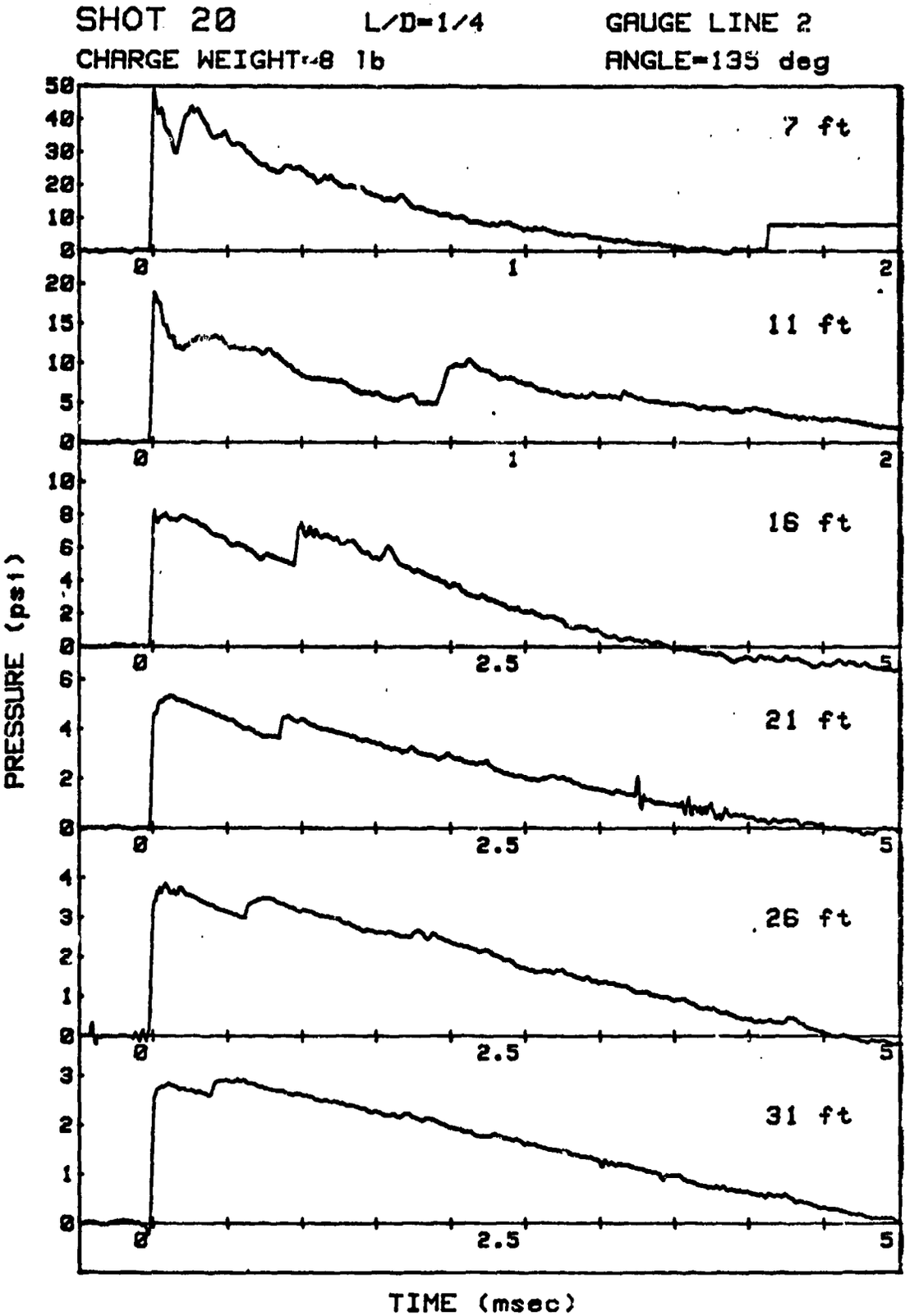
SHOT 20
L/D=1/4
GAUGE LINE 2
CHARGE WEIGHT=8 lb
ANGLE=135 deg
7 ft
11 ft
16 ft
21 ft
26 ft
31 ft
PRESSURE (psi)
TIME (msec)

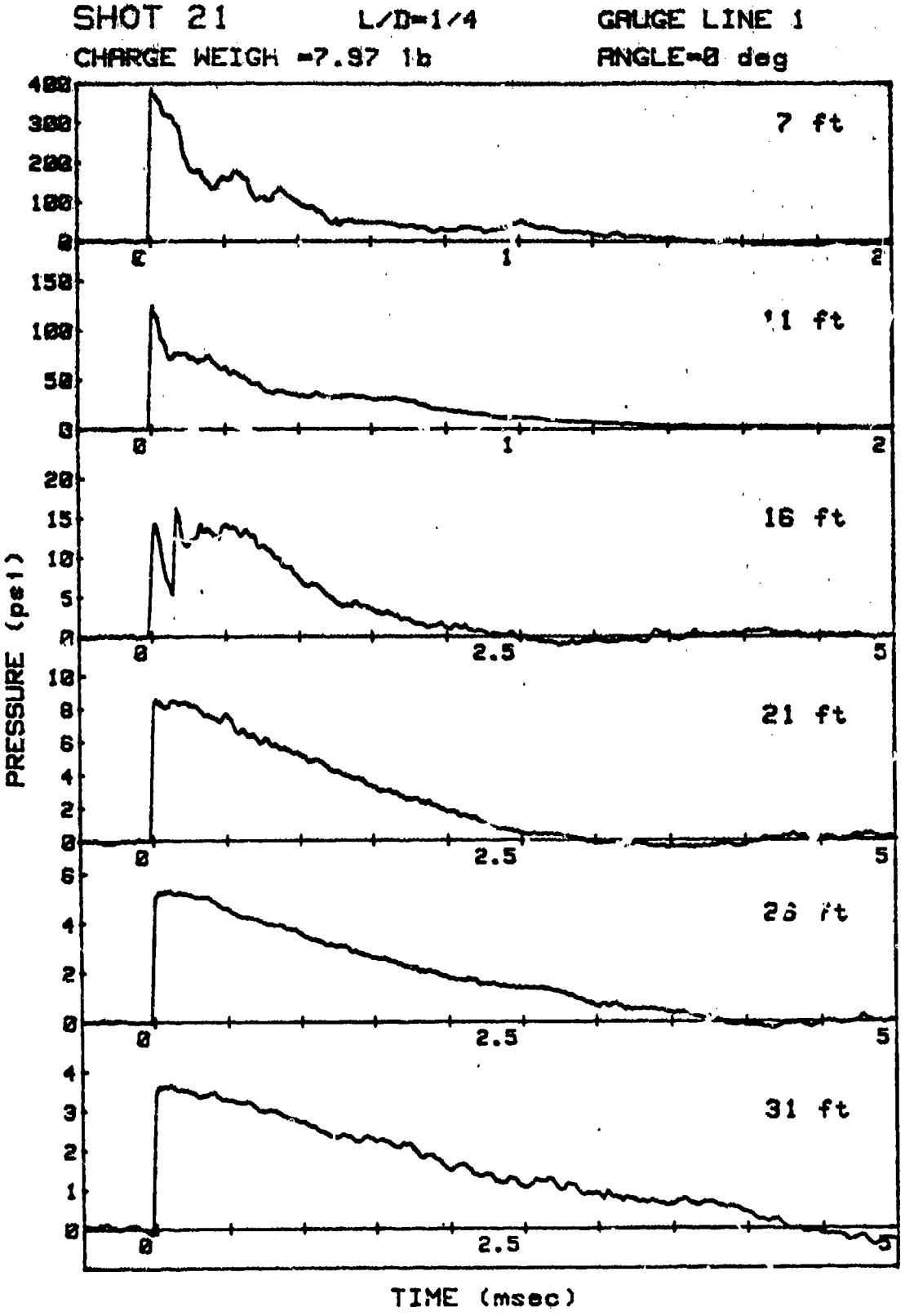
SHOT 21
L/D=1/4
GAUGE LINE 1
CHARGE WEIGH =7.97 lb
ANGLE=0 deg
7 ft
11 ft
16 ft
21 ft
26 ft
31 ft
PRESSURE (psi)
TIME (msec)

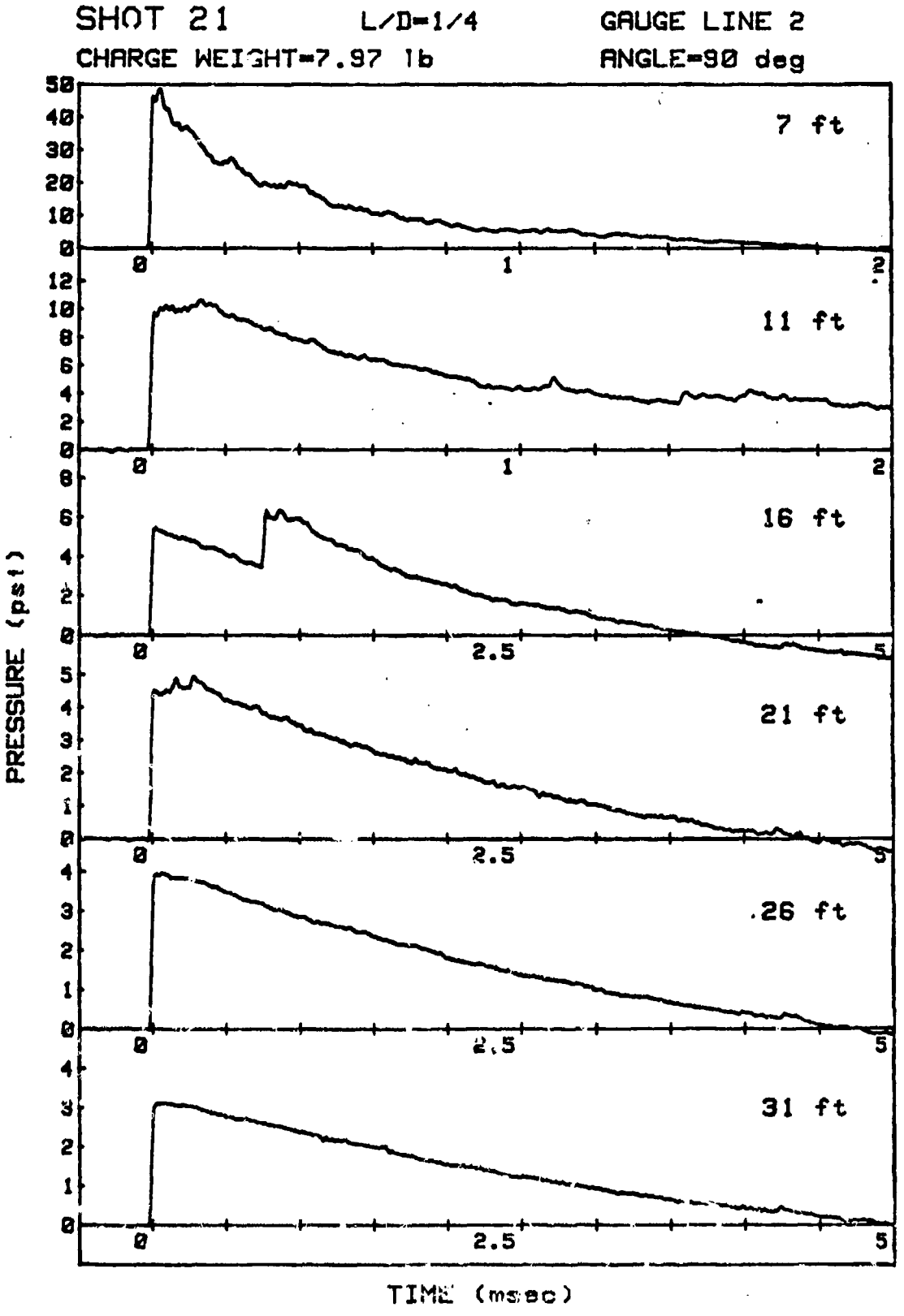
SHOT 21
L/D=1/4
GAUGE LINE 2
CHARGE WEIGHT=7.97 lb
ANGLE=90 deg
7 ft
11 ft
16 ft
21 ft
26 ft
31 ft
PRESSURE (psi)
TIME (msec)

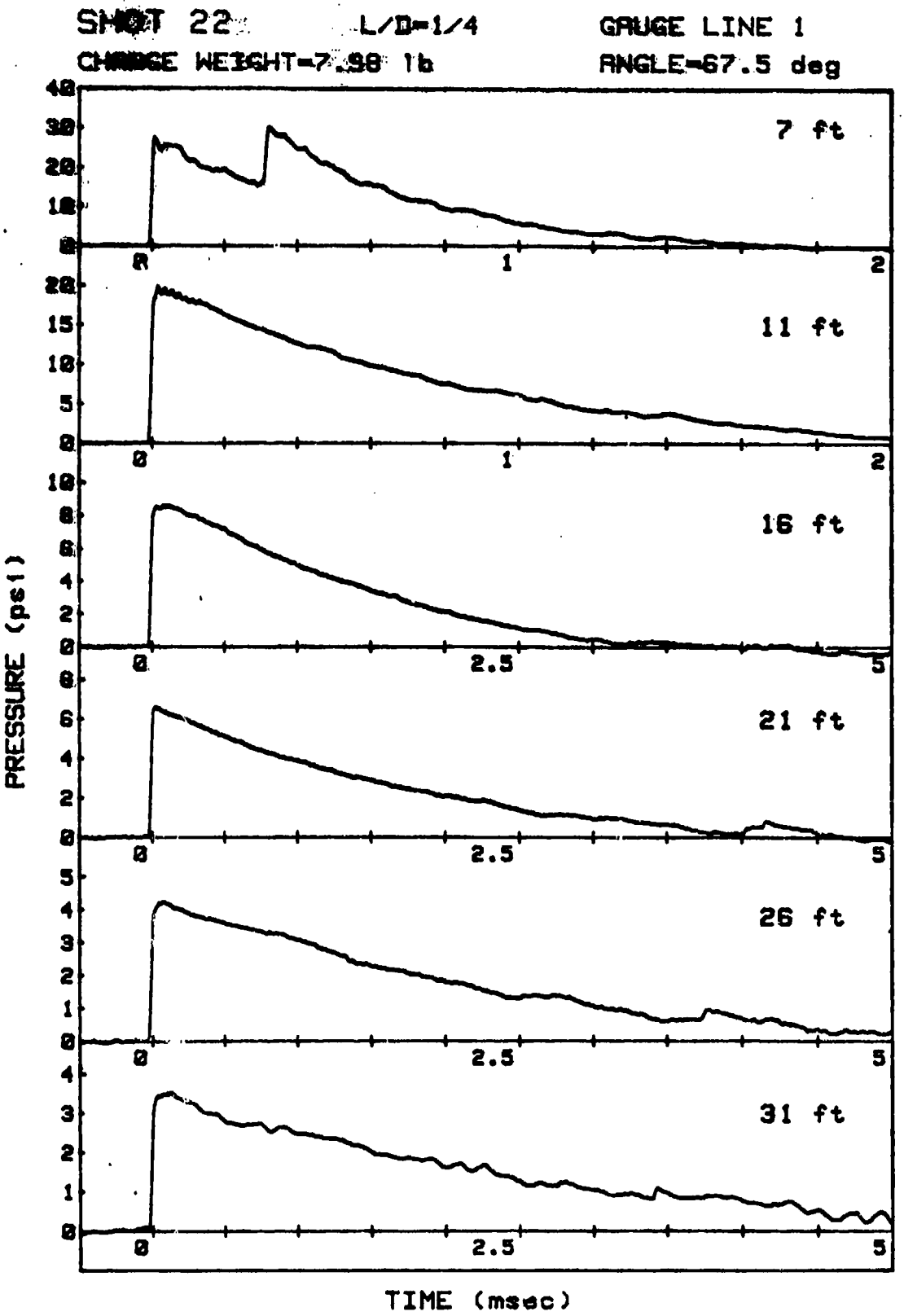
SHOT 22
L/D=1/4
GAUGE LINE 1
CHARGE WEIGHT=7.98 lb
ANGLE=67.5 deg
7 ft
11 ft
16 ft
21 ft
26 ft
31 ft
PRESSURE (psi)
TIME (msec)

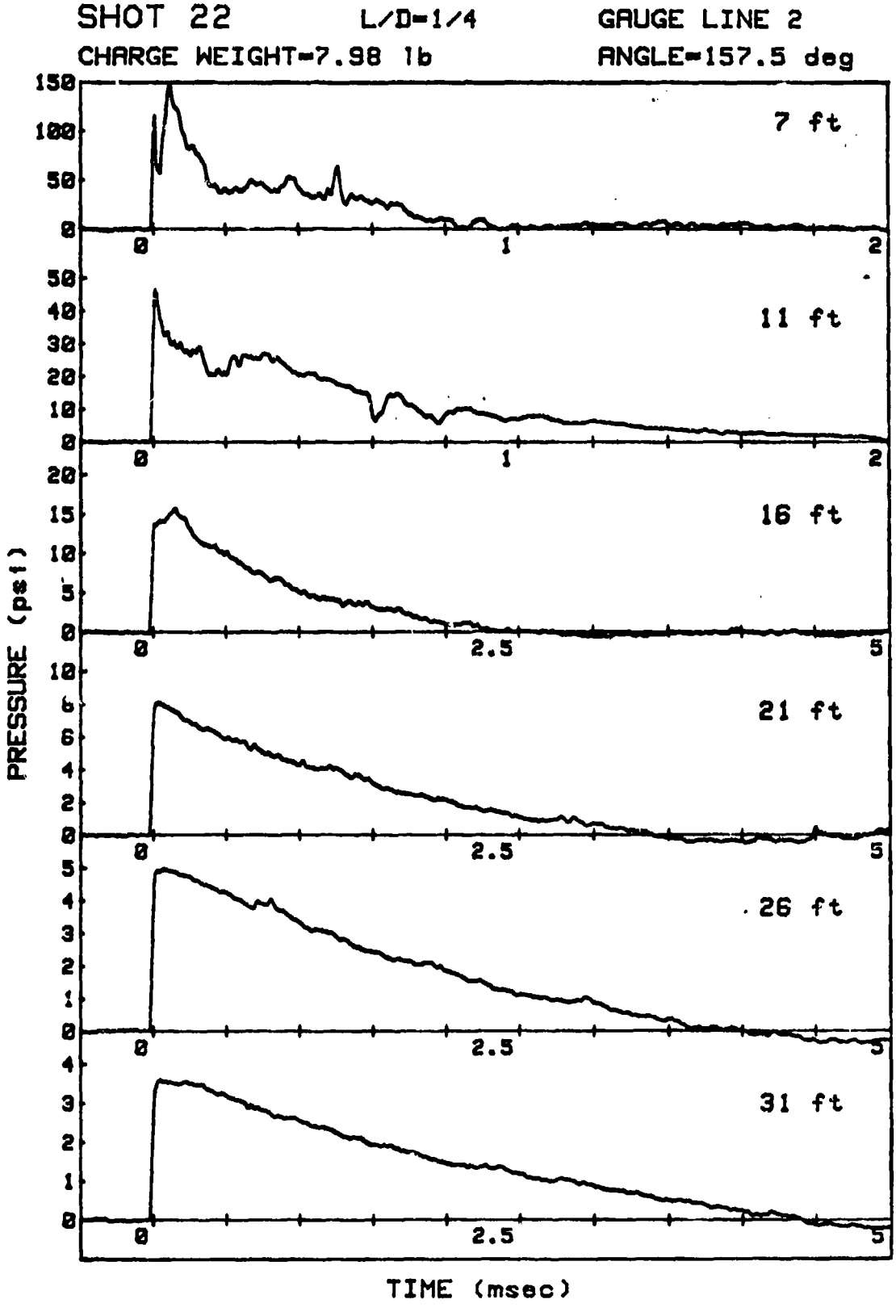
SHOT 22
L/D=1/4
GAUGE LINE 2
CHARGE WEIGHT=7.98 lb
ANGLE=157.5 deg
7 ft
11 ft
16 ft
21 ft
26 ft
31 ft
PRESSURE (psi)
TIME (msec)

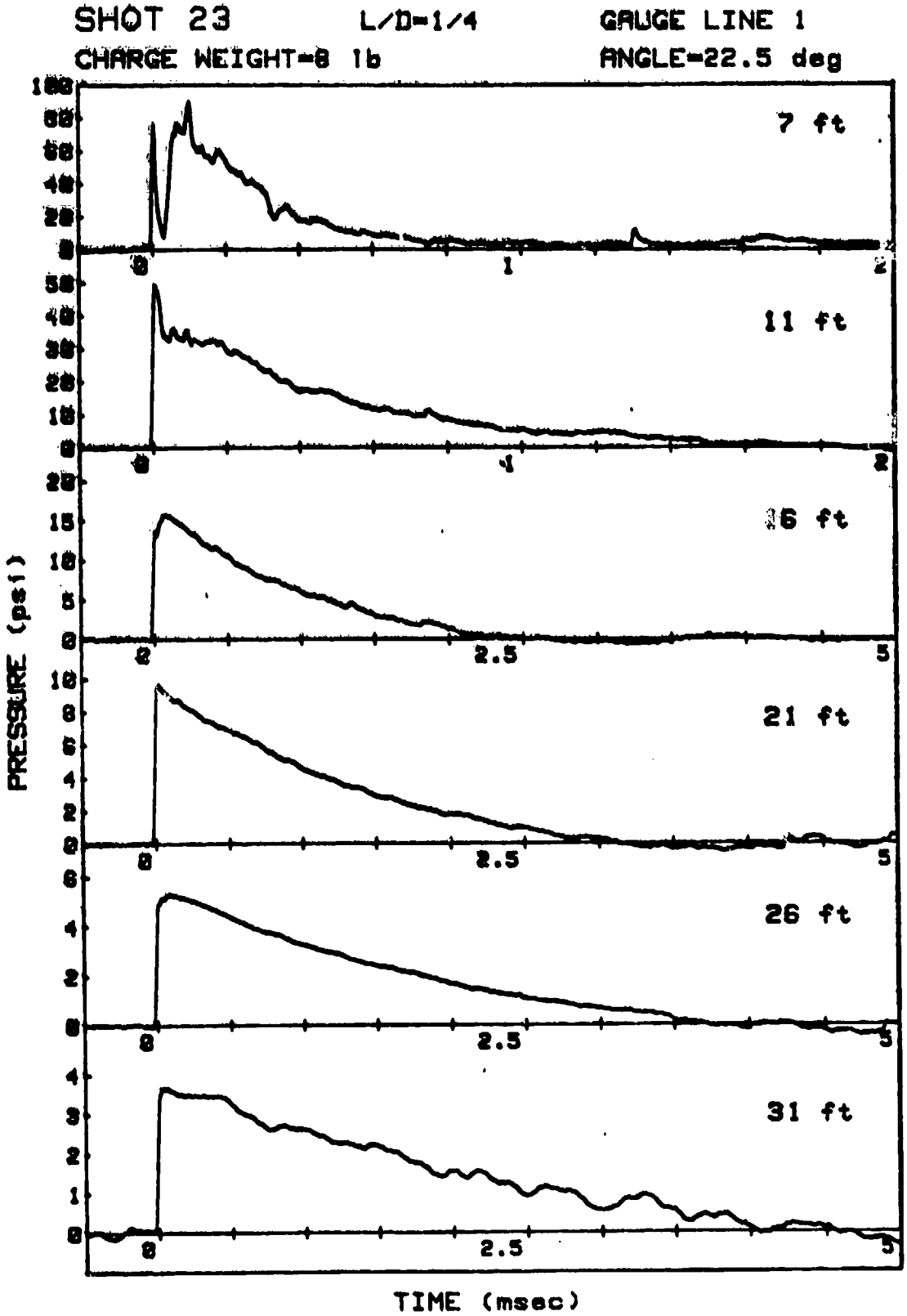
SHOT 23
L/D=1/4
GAUGE LINE 1
CHARGE WEIGHT=8 lb
ANGLE=22.5 deg
7 ft
11 ft
16 ft
21 ft
26 ft
31 ft
PRESSURE (psi)
TIME (msec)

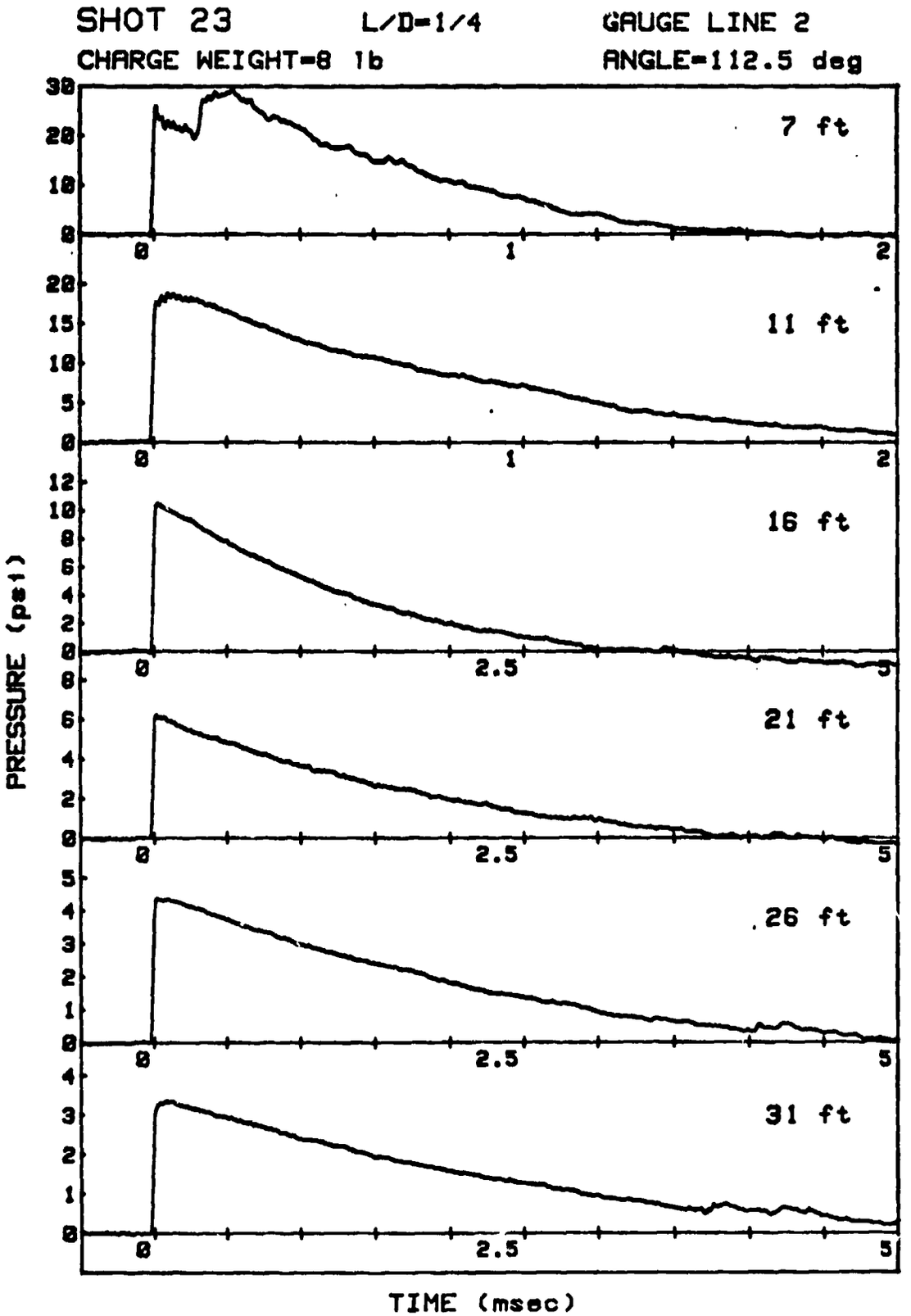
SHOT 23
L/D=1/4
GAUGE LINE 2
CHARGE WEIGHT=8 lb
ANGLE=112.5 deg
7 ft
11 ft
16 ft
21 ft
26 ft
31 ft
PRESSURE (psi)
TIME (msec)

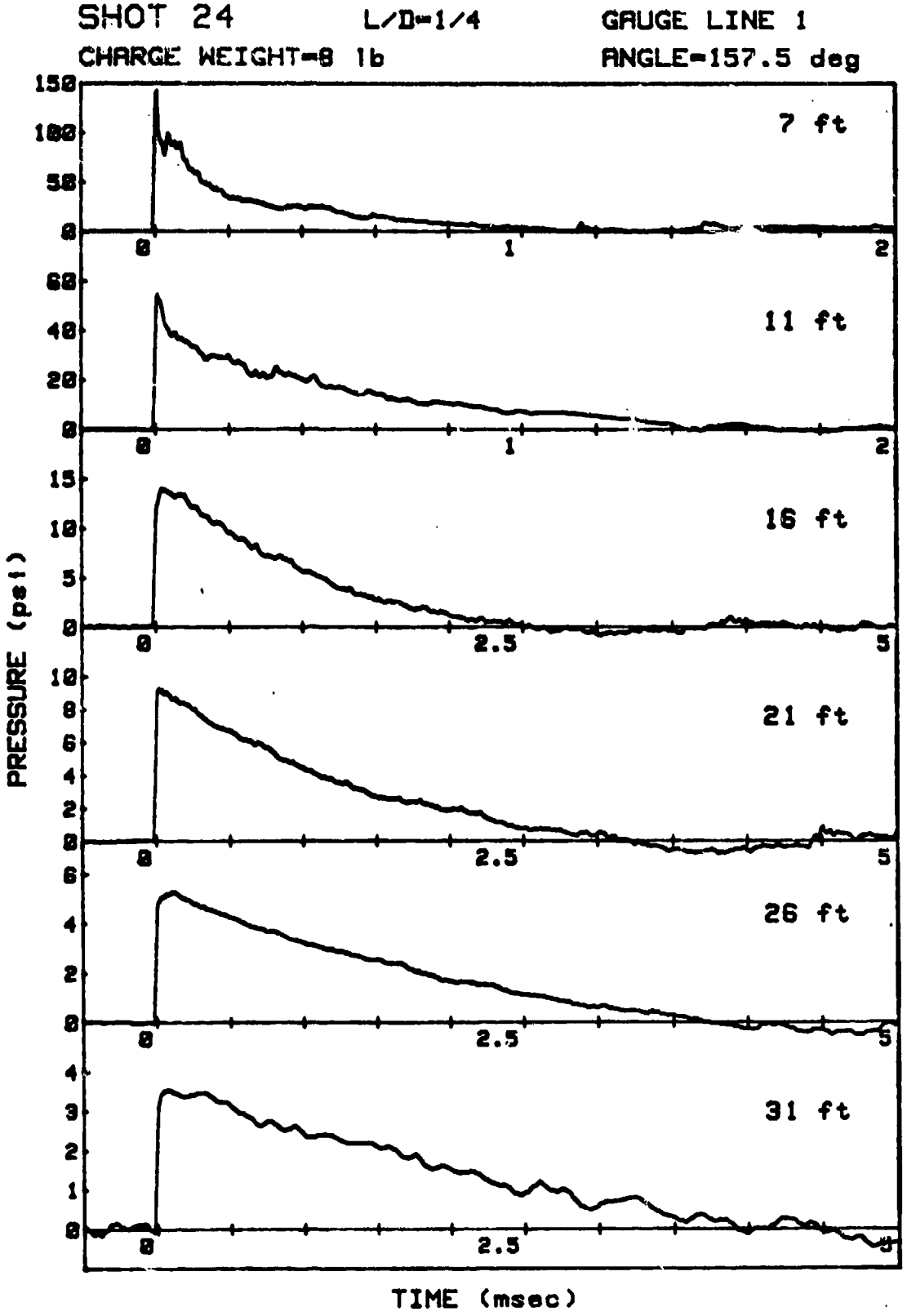
SHOT 24
L/D=1/4
GAUGE LINE 1
CHARGE WEIGHT=8 lb
ANGLE=157.5 deg
7 ft
11 ft
16 ft
21 ft
26 ft
31 ft
PRESSURE (psi)
TIME (msec)

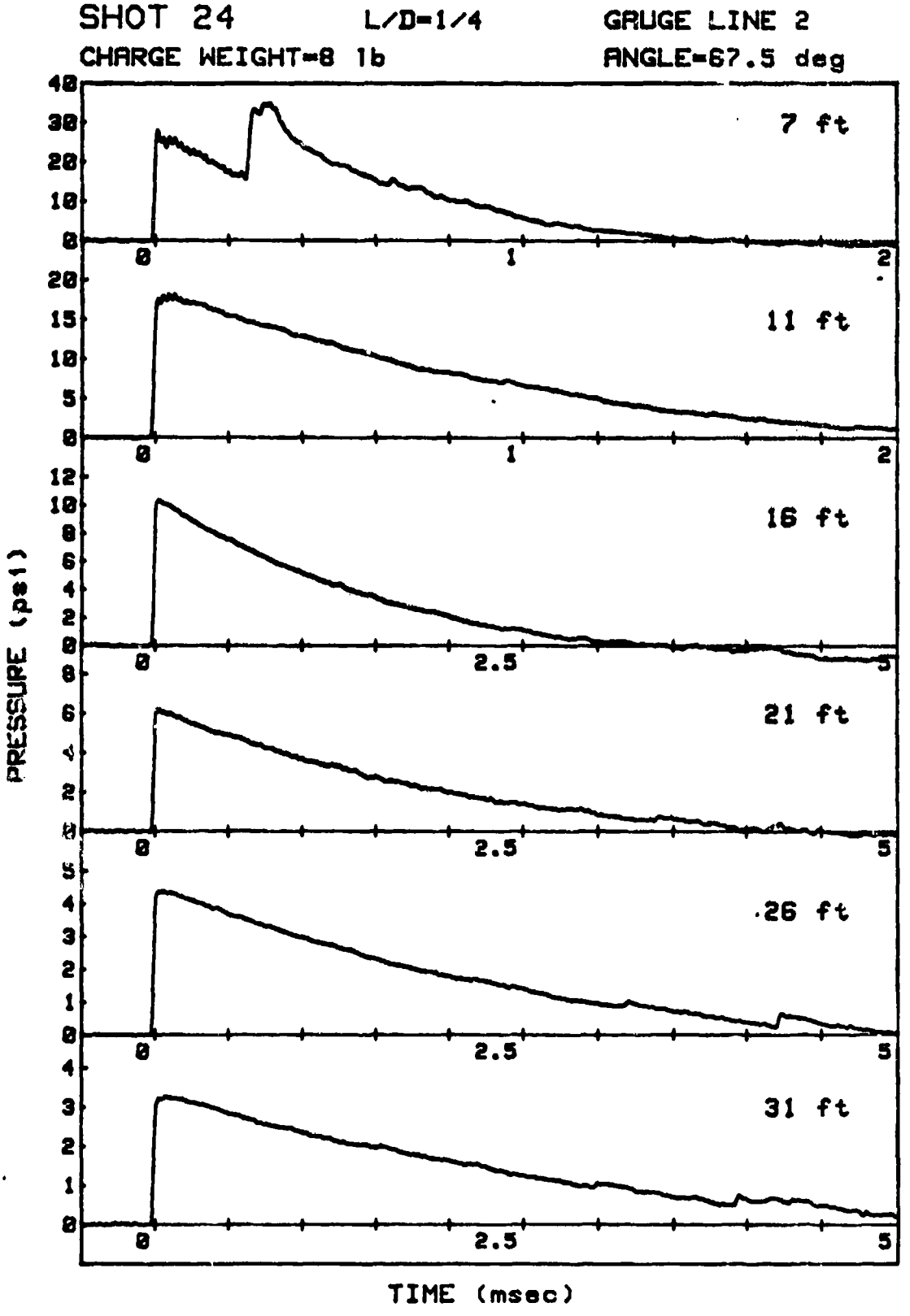
SHOT 24
L/D=1/4
GRUGE LINE 2
CHARGE WEIGHT=8 lb
ANGLE=67.5 deg
7 ft
11 ft
16 ft
21 ft
26 ft
31 ft
PRESSURE (psi)
TIME (msec)

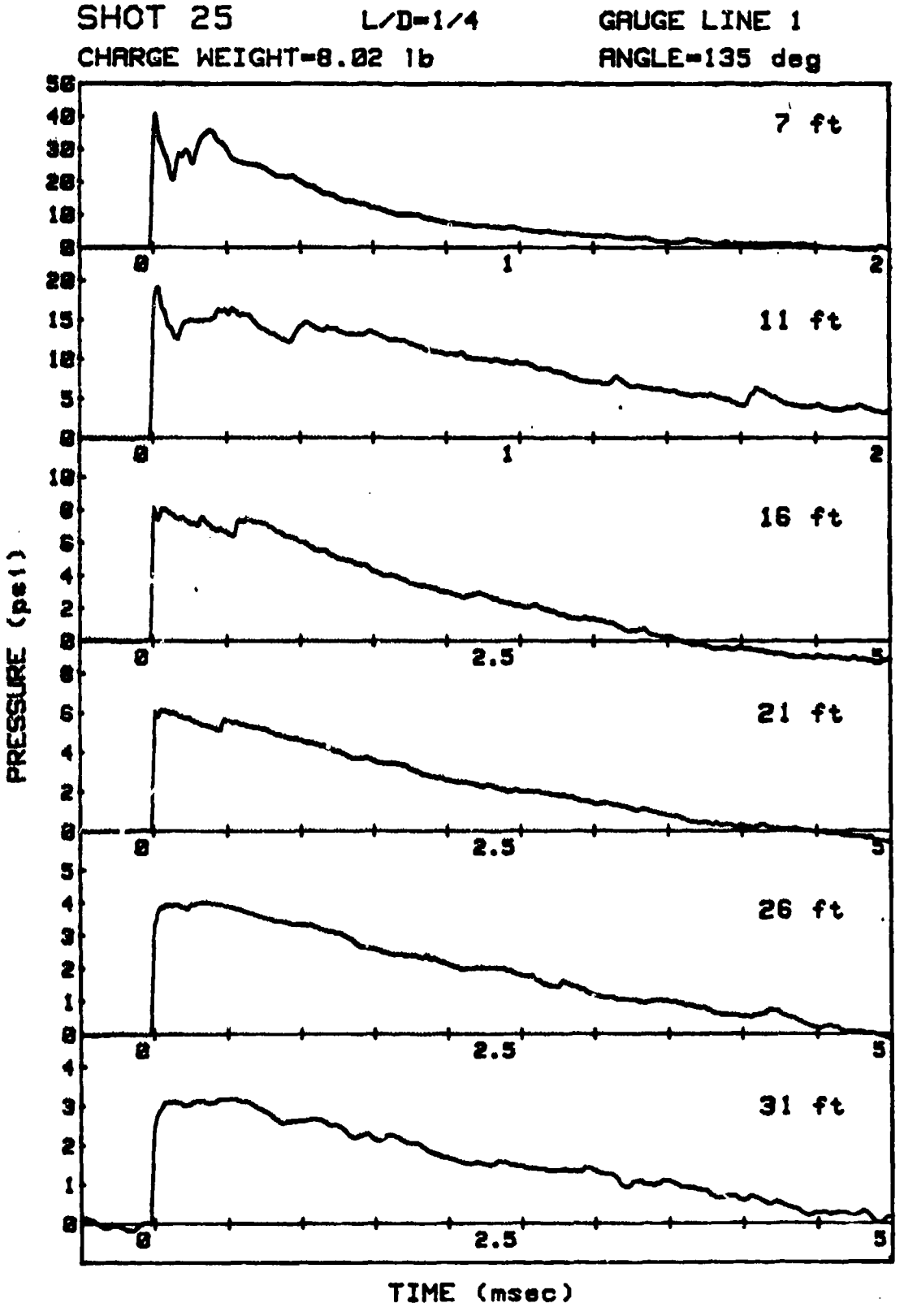
SHOT 25
L/D=1/4
GAUGE LINE 1
CHARGE WEIGHT=8.02 lb
ANGLE=135 deg
7 ft
11 ft
16 ft
21 ft
26 ft
31 ft
PRESSURE (psi)
TIME (msec)

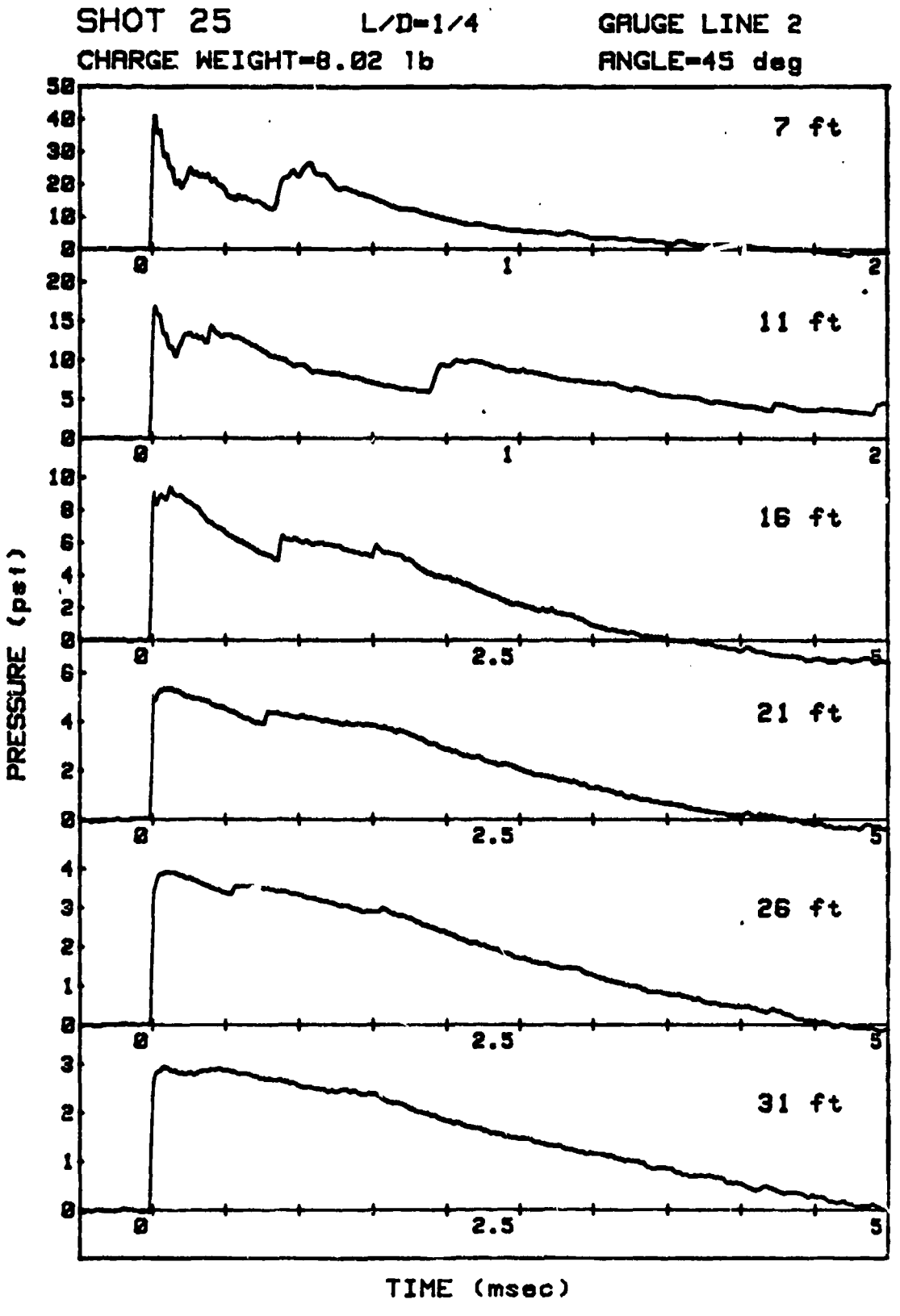
SHOT 25
L/D=1/4
GAUGE LINE 2
CHARGE WEIGHT=8.02 lb
ANGLE=45 deg
7 ft
11 ft
16 ft
21 ft
26 ft
31 ft
PRESSURE (psi)
TIME (msec)

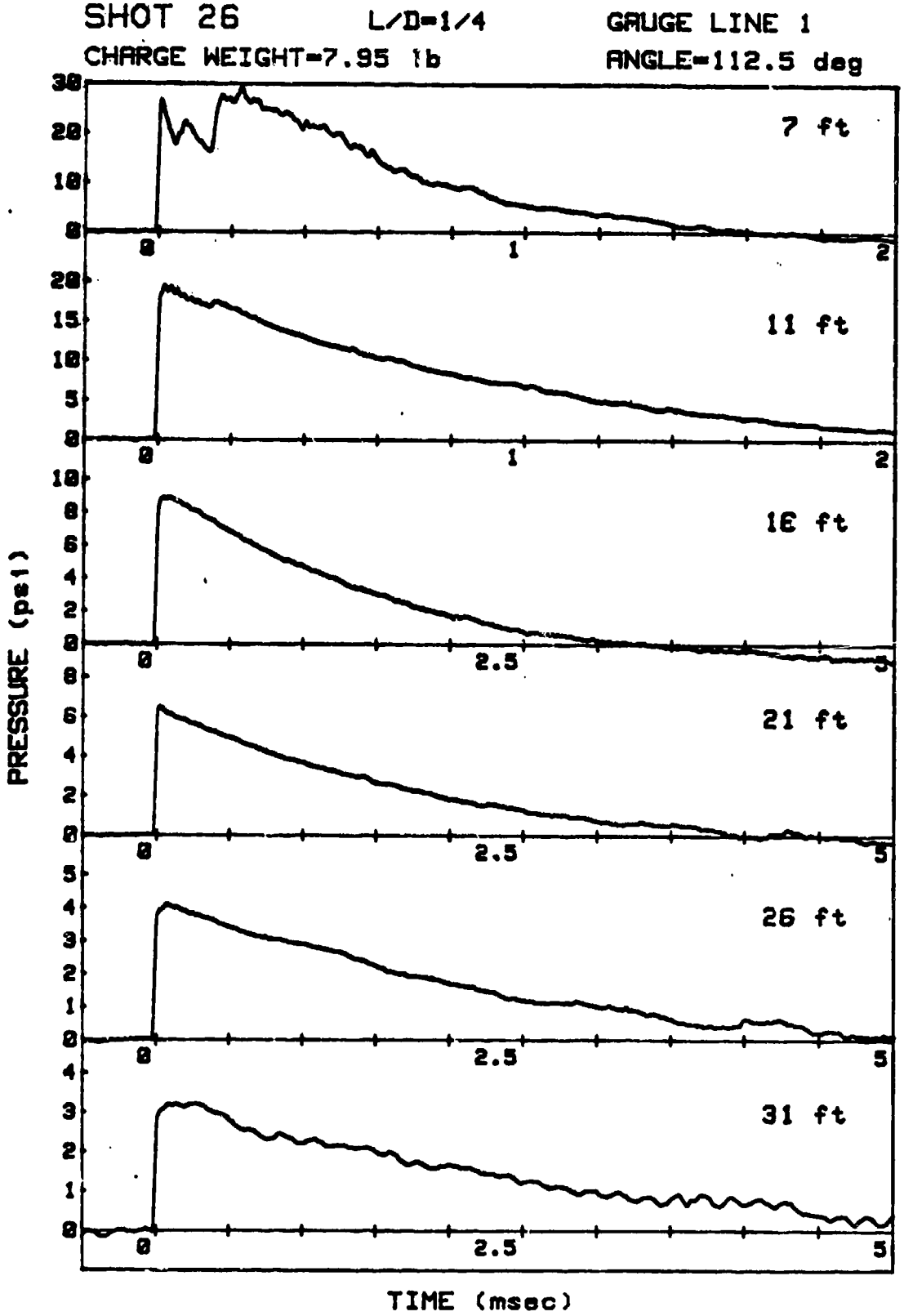
SHOT 26
L/D=1/4
GAUGE LINE 1
CHARGE WEIGHT=7.95 lb
ANGLE=112.5 deg
7 ft
11 ft
16 ft
21 ft
26 ft
31 ft
PRESSURE (psi)
TIME (msec)

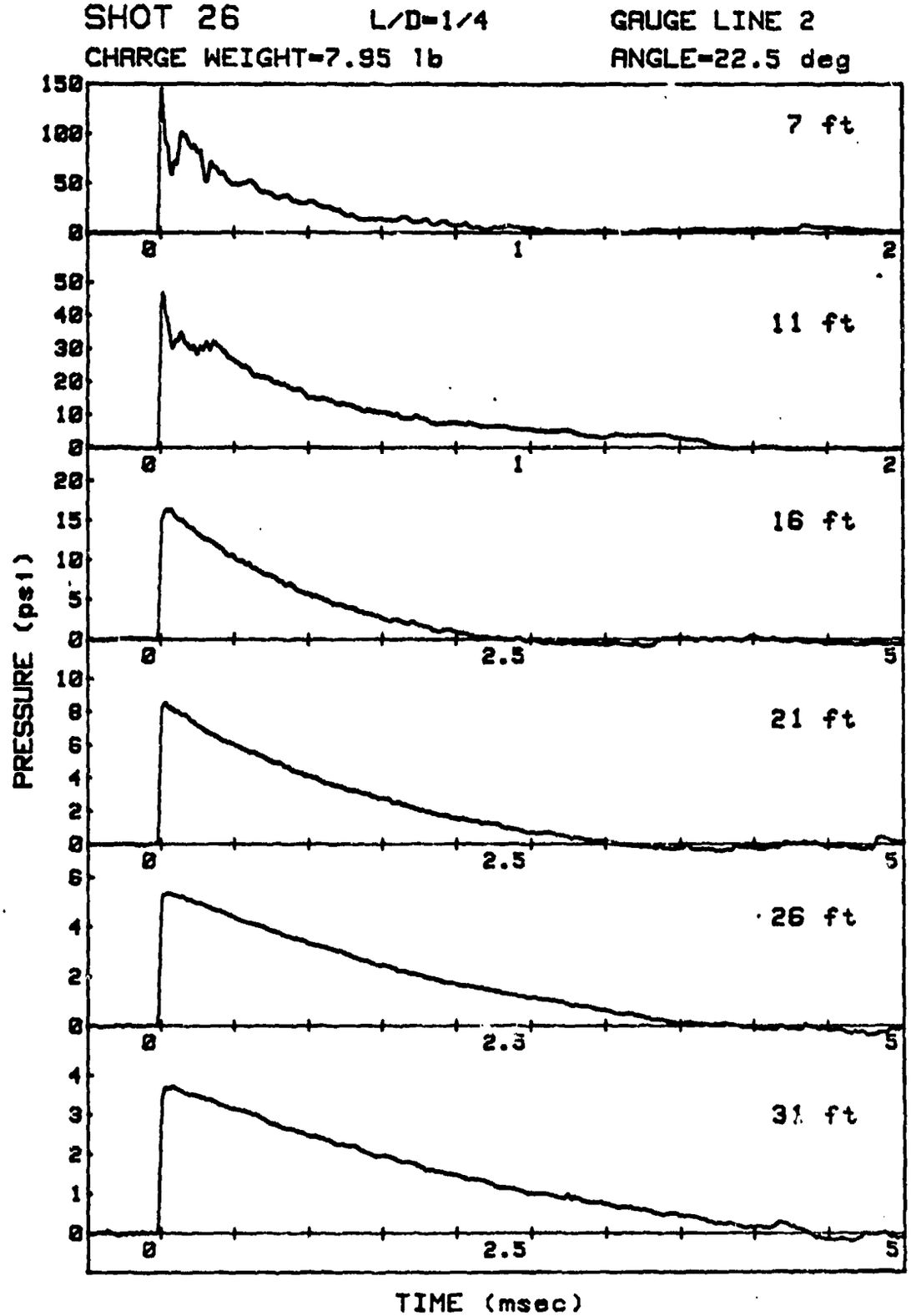
SHOT 26
L/D=1/4
GAUGE LINE 2
CHARGE WEIGHT=7.95 lb
ANGLE=22.5 deg
7 ft
11 ft
16 ft
21 ft
26 ft
31 ft
PRESSURE (psi)
TIME (msec)

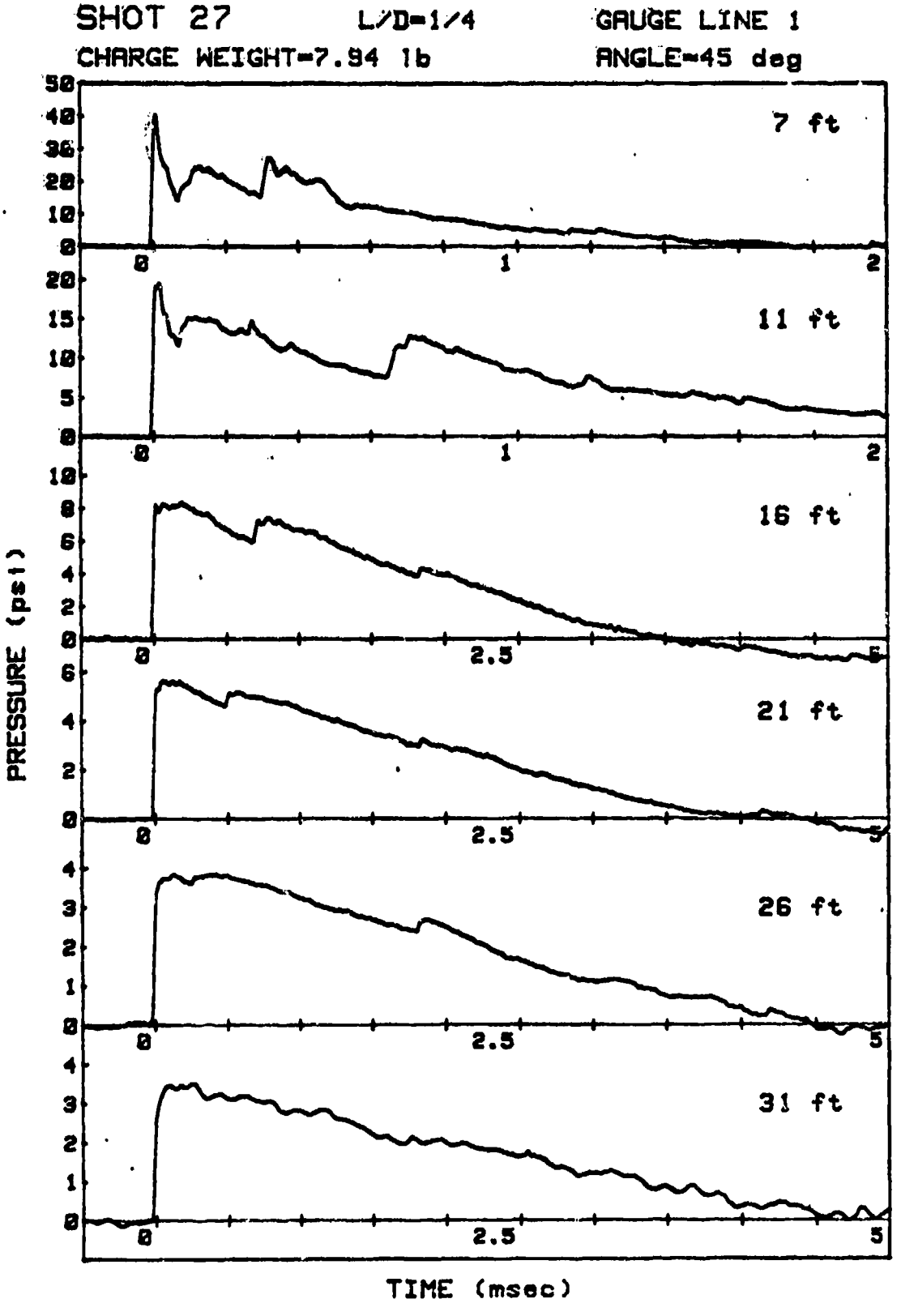
SHOT 27
L/D=1/4
GAUGE LINE 1
CHARGE WEIGHT=7.94 lb
ANGLE=45 deg
7 ft
11 ft
16 ft
21 ft
26 ft
31 ft
PRESSURE (psi)
TIME (msec)

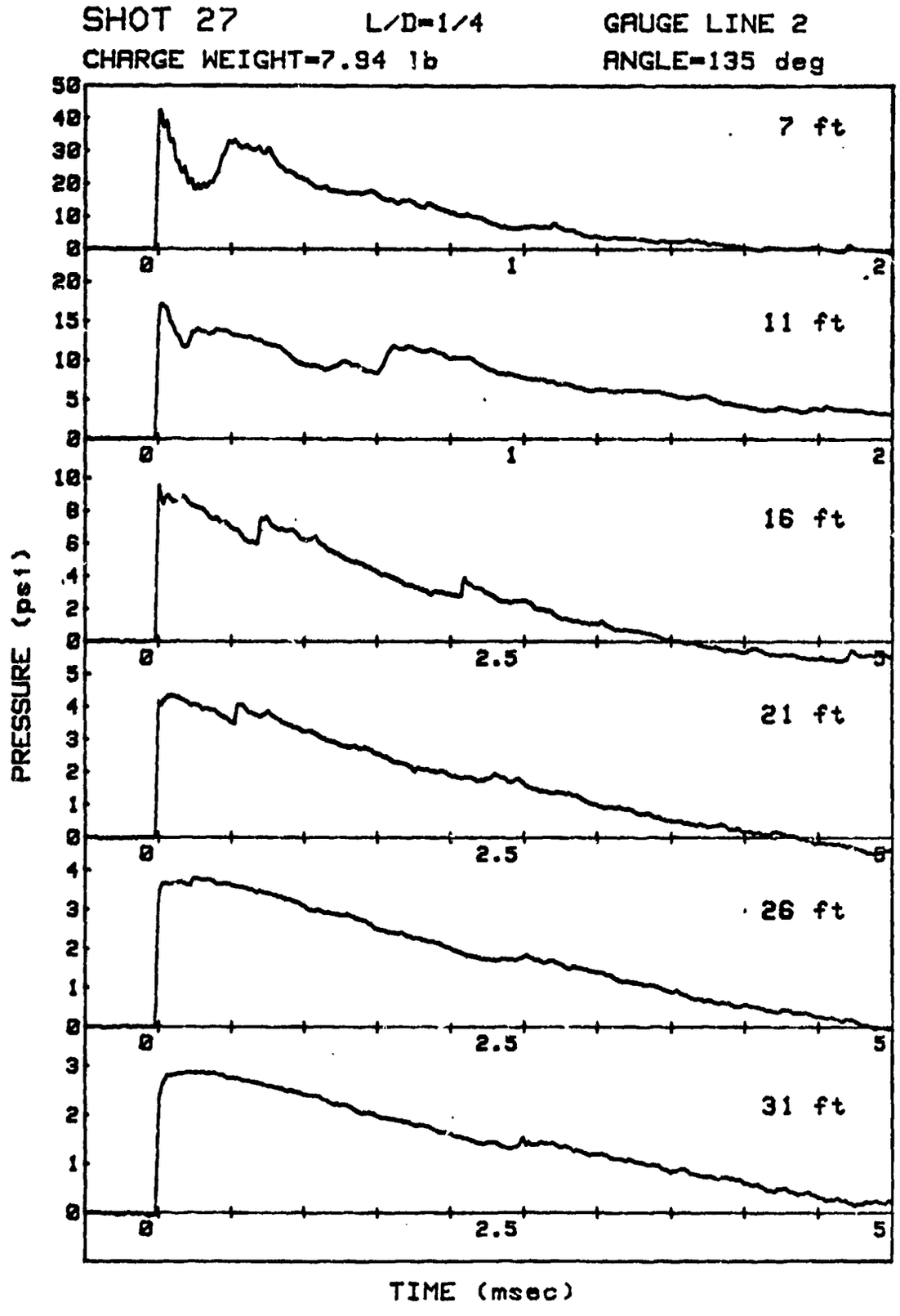
SHOT 27
L/D=1/4
GAUGE LINE 2
CHARGE WEIGHT=7.94 lb
ANGLE=135 deg
7 ft
11 ft
16 ft
21 ft
26 ft
31 ft
PRESSURE (psi)
TIME (msec)

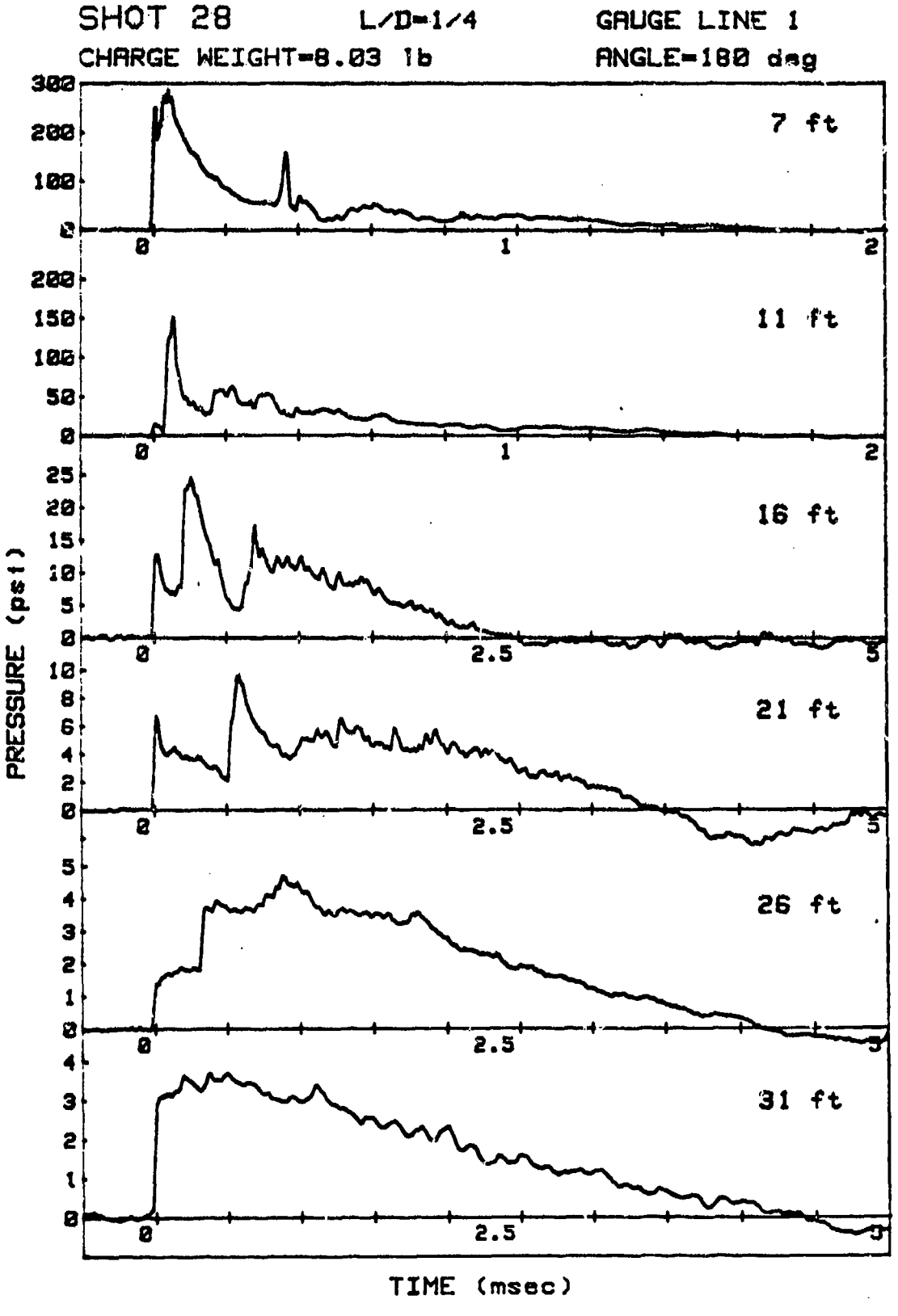
SHOT 28
L/D=1/4
GAUGE LINE 1
CHARGE WEIGHT=8.03 lb
ANGLE=180 deg
7 ft
11 ft
16 ft
21 ft
26 ft
31 ft
PRESSURE (psi)
TIME (msec)

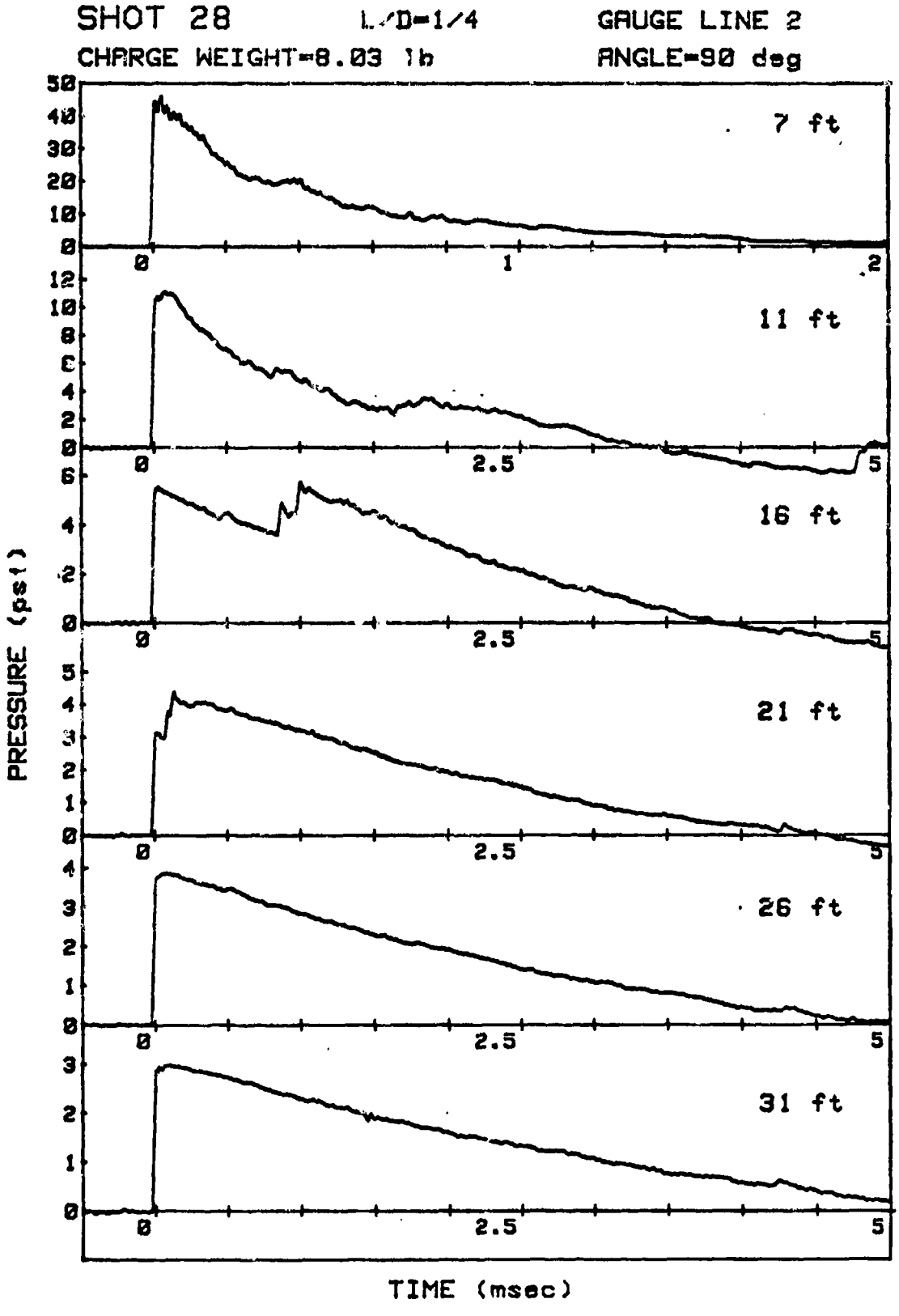
SHOT 28
L/D=1/4
GAUGE LINE 2
CHARGE WEIGHT=8.03 lb
ANGLE=90 deg
7 ft
11 ft
16 ft
21 ft
26 ft
31 ft
PRESSURE (psi)
TIME (msec)

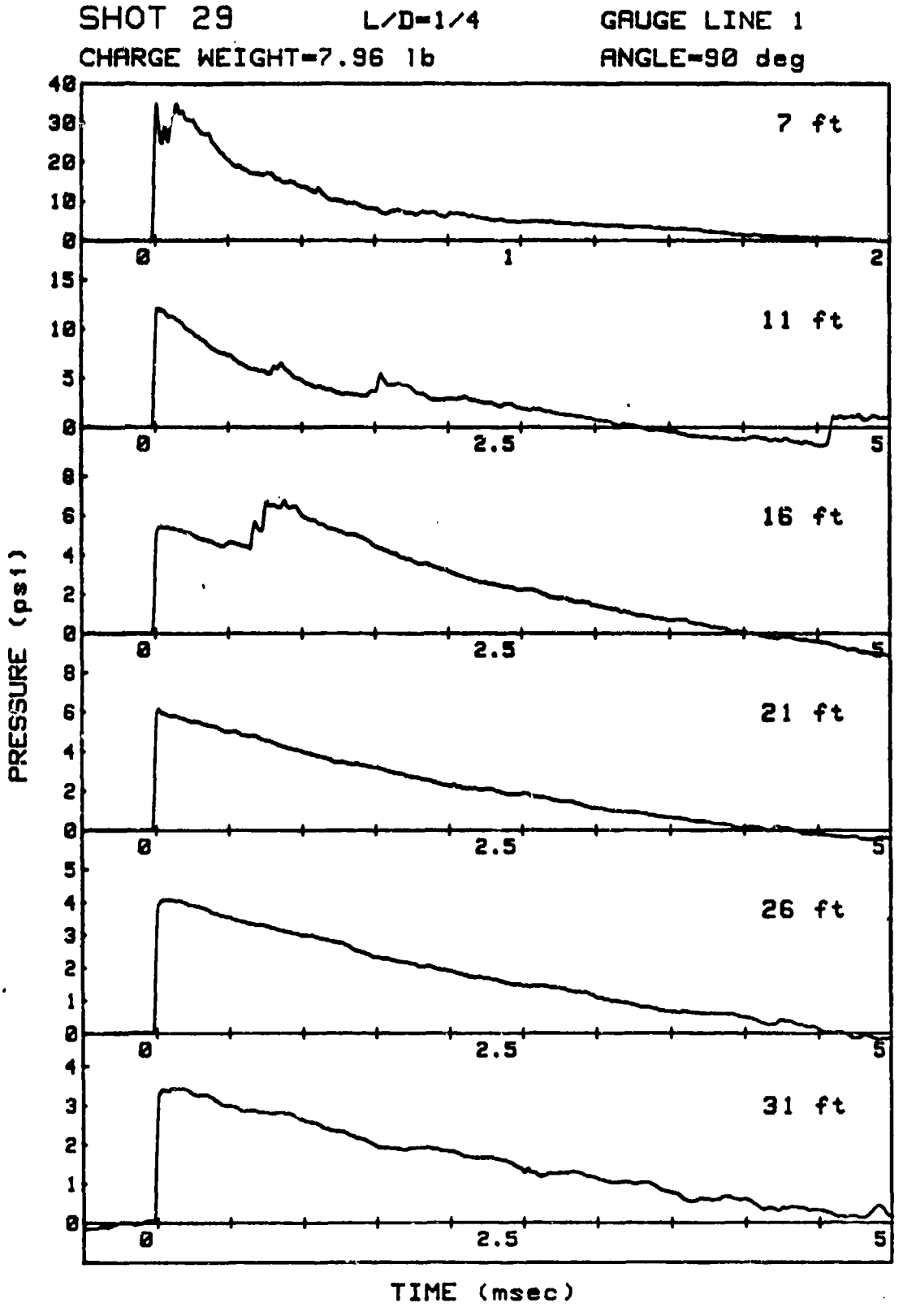
SHOT 29
L/D=1/4
GAUGE LINE 1
CHARGE WEIGHT=7.96 lb
ANGLE=90 deg
7 ft
11 ft
16 ft
21 ft
26 ft
31 ft
PRESSURE (psi)
TIME (msec)

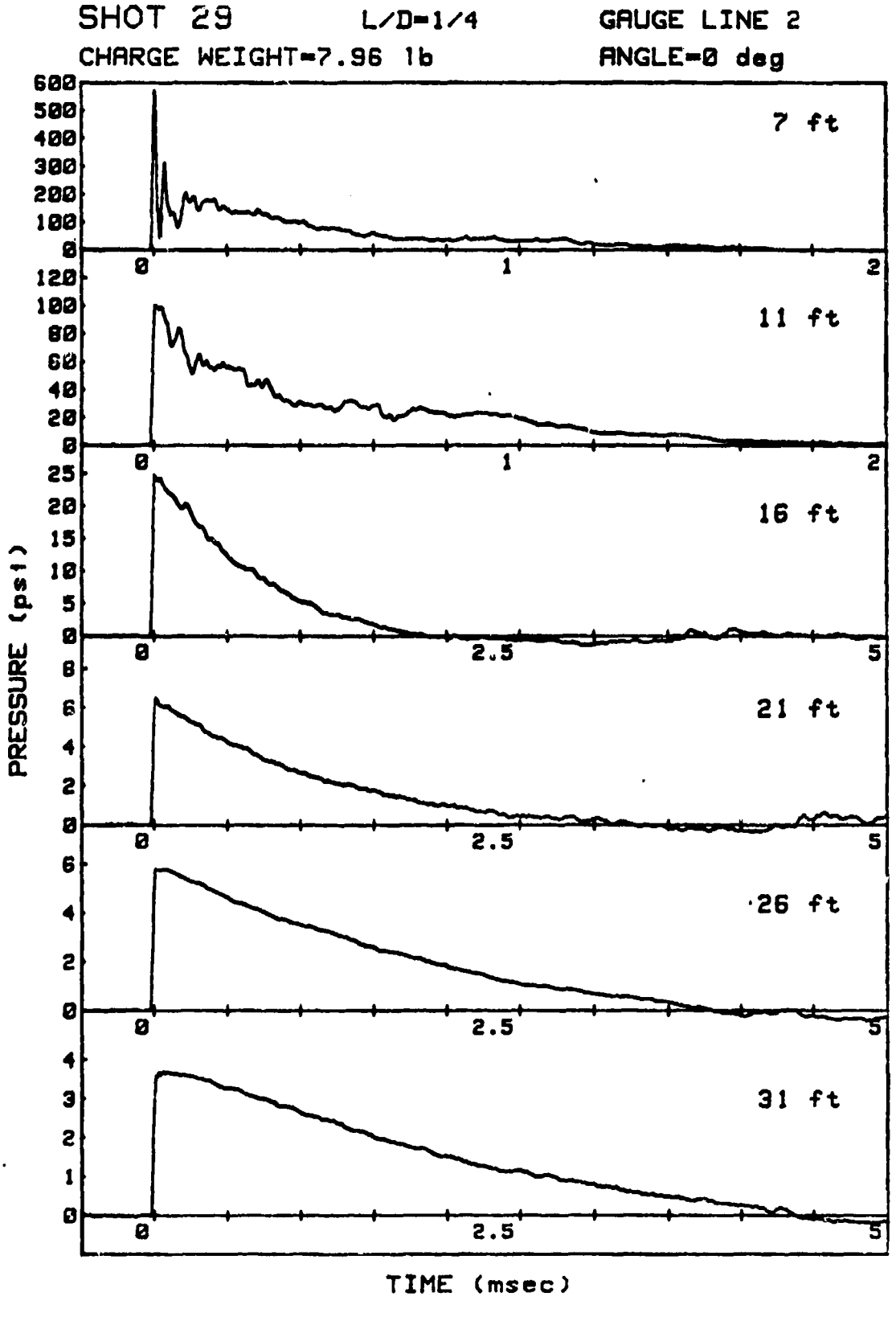
SHOT 29
L/D=1/4
GAUGE LINE 2
CHARGE WEIGHT=7.96 lb
ANGLE=0 deg
7 ft
11 ft
16 ft
21 ft
26 ft
31 ft
PRESSURE (psi)
TIME (msec)

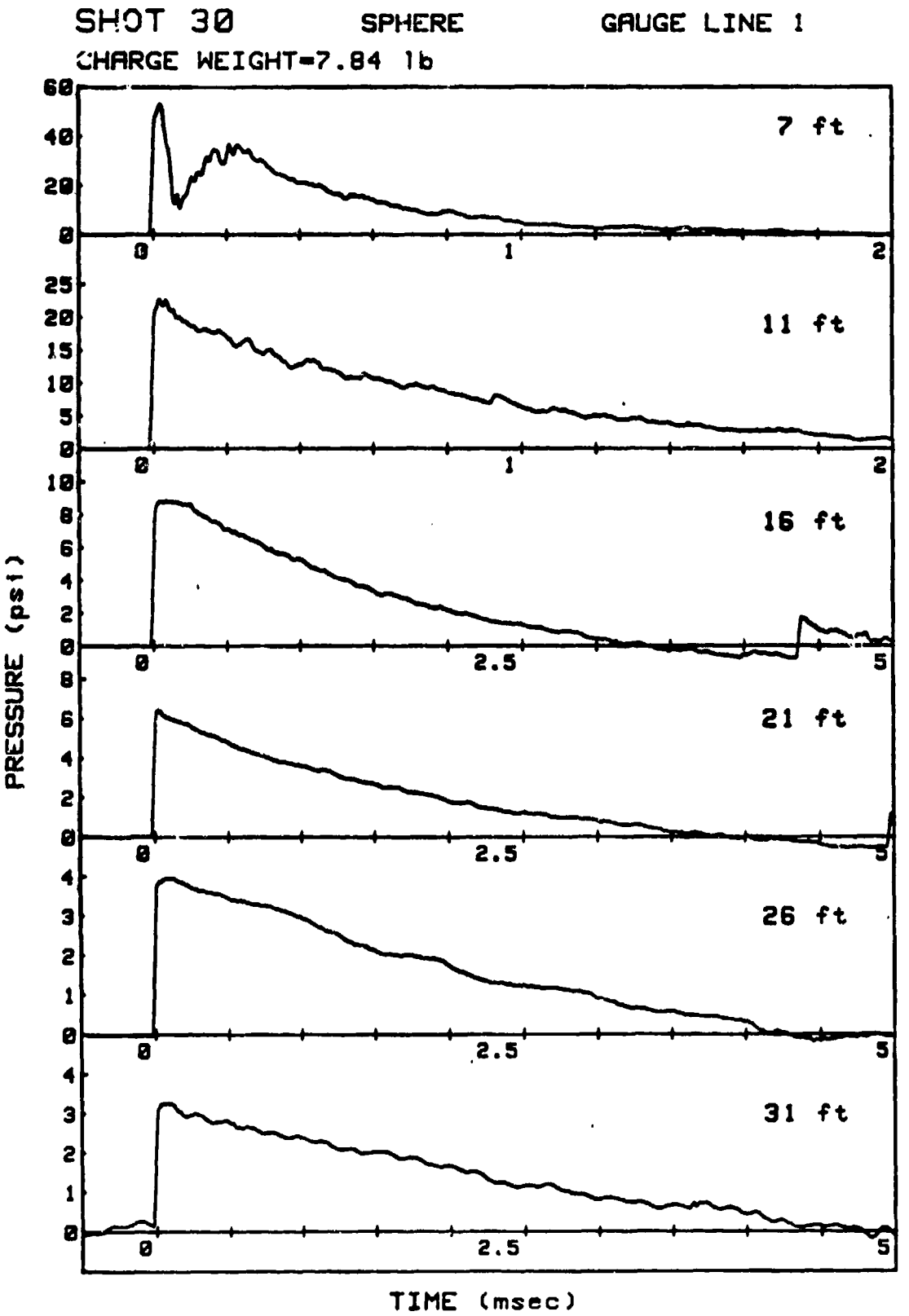
SHOT 30
SPHERE
GAUGE LINE 1
CHARGE WEIGHT=7.84 lb
7 ft
11 ft
16 ft
21 ft
26 ft
31 ft
PRESSURE (psi)
TIME (msec)

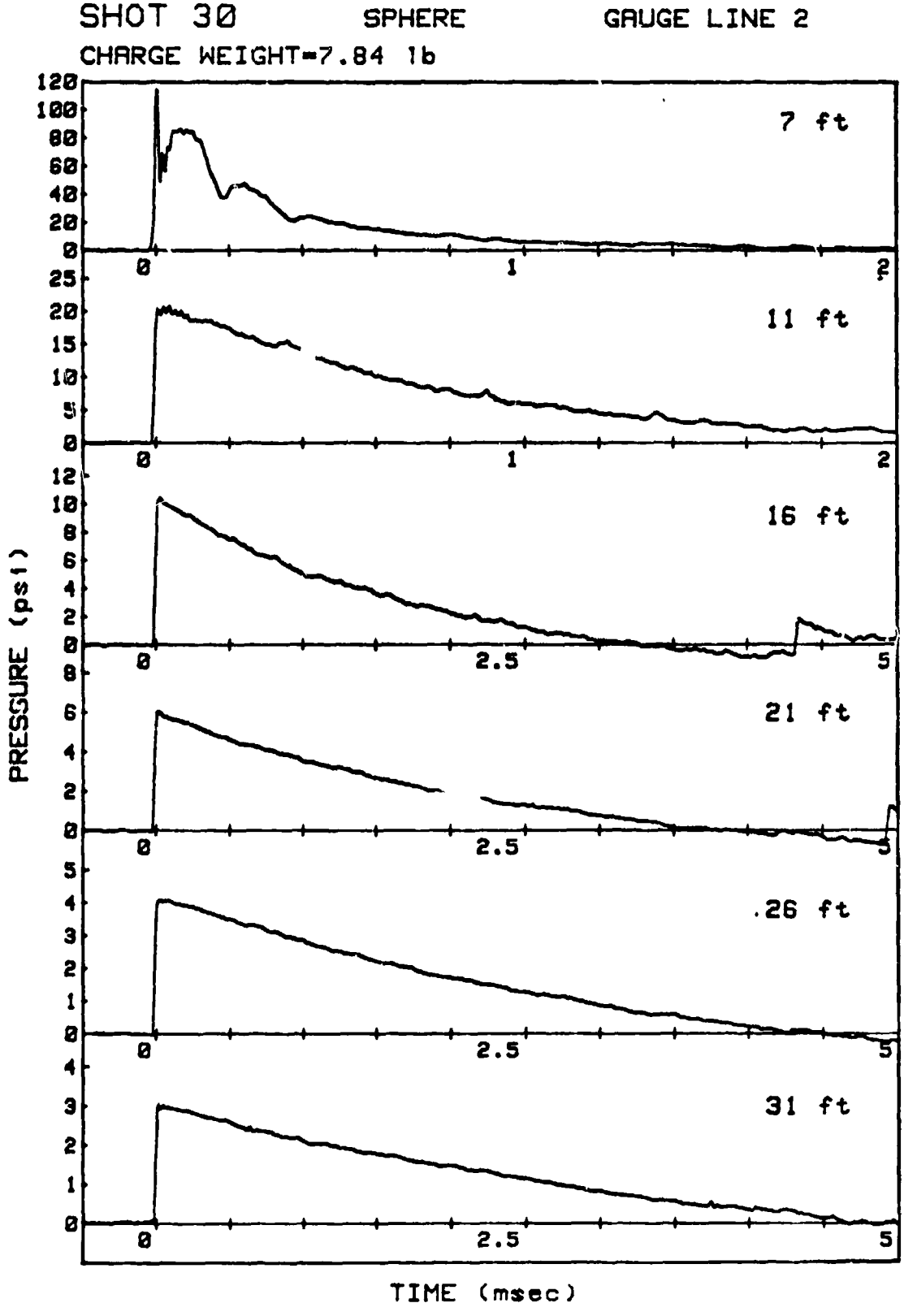
SHOT 30
SPHERE
GAUGE LINE 2
CHARGE WEIGHT=7.84 lb
7 ft
11 ft
16 ft
21 ft
.26 ft
31 ft
PRESSURE (psi)
TIME (msec)

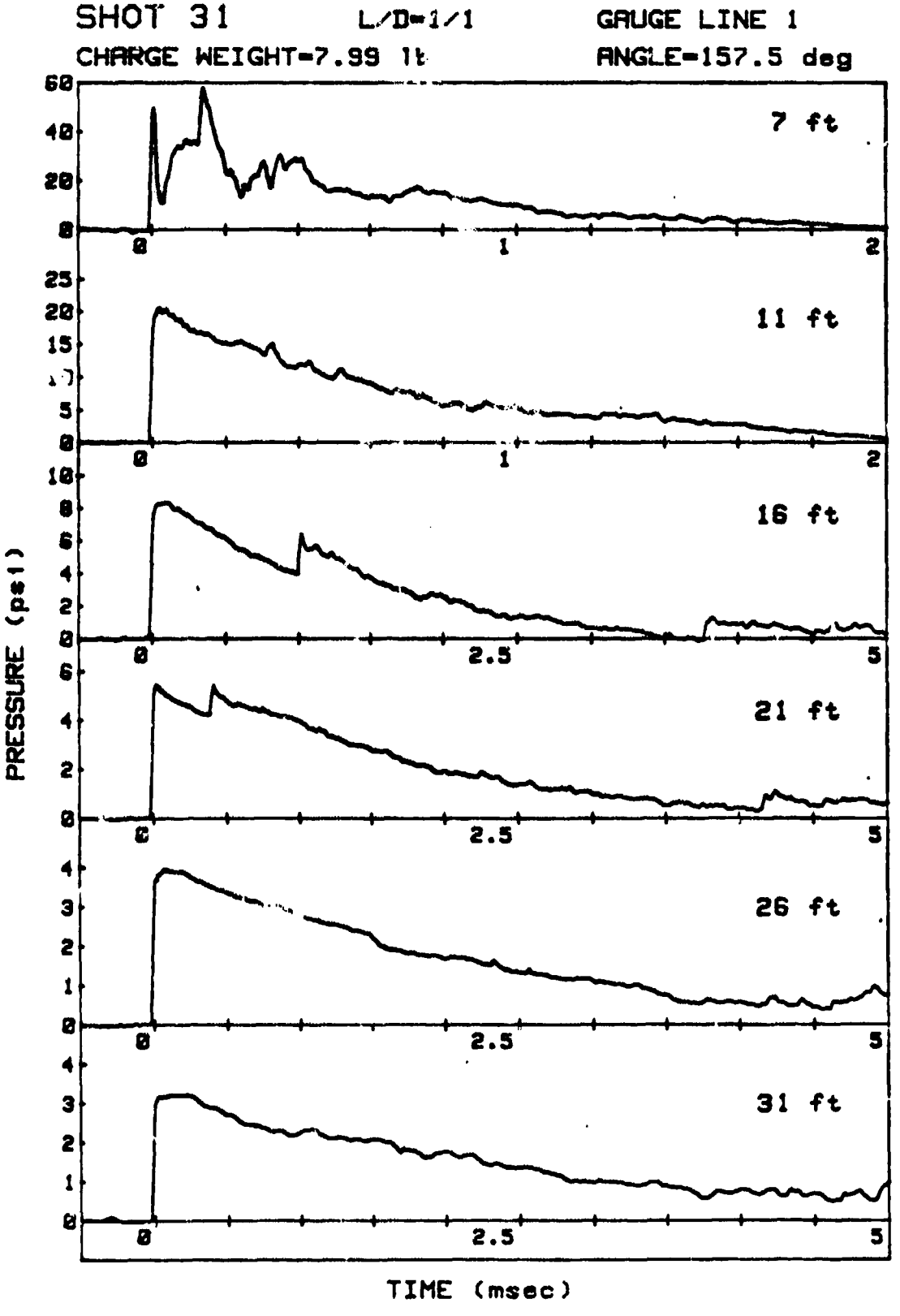
SHOT 31
L/D=1/1
GAUGE LINE 1
CHARGE WEIGHT=7.99 lb
ANGLE=157.5 deg
7 ft
11 ft
16 ft
21 ft
26 ft
31 ft
PRESSURE (psi)
TIME (msec)

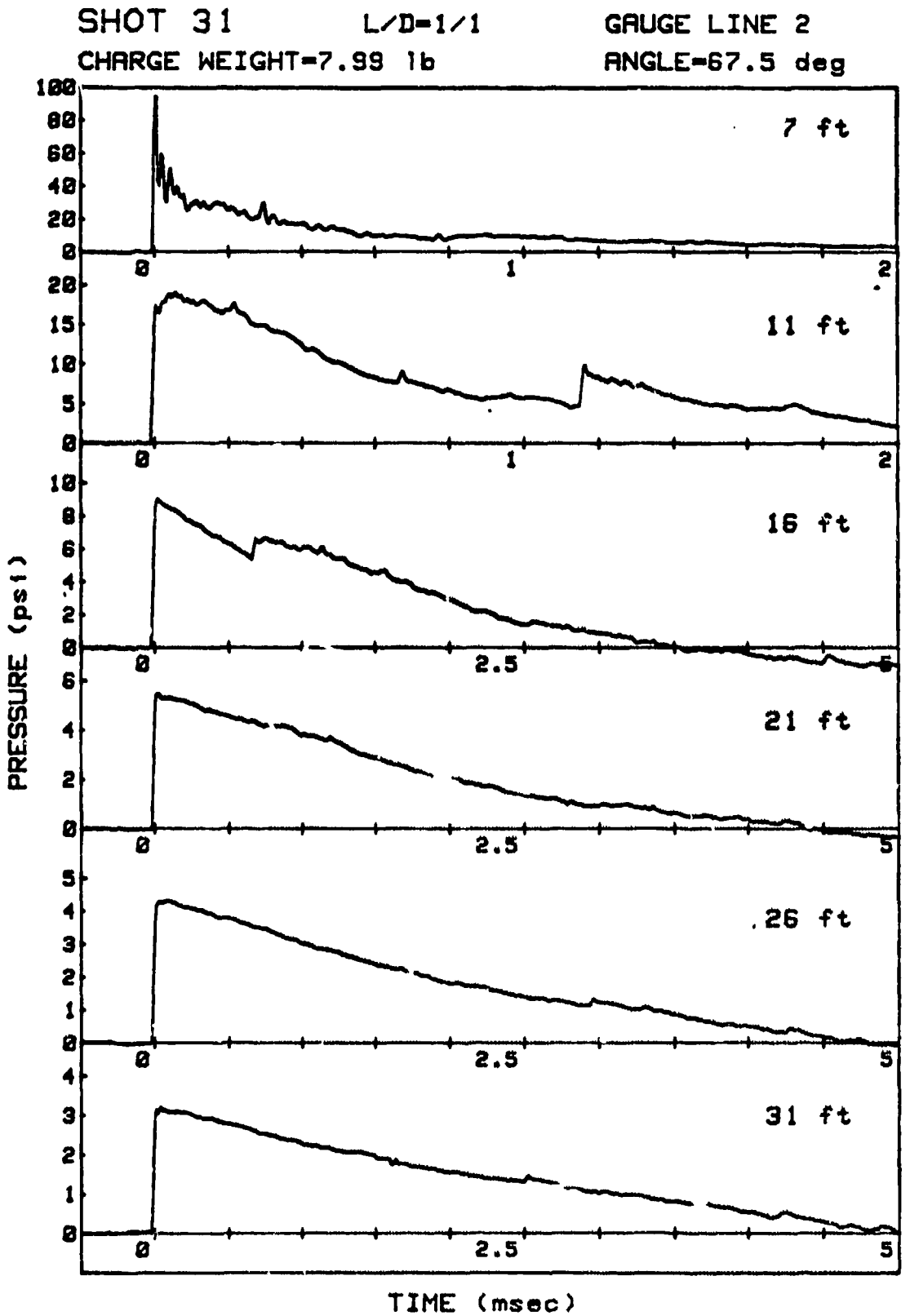
SHOT 31
L/D=1/1
GAUGE LINE 2
CHARGE WEIGHT=7.99 lb
ANGLE=67.5 deg
7 ft
11 ft
16 ft
21 ft
26 ft
31 ft
PRESSURE (psi)
TIME (msec)

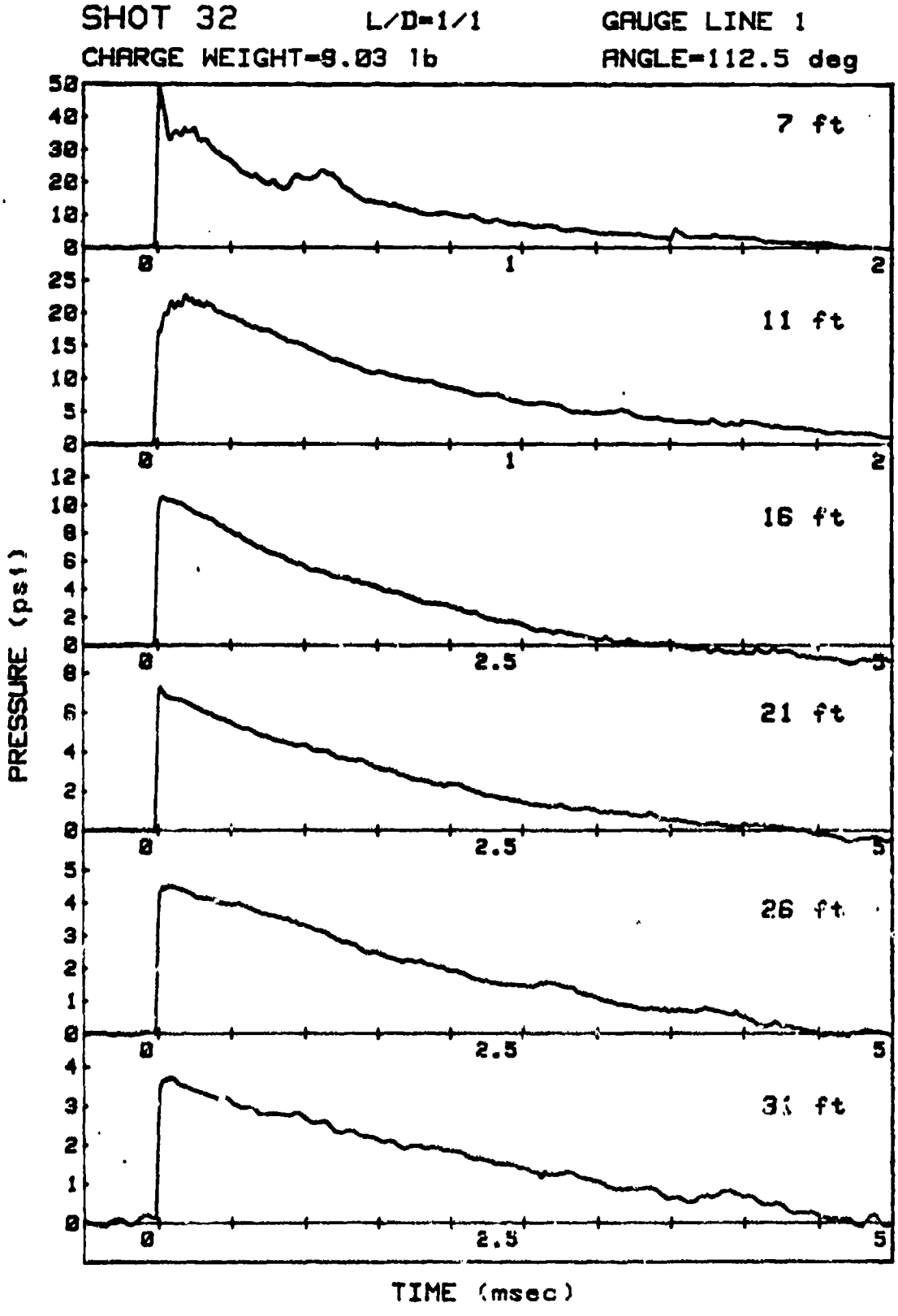
SHOT 32
L/D=1/1
GAUGE LINE 1
CHARGE WEIGHT=9.03 lb
ANGLE=112.5 deg
7 ft
11 ft
16 ft
21 ft
26 ft
31 ft
PRESSURE (psi)
TIME (msec)

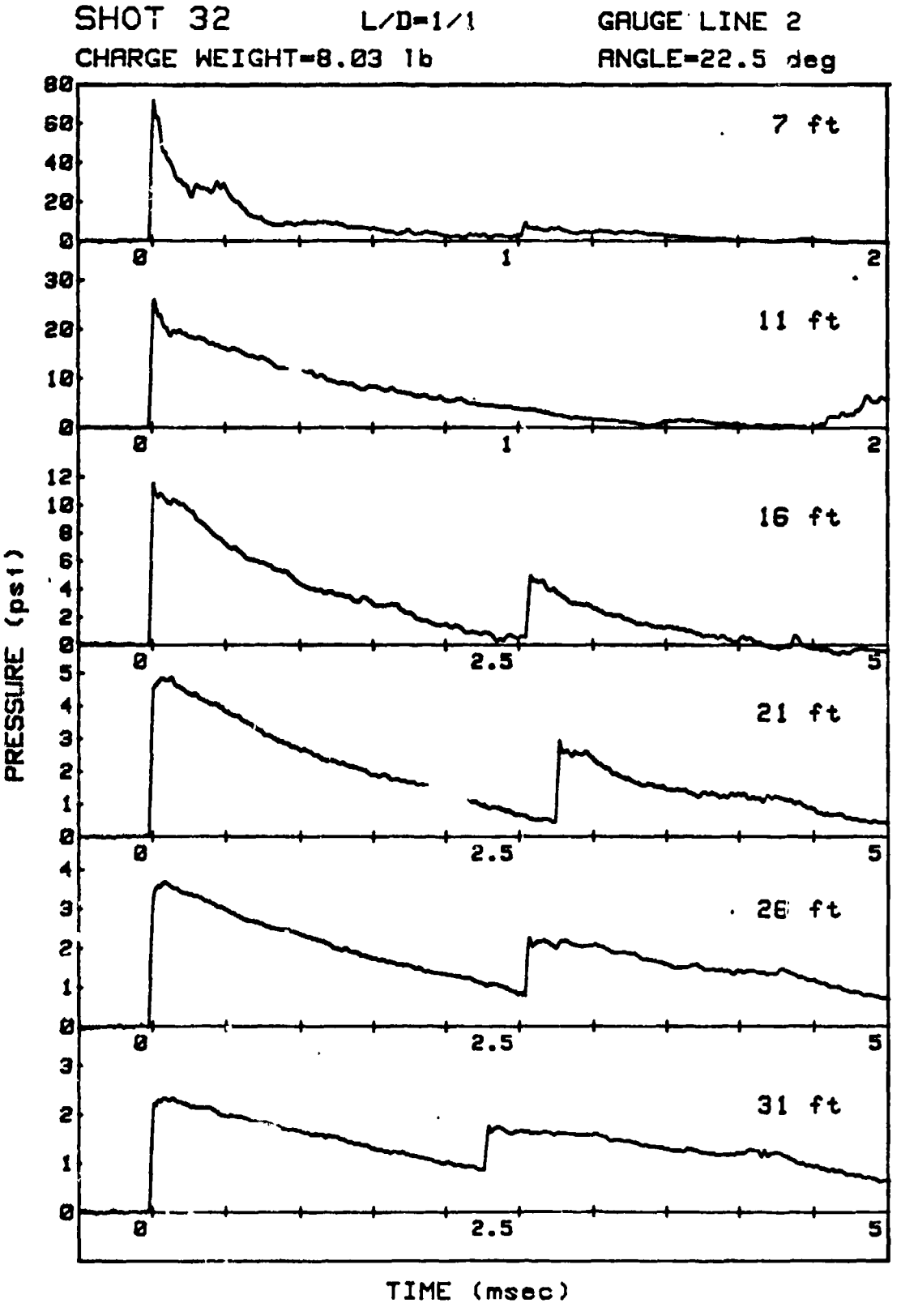
SHOT 32
L/D=1/1
GAUGE LINE 2
CHARGE WEIGHT=8.03 lb
ANGLE=22.5 deg
7 ft
11 ft
16 ft
21 ft
26 ft
31 ft
PRESSURE (psi)
TIME (msec)

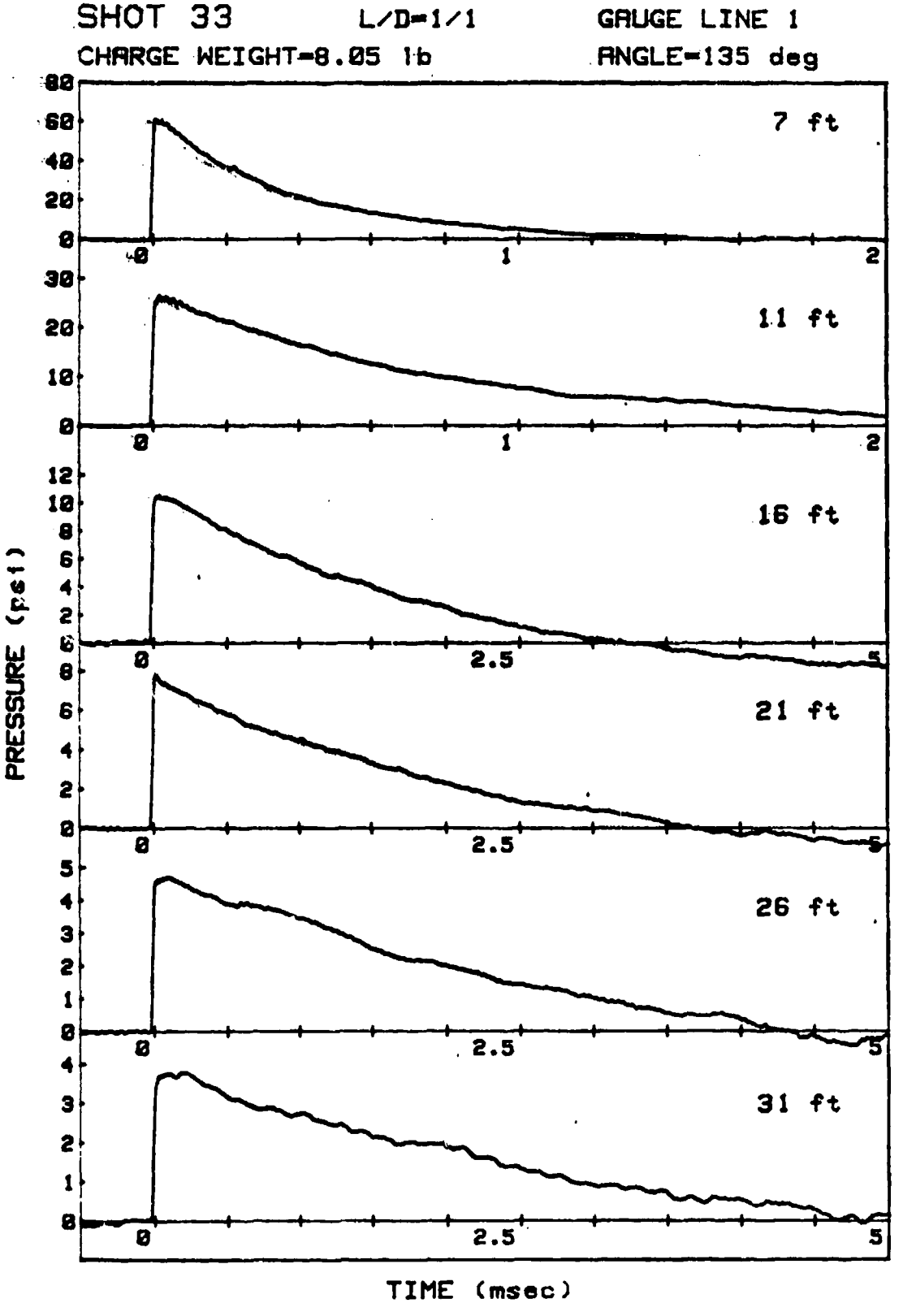
SHOT 33
L/D=1/1
GAUGE LINE 1
CHARGE WEIGHT=8.05 lb
ANGLE=135 deg
7 ft
11 ft
16 ft
21 ft
26 ft
31 ft
PRESSURE (psi)
TIME (msec)

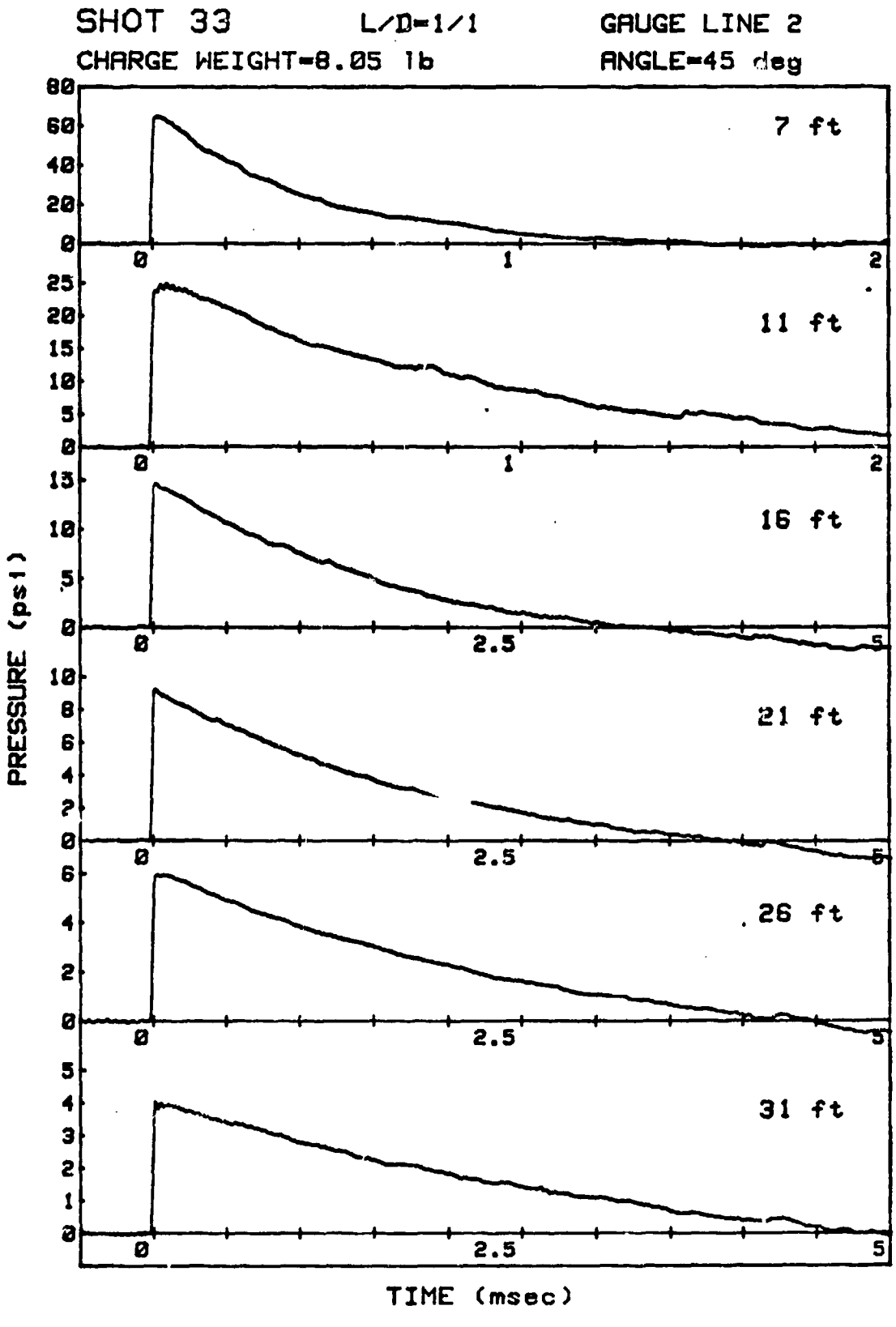
SHOT 33
L/D=1/1
GAUGE LINE 2
CHARGE WEIGHT=8.05 lb
ANGLE=45 deg
7 ft
11 ft
16 ft
21 ft
26 ft
31 ft
PRESSURE (psi)
TIME (msec)

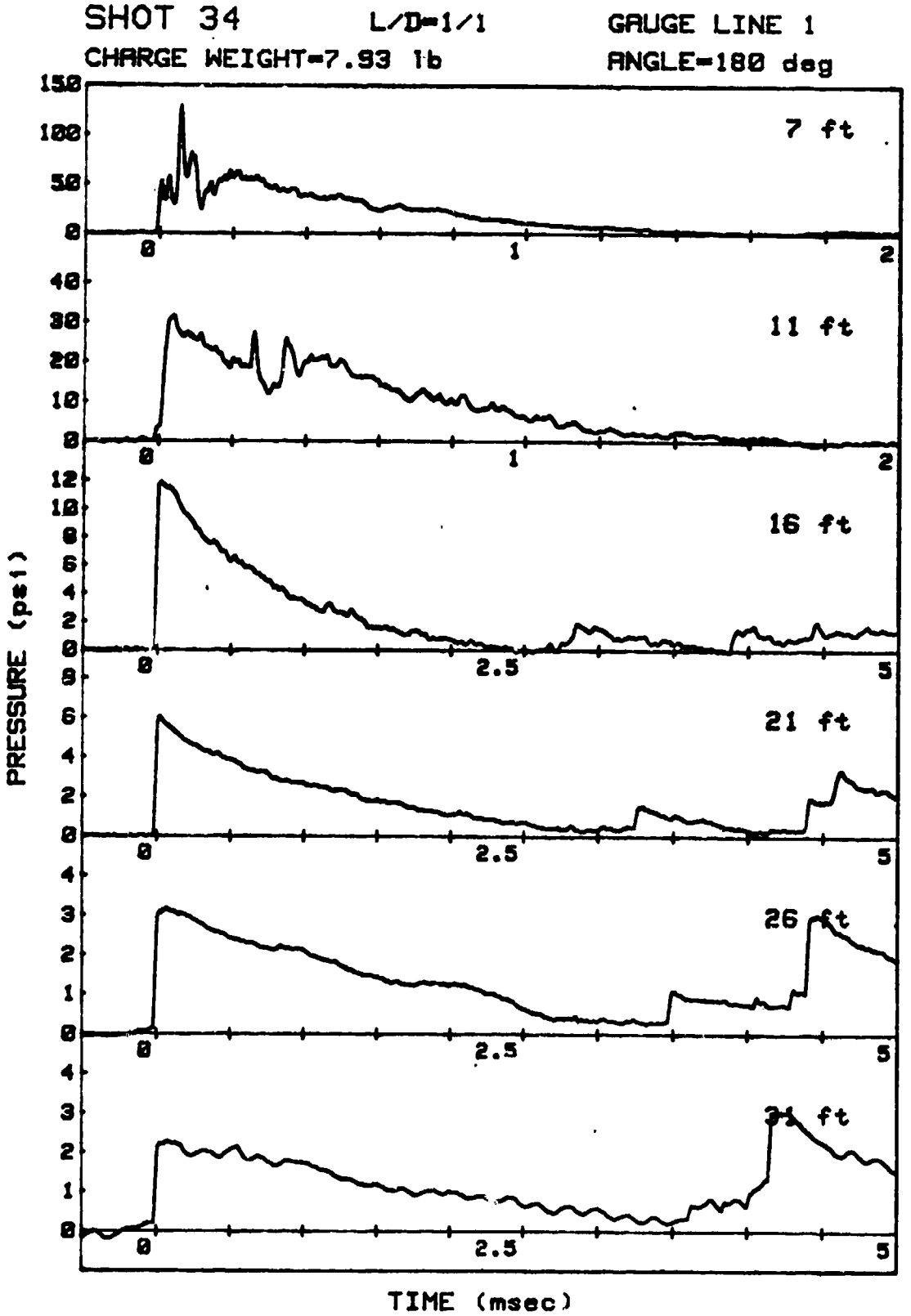
SHOT 34
L/D=1/1
GAUGE LINE 1
CHARGE WEIGHT=7.93 lb
ANGLE=180 deg
7 ft
11 ft
16 ft
21 ft
26 ft
31 ft
PRESSURE (psi)
TIME (msec)

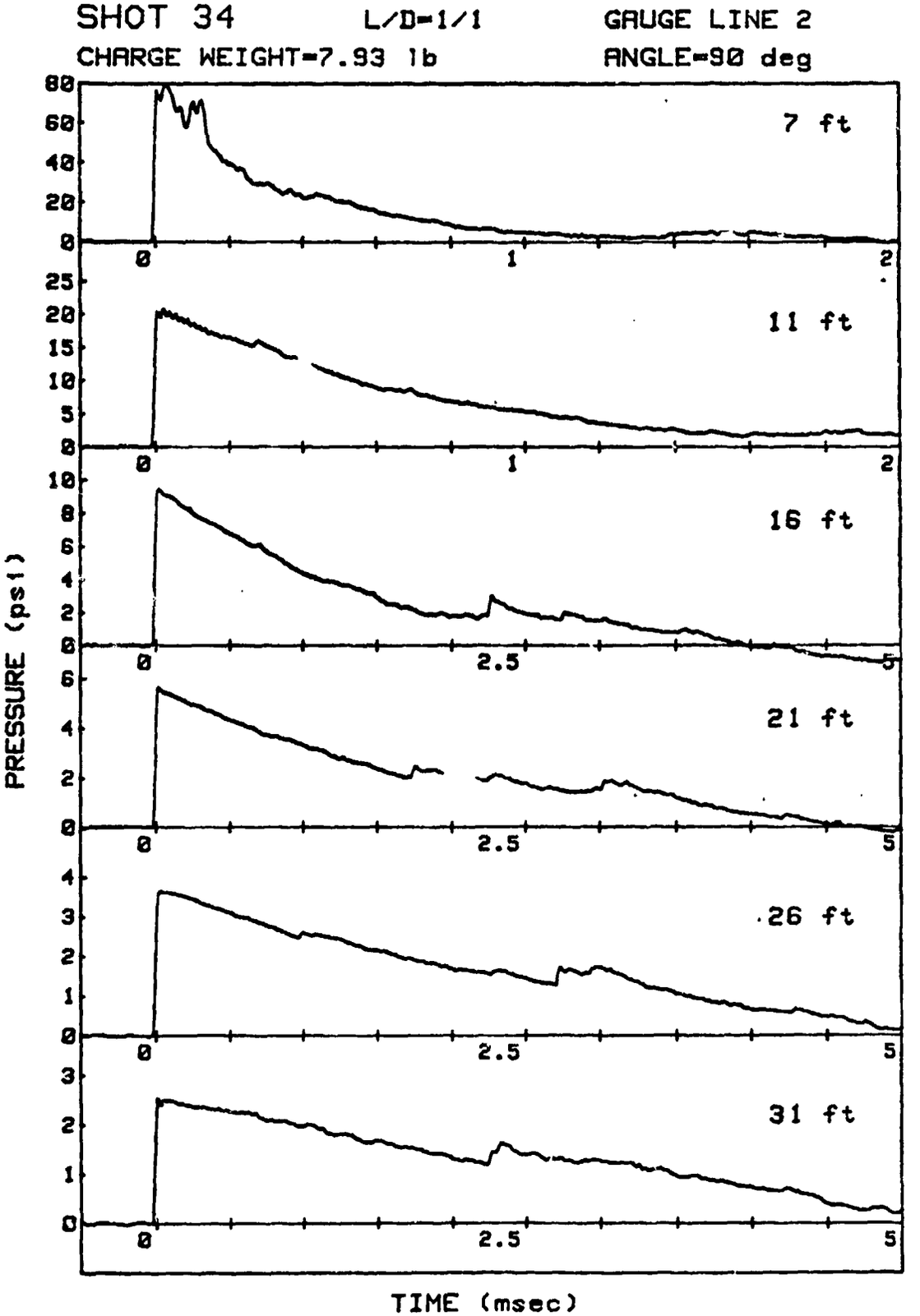
SHOT 34
L/D=1/1
GAUGE LINE 2
CHARGE WEIGHT=7.93 lb
ANGLE=90 deg
7 ft
11 ft
16 ft
21 ft
26 ft
31 ft
PRESSURE (psi)
TIME (msec)

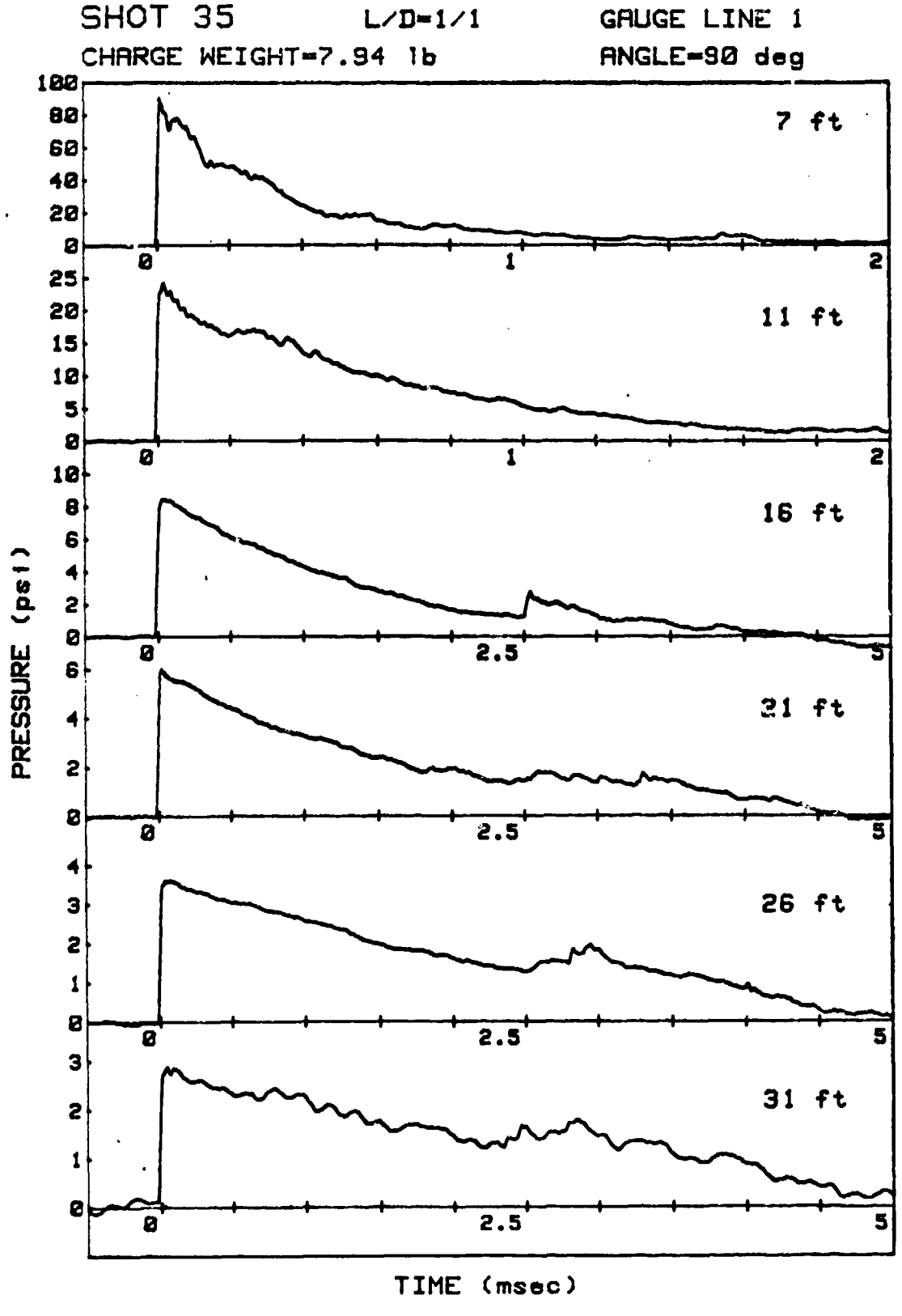
SHOT 35
L/D=1/1
GAUGE LINE 1
CHARGE WEIGHT=7.94 lb
ANGLE=90 deg
7 ft
11 ft
16 ft
21 ft
26 ft
31 ft
PRESSURE (psi)
TIME (msec)

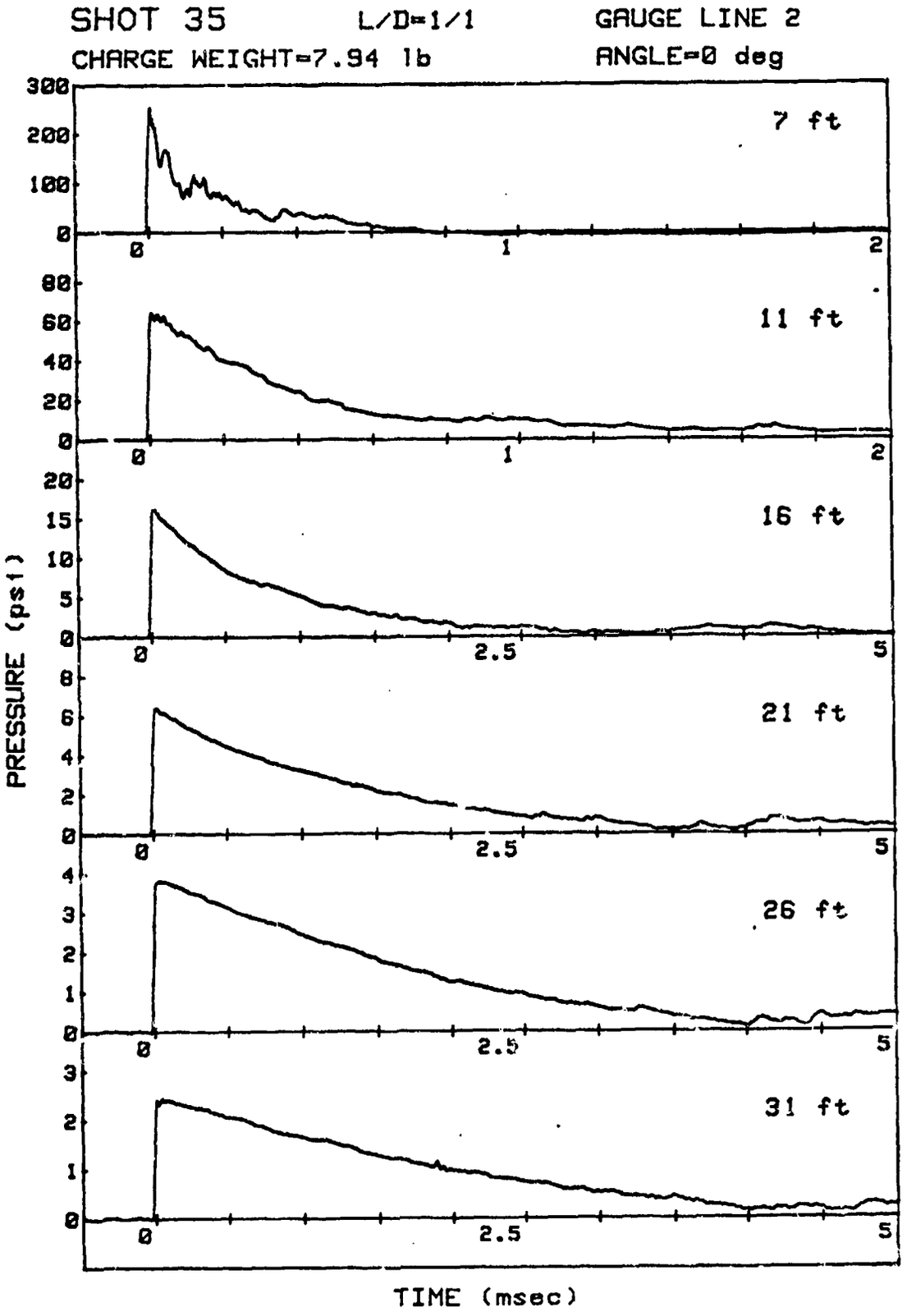
SHOT 35
L/D=1/1
GAUGE LINE 2
CHARGE WEIGHT=7.94 lb
ANGLE=0 deg
7 ft
11 ft
16 ft
21 ft
26 ft
31 ft
PRESSURE (psi)
TIME (msec)

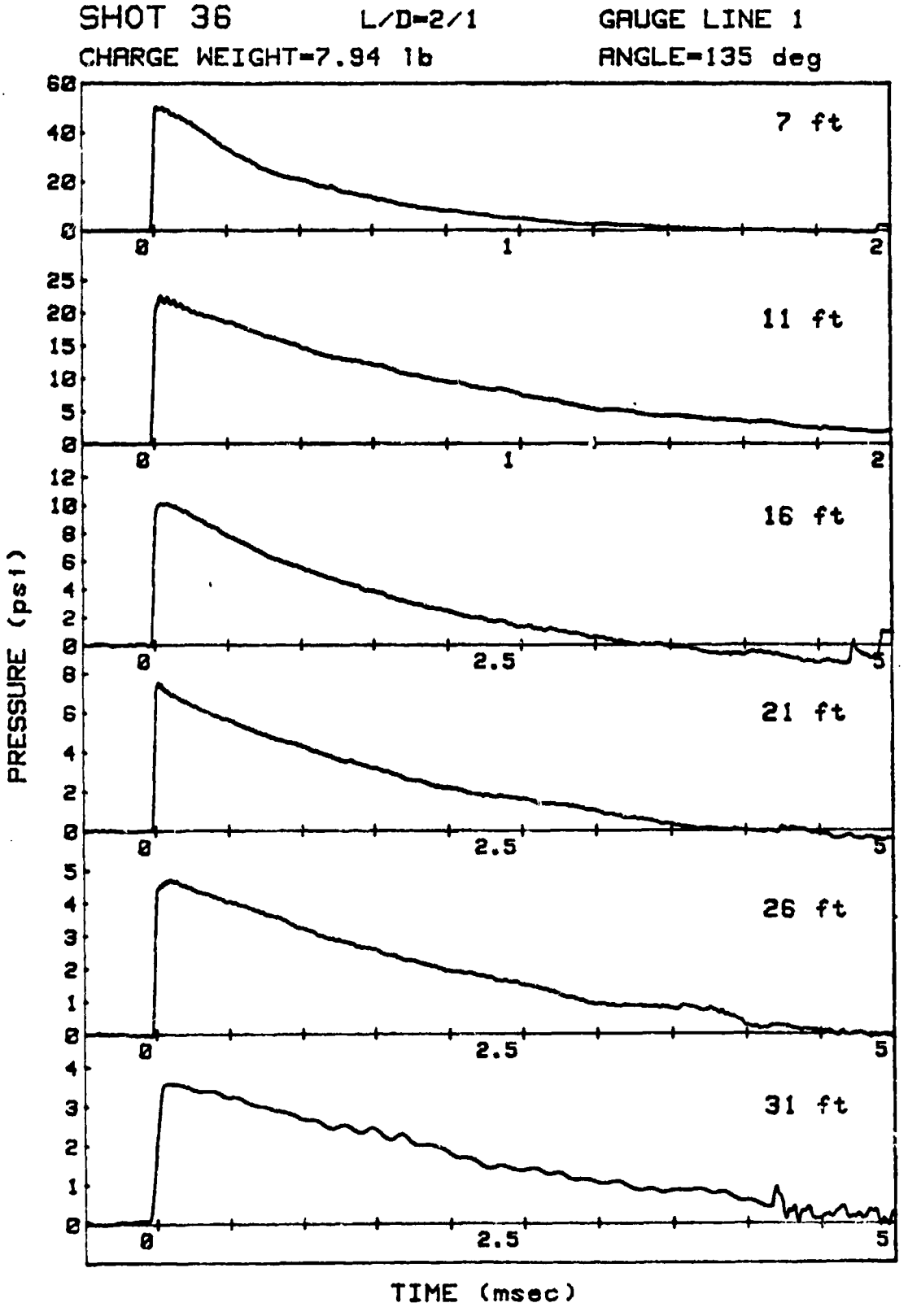
SHOT 36
L/D=2/1
GAUGE LINE 1
CHARGE WEIGHT=7.94 lb
ANGLE=135 deg
7 ft
11 ft
16 ft
21 ft
26 ft
31 ft
PRESSURE (psi)
TIME (msec)

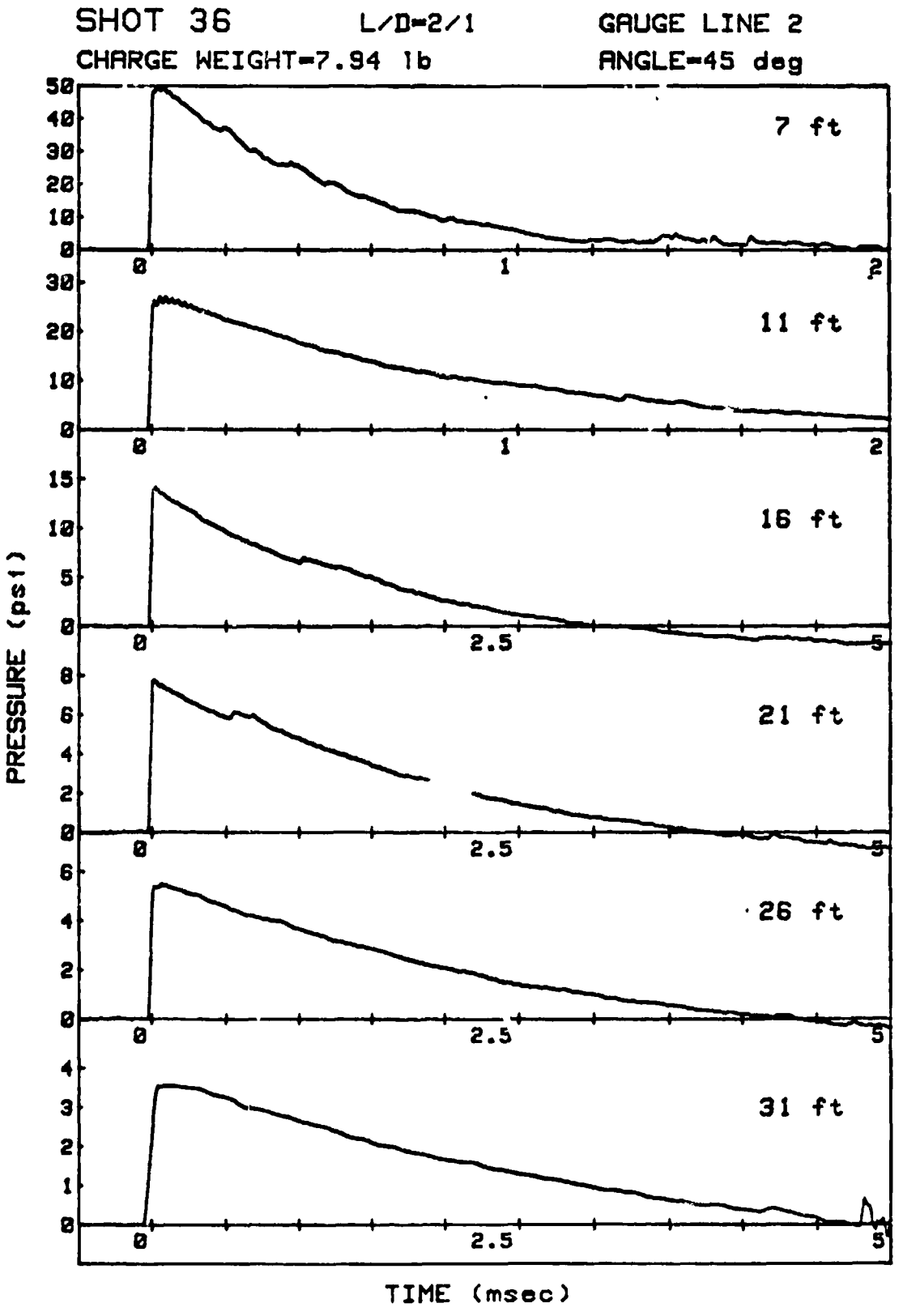
SHOT 36
L/D=2/1
GAUGE LINE 2
CHARGE WEIGHT=7.94 lb
ANGLE=45 deg
7 ft
11 ft
16 ft
21 ft
26 ft
31 ft
PRESSURE (psi)
TIME (msec)

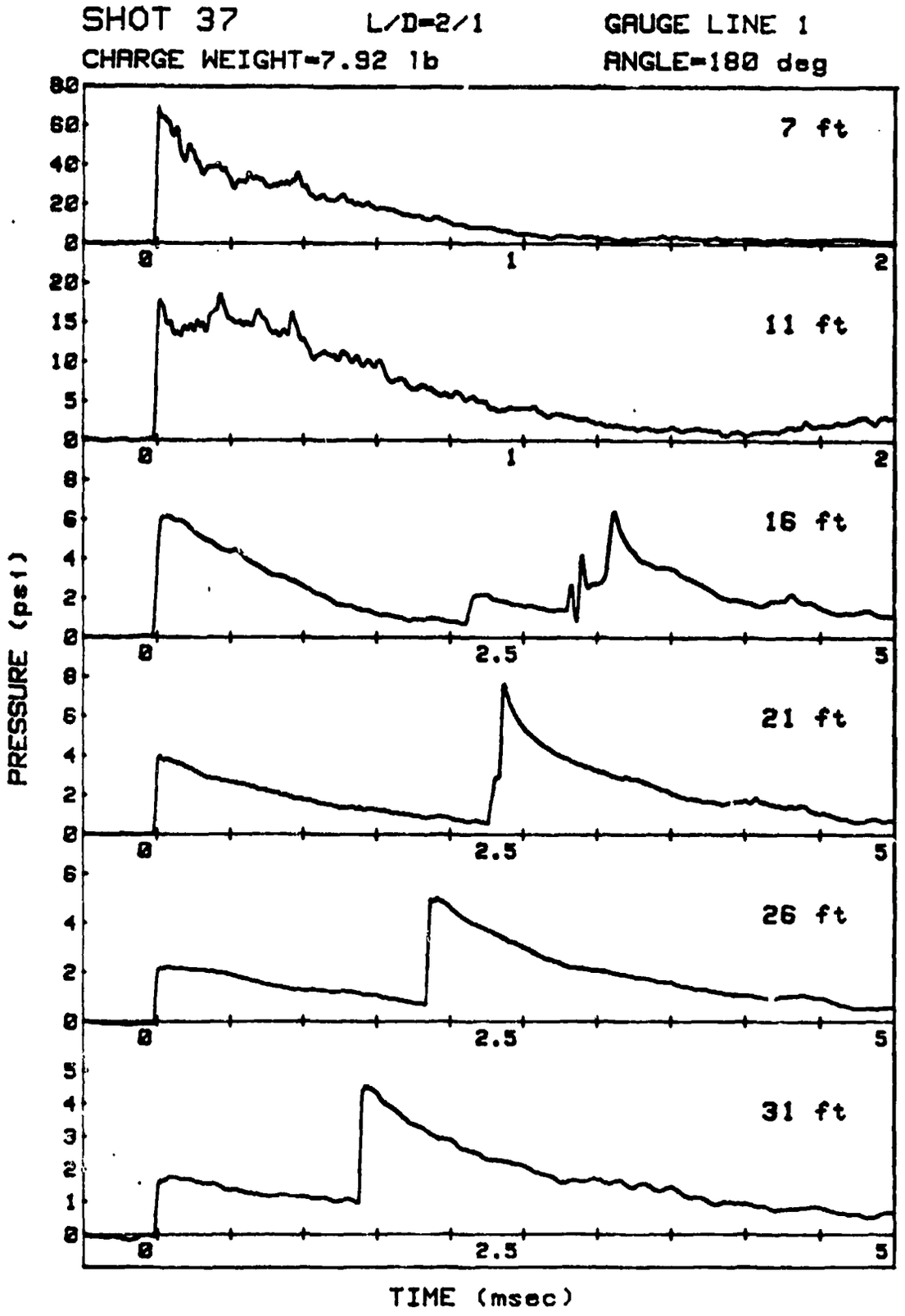
SHOT 37
L/D=2/1
GAUGE LINE 1
CHARGE WEIGHT=7.92 lb
ANGLE=180 deg
7 ft
11 ft
16 ft
21 ft
26 ft
31 ft
PRESSURE (psi)
TIME (msec)

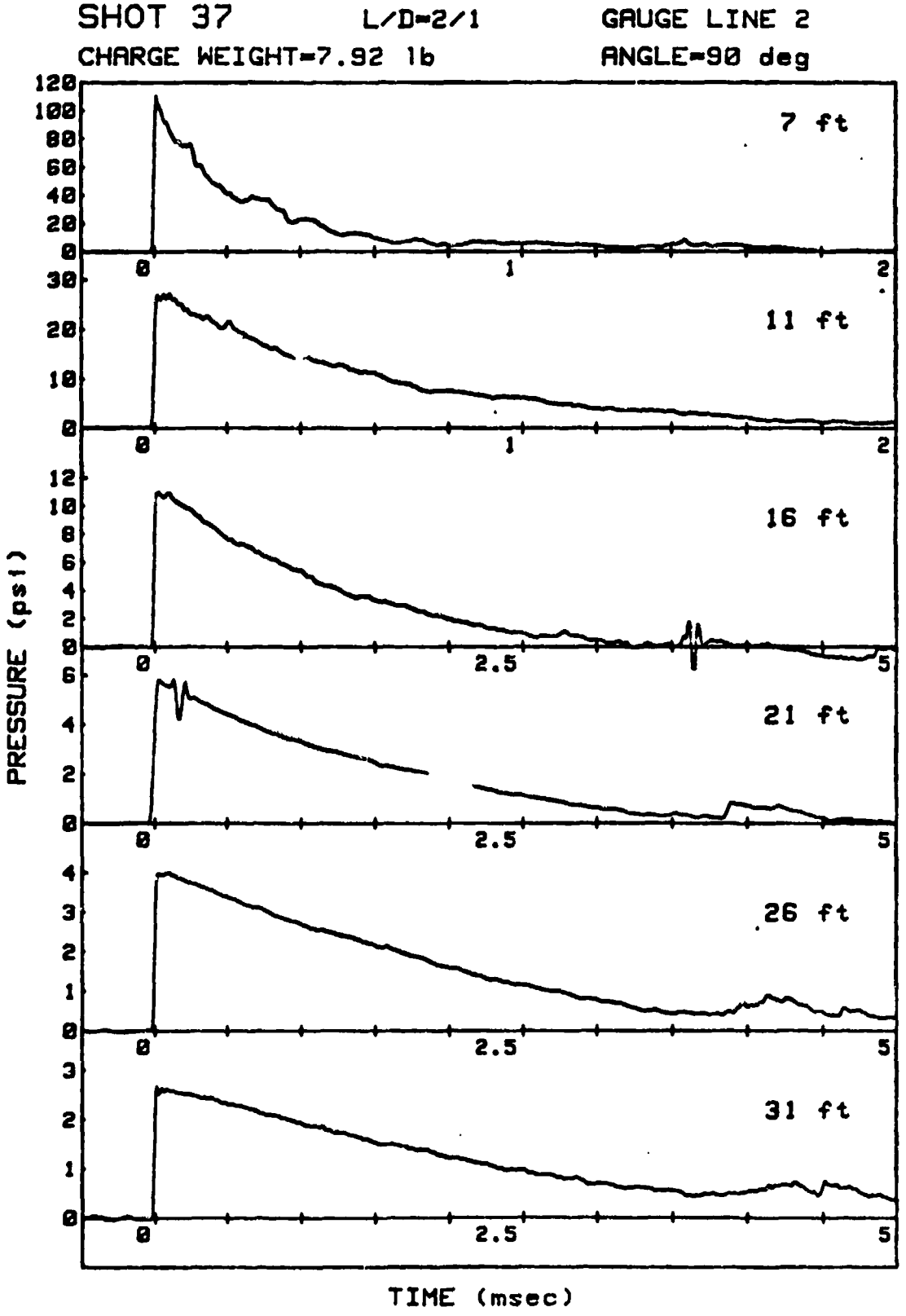
SHOT 37
L/D=2/1
GAUGE LINE 2
CHARGE WEIGHT=7.92 lb
ANGLE=90 deg
7 ft
11 ft
16 ft
21 ft
26 ft
31 ft
PRESSURE (psi)
TIME (msec)

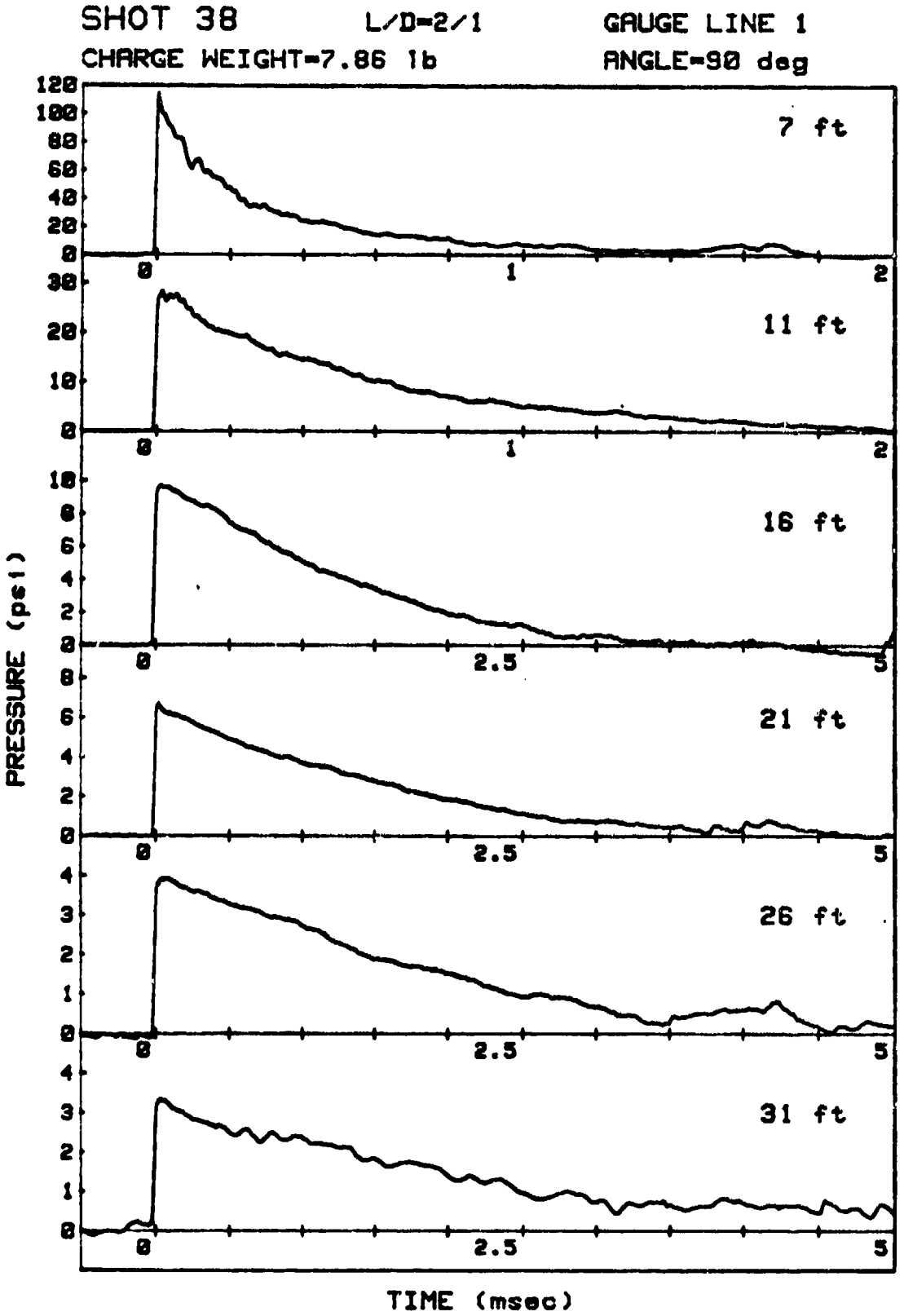
SHOT 38
L/D=2/1
GAUGE LINE 1
CHARGE WEIGHT=7.86 lb
ANGLE=90 deg
7 ft
11 ft
16 ft
21 ft
26 ft
31 ft
PRESSURE (psi)
TIME (msec)

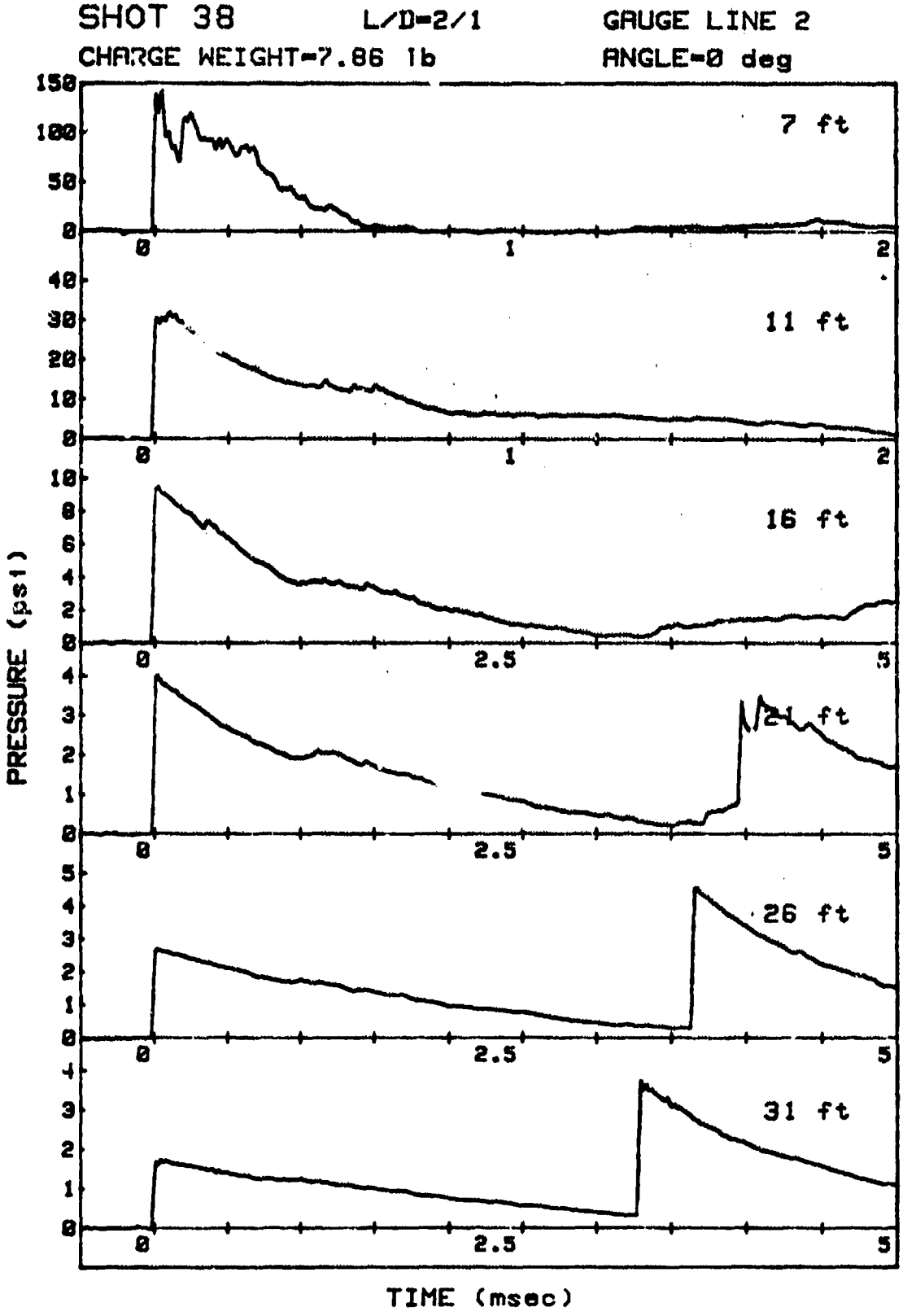
SHOT 38
L/D=2/1
GAUGE LINE 2
CHARGE WEIGHT=7.86 lb
ANGLE=0 deg
7 ft
11 ft
16 ft
21 ft
26 ft
31 ft
PRESSURE (psi)
TIME (msec)

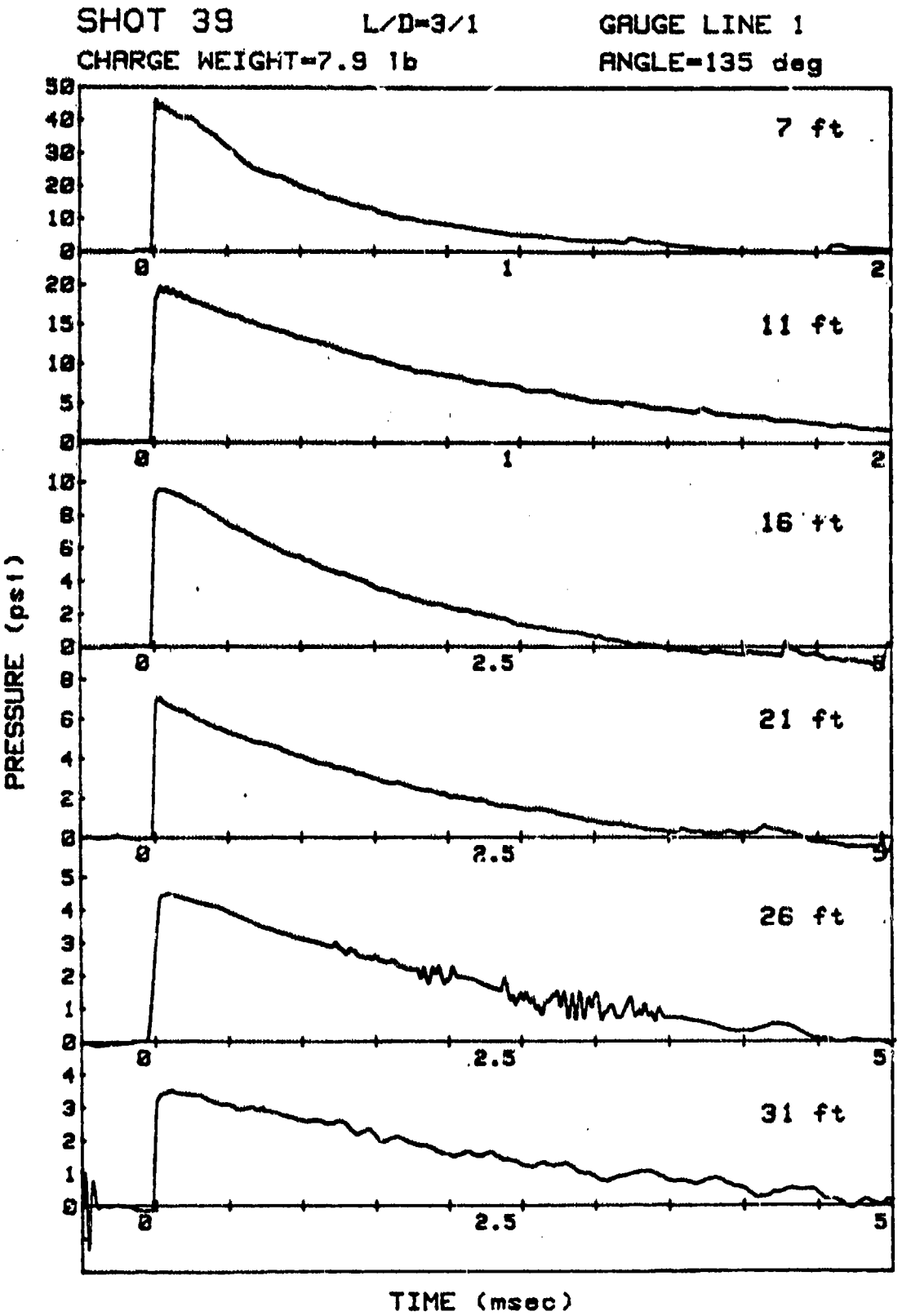
SHOT 39
L/D=3/1
GAUGE LINE 1
CHARGE WEIGHT=7.9 lb
ANGLE=135 deg
7 ft
11 ft
16 ft
21 ft
26 ft
31 ft
PRESSURE (psi)
TIME (msec)

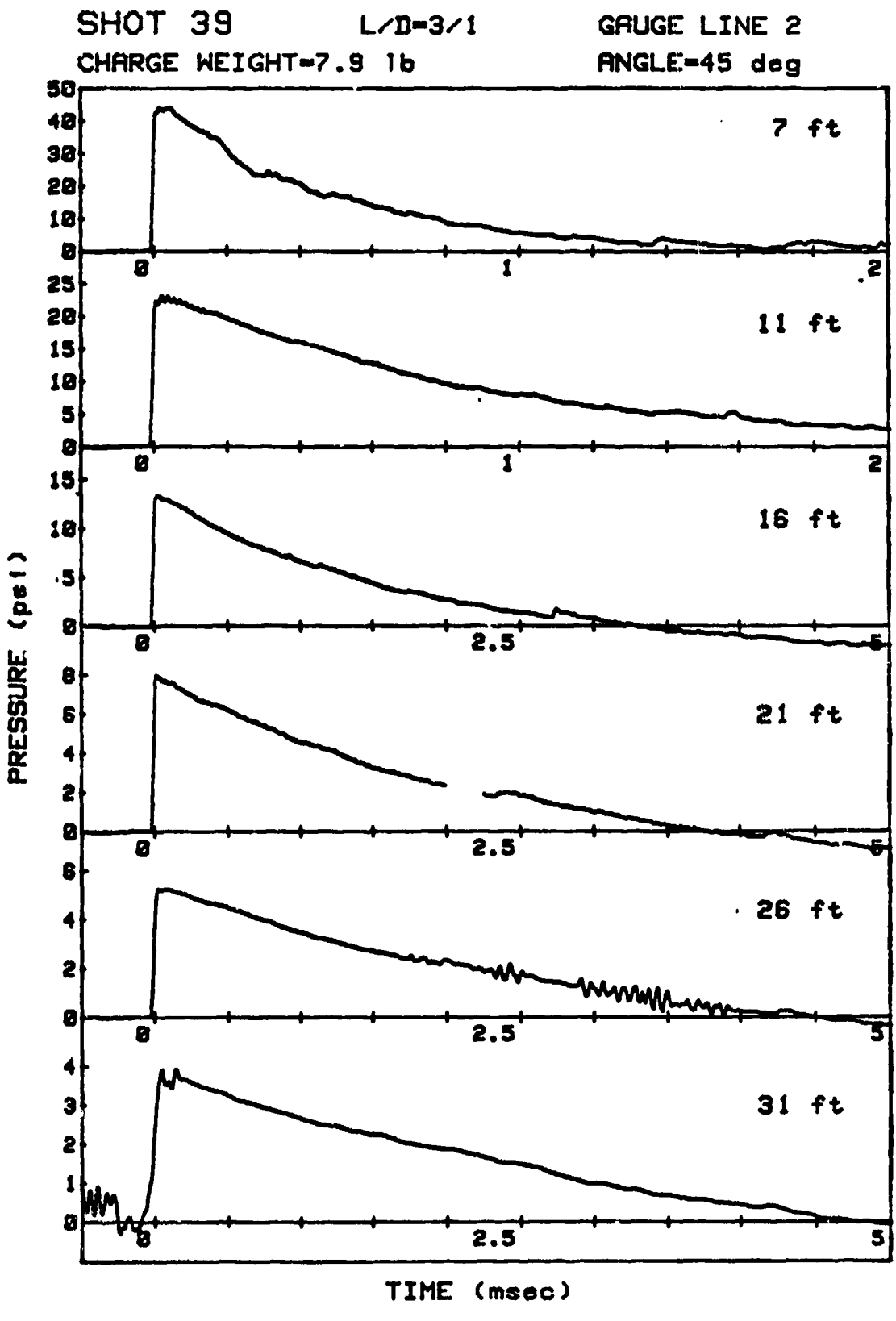
SHOT 39
L/D=3/1
GAUGE LINE 2
CHARGE WEIGHT=7.9 lb
ANGLE=45 deg
7 ft
11 ft
16 ft
21 ft
26 ft
31 ft
PRESSURE (psi)
TIME (msec)

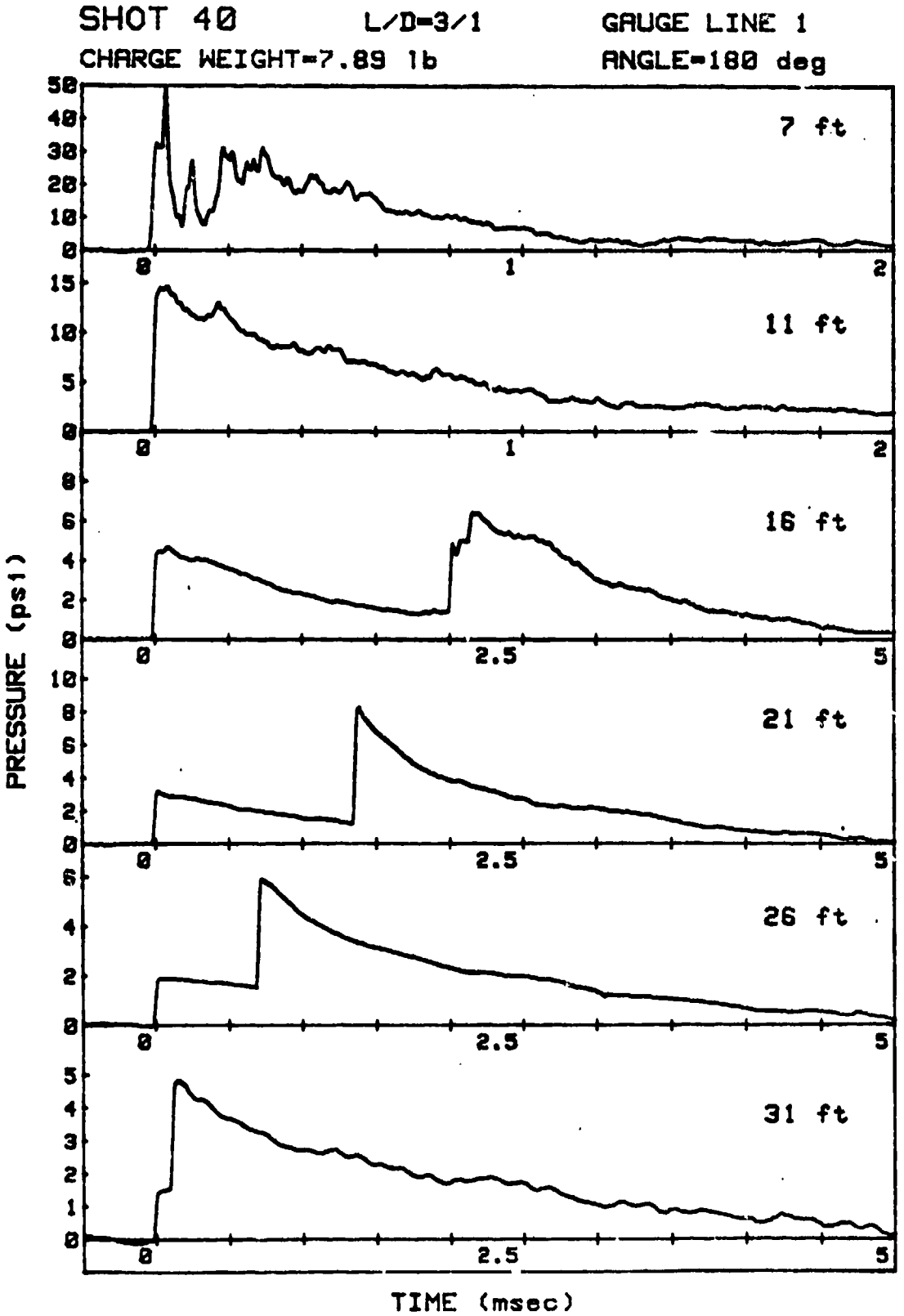
SHOT 40
L/D=3/1
GAUGE LINE 1
CHARGE WEIGHT=7.89 lb
ANGLE=180 deg
7 ft
11 ft
16 ft
21 ft
26 ft
31 ft
PRESSURE (psi)
TIME (msec)

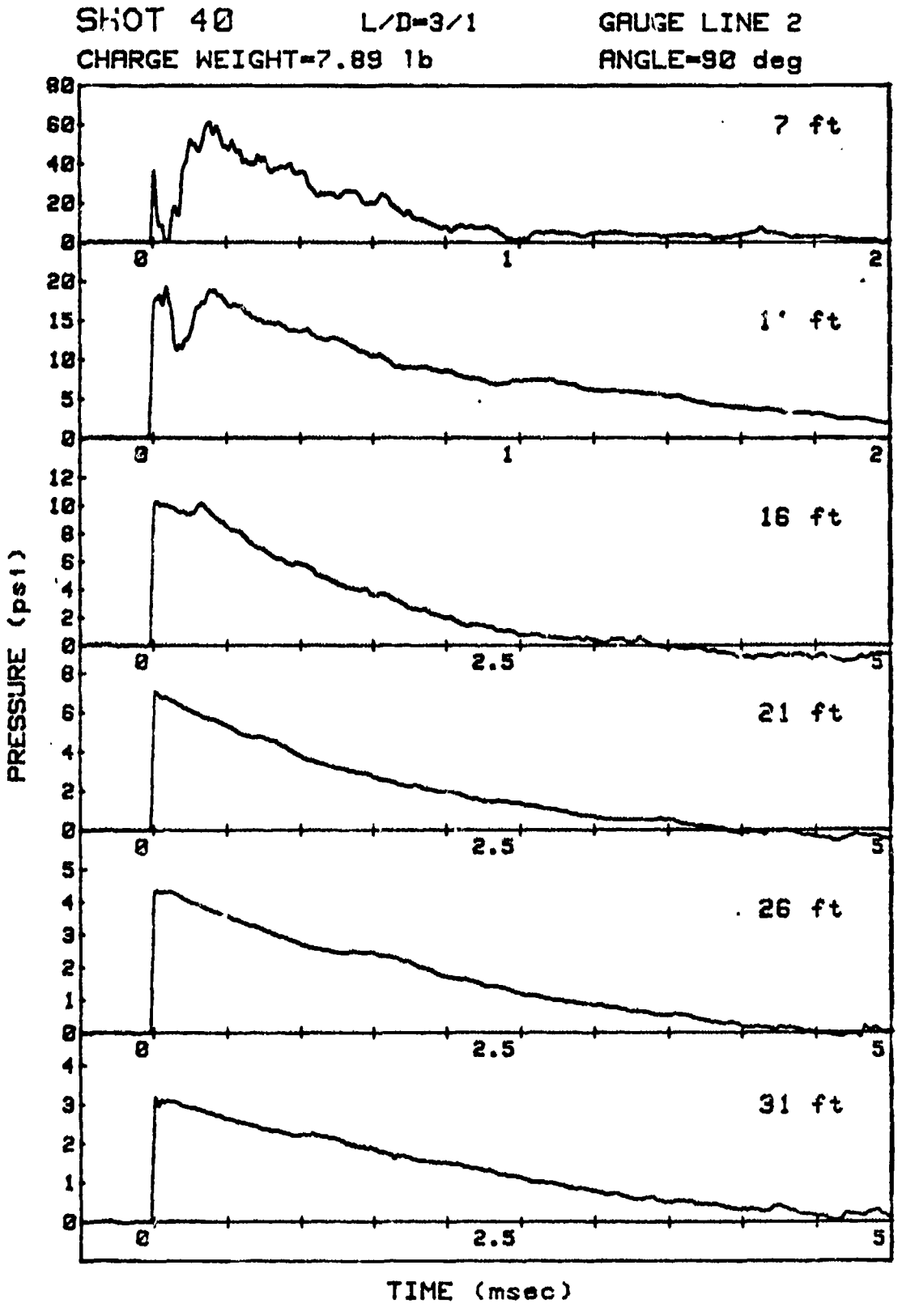
SHOT 40
L/D=3/1
GAUGE LINE 2
CHARGE WEIGHT=7.89 lb
ANGLE=90 deg
7 ft
11 ft
16 ft
21 ft
26 ft
31 ft
PRESSURE (psi)
TIME (msec)

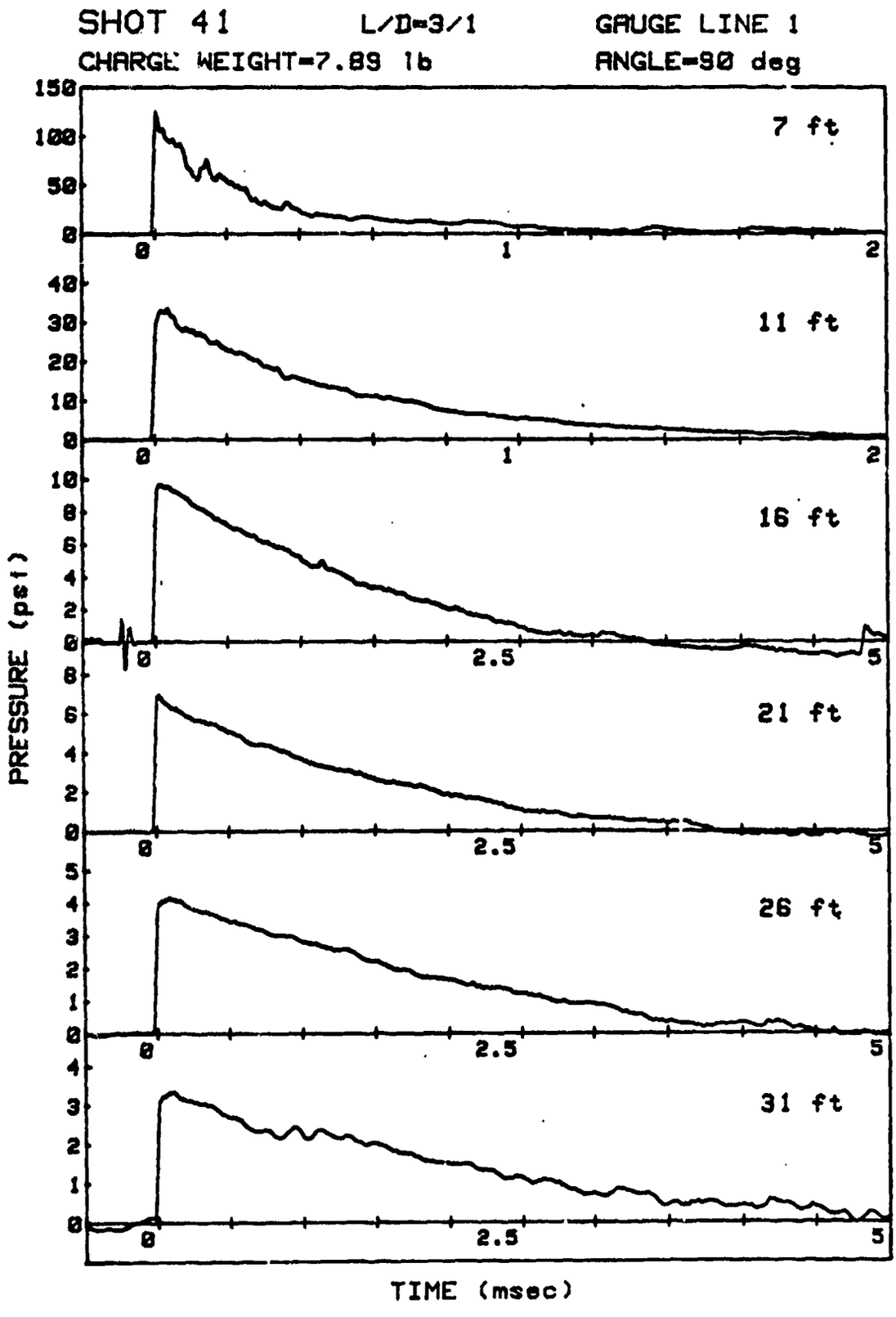
SHOT 41
L/D=3/1
GAUGE LINE 1
CHARGE WEIGHT=7.89 lb
ANGLE=90 deg
7 ft
11 ft
16 ft
21 ft
26 ft
31 ft
PRESSURE (psi)
TIME (msec)

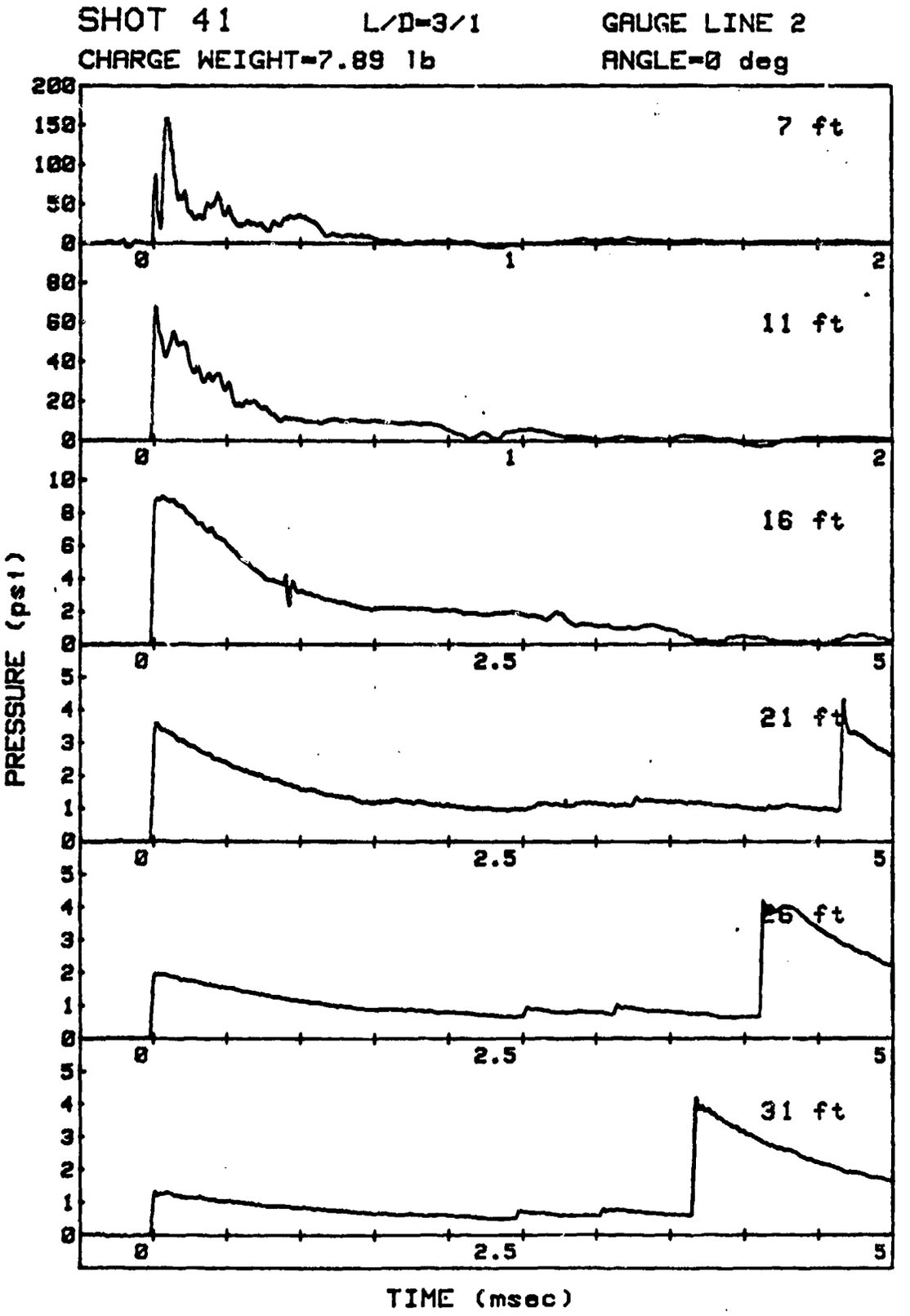
SHOT 41
L/D=3/1
GAUGE LINE 2
CHARGE WEIGHT=7.89 lb
ANGLE=0 deg
7 ft
11 ft
16 ft
21 ft
26 ft
31 ft
PRESSURE (psi)
TIME (msec)

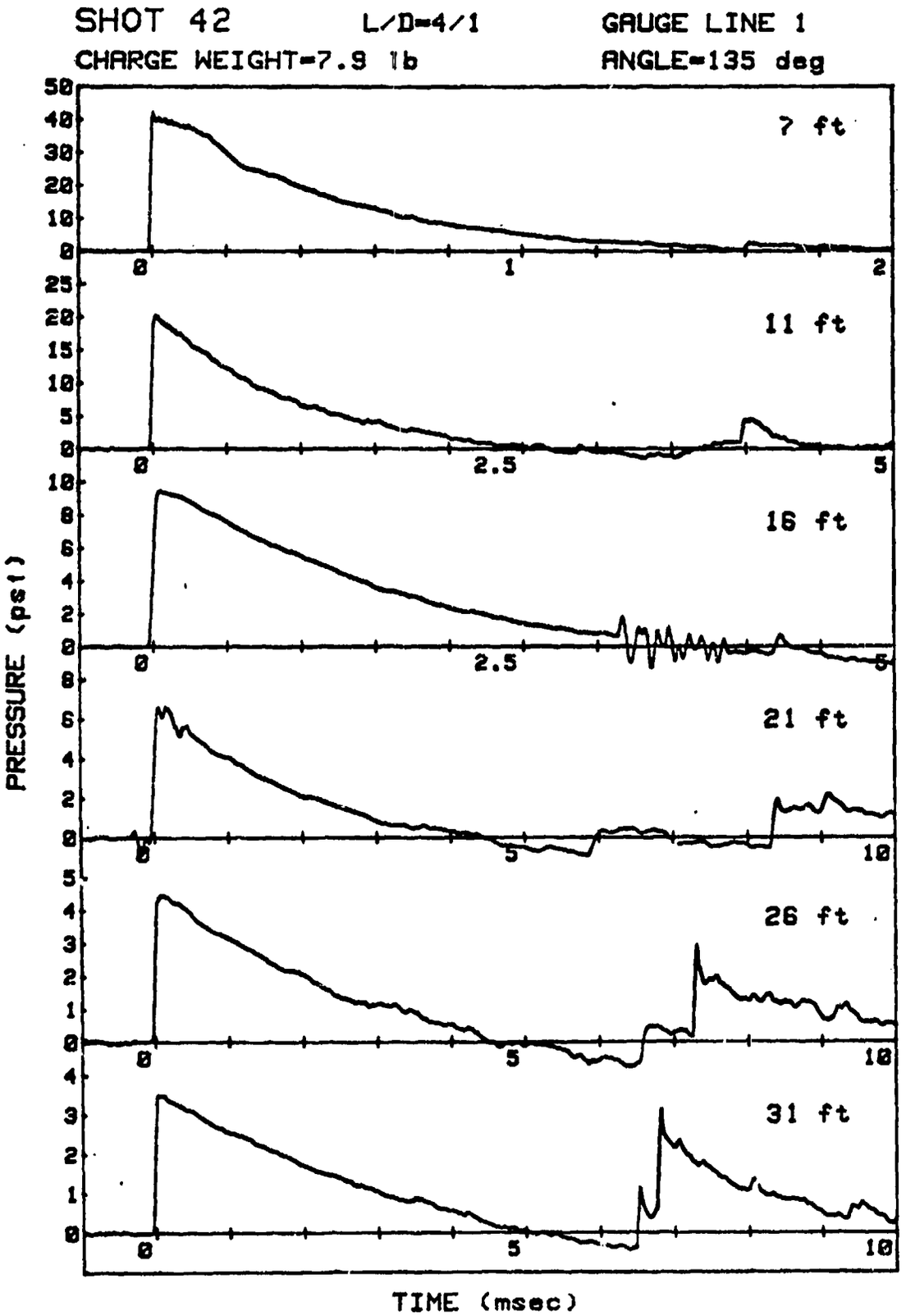
SHOT 42
L/D=4/1
GAUGE LINE 1
CHARGE WEIGHT=7.9 lb
ANGLE=135 deg
7 ft
11 ft
16 ft
21 ft
26 ft
31 ft
PRESSURE (psi)
TIME (msec)

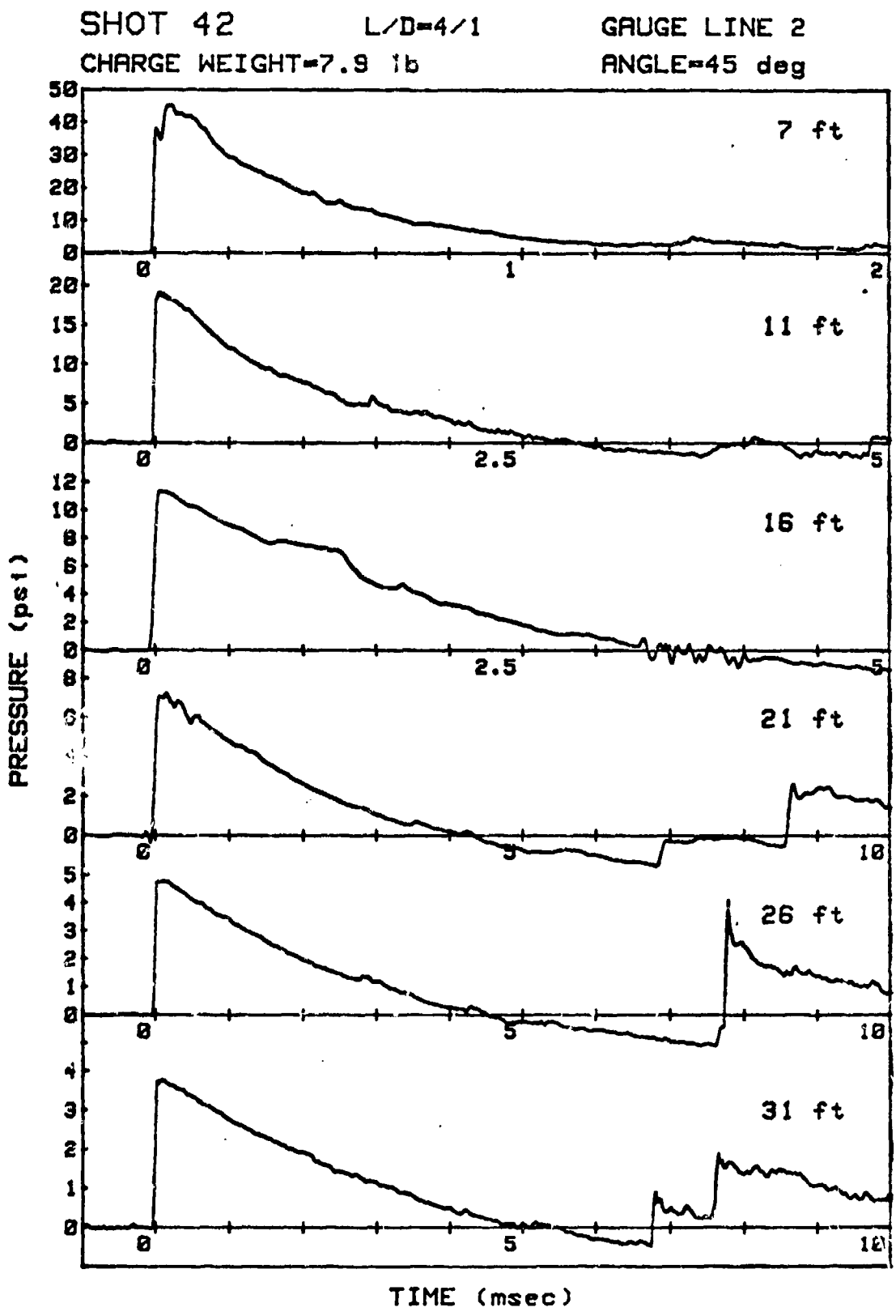
SHOT 42
L/D=4/1
GAUGE LINE 2
CHARGE WEIGHT=7.9 lb
ANGLE=45 deg
7 ft
11 ft
16 ft
21 ft
26 ft
31 ft
PRESSURE (psi)
TIME (msec)

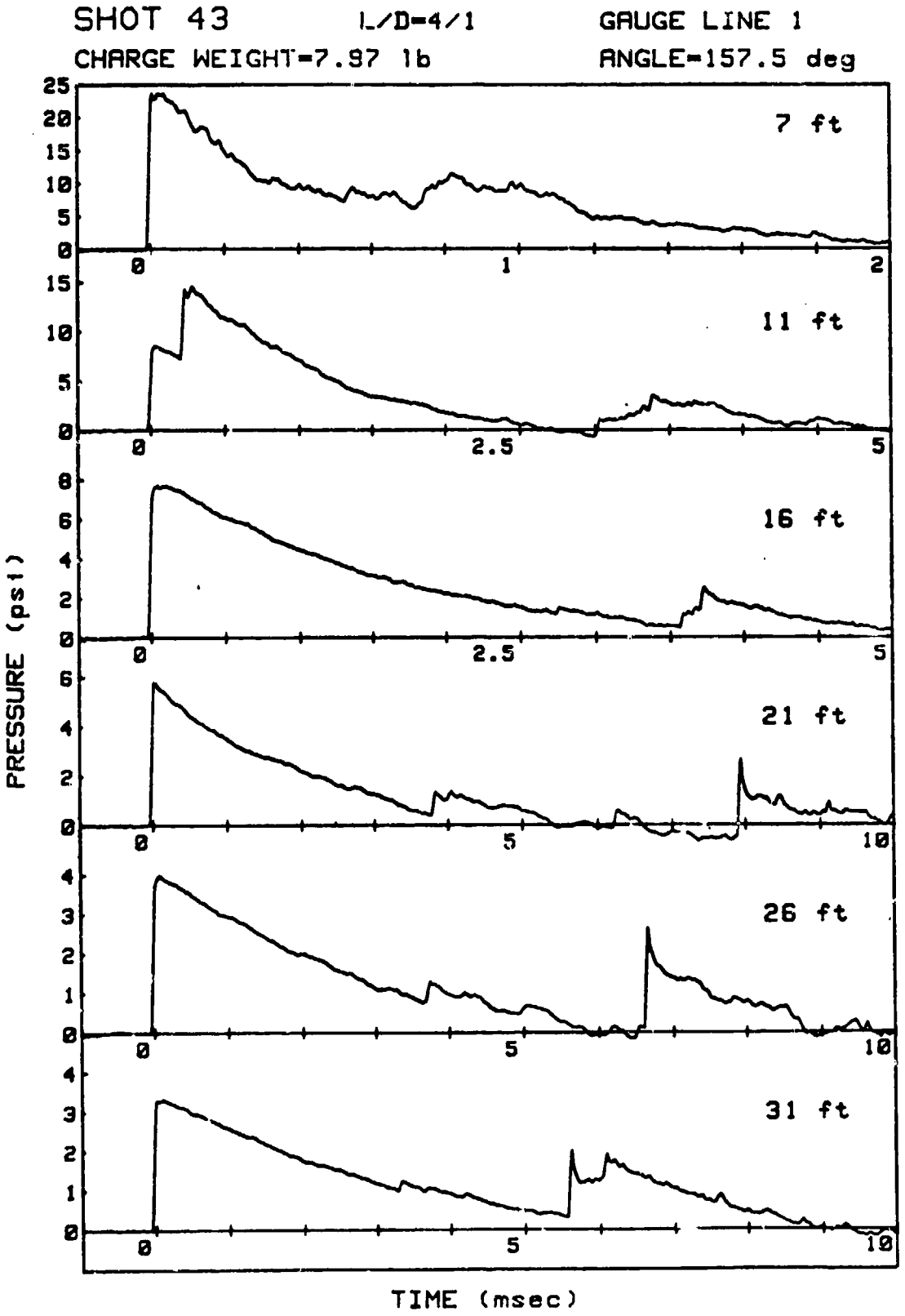
SHOT 43
L/D=4/1
GAUGE LINE 1
CHARGE WEIGHT=7.97 lb
ANGLE=157.5 deg
7 ft
11 ft
16 ft
21 ft
26 ft
31 ft
PRESSURE (psi)
TIME (msec)

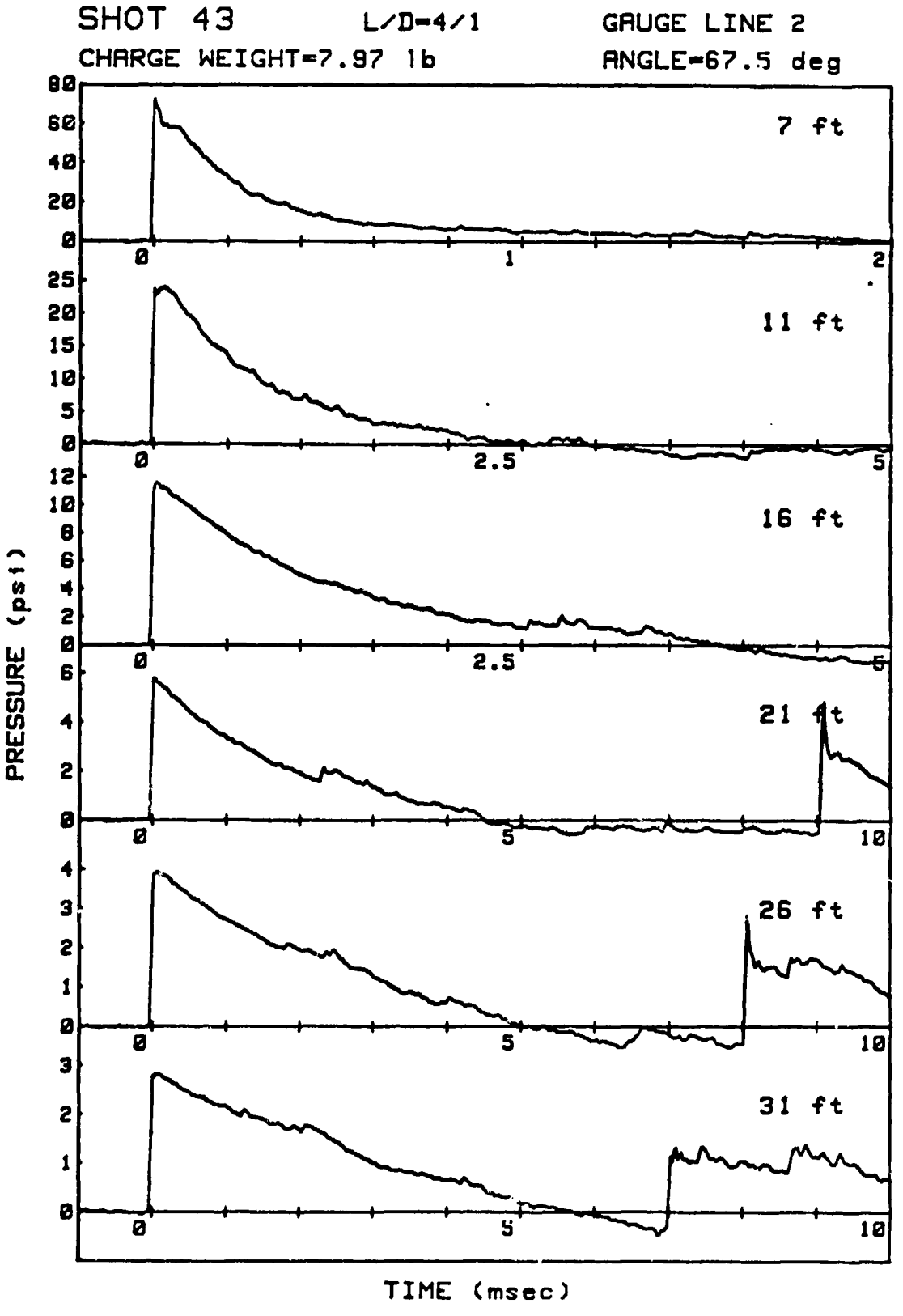
SHOT 43
L/D=4/1
GAUGE LINE 2
CHARGE WEIGHT=7.97 lb
ANGLE=67.5 deg
7 ft
11 ft
16 ft
21 ft
26 ft
31 ft
PRESSURE (psi)
TIME (msec)

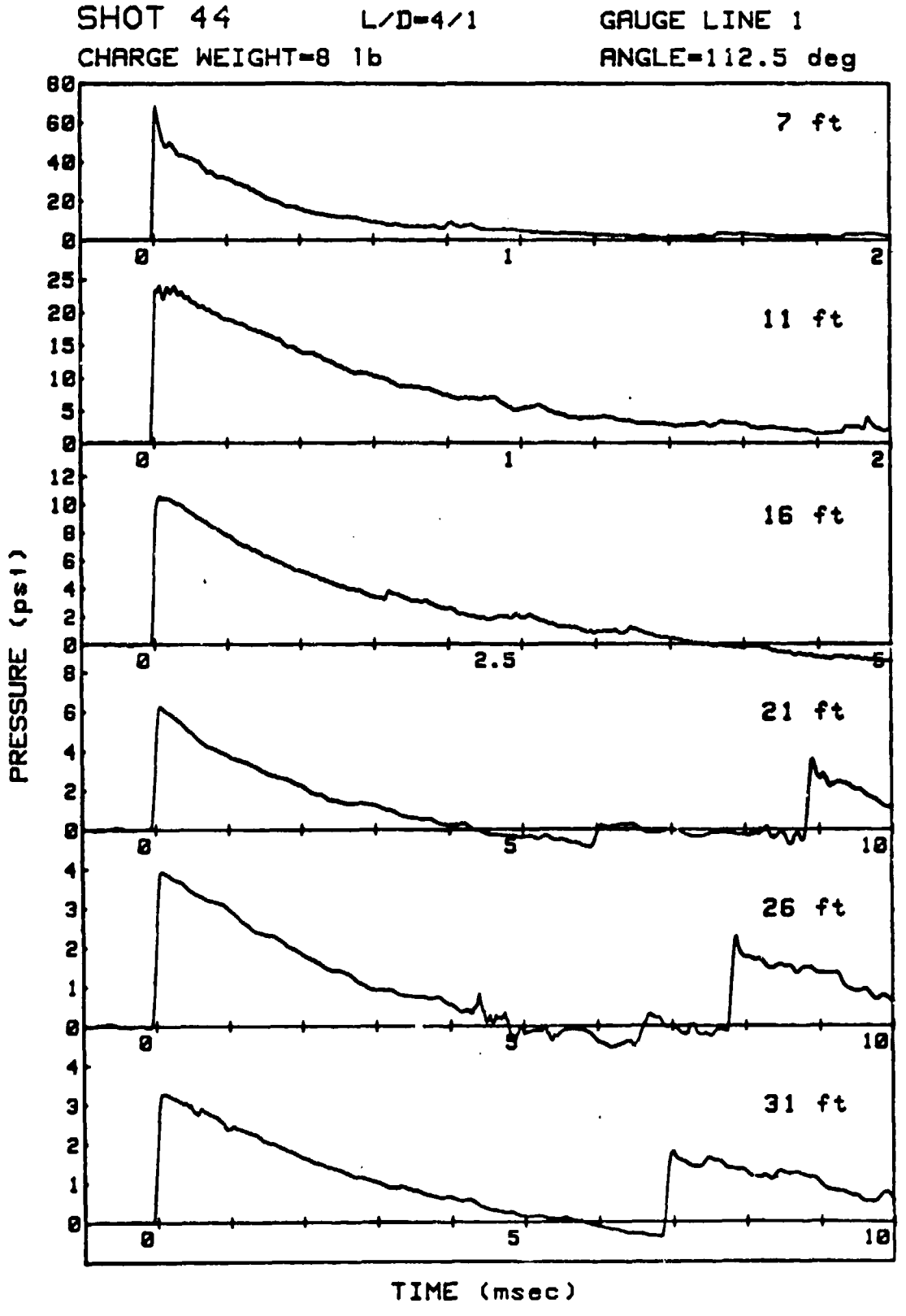
SHOT 44
L/D=4/1
GAUGE LINE 1
CHARGE WEIGHT=8 lb
ANGLE=112.5 deg
7 ft
11 ft
16 ft
21 ft
26 ft
31 ft
PRESSURE (psi)
TIME (msec)

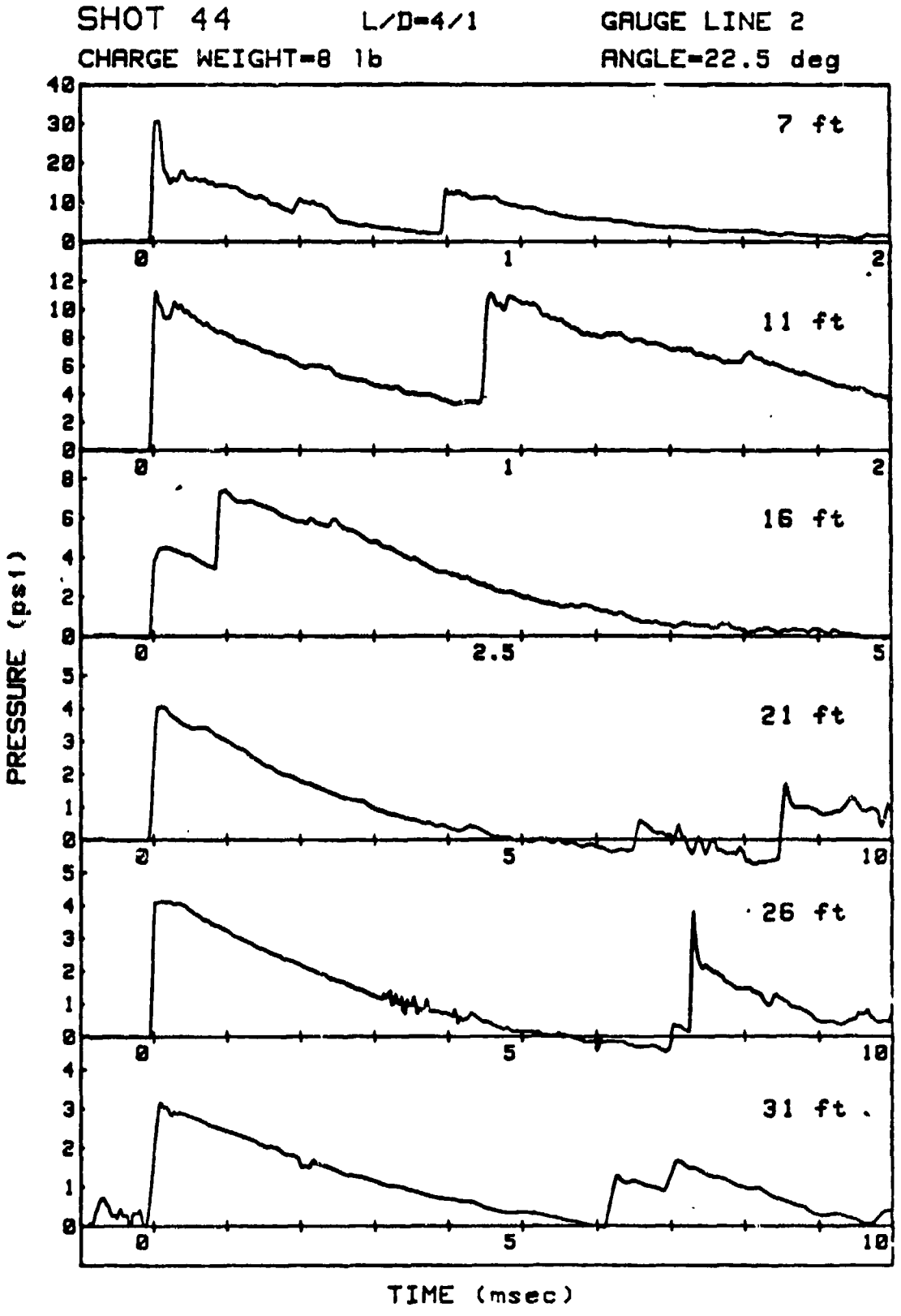
SHOT 44
L/D=4/1
GAUGE LINE 2
CHARGE WEIGHT=8 lb
ANGLE=22.5 deg
7 ft
11 ft
16 ft
21 ft
26 ft
31 ft
PRESSURE (psi)
TIME (msec)

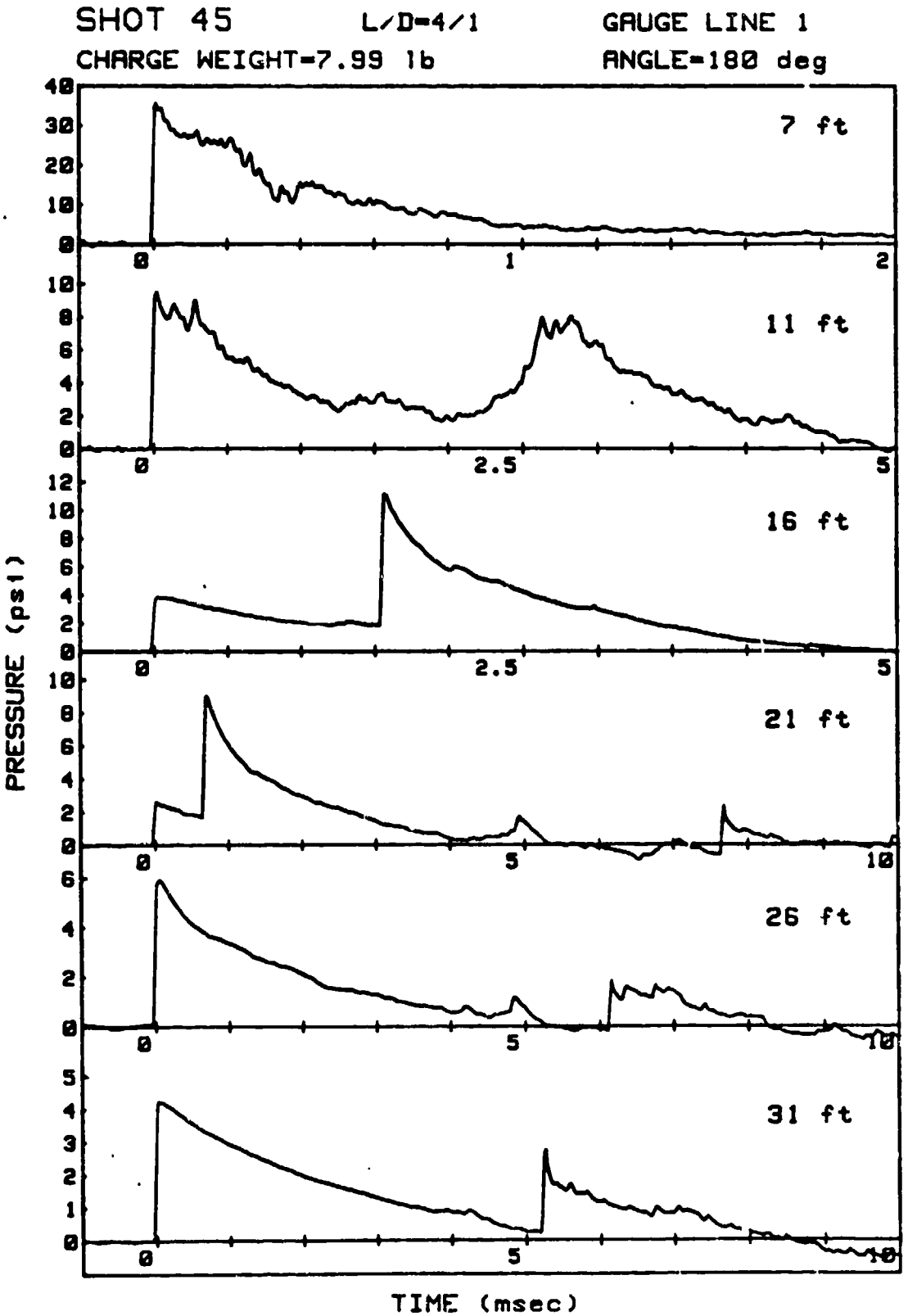
SHOT 45
L/D=4/1
GAUGE LINE 1
CHARGE WEIGHT=7.99 lb
ANGLE=180 deg
7 ft
11 ft
16 ft
21 ft
26 ft
31 ft
PRESSURE (psi)
TIME (msec)

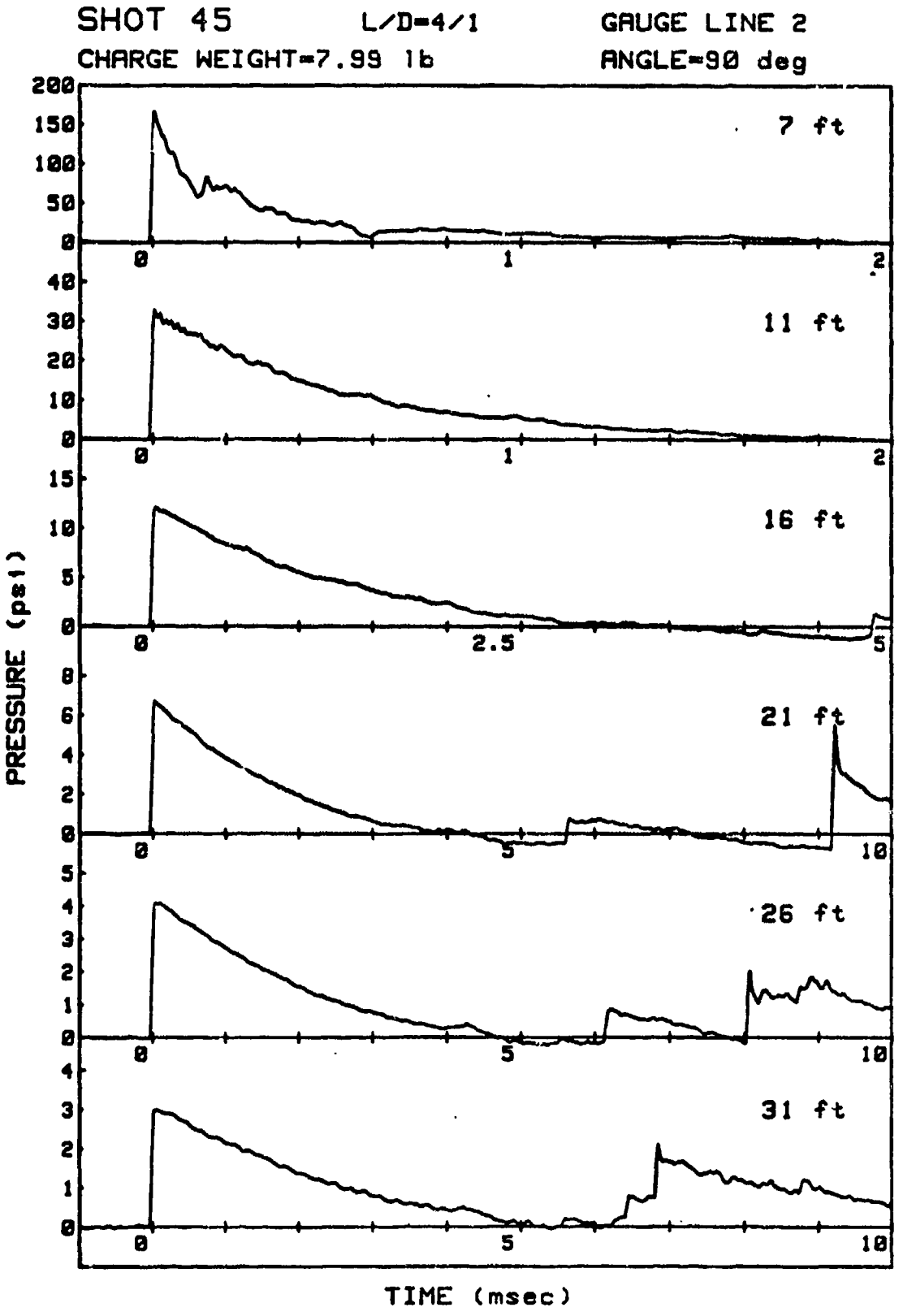
SHOT 45
L/D=4/1
GAUGE LINE 2
CHARGE WEIGHT=7.99 lb
ANGLE=90 deg
7 ft
11 ft
16 ft
21 ft
26 ft
31 ft
PRESSURE (psi)
TIME (msec)

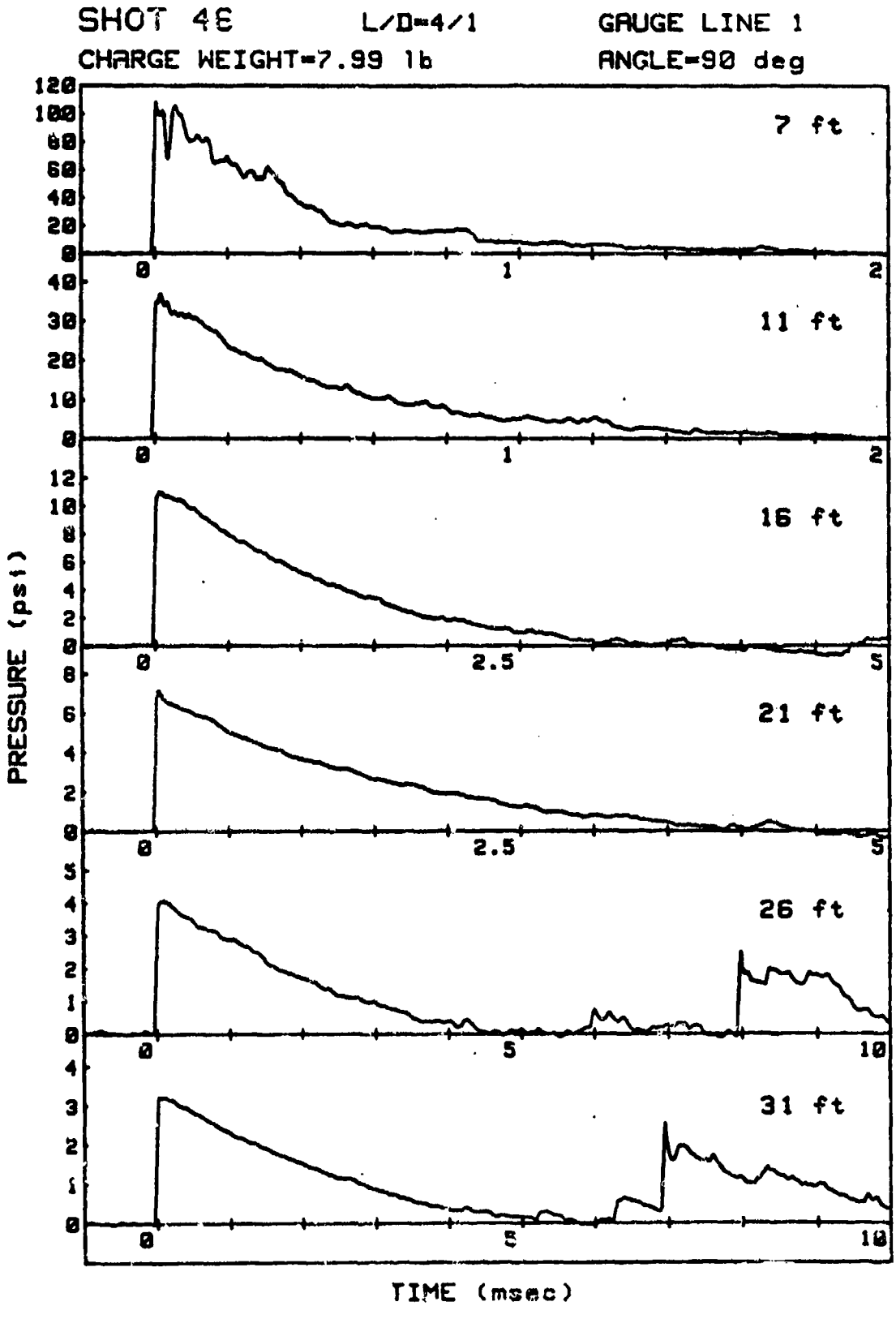
SHOT 4E
L/D=4/1
GAUGE LINE 1
CHARGE WEIGHT=7.99 lb
ANGLE=90 deg
7 ft
11 ft
16 ft
21 ft
26 ft
31 ft
PRESSURE (psi)
TIME (msec)

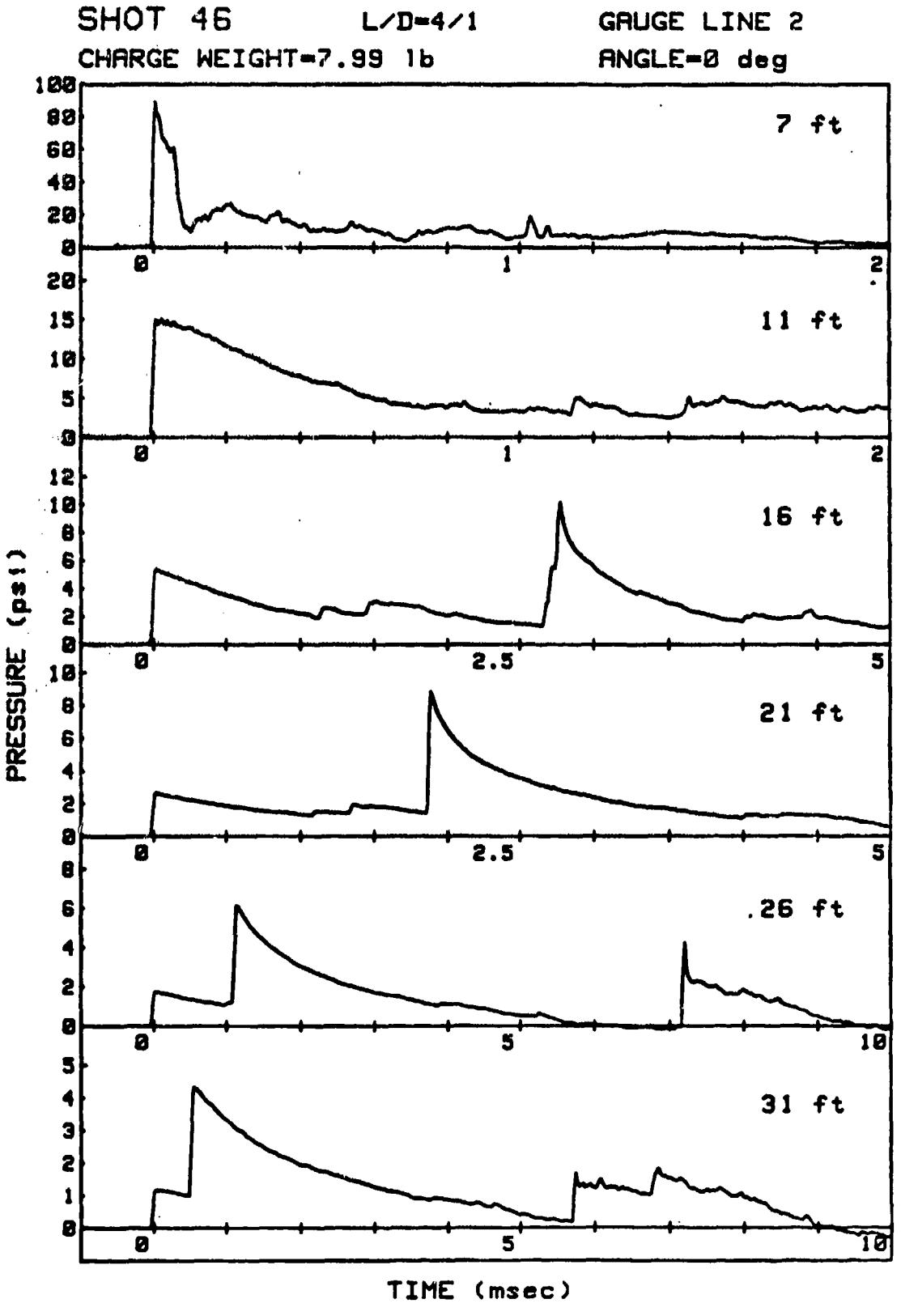
SHOT 46
L/D=4/1
GAUGE LINE 2
CHARGE WEIGHT=7.99 lb
ANGLE=0 deg
7 ft
11 ft
16 ft
21 ft
.26 ft
31 ft
PRESSURE (psi)
TIME (msec)

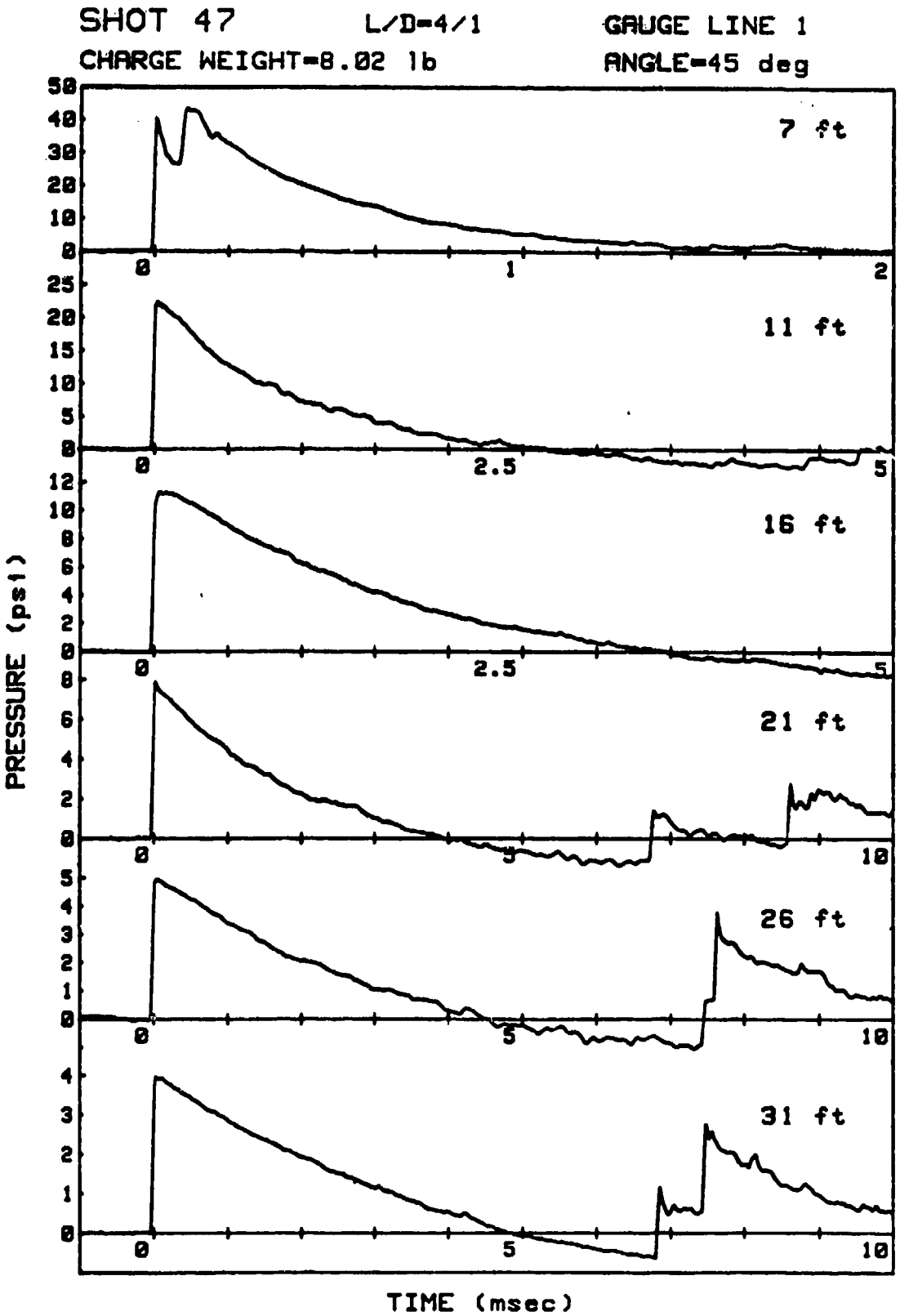
SHOT 47
L/D=4/1
GAUGE LINE 1
CHARGE WEIGHT=8.02 lb
ANGLE=45 deg
7 ft
11 ft
16 ft
21 ft
26 ft
31 ft
PRESSURE (psi)
TIME (msec)

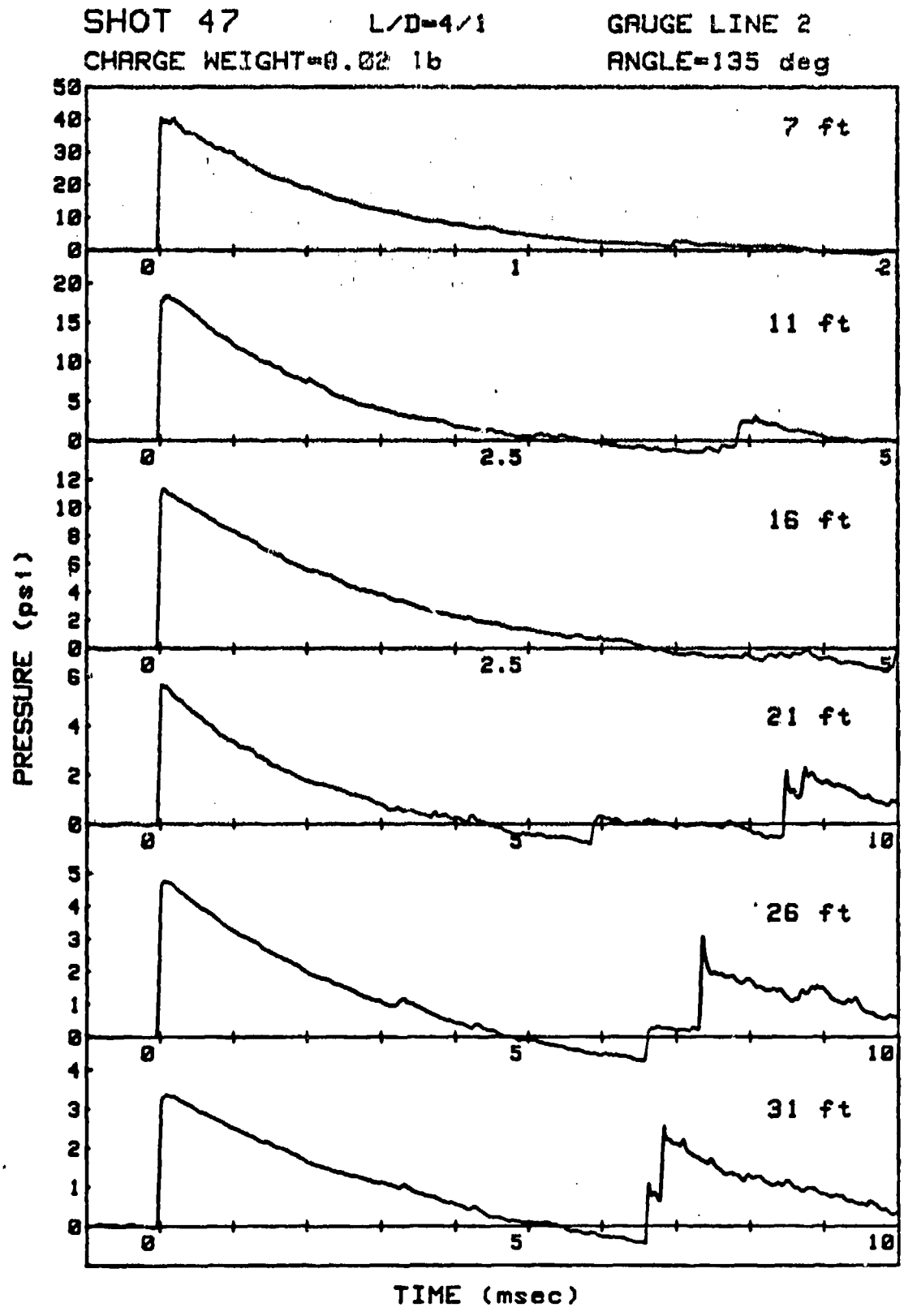
SHOT 47
L/D=4/1
GAUGE LINE 2
CHARGE WEIGHT=0.02 lb
ANGLE=135 deg
7 ft
11 ft
16 ft
21 ft
26 ft
31 ft
PRESSURE (psi)
TIME (msec)

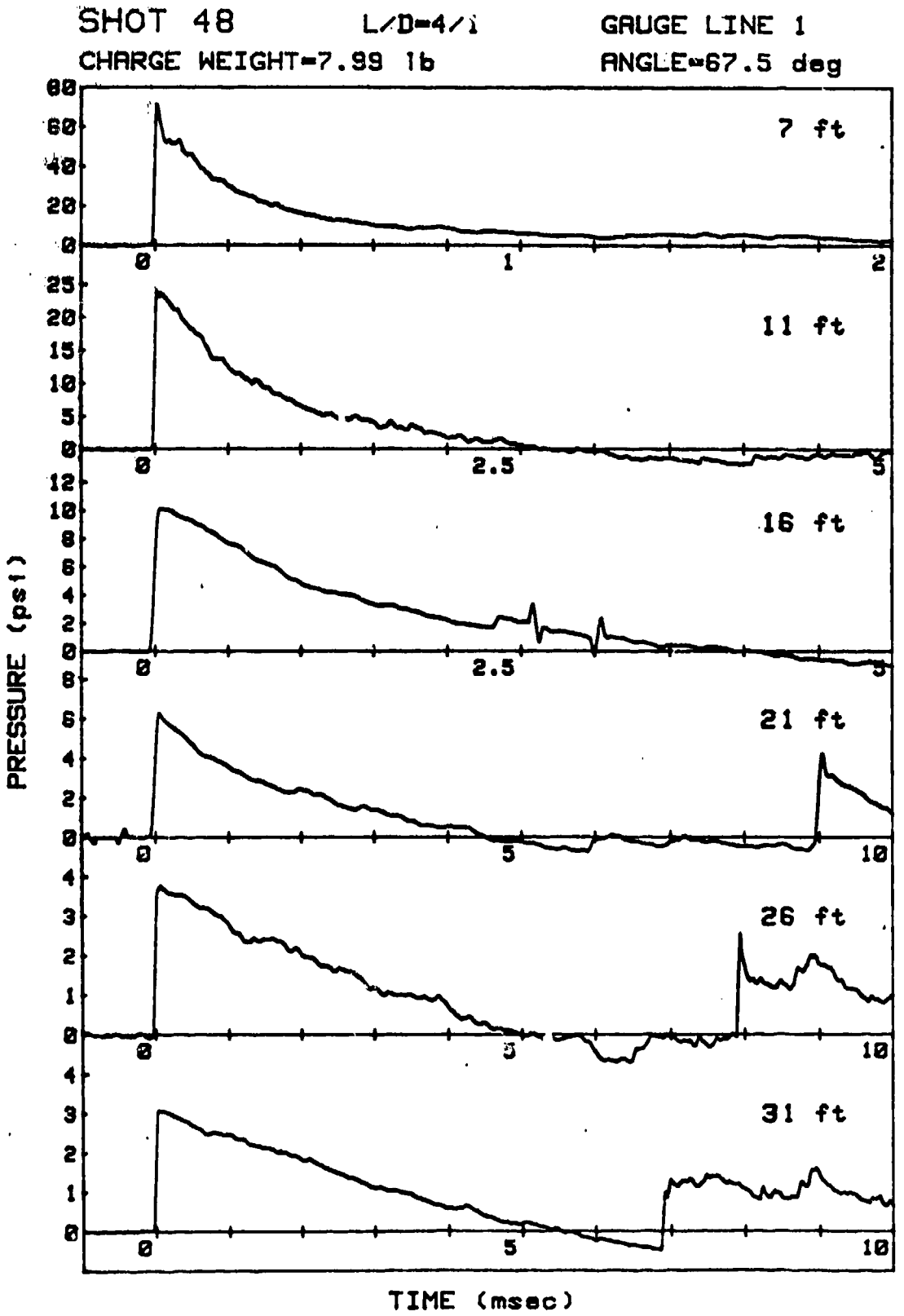
SHOT 48
L/D=4/1
GAUGE LINE 1
CHARGE WEIGHT=7.99 lb
ANGLE=67.5 deg
7 ft
11 ft
16 ft
21 ft
26 ft
31 ft
PRESSURE (psi)
TIME (msec)

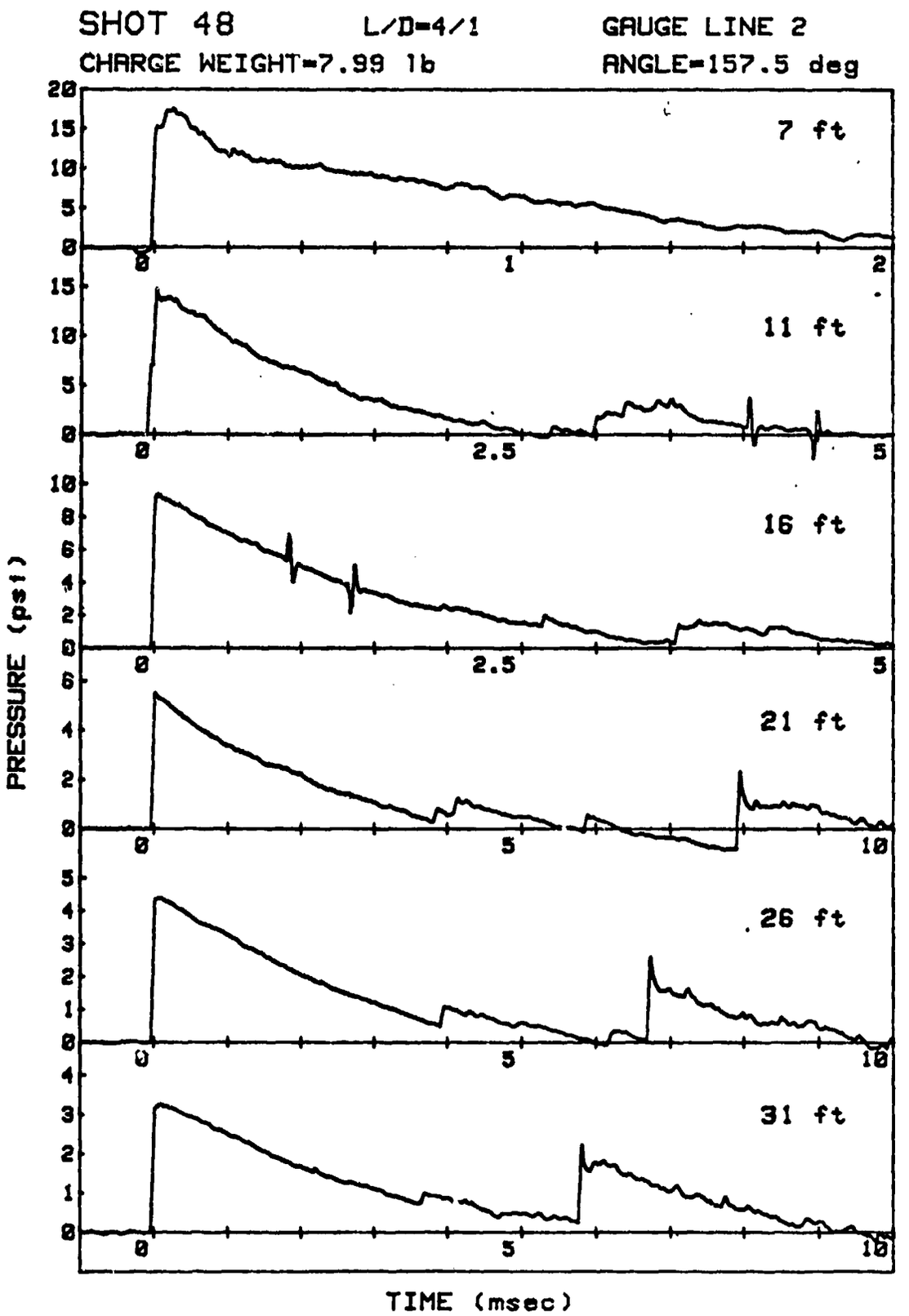
SHOT 48
L/D=4/1
GAUGE LINE 2
CHARGE WEIGHT=7.99 lb
ANGLE=157.5 deg
7 ft
11 ft
16 ft
21 ft
26 ft
31 ft
PRESSURE (psi)
TIME (msec)

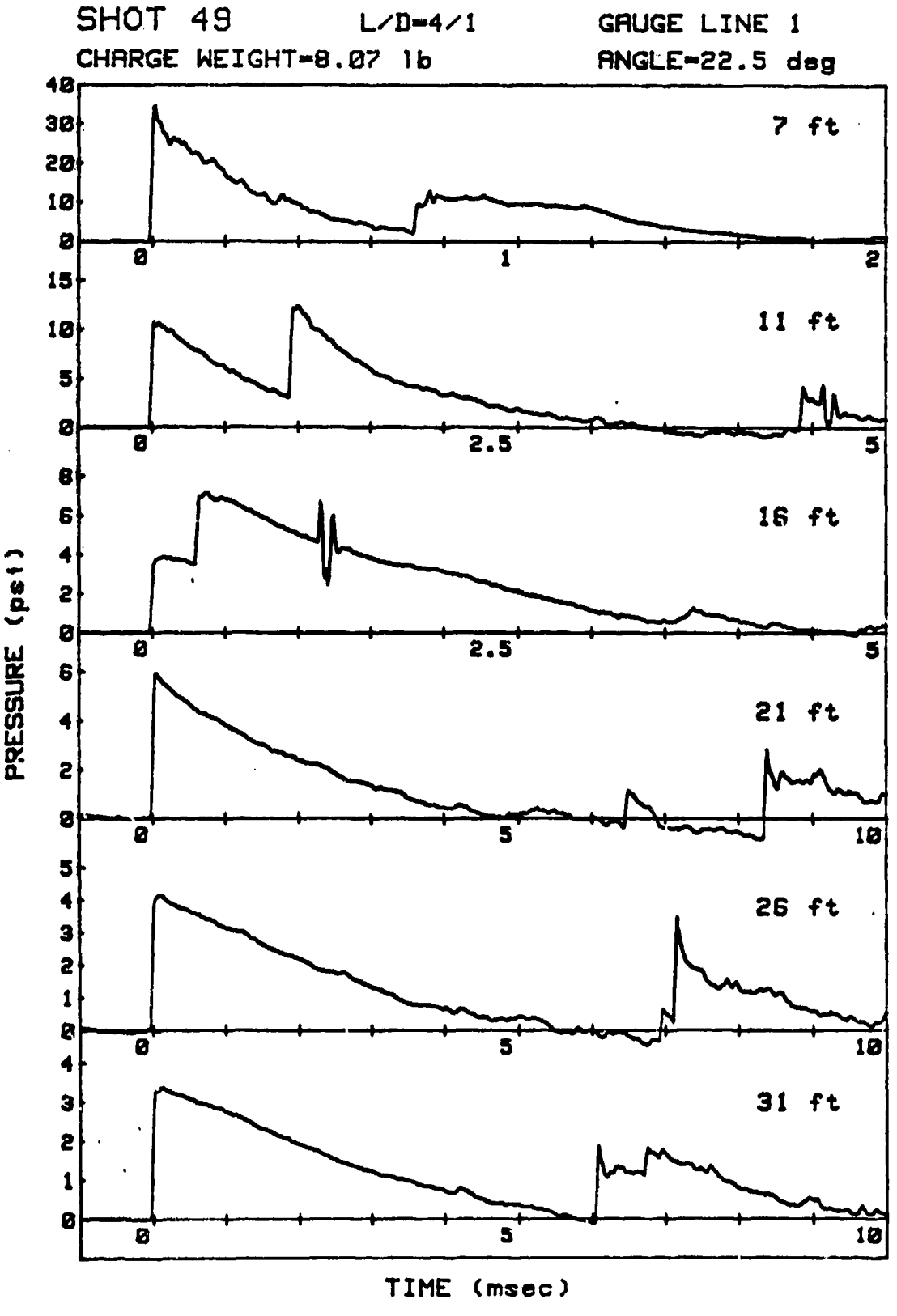
SHOT 49
L/D=4/1
GAUGE LINE 1
CHARGE WEIGHT=8.07 lb
ANGLE=22.5 deg
7 ft
11 ft
16 ft
21 ft
26 ft
31 ft
PRESSURE (psi)
TIME (msec)

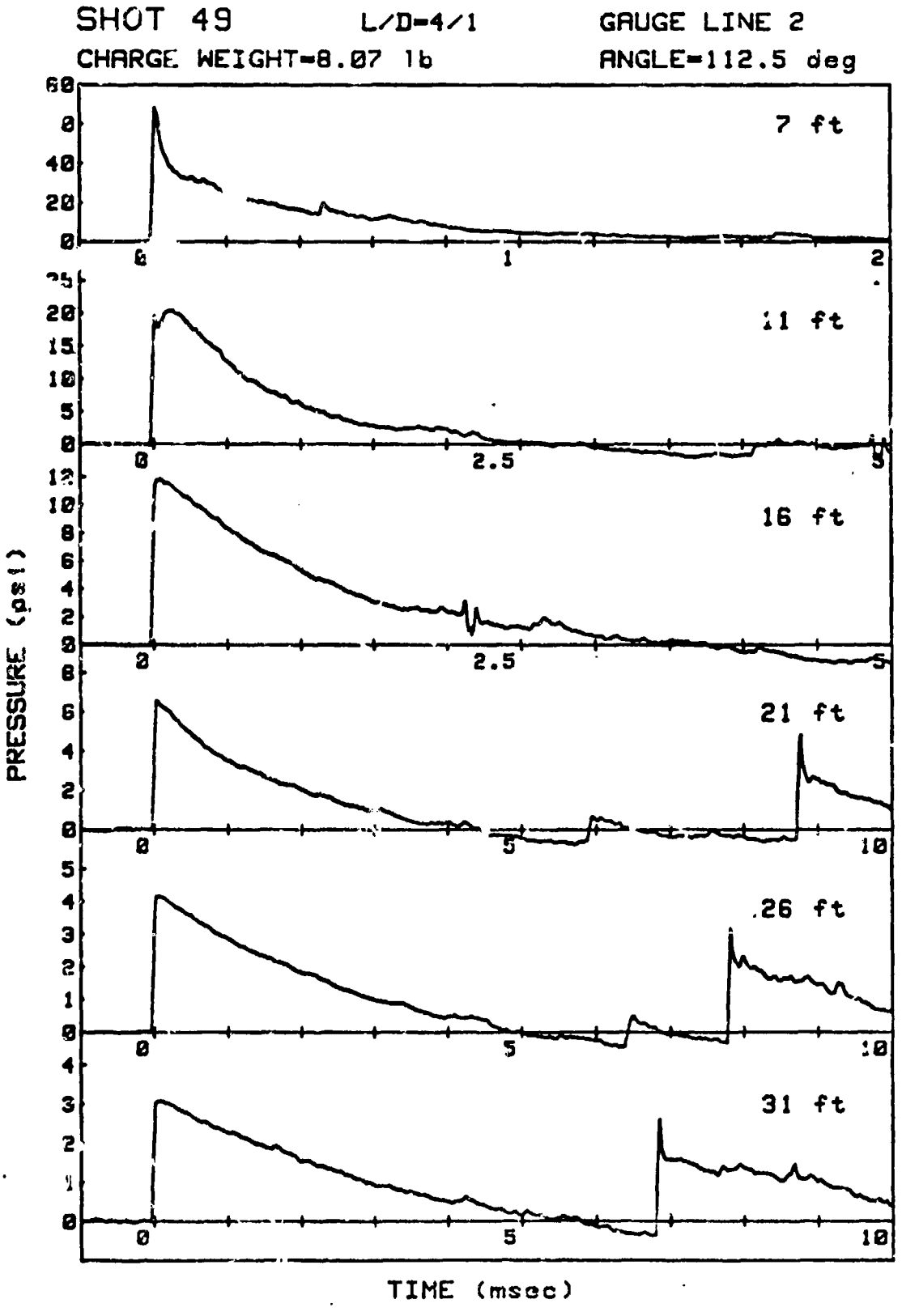
SHOT 49
L/D=4/1
GAUGE LINE 2
CHARGE WEIGHT=8.07 lb
ANGLE=112.5 deg
7 ft
11 ft
16 ft
21 ft
26 ft
31 ft
PRESSURE (psi)
TIME (msec)

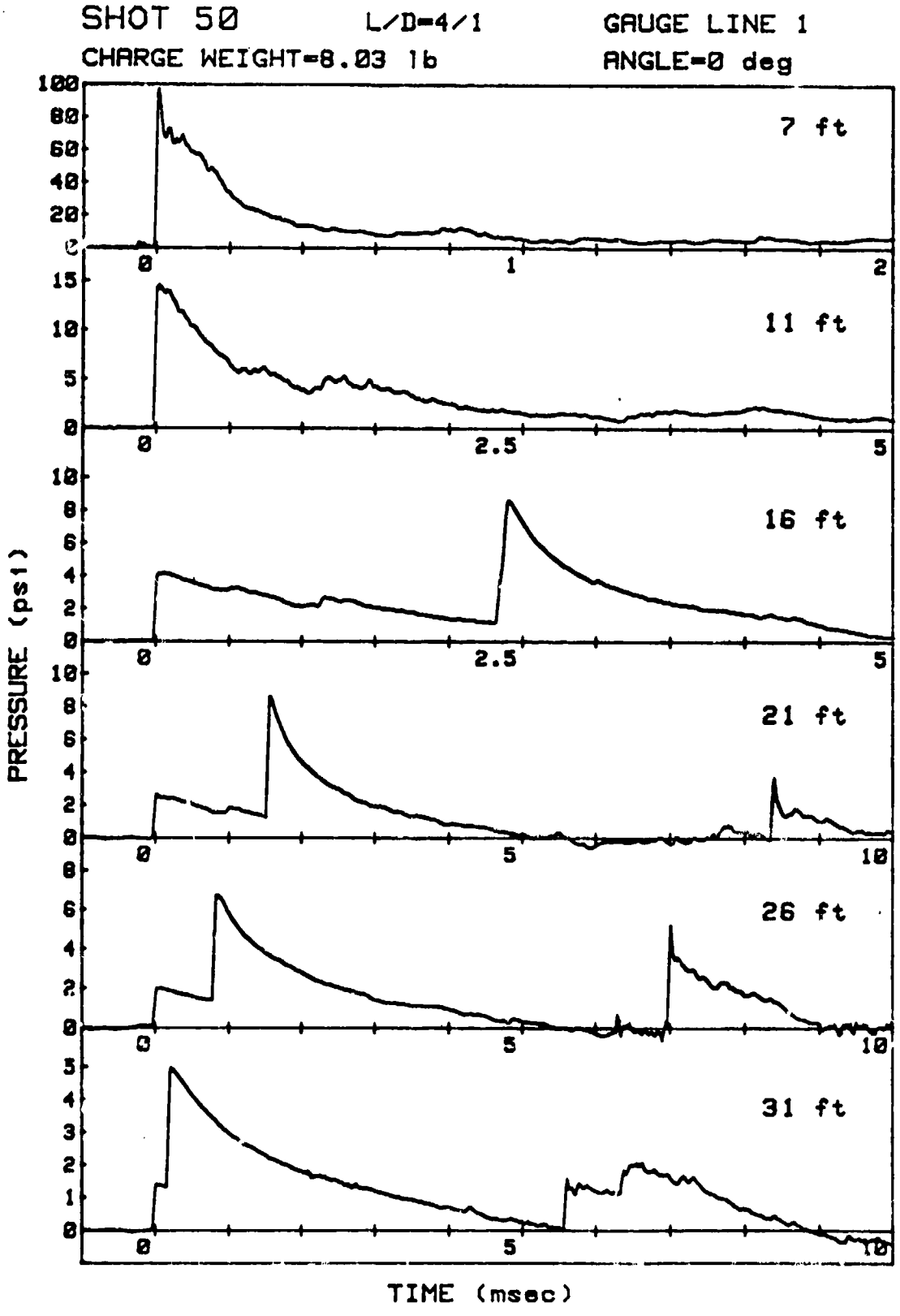
SHOT 50
L/D=4/1
GAUGE LINE 1
CHARGE WEIGHT=8.03 lb
ANGLE=0 deg
7 ft
11 ft
16 ft
21 ft
26 ft
31 ft
PRESSURE (psi)
TIME (msec)

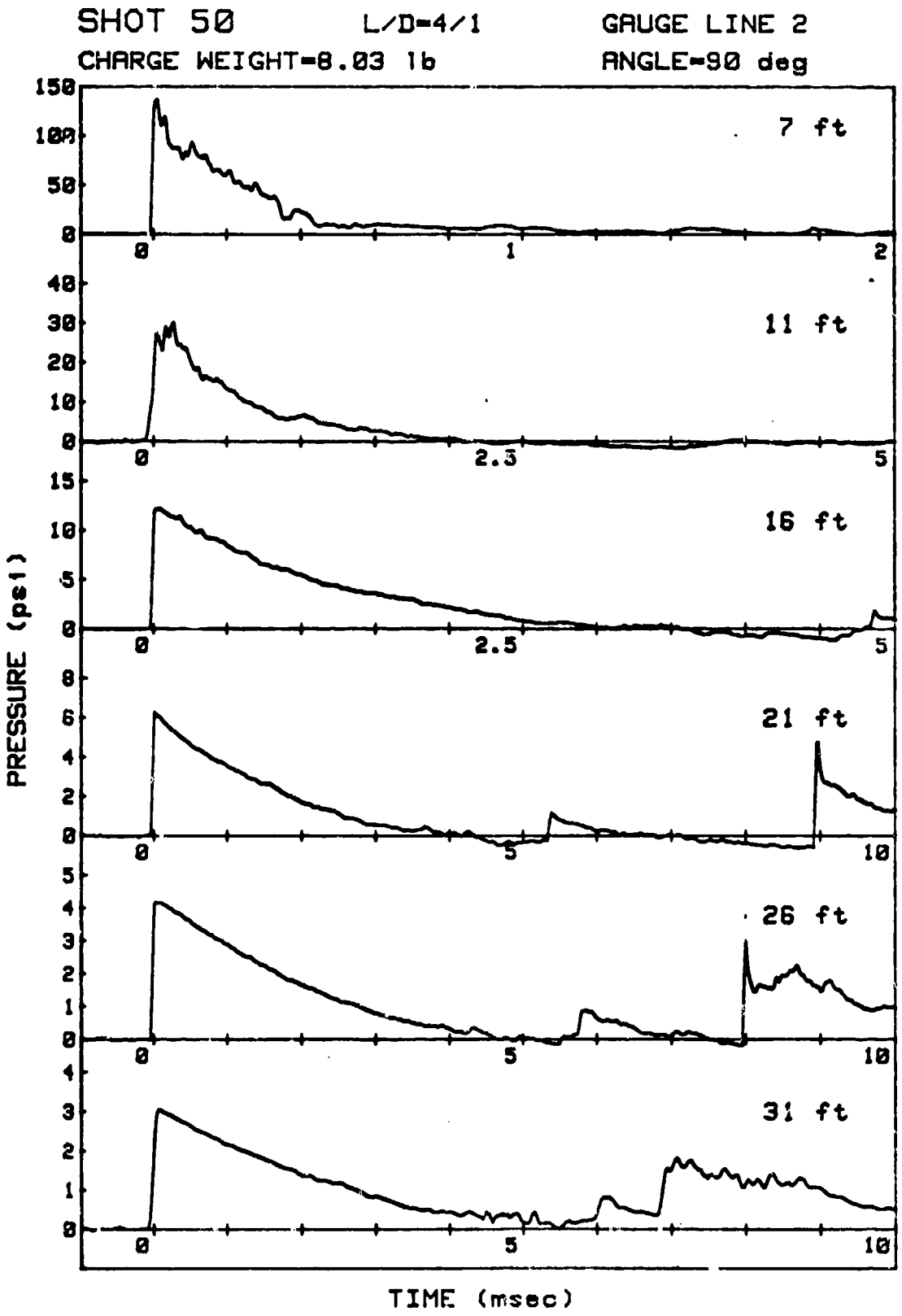
SHOT 50
L/D=4/1
GAUGE LINE 2
CHARGE WEIGHT=8.03 lb
ANGLE=90 deg
7 ft
11 ft
16 ft
21 ft
26 ft
31 ft
PRESSURE (psi)
TIME (msec)

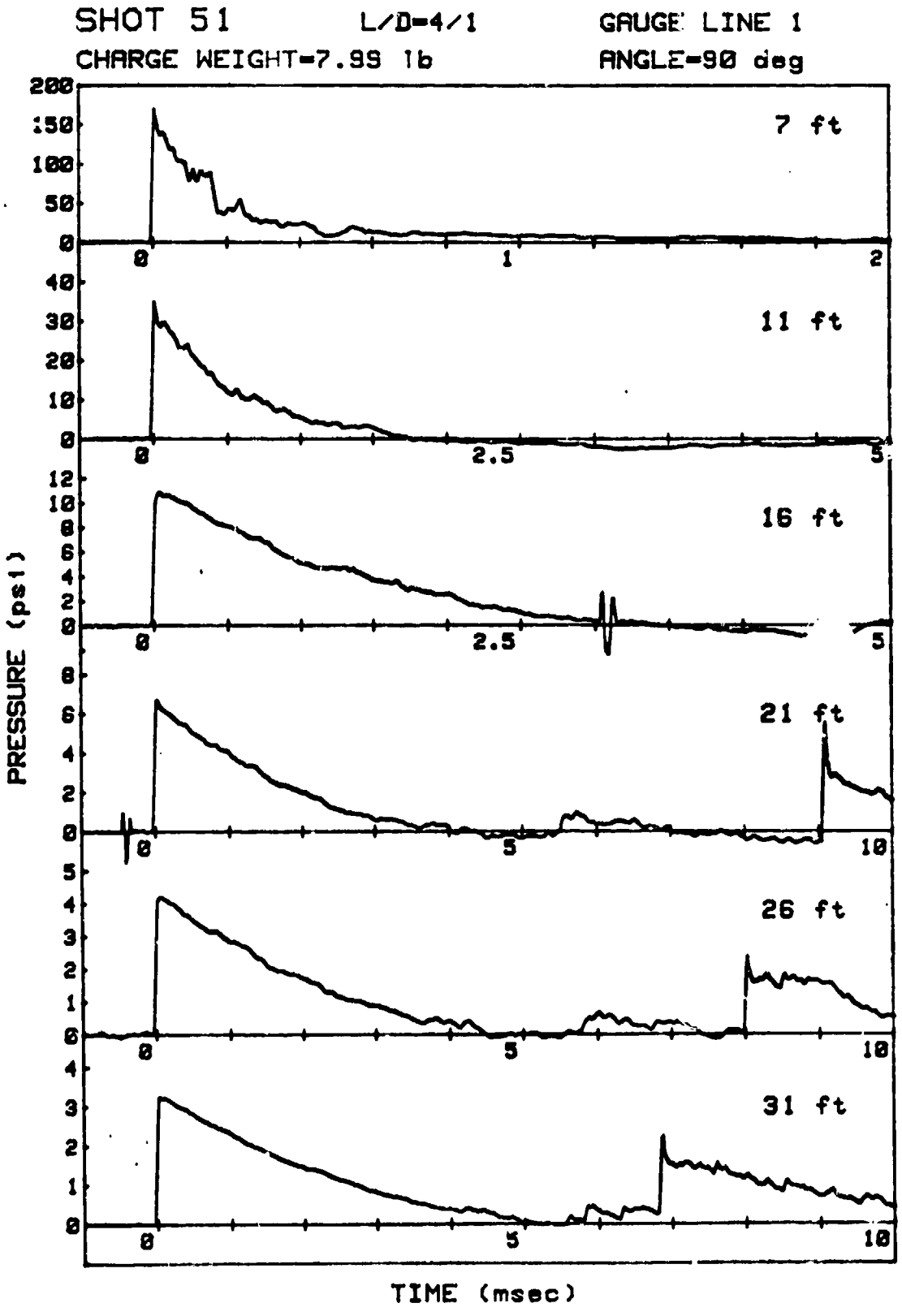
SHOT 51
L/D=4/1
GAUGE LINE 1
CHARGE WEIGHT=7.99 lb
ANGLE=90 deg
7 ft
11 ft
16 ft
21 ft
26 ft
31 ft
PRESSURE (psi)
TIME (msec)

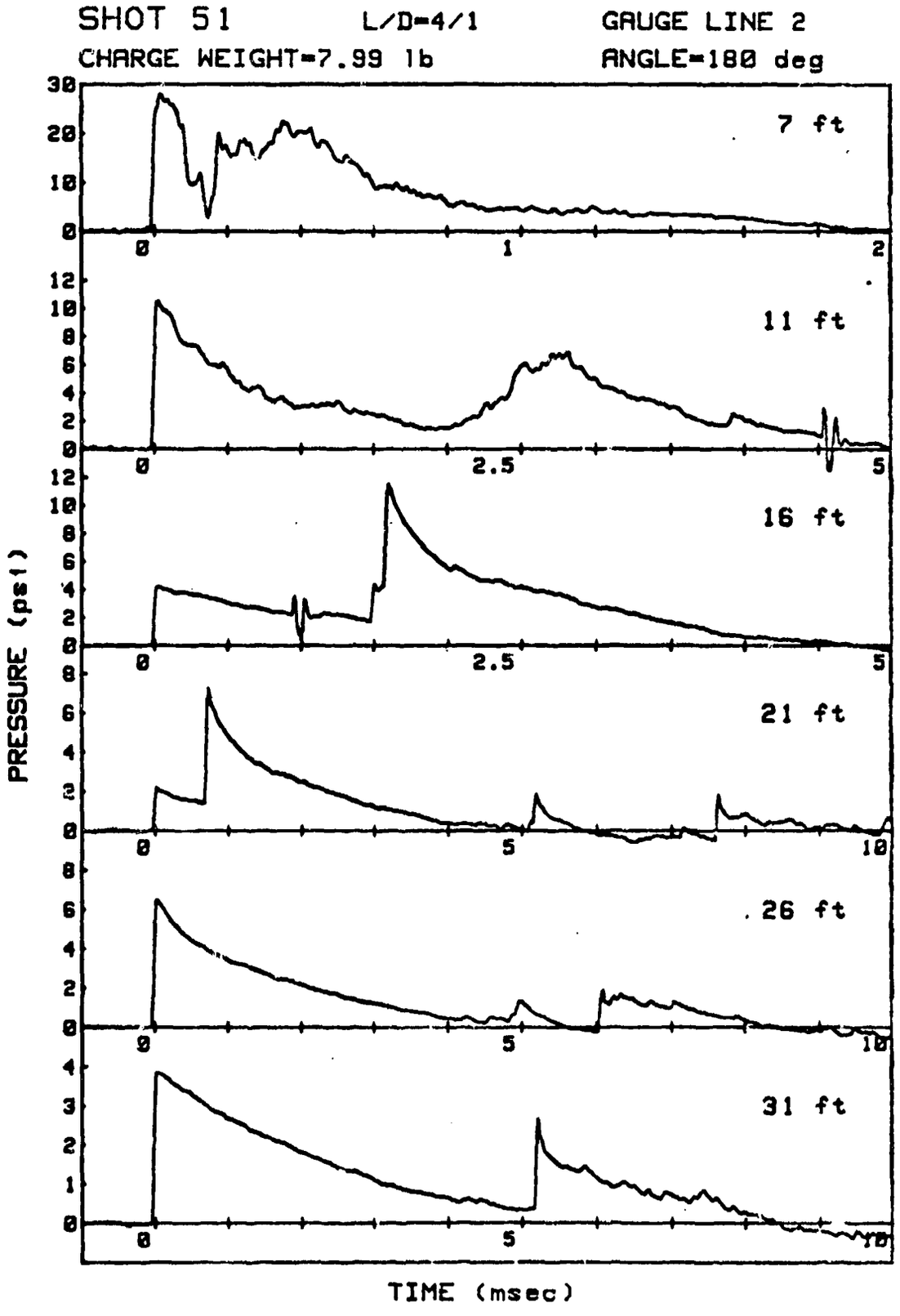
SHOT 51
L/D=4/1
GAUGE LINE 2
CHARGE WEIGHT=7.99 lb
ANGLE=180 deg
7 ft
11 ft
16 ft
21 ft
26 ft
31 ft
PRESSURE (psi)
TIME (msec)

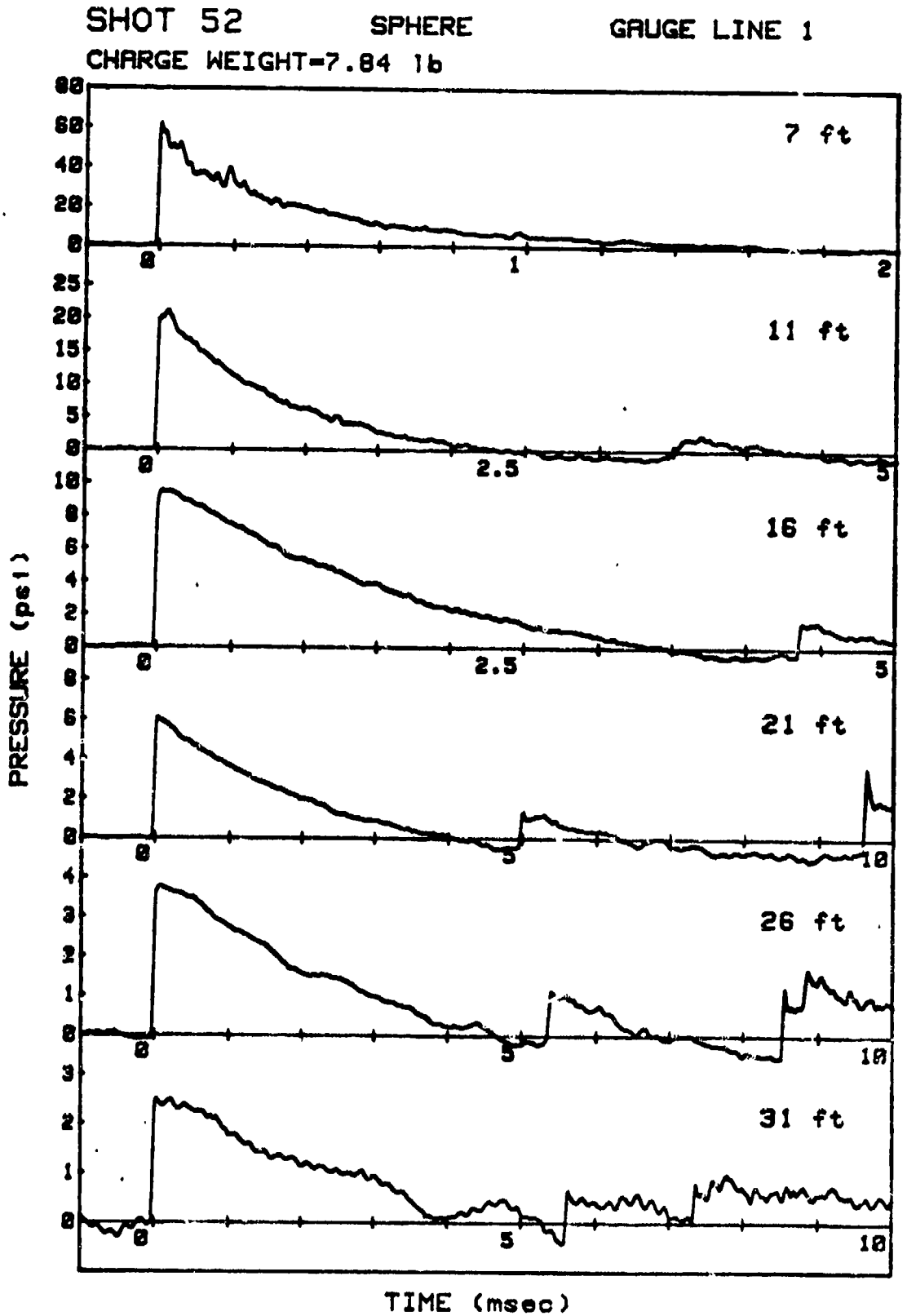
SHOT 52
SPHERE
GAUGE LINE 1
CHARGE WEIGHT=7.84 lb
7 ft
11 ft
16 ft
21 ft
26 ft
31 ft
PRESSURE (psi)
TIME (msec)

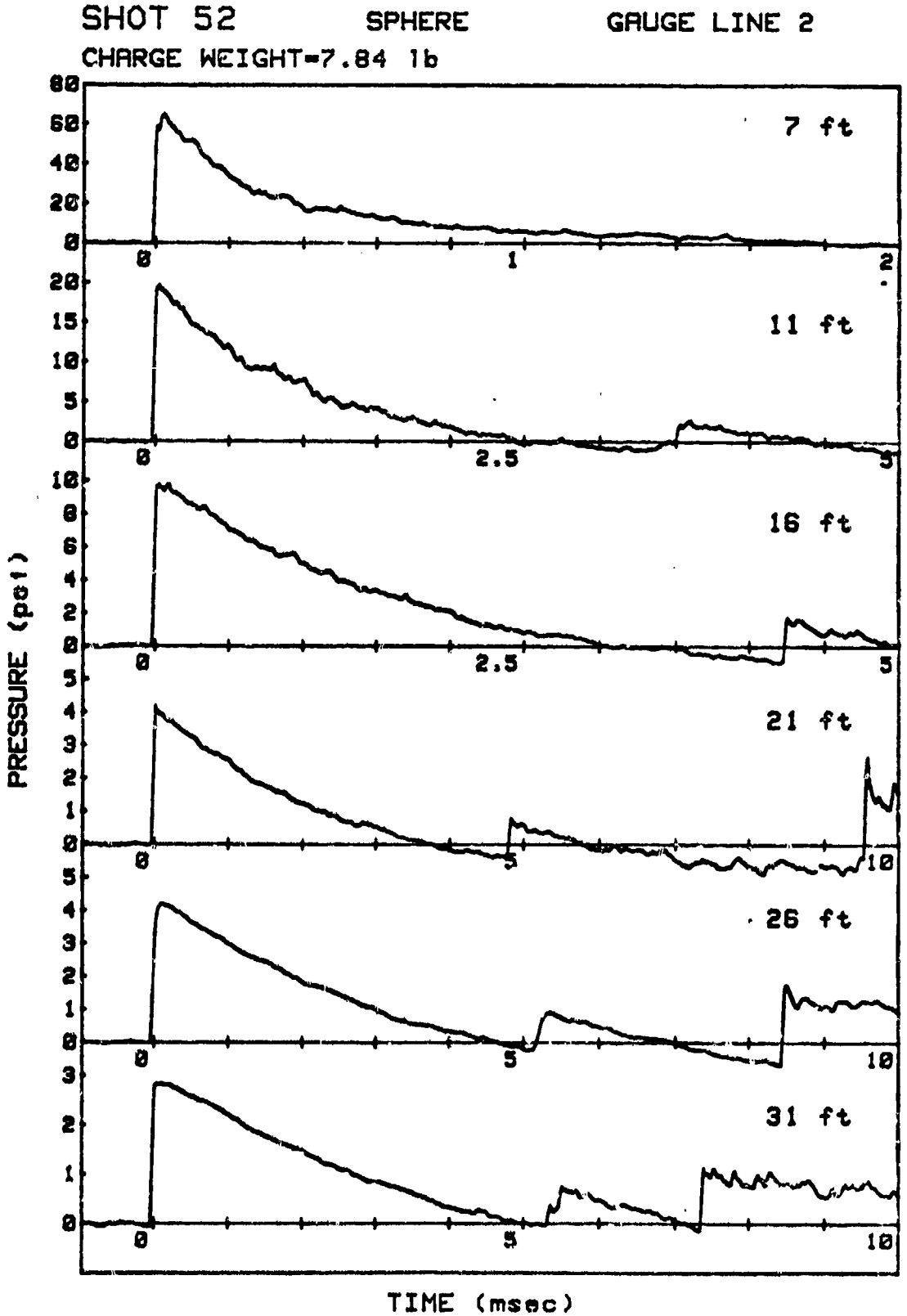
SHOT 52
SPHERE
GAUGE LINE 2
CHARGE WEIGHT=7.84 lb
7 ft
11 ft
16 ft
21 ft
26 ft
31 ft
PRESSURE (psi)
TIME (msec)

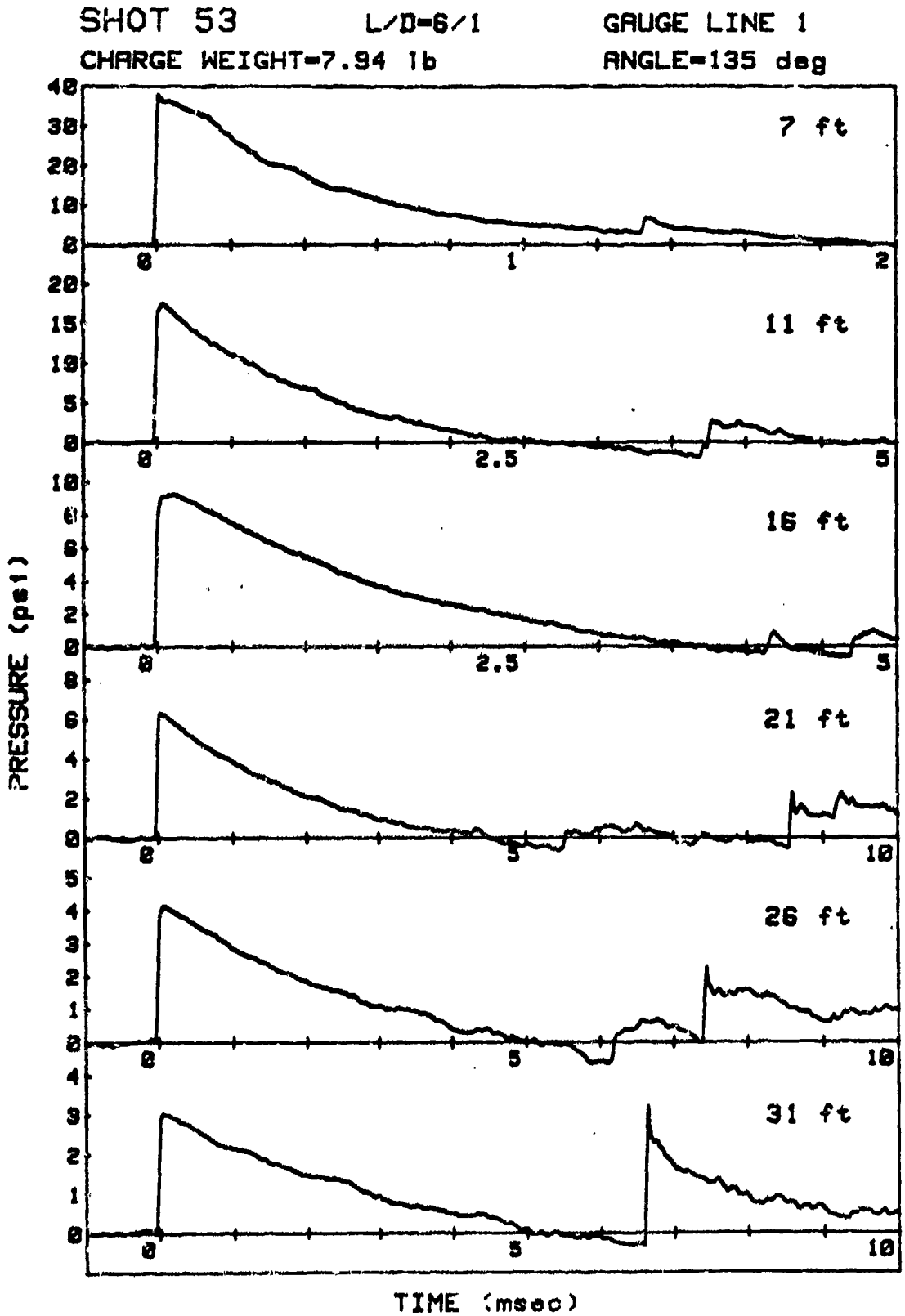
SHOT 53
L/D=6/1
GAUGE LINE 1
CHARGE WEIGHT=7.94 lb
ANGLE=135 deg
7 ft
11 ft
16 ft
21 ft
26 ft
31 ft
PRESSURE (psi)
TIME (msec)

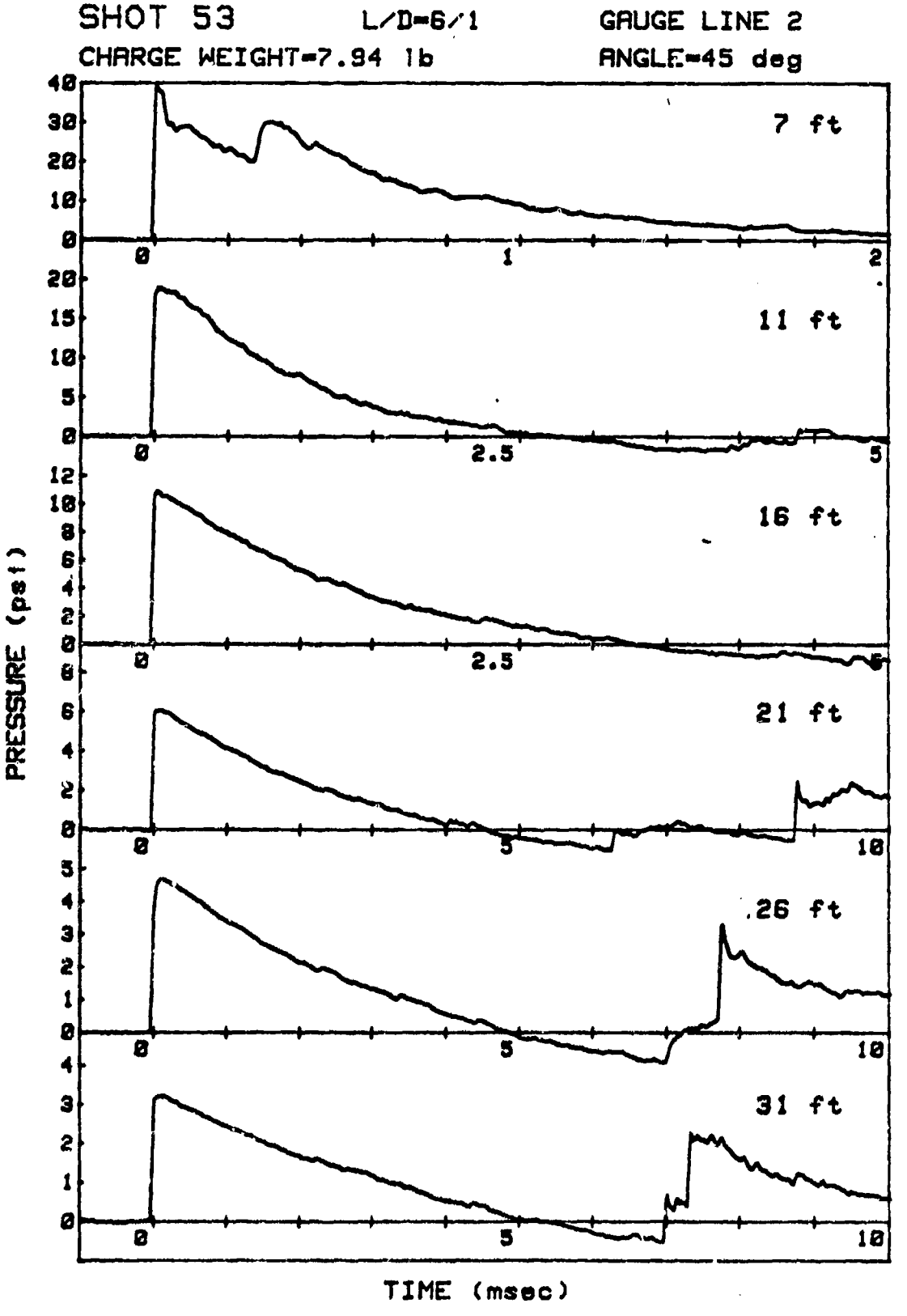
SHOT 53
L/D=6/1
GAUGE LINE 2
CHARGE WEIGHT=7.94 lb
ANGLE=45 deg
7 ft
11 ft
16 ft
21 ft
26 ft
31 ft
PRESSURE (psi)
TIME (msec)

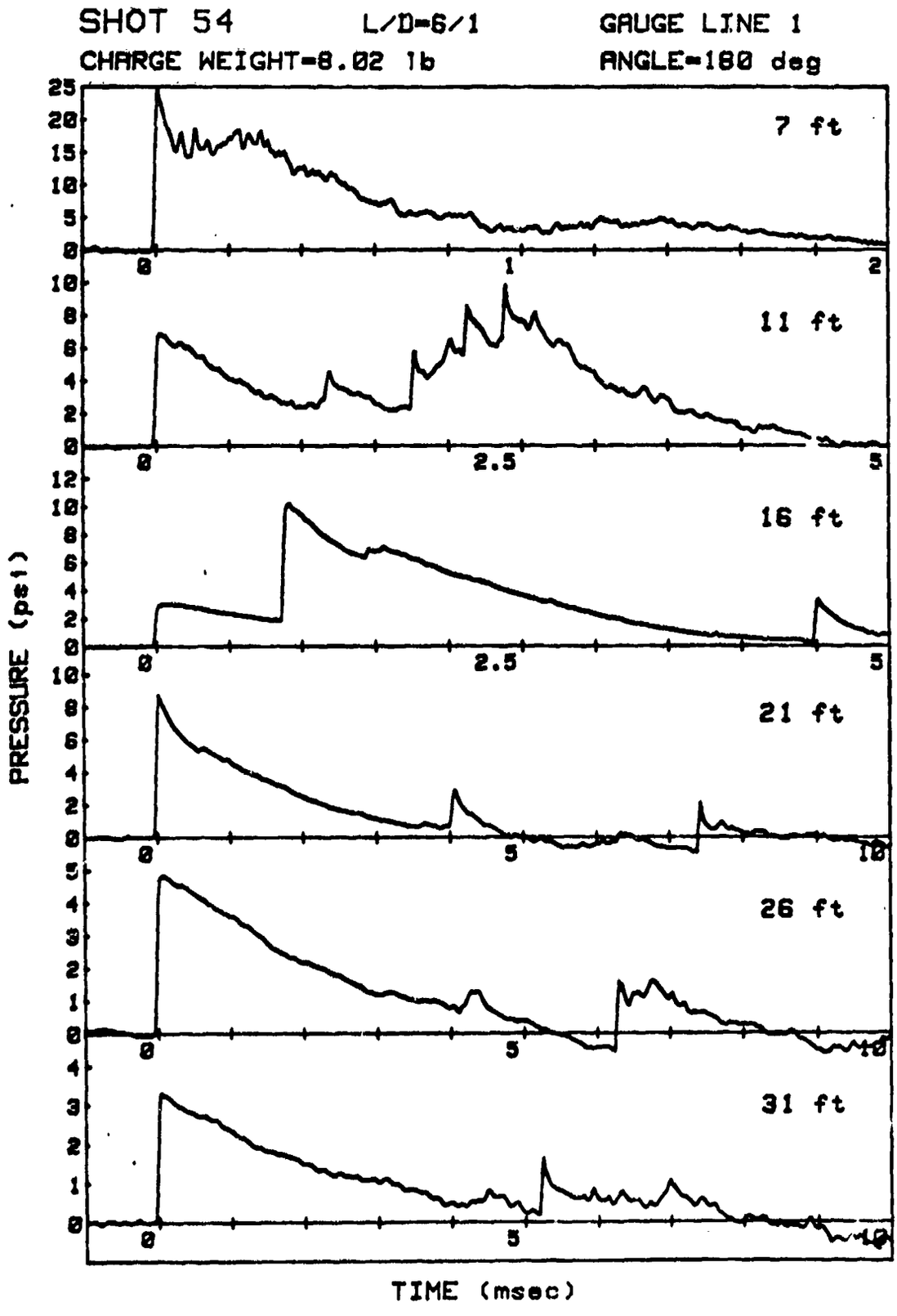
SHOT 54
L/D=6/1
GAUGE LINE 1
CHARGE WEIGHT=8.02 lb
ANGLE=180 deg
7 ft
11 ft
16 ft
21 ft
26 ft
31 ft
PRESSURE (psi)
TIME (msec)

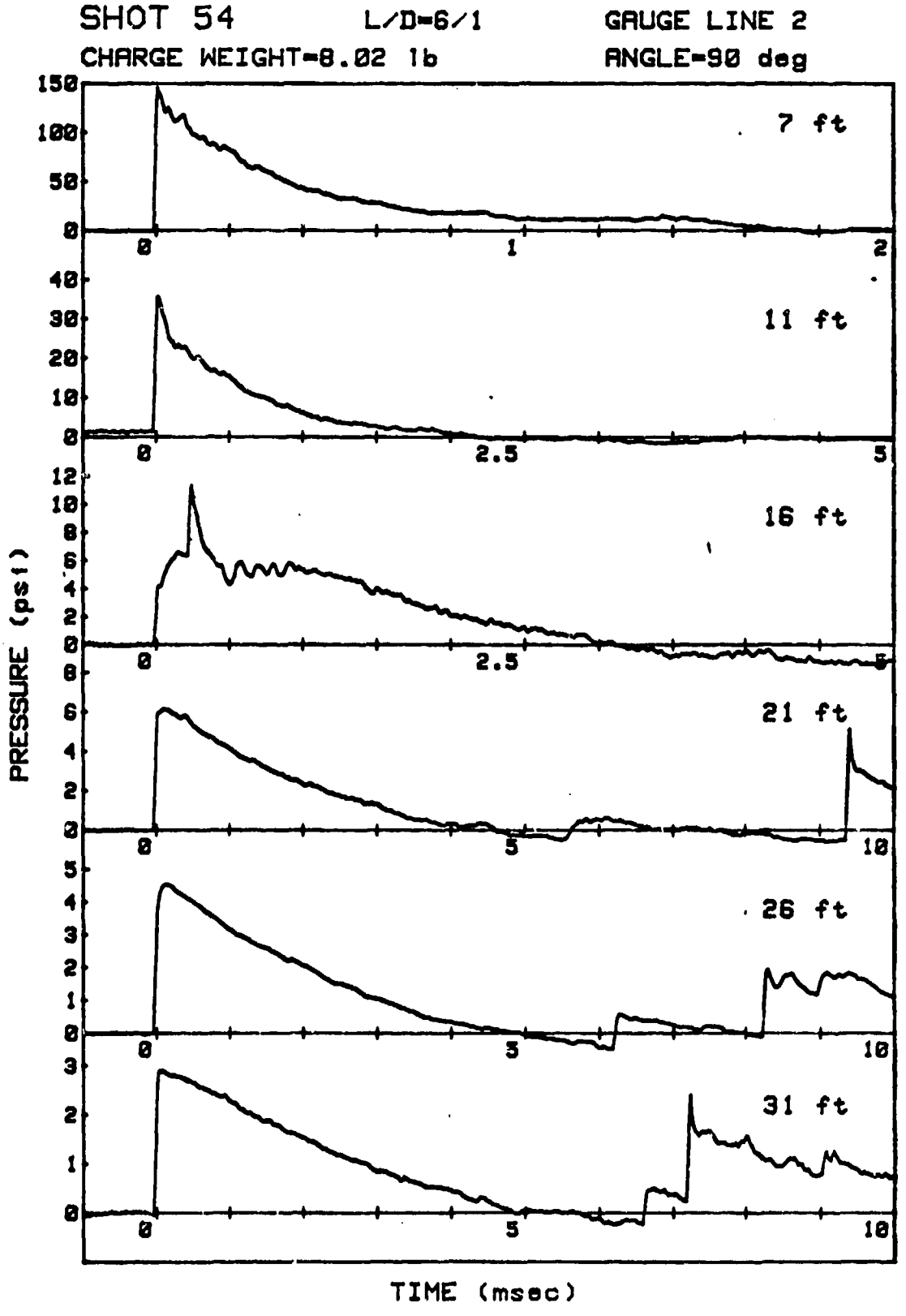
SHOT 54
L/D=6/1
GAUGE LINE 2
CHARGE WEIGHT=8.02 lb
ANGLE=90 deg
7 ft
11 ft
16 ft
21 ft
26 ft
31 ft
PRESSURE (psi)
TIME (msec)

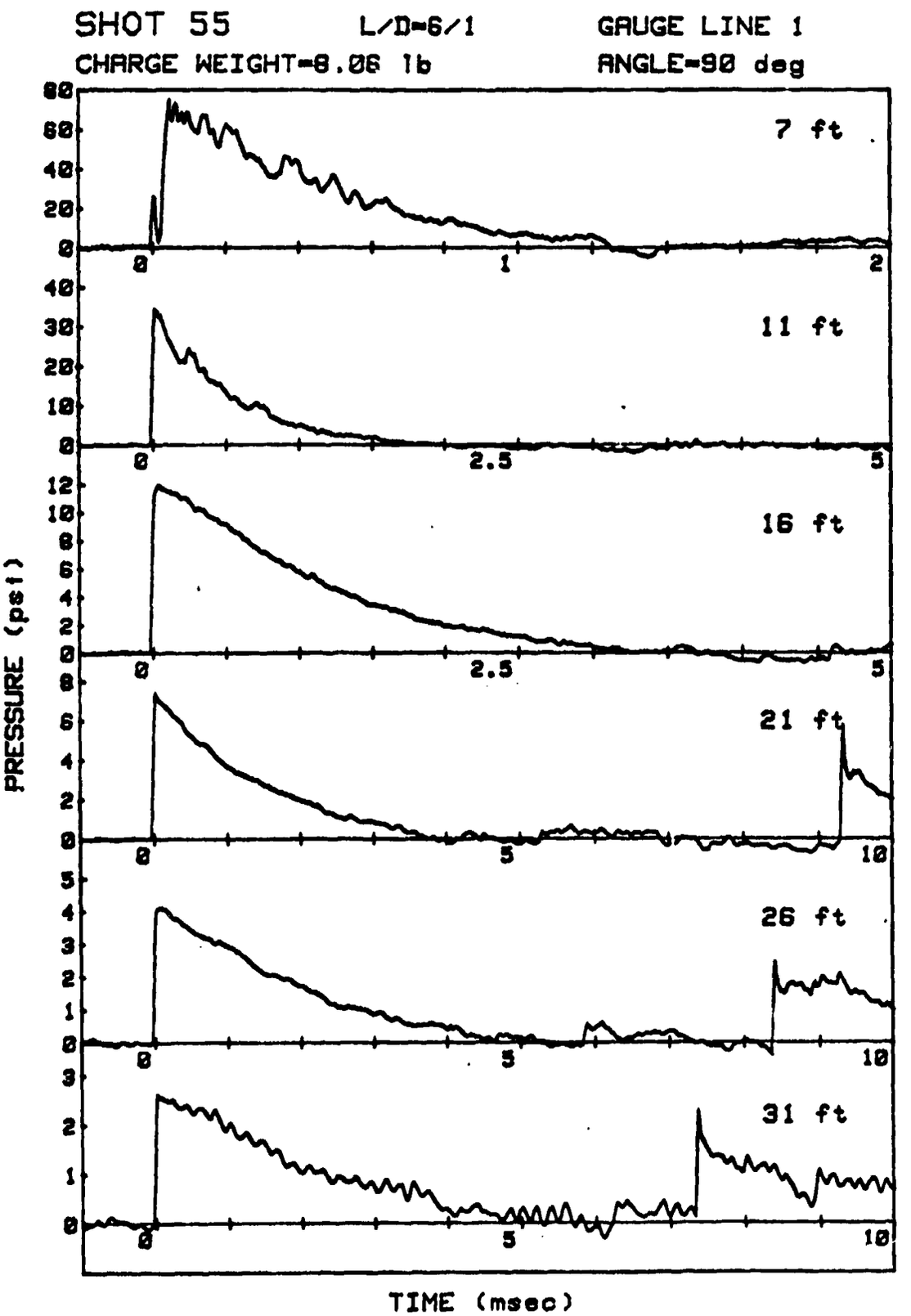
SHOT 55
L/D=6/1
GAUGE LINE 1
CHARGE WEIGHT=8.06 lb
ANGLE=90 deg
7 ft
11 ft
16 ft
21 ft
26 ft
31 ft
PRESSURE (psi)
TIME (msec)

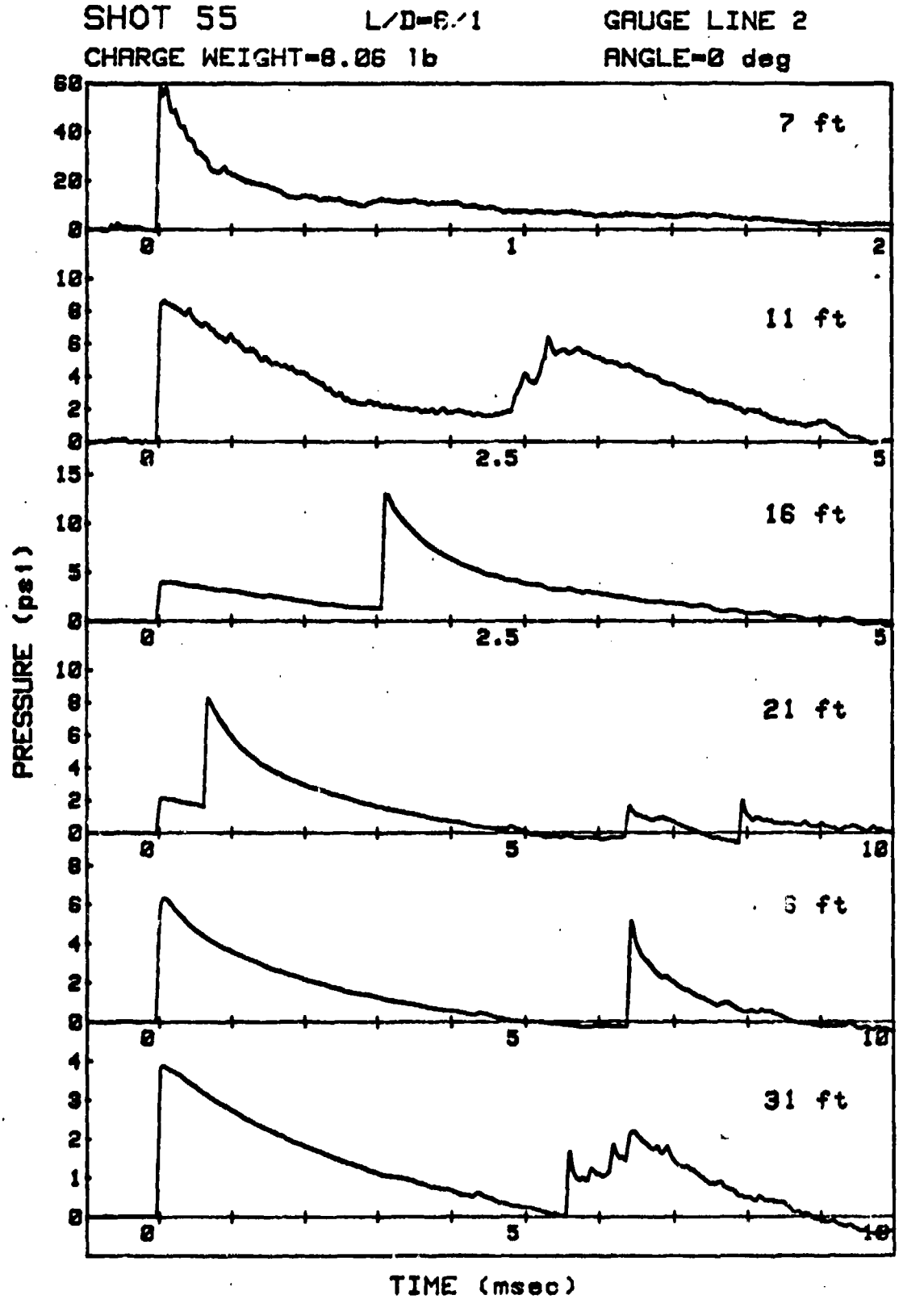
SHOT 55
L/D=6.1
GAUGE LINE 2
CHARGE WEIGHT=8.06 lb
ANGLE=0 deg
7 ft
11 ft
16 ft
21 ft
6 ft
31 ft
PRESSURE (psi)
TIME (msec)

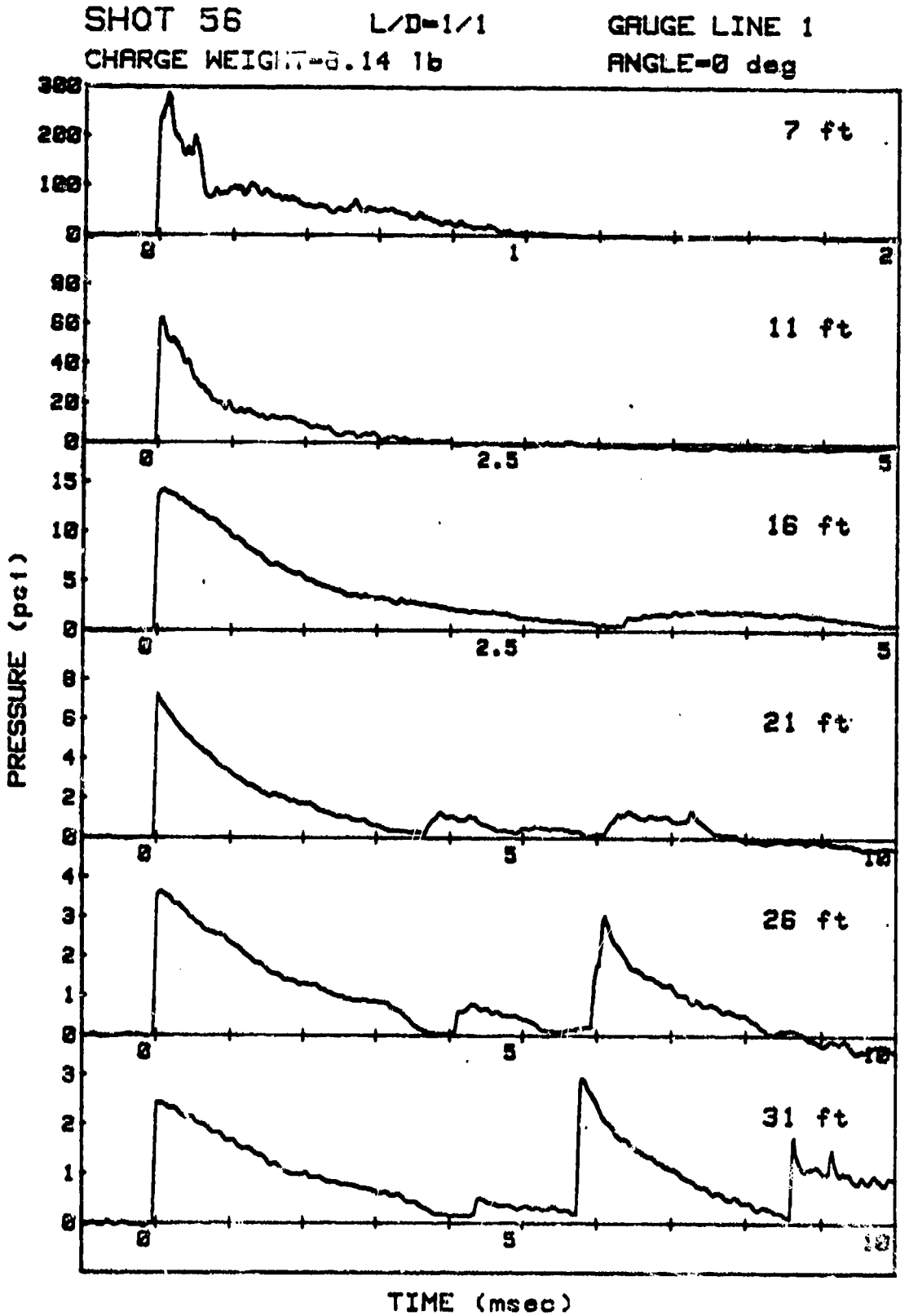
SHOT 56
L/D=1/1
GAUGE LINE 1
CHARGE WEIGHT=0.14 lb
ANGLE=0 deg
7 ft
11 ft
16 ft
21 ft
26 ft
31 ft
PRESSURE (psi)
TIME (msec)

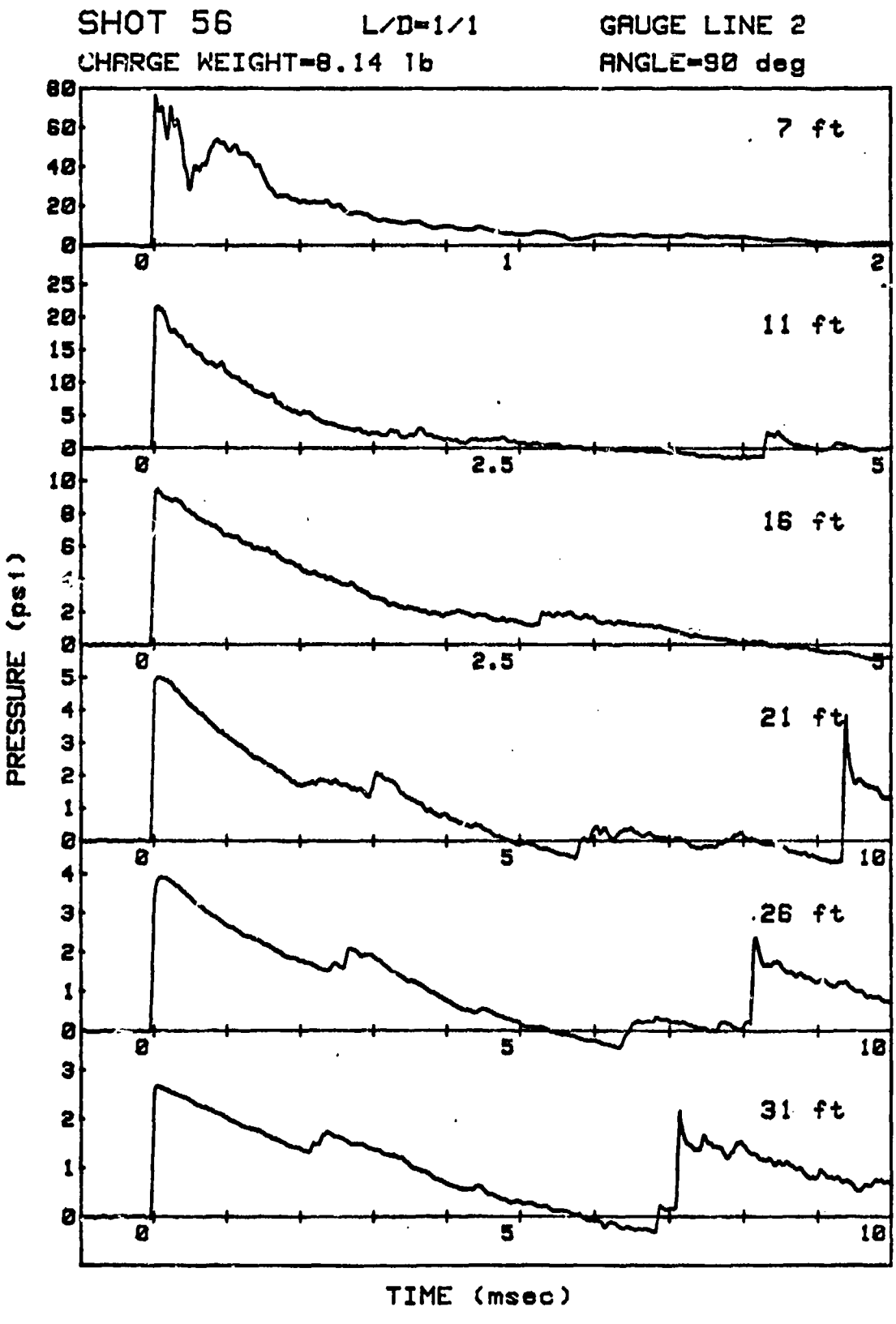
SHOT 56
L/D=1/1
GAUGE LINE 2
CHARGE WEIGHT=8.14 lb
ANGLE=90 deg
7 ft
11 ft
16 ft
21 ft
26 ft
31 ft
PRESSURE (psi)
TIME (msec)

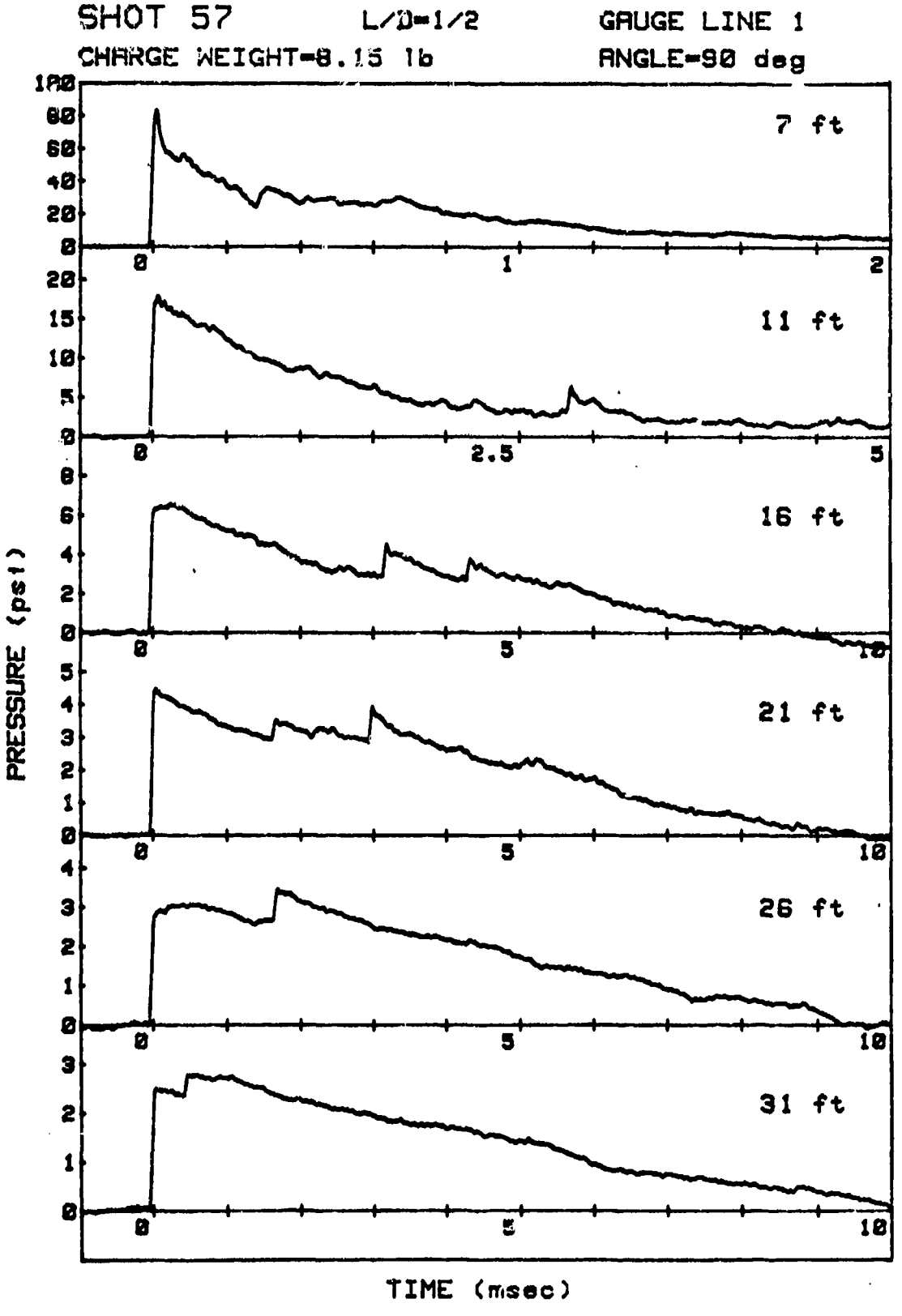
SHOT 57
L/D=1/2
GAUGE LINE 1
CHARGE WEIGHT=8.15 lb
ANGLE=90 deg
7 ft
11 ft
16 ft
21 ft
26 ft
31 ft
PRESSURE (psi)
TIME (msec)

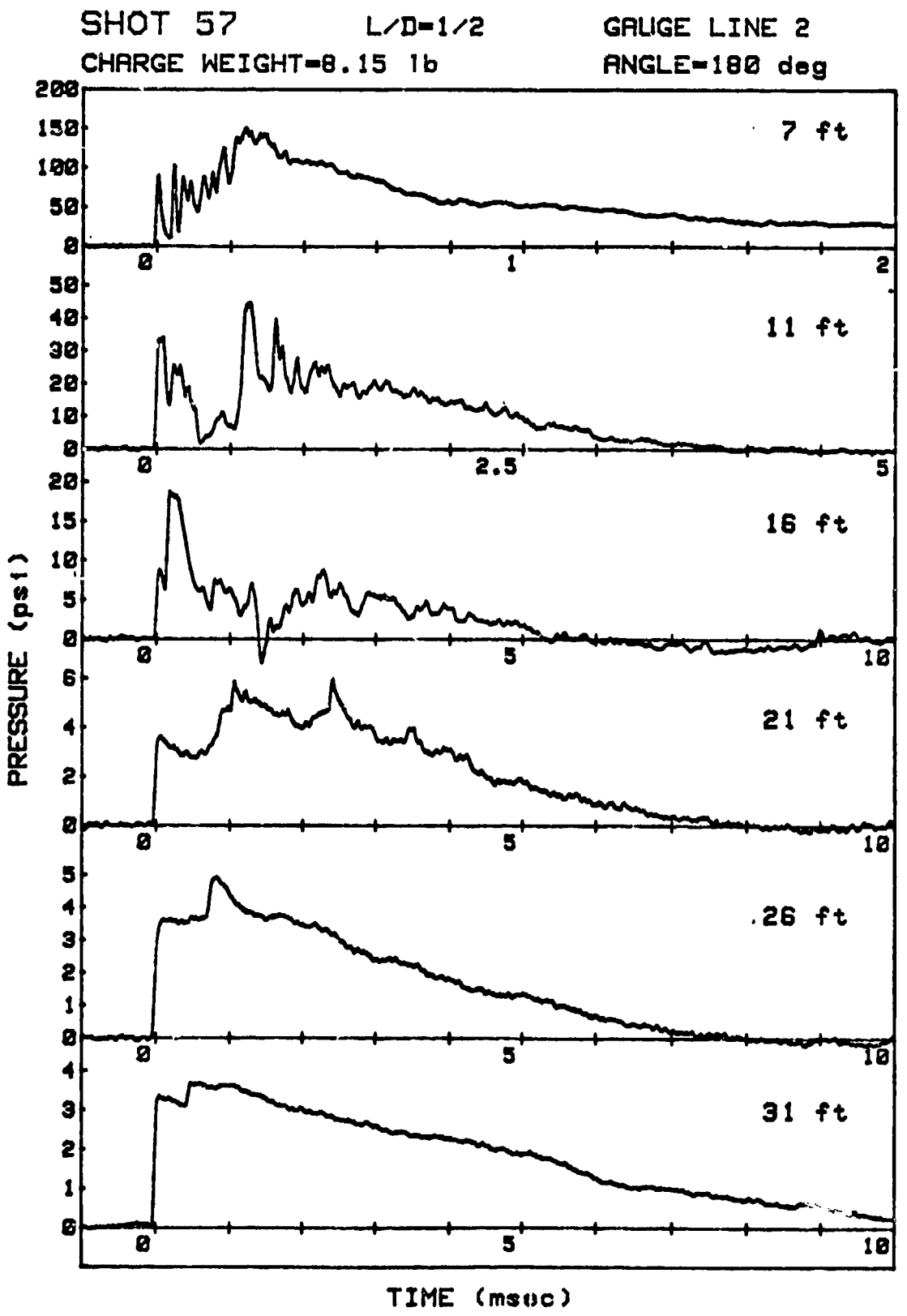
SHOT 57
L/D=1/2
GAUGE LINE 2
CHARGE WEIGHT=8.15 lb
ANGLE=180 deg
7 ft
11 ft
16 ft
21 ft
26 ft
31 ft
PRESSURE (psi)
TIME (msec)

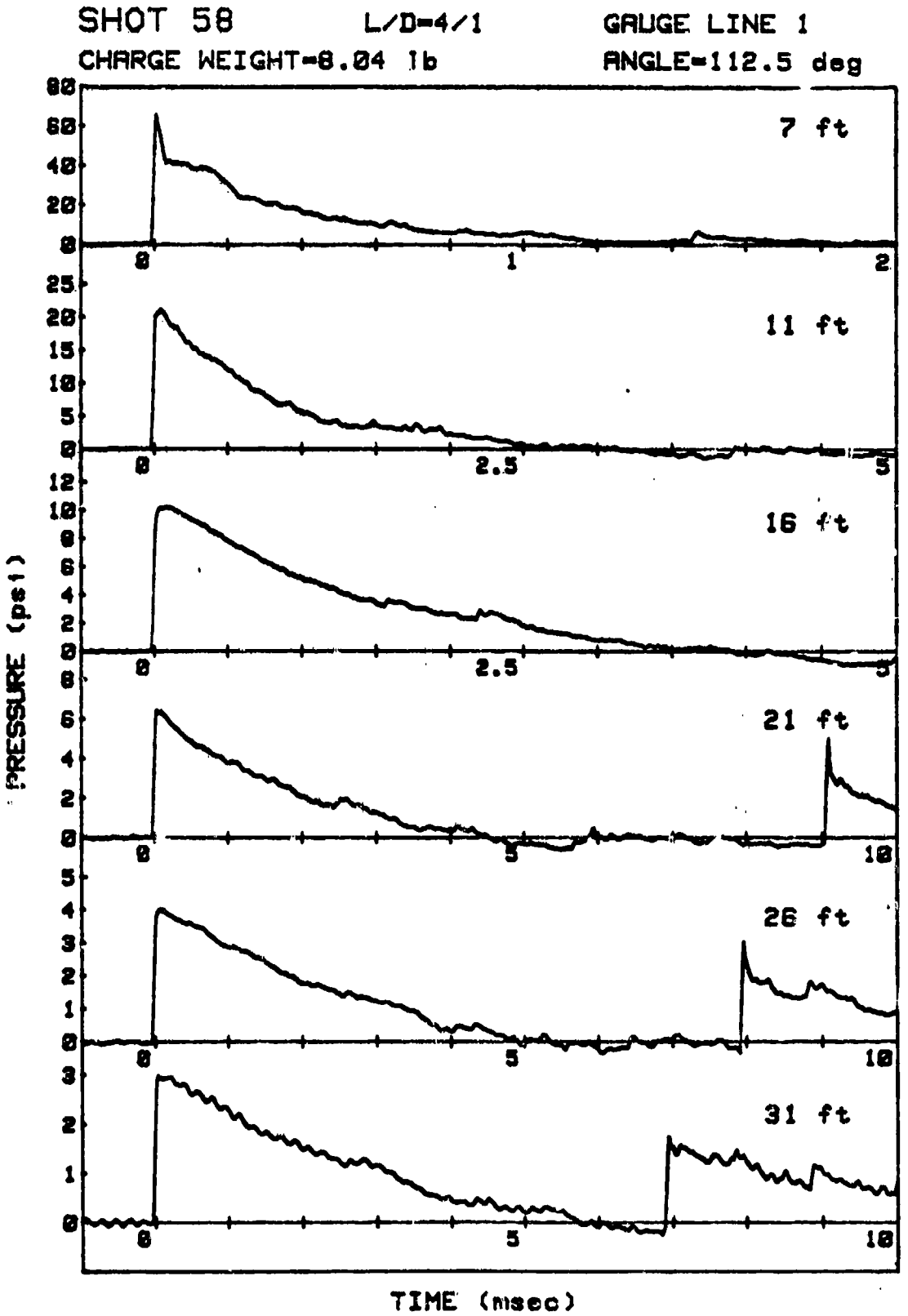
SHOT 58
L/D=4/1
GAUGE LINE 1
CHARGE WEIGHT=8.04 lb
ANGLE=112.5 deg
7 ft
11 ft
16 ft
21 ft
26 ft
31 ft
PRESSURE (psi)
TIME (msec)

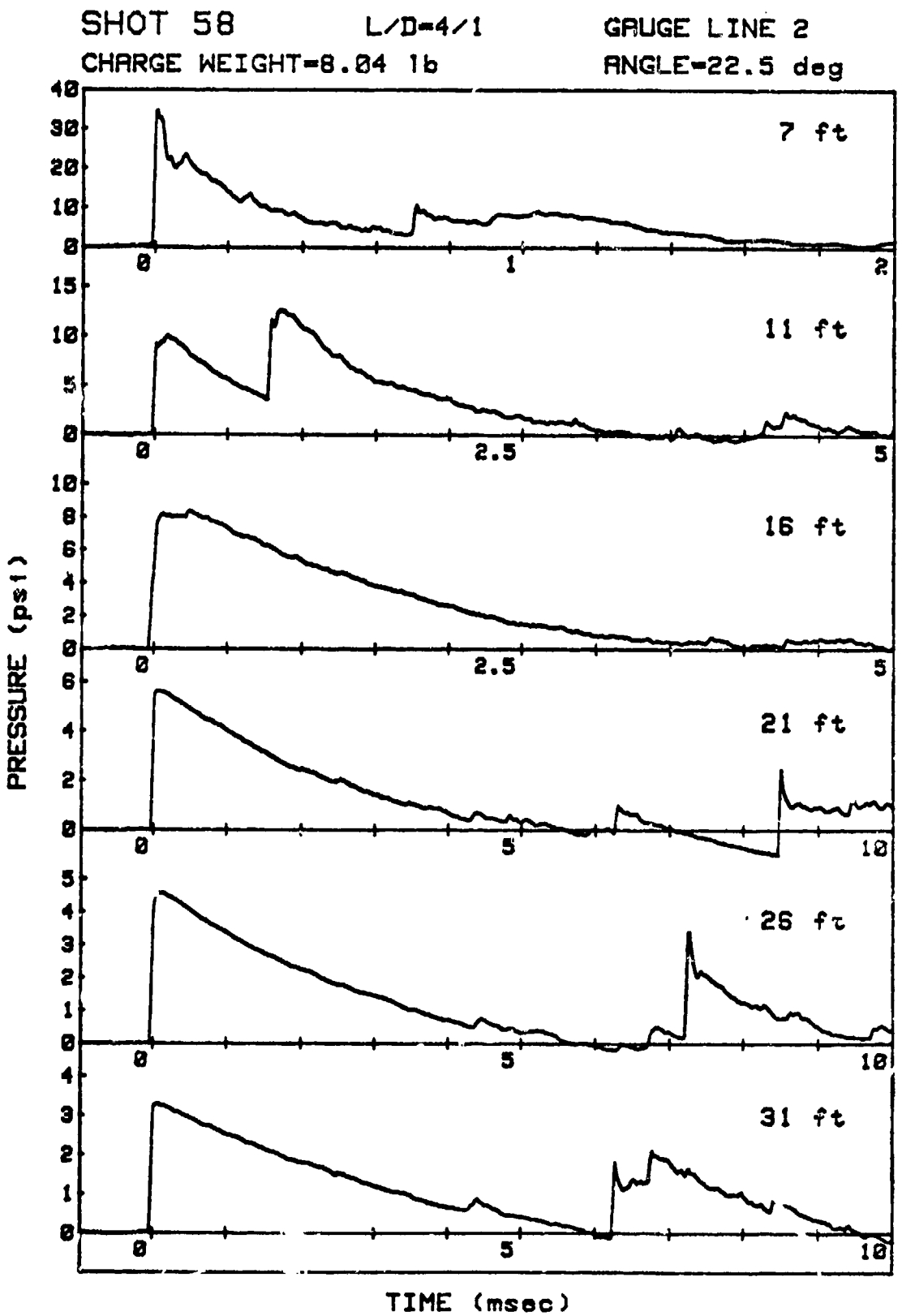
SHOT 58
L/D=4/1
GAUGE LINE 2
CHARGE WEIGHT=8.04 lb
ANGLE=22.5 deg
7 ft
11 ft
16 ft
21 ft
26 ft
31 ft
PRESSURE (psi)
TIME (msec)

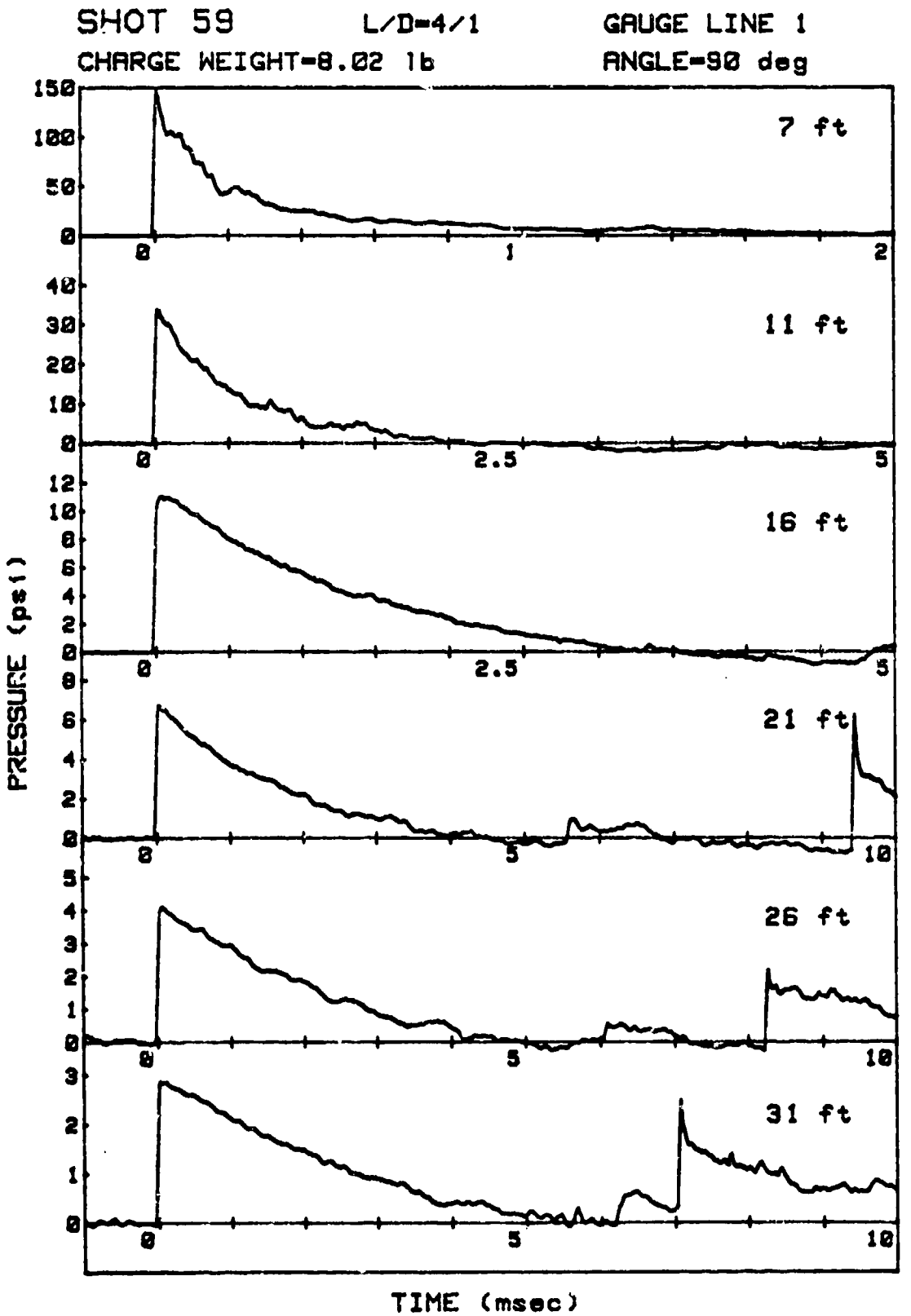
SHOT 59
L/D=4/1
GAUGE LINE 1
CHARGE WEIGHT=8.02 lb
ANGLE=90 deg
7 ft
11 ft
16 ft
21 ft
26 ft
31 ft
PRESSURE (psi)
TIME (msec)

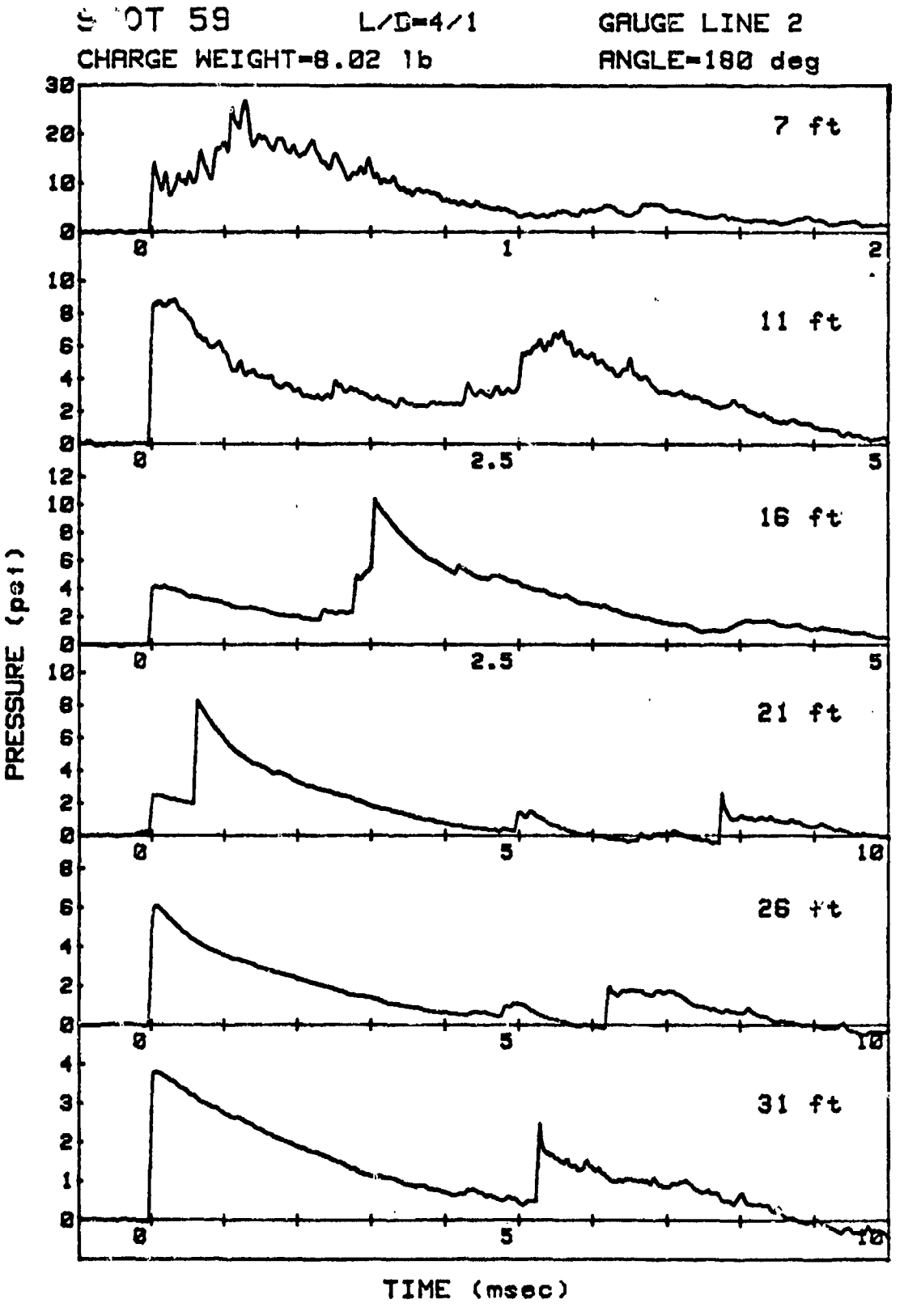
SHOT 59
L/D=4/1
GAUGE LINE 2
CHARGE WEIGHT=8.02 lb
ANGLE=180 deg
7 ft
11 ft
16 ft
21 ft
26 ft
31 ft
PRESSURE (psi)
TIME (msec)

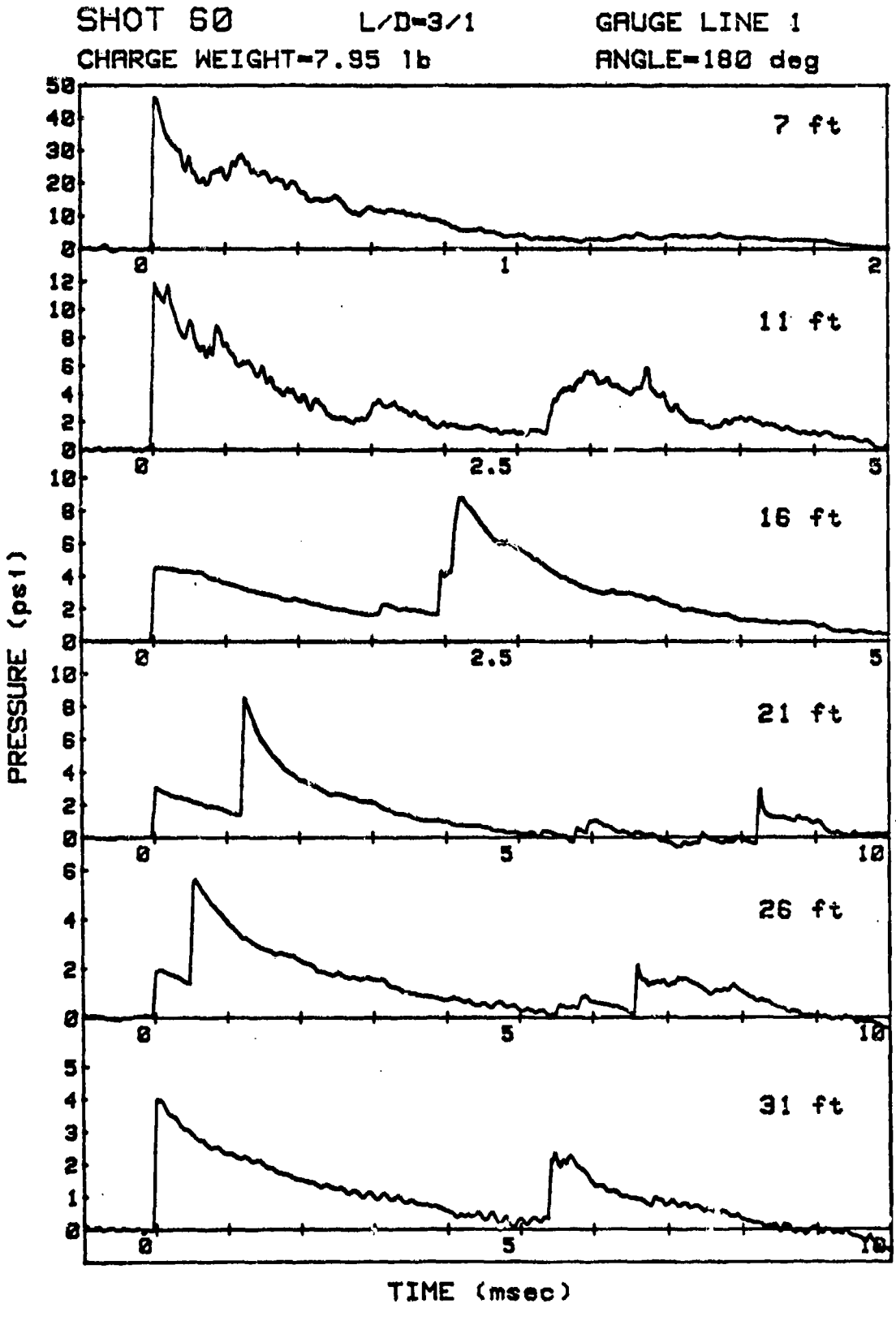
SHOT 60
L/D=3/1
GAUGE LINE 1
CHARGE WEIGHT=7.95 lb
ANGLE=180 deg
7 ft
11 ft
16 ft
21 ft
26 ft
31 ft
PRESSURE (psi)
TIME (msec)

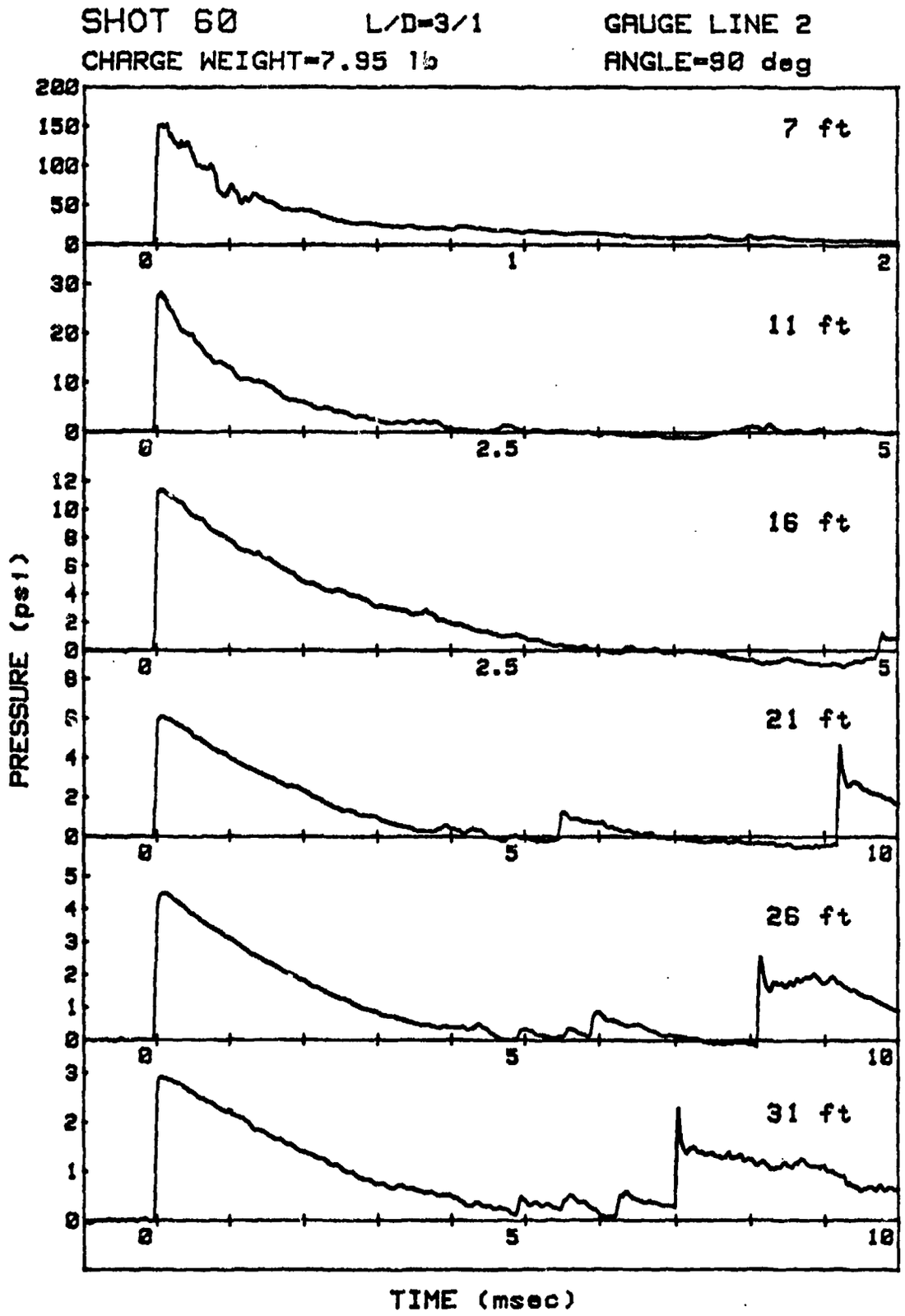
SHOT 60
L/D=3/1
GAUGE LINE 2
CHARGE WEIGHT=7.95 lb
ANGLE=90 deg
7 ft
11 ft
16 ft
21 ft
26 ft
31 ft
PRESSURE (psi)
TIME (msec)

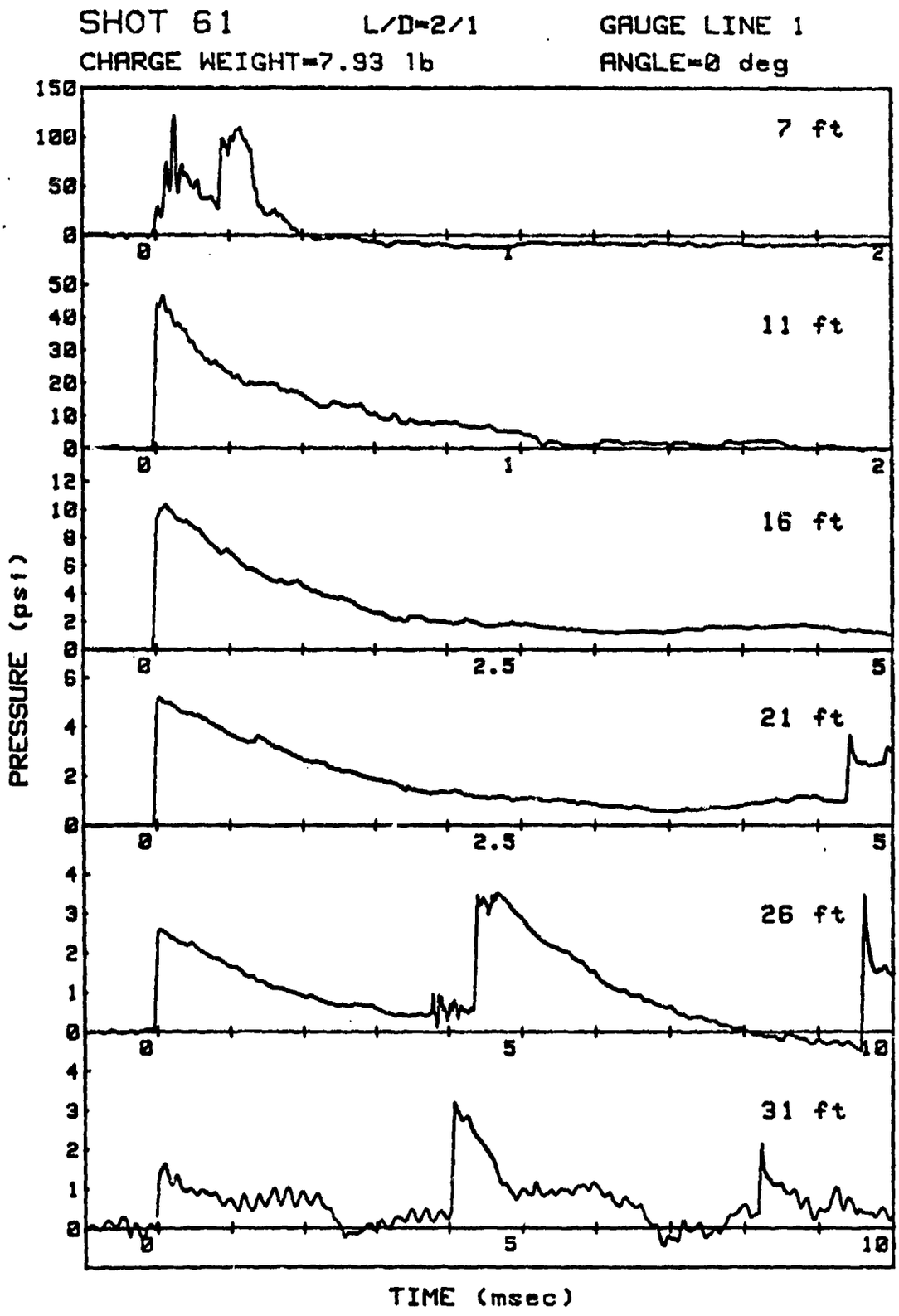
SHOT 61
L/D=2/1
GAUGE LINE 1
CHARGE WEIGHT=7.93 lb
ANGLE=0 deg
7 ft
11 ft
16 ft
21 ft
26 ft
31 ft
PRESSURE (psi)
TIME (msec)

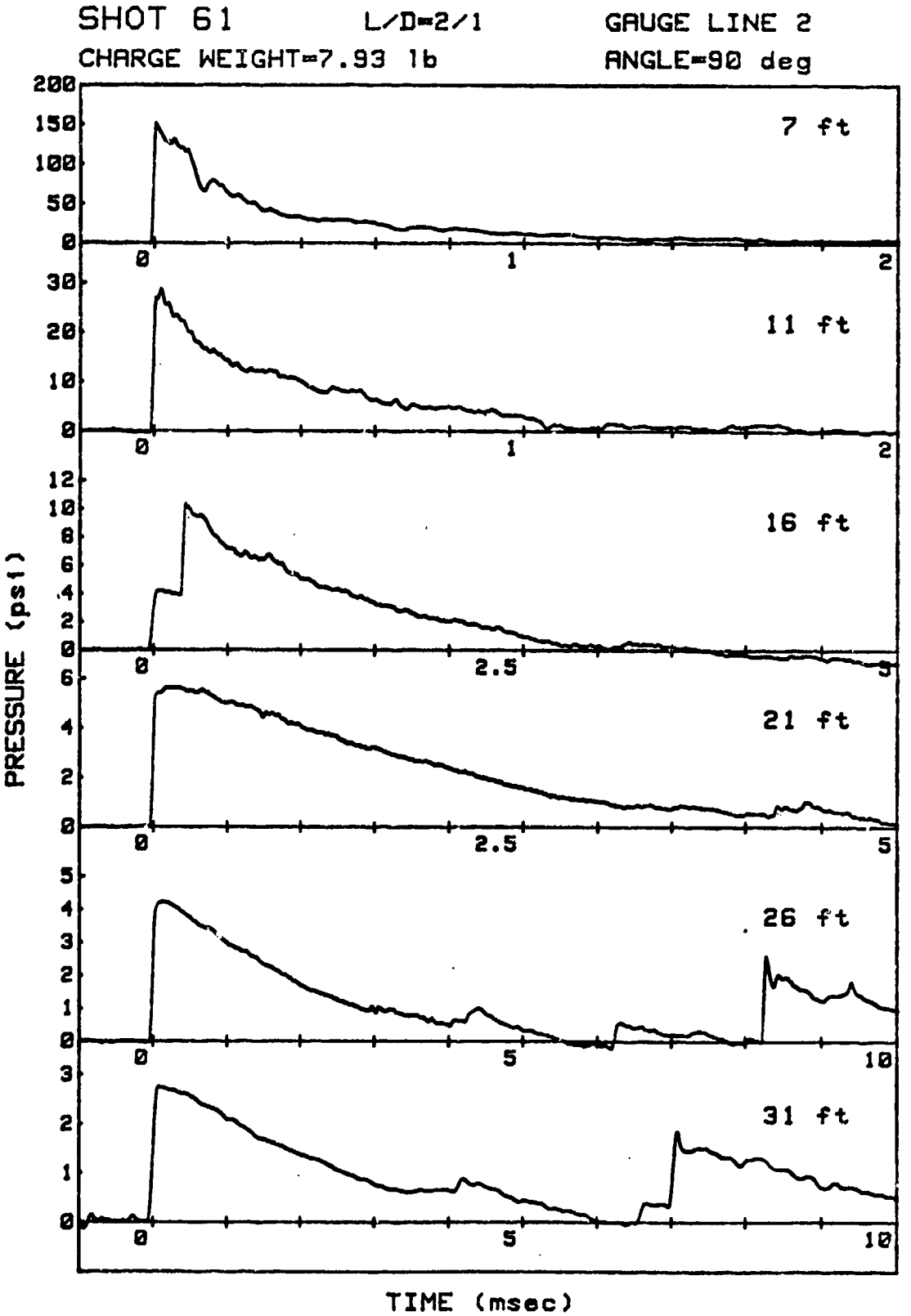
SHOT 61
L/D=2/1
GAUGE LINE 2
CHARGE WEIGHT=7.93 lb
ANGLE=90 deg
7 ft
11 ft
16 ft
21 ft
26 ft
31 ft
PRESSURE (psi)
TIME (msec)

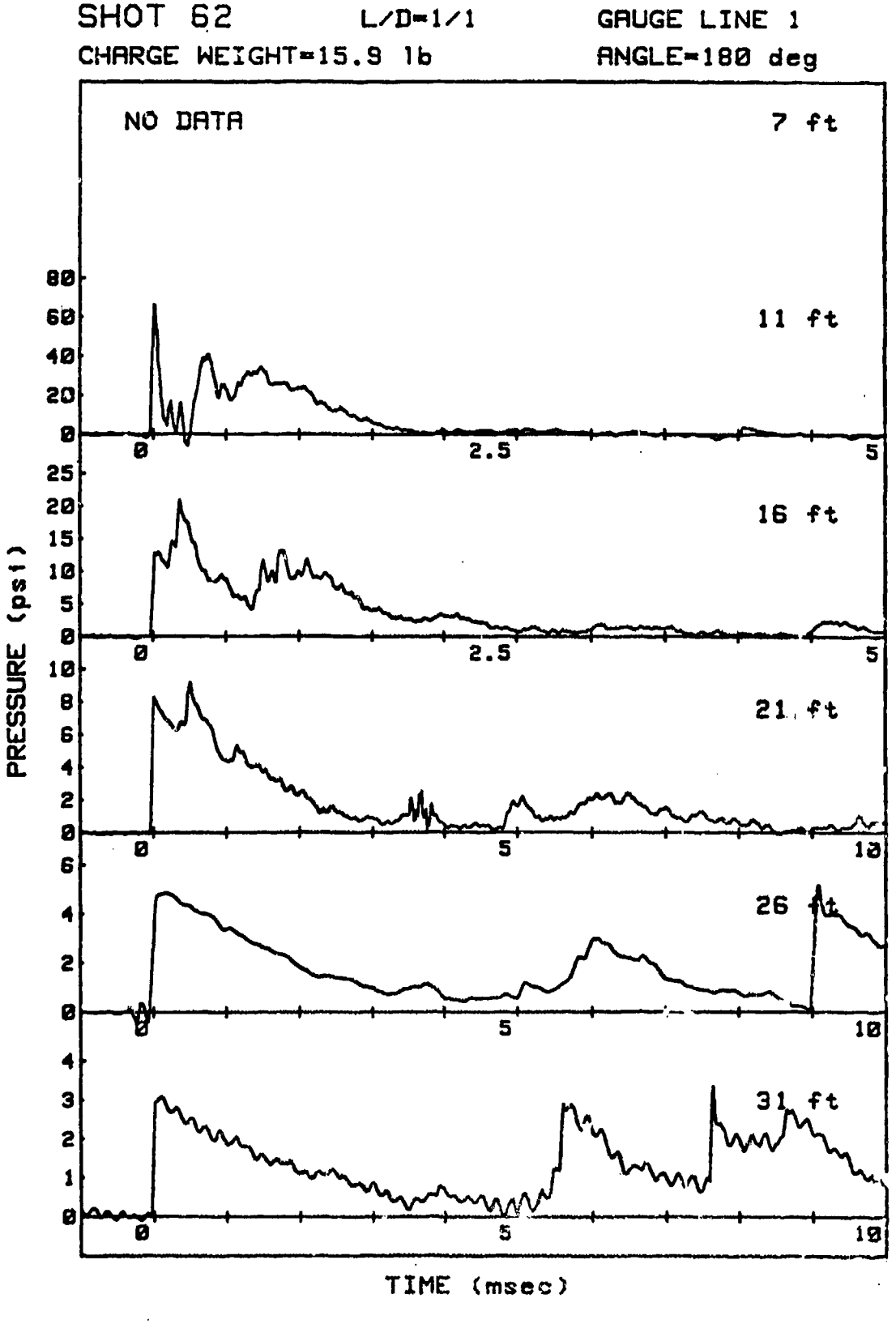
SHOT 62
L/D=1/1
GAUGE LINE 1
CHARGE WEIGHT=15.9 lb
ANGLE=180 deg
NO DATA
7 ft
11 ft
16 ft
21 ft
26 ft
31 ft
PRESSURE (psi)
TIME (msec)

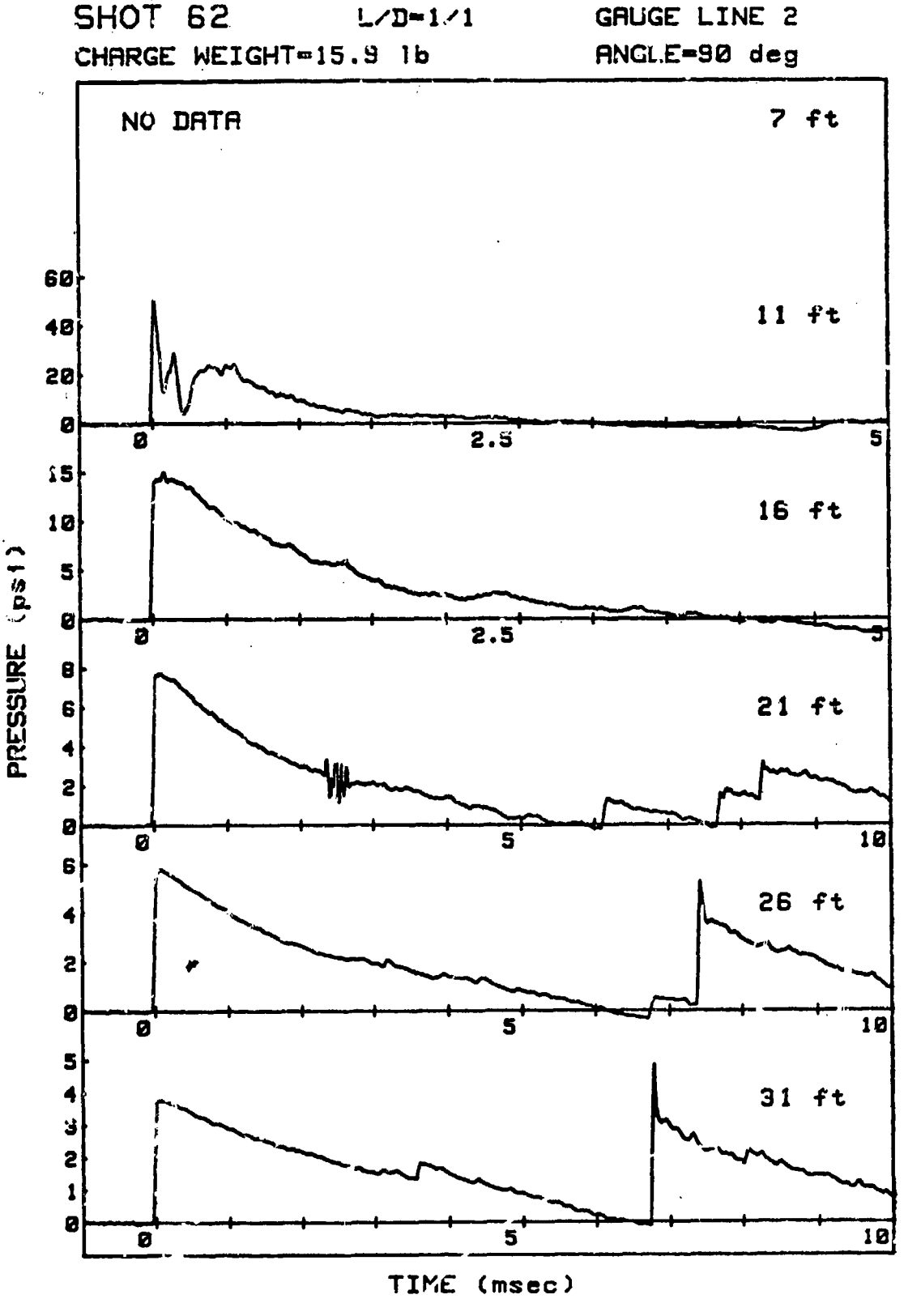
SHOT 62
L/D=1/1
GAUGE LINE 2
CHARGE WEIGHT=15.9 lb
ANGLE=90 deg
NO DATA
7 ft
11 ft
16 ft
21 ft
26 ft
31 ft
PRESSURE (psi)
TIME (msec)

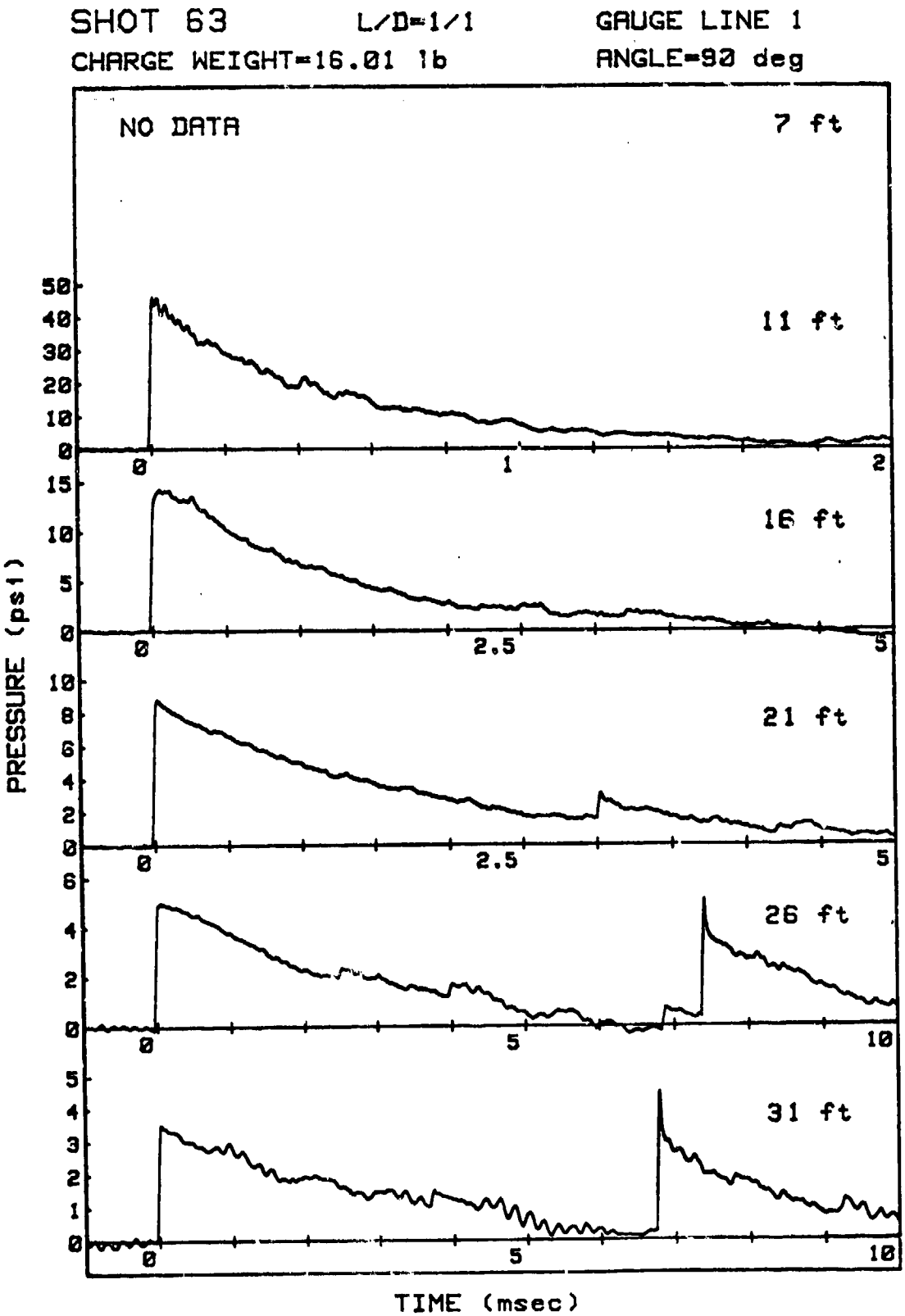
SHOT 63
L/D=1/1
GAUGE LINE 1
CHARGE WEIGHT=16.01 lb
ANGLE=90 deg
NO DATA
7 ft
11 ft
16 ft
21 ft
26 ft
31 ft
PRESSURE (psi)
TIME (msec)

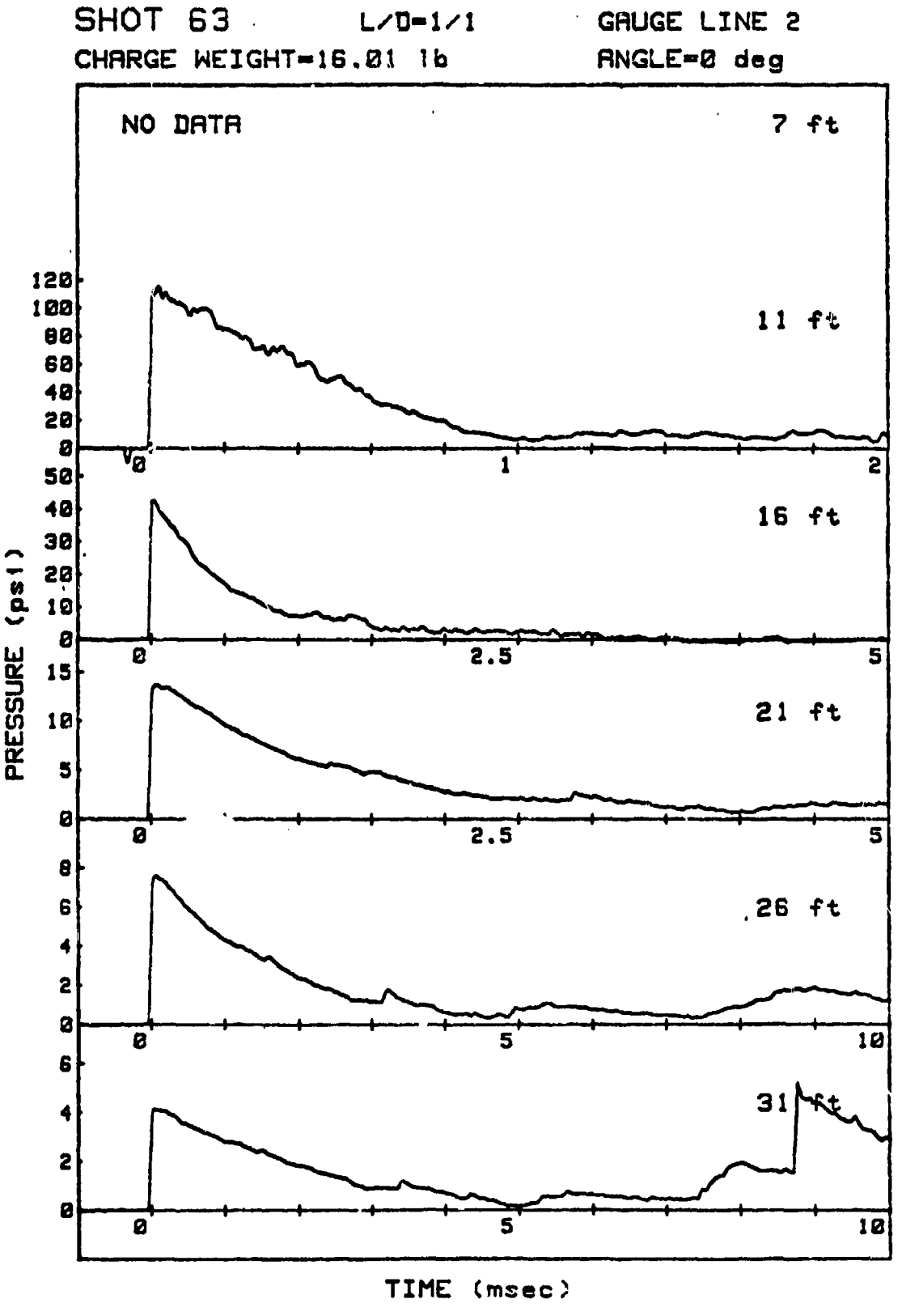
SHOT 63
L/D=1/1
GAUGE LINE 2
CHARGE WEIGHT=16.01 lb
ANGLE=0 deg
NO DATA
7 ft
11 ft
16 ft
21 ft
26 ft
31 ft
PRESSURE (psi)
TIME (msec)

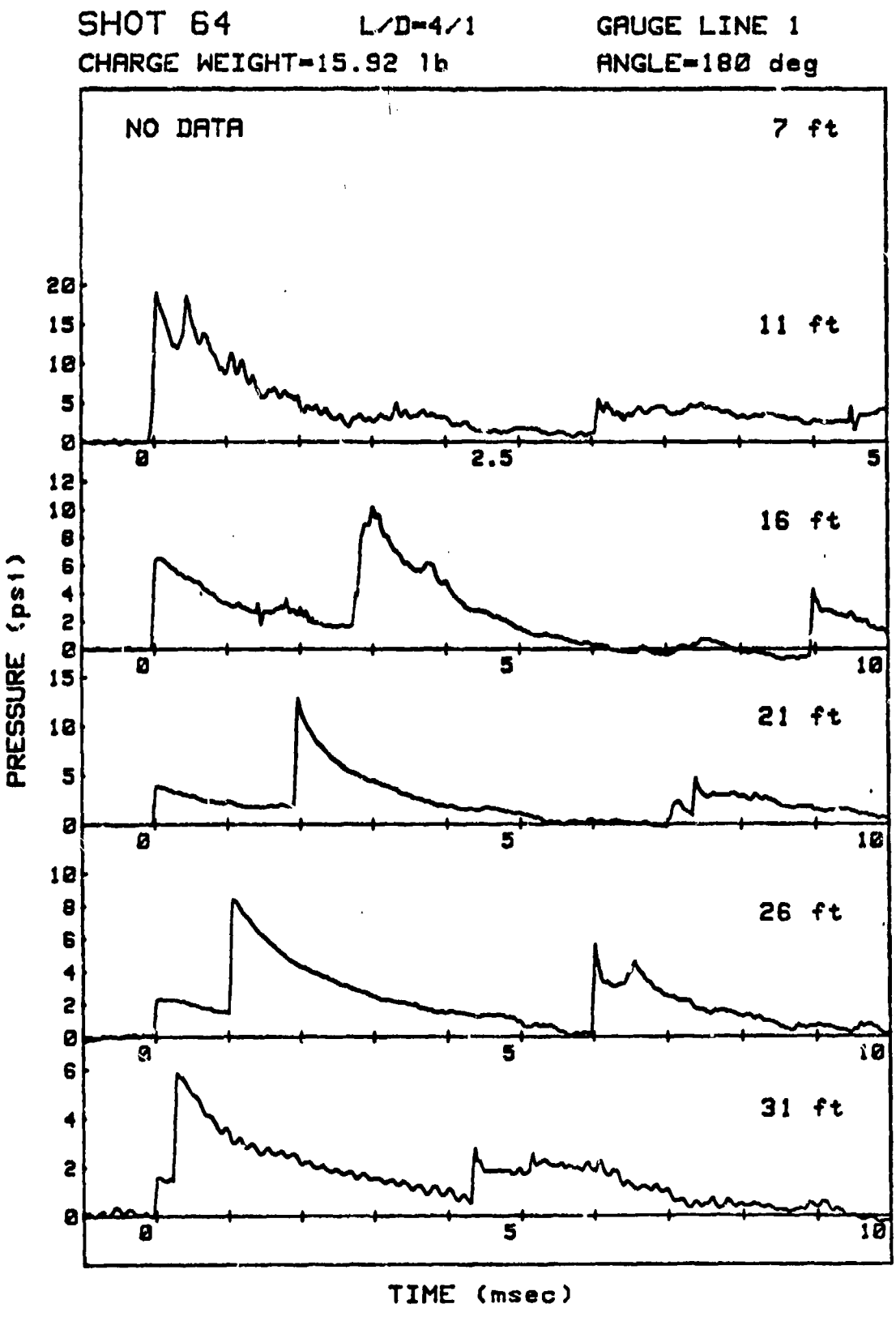
SHOT 64
L/D=4/1
GAUGE LINE 1
CHARGE WEIGHT=15.92 lb
ANGLE=180 deg
NO DATA
7 ft
11 ft
16 ft
21 ft
26 ft
31 ft
PRESSURE (psi)
TIME (msec)

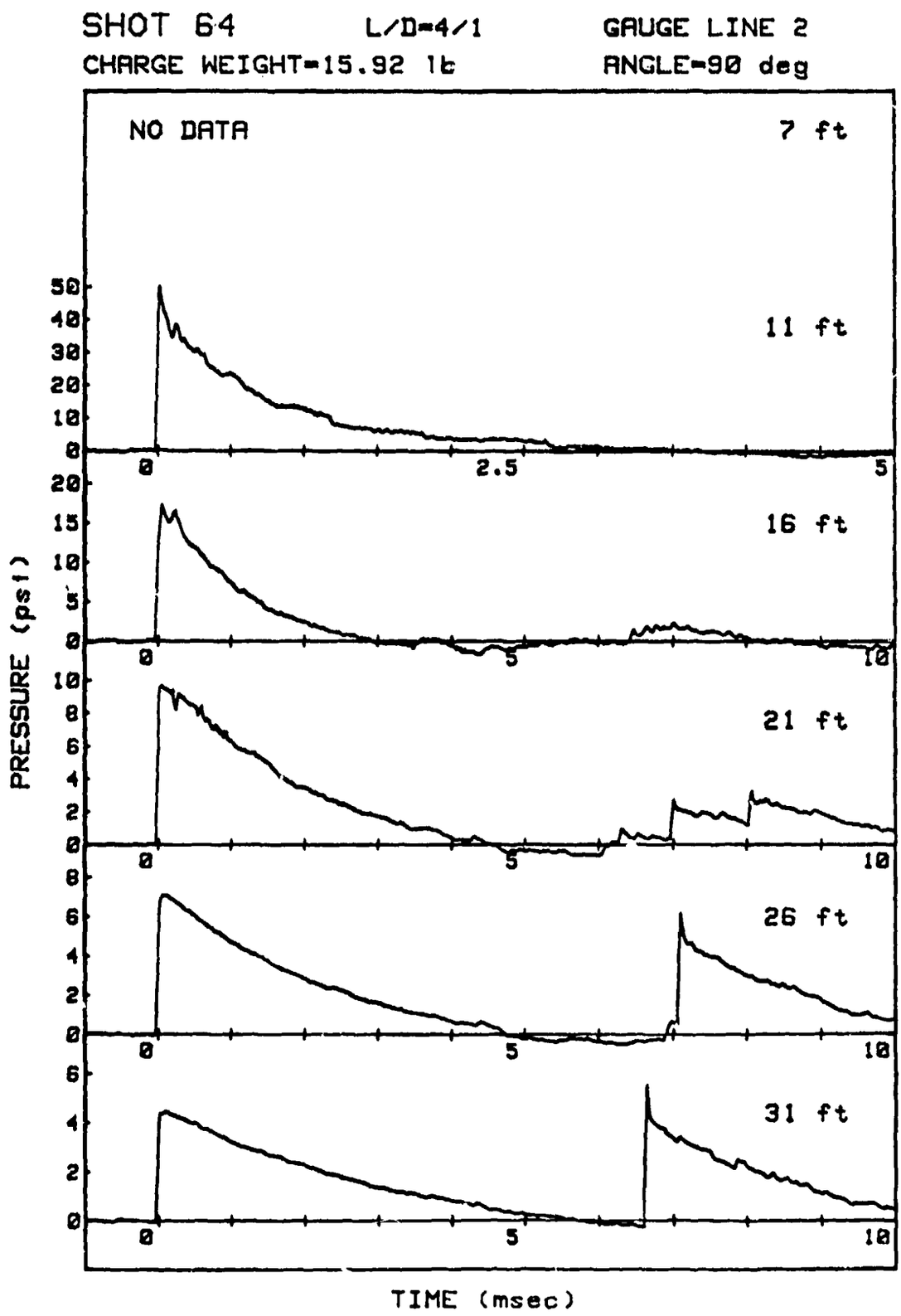
SHOT 64
L/D=4/1
GAUGE LINE 2
CHARGE WEIGHT=15.92 lb
ANGLE=90 deg
NO DATA
7 ft
11 ft
16 ft
21 ft
26 ft
31 ft
PRESSURE (psi)
TIME (msec)

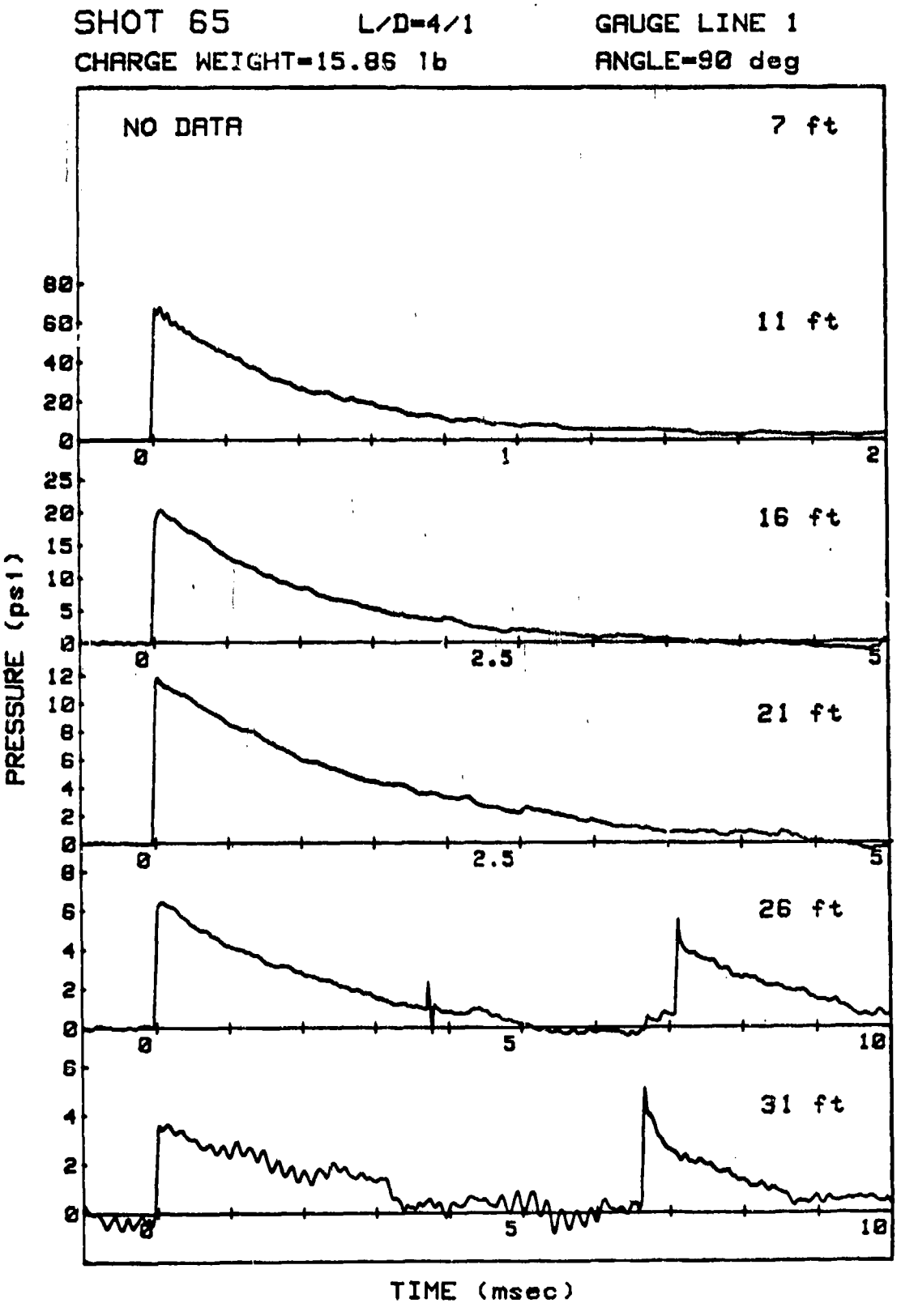
SHOT 65
L/D=4/1
GAUGE LINE 1
CHARGE WEIGHT=15.86 lb
ANGLE=90 deg
NO DATA
7 ft
11 ft
16 ft
21 ft
26 ft
31 ft
PRESSURE (psi)
TIME (msec)

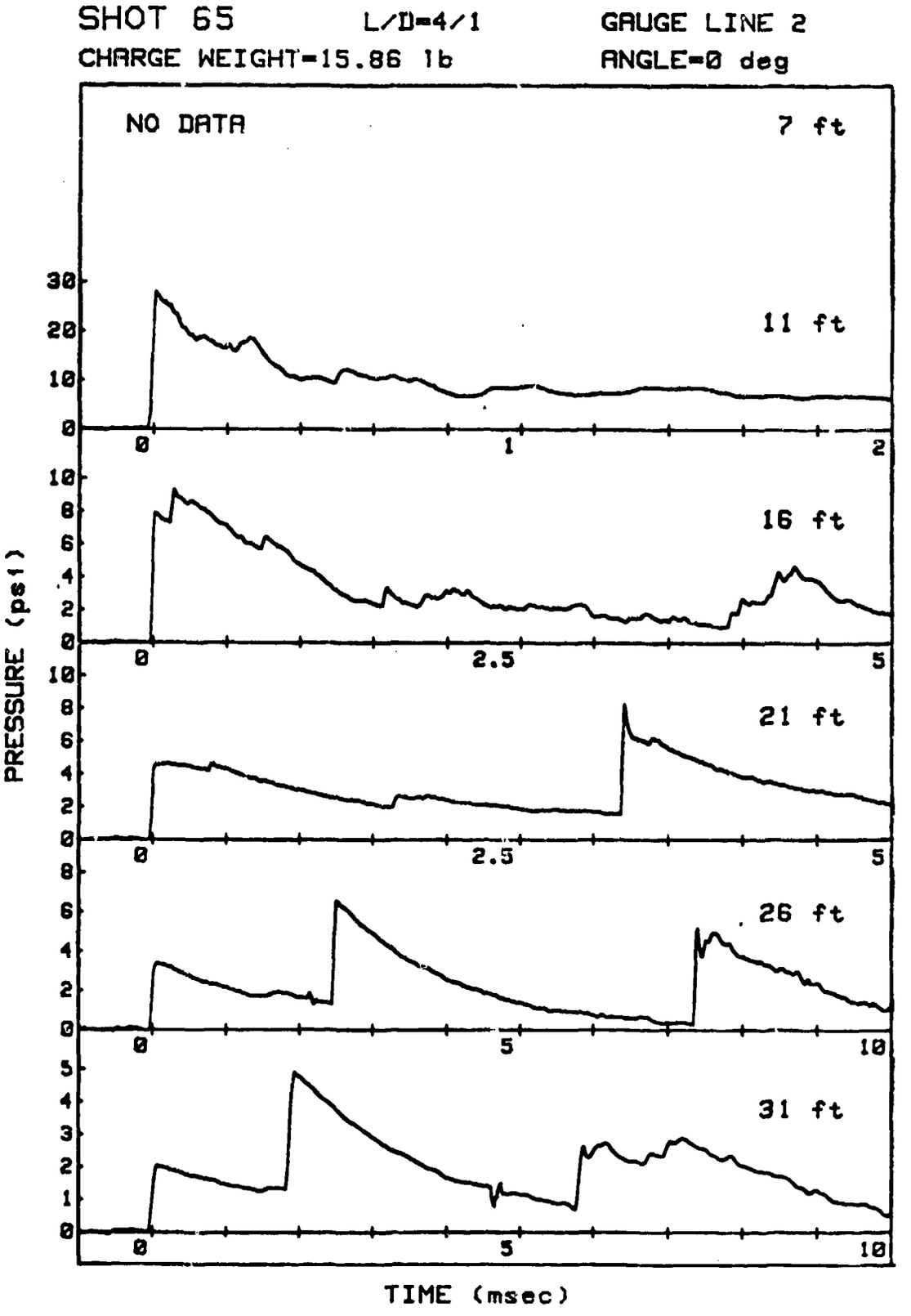
SHOT 65
L/D=4/1
GAUGE LINE 2
CHARGE WEIGHT=15.86 lb
ANGLE=0 deg
NO DATA
7 ft
11 ft
16 ft
21 ft
26 ft
31 ft
PRESSURE (psi)
TIME (msec)

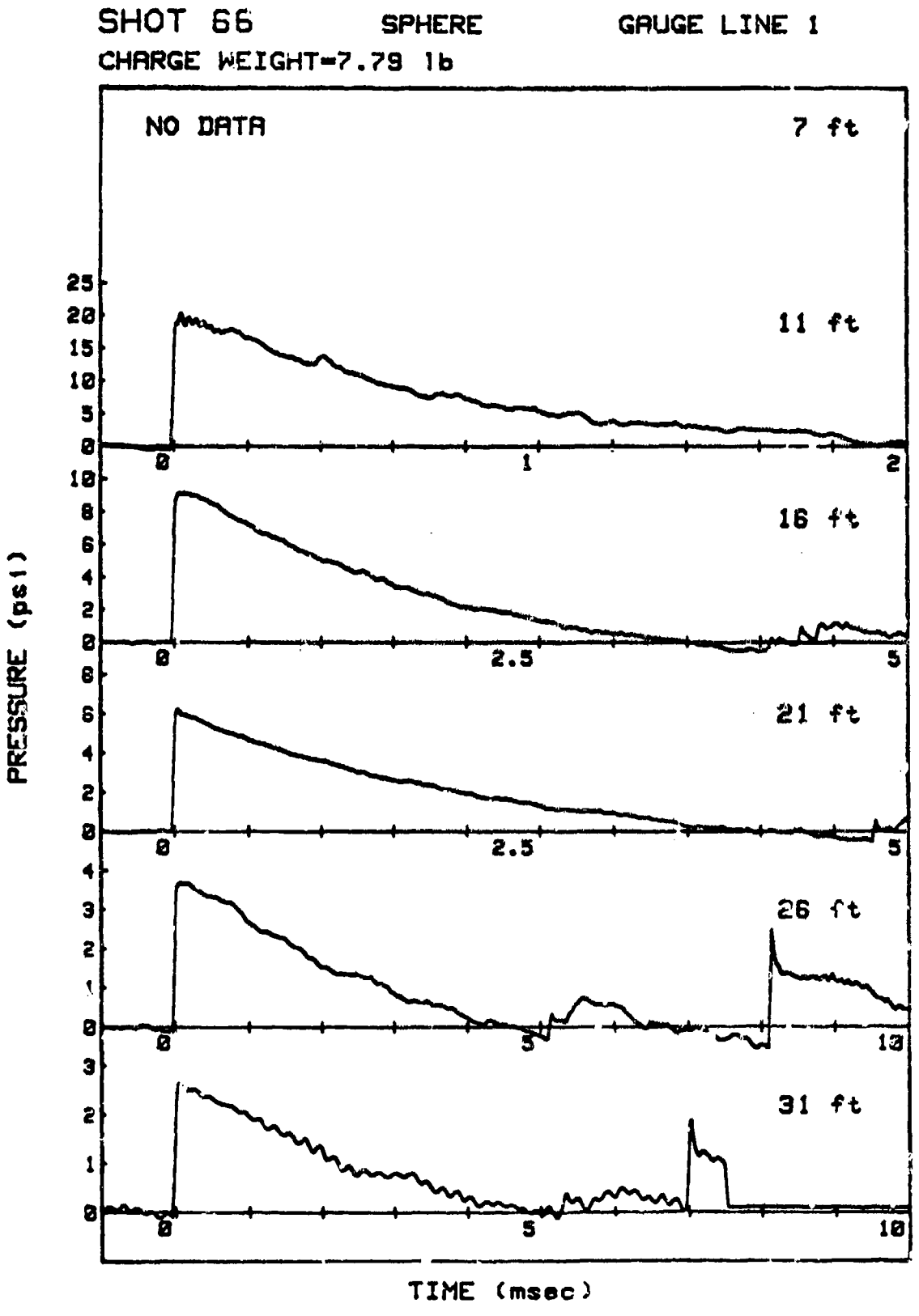
SHOT 66
SPHERE
GAUGE LINE 1
CHARGE WEIGHT=7.79 lb
NO DATA
7 ft
11 ft
16 ft
21 ft
26 ft
31 ft
PRESSURE (psi)
TIME (msec)

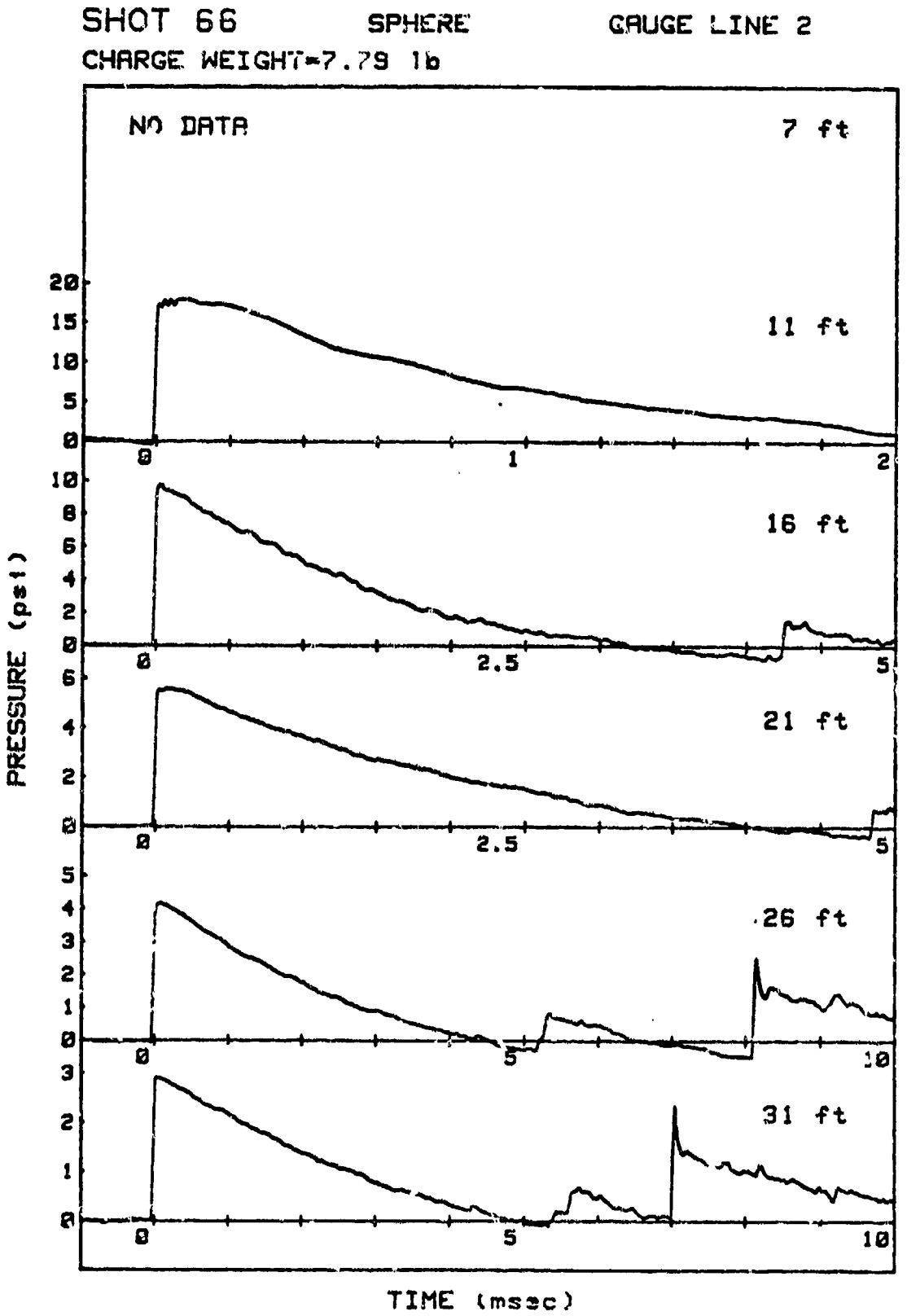
SHOT 66
SPHERE
GAUGE LINE 2
CHARGE WEIGHT=7.79 lb
NO DATA
7 ft
11 ft
16 ft
21 ft
26 ft
31 ft
PRESSURE (psi)
TIME (msec)

NWC TP 6382

Appendix B

ESTIMATION OF POSITIVE IMPULSE FROM PEAK PRESSURE DATA FOR CYLINDRICAL EXPLOSIVE CHARGES: PRELIMINARY INVESTIGATION

March 1979

by

M. N. Plooster and J. D. Yatteau

Prepared for

Naval Weapons Center
China Lake, CA 93555

Contract No. N))123-76-C-0166

INTRODUCTION

This report covers the third phase of a continuing study of blast effects from cylindrical charges of high explosive. The first phases of this study were devoted to a characterization of the angular and radial variation of blast front pressure (the overpressure of the first shock wave to reach a given point). That work was carried to a successful conclusion. The third phase has been directed toward an analogous study of the impulse from a cylindrical charge.

Since theoretical calculations of pressure and impulse from cylindrical charges is difficult, this study has concentrated on the analysis of experimental data. The best, and nearly the only, source of data on free air blast effects from cylindrical charges is a report by Wisotski and Snyer (1965), which summarizes work done here at the Denver Research Institute in the late 1950's and early 1960's. Wisotski and Snyer reported blast front pressures and positive impulses for cylindrical charges with length-to-diameter (L/D) rations ranging from 1/4 to 10/1. A descriptive model for the blast front pressure was made possible by two features of this data set: (1) for three widely separated L/D ratios (1/4, 1/1, and 6/1) blast front pressures were given with high resolution in both the angular and radial coordinates; and (2) a simple interpolation method was found to give good agreement with data at other L/D ratios, where less data on the angular variation were available.

Unfortunately, the impulse data of Wisotski and Snyer do not cover the same range of angular and radial variation. For a few L/D ratios, impulse data were given with high angular resolution, but at only two radial distances; for others, impulse data were given at several distances but at only one angle. Thus it is not possible to develop a detailed impulse model at any L/D ratio using only the experimental impulse data.

A hybrid approach was used in this study. A theoretical relationship between the peak pressure and the impulse, derived by Brinkley and Kirkwood (1947), was used in connection with the descriptive model of blast front pressure obtained in the first phase of this study and reported by Plooster (1978). This gave a set of predicted impulse curves, which were then compared with the experimental impulse data reported by Wisotski and Snyer. The results of this approach, which was promising but not entirely successful, are presented in this report.

APPROACH

The physical basis for the approach used here is the fact that the pressure-time curve, from which the impulse is obtained, is related to the peak pressure-distance curve. The important features of a typical blast wave are an initial discontinuous rise in pressure, the shock front, followed by a continuous pressure drop. The pressure drop is caused by a rarefaction wave; it moves faster than the shock wave, and leads to an attenuation of shock strength with distance. If the rarefaction wave is strong, the pressure will decay rapidly with time after passage of the shock front, and the impulse will be small. A strong rarefaction wave will also rapidly attenuate the shock wave, however, and thus lead to a rapid decay of shock front pressure with distance from the blast source. Conversely, a weak rarefaction wave will lead to a higher impulse and a slow decay of shock pressure with distance. Thus the impulse is directly proportional to the blast front overpressure, but inversely proportional to its rate of decay with distance from the charge.

Brinkley and Kirkwood have derived a relationship between the impulse and the peak pressure-distance curve, starting from the fundamental equations of hydrodynamics, using two simplifying assumptions. The first assumption is that there is only one shock front in the blast wave, or at least that there are no other shock fronts between the primary shock and the point at which the pressure first decays back to the ambient value. The second assumption is that the pressure behind the primary shock decays exponentially with time when the shock is very strong, and gradually approaches a linear decay rate as shock strength decreases. With these assumptions, they obtain the following expression for the impulse, I:

$$I = \nu p \theta, \tag{1}$$

where p is the shock front overpressure and ν and θ are defined by the equations

$$\nu = 1 - \tfrac{1}{2} \exp[-\sqrt{p/p_o}], \tag{2}$$

and

$$-\frac{1}{\theta} = \frac{U}{G}\,\frac{\alpha}{R} + \left\{\left[\frac{\rho}{\rho_o}\,(1+g) + \left(1-\frac{\rho}{\rho_o}\right) G\right]\frac{1}{p}\,\frac{dp}{dR}\right\}, \tag{3}$$

with

$$g = 1 - \frac{p}{U}\,\frac{dU}{dp} \quad \text{and} \quad G = 1 - \left(\frac{\rho_o U}{\rho c}\right)^2.$$

The variables in these equations are:

- U shock velocity
- ρ gas density
- c velocity of sound
- R radial position of shock front

Subscript zero on p and ρ denote ambient pressure and density; all unsubscripted variables represent the values of the variables at the shock front itself.

The parameter α is determined by the geometry of the blast wave; we have $\alpha = d(\log A)/d(\log R)$, where A is the area of the shock front. The value of α is 2 for spherical shocks, 1 for cylindrical shocks and 0 for plane shock waves. Blast waves from cylindrical explosive charges will not be precisely spherical except at very large distances from the charge. However, they will be nearly spherical at distances which are large compared with the largest dimension of the charge, which is the case for all the situations studied here. α will be assumed to be equal to 2 in all the work in this report.

The values of U, ρ, and c at the shock front can all be expressed in terms of the shock overpressure, p, or the ratio p/p_o, by using the Rankine-Hugoniot equations. Assuming that air is an ideal gas with specific heat ratio $\gamma = 1.4$, and using $P = p/p_o$ to simplify the notation, the above relationships can be reduced to the single equation

$$I = -\frac{6\, p_o R P \quad (7 + P)\left(1 - \frac{1}{2} e^{-\sqrt{P}}\right)}{C_o \sqrt{1 + \frac{6}{7} P}\left[14(7 + 8P + p^2) + (98 + 161P + 33P^2)\frac{R}{P}\frac{dP}{dR}\right]} \qquad (4)$$

where C_o is the velocity of sound in the ambient atmosphere. This is the impulse equation used in this study.

The blast front pressure model developed in the first phase of this study approximated the peak pressure as a function of radial distance by a simple quadratic equation,

$$y = A + Bx + Cx^2, \qquad (5)$$

where $y = \log p$ and $x = \log (\lambda/10)$, with λ being the scaled distance from the charge. The term $(R/P)\, dp/dR$ in equation (4) is just $d(\log p)/d(\log R)$, which is equal to dy/dx in the notation of equation (5), since the ambient pressure and the scale factors cancel out. The coefficients A, B, and C were computed in the course of the work leading to the blast front pressure model. Thus the parameters needed to test

the applicability of the Brinkley-Kirkwood theory were already available from the previous study.

There are actually two ways to estimate dy/dx from the previous work: (1) use the values of A, B, and C determined from the experimental peak pressure data for each combination of charge L/D ratio and angle of observation; or (2) use the values of A, B, and C determined from the composite model of blast front pressure, i.e., from either equation (4) or (5) of the report by Plooster (1978). Both of these methods were tried in this study. In general, the best results were obtained using the first of these alternatives; these are the only results reported here.

RESULTS

Since the Brinkley-Kirkwood (B-K) theory was initially developed for simple charge geometries, it was first tested with spherical-charge peak pressure and impulse data. These tests were successful. It was then applied to the cylindrical charge problem. The results of the spherical charge tests are briefly described here before going to the cylindrical charge results.

SPHERICAL CHARGE TESTS

Peak overpressure and impulse data for bare spherical charges have been reported by many investigators. The data used in this study were taken from reports by Swisdak (1975) on TNT, Wisotski (1971) on pentolite, and Wisotski and Snyer (1965) on Composition B. The pentolite and Composition B data were taken at an altitude of over 5000', while Swisdak's data are reported for sea-level conditions. The former two data sets were scaled to sea level using Sachs' scaling laws for this study. Also, their charge weights were adjusted to equivalent charge weights of TNT. One pound of Composition B was set equal to 1.11 pounds of TNT for the peak pressure data, and to 0.98 pounds of TNT for impulse data; the corresponding factors for pentolite were 1.42 and 1.00. All three sets of peak pressure data are plotted on a single graph in Figure 1. The three pressure curves agree very well. Equation (5) was fitted to this composite pressure data set by the method of least squares; the resultant curve is also shown in Figure 1.

Figure 2 shows the scaled impulse data for these three charge compositions. The impulse data show much more scatter than the peak pressures. This is probably due largely to the increased error typical of impulse measurements. Swisdak suggests that the TNT impulse data carry an uncertainty of the order of $\pm$ 20%. Wisotski and Snyer simply remark that their impulse data are much less reliable than their peak pressure measurements. Nevertheless, the B-K equation for impulse (equation 4), obtained using the empirical fit of the peak pressure described above, is in reasonable agreement with the experimental

measurements; it is shown as the smooth curve on the impulse plot in Figure 2. The B-K impulse curve is seen to turn upwards at scaled distances above 15 ft/lb $^{1/3}$. This is clearly not correct. Inspection of equation (4) shows that its denominator is the difference between two relatively large terms, since the factor (R/P) dP/dR in the second term is negative. Thus it can be very sensitive to the slope of the pressure-distance curve as P becomes small. The empirical pressure curve, equation (5), does not give the correct asymptotic behavior, as was done for example by Goodman (1960) in his compilation of spherical blast wave parameters.

CYLINDRICAL CHARGE TESTS

This section presents the main results of this study. Wisotski and Snyer report impulse measurements for end-initiated cylindrical charges of Composition B, with L/D ratios of 1/4, 1/2, 1/1, 2/1, 3/1, 4/1, 6/1, and 8/1. The impulse data are tabulated in Tables 1 to 8. Each table contains the following information:

ϕ - The angle in degrees from the charge axis at which impulse measurements were made. All charges were initiated at the 180° end of the charge, so that the detonation wave propagated toward the 0° end.

R - The radial distance in feet from the center of the charge to the pressure sensor.

I - The measured impulse in psi-msec. A dash in the tables means that no impulse measurements were given at that combination of angular and radial coordinates. When more than one measurement of impulse was available at a given location, the value of I given here is the mean of those measurements.

σ - The standard deviation of the measured impulse at a location. A dash in the table means that only one measurement was available at that point.

I_p - The predicted value of the impulse at that point, using the B-K theory (equation 4). These predicted values of impulse were obtained by fitting equation (5) to Wisotski and Snyer's peak pressure vs distance measurements for a charge of the same L/D ratio and at the same angle from the charge axis.

I_s - The impulse from a spherical charge of the same weight and at the same distance. The spherical charge impulses are obviously independent of the angle of observation. It was calculated using Wisotski and Snyer's empirical fit to their spherical impulse data.

The ambient pressure p_o and the speed of sound c_o were assumed to be 12 psi and 1103 ft/sec, respectively, in all these tests.

These tables constitute a rather uneven data set for the purposes of this study. Tables 1 and 3 (L/D ratios of 1/4 and 1/1) show impulse data at 15° increments in the angle of observation, but at only two radial distances. Tables 4, 5, and 8 (L/D ratios of 2/1, 3/1, and 8/1) give data only at $\phi = 90°$, but at a number of radial distances. Tables 2, 6, and 7 (L/D ratios of 1/2, 4/1, and 6/1) are somewhere between, giving data at 3 to 5 angles and 2 to 4 radial distances. Thus it is difficult to establish trends that apply to the entire range of interest.

Still, there are some generalizations that can be drawn from the data tabulated here. First, the impulse from cylindrical charges appears to be higher than that from spherical charges of equal weight. This difference is greatest for disc-shaped or equi-dimensional cylinders ($L/D \leq 1$), and diminishes as the charges become more elongated (although most of the data on long charges is only for blast off the sides of the charges, i.e., for $\phi = 90°$). Second, for long charges, the impulses predicted using the B-K theory and peak pressure data agree fairly well with the measured impulses at $\phi = 90°$. In particular the B-K equation gives a good estimate of the dependence of impulse on distance from the charge. Figure 3 shows a plot of measured versus predicted impulse (I vs I_p) for all the data at $\phi = 90°$ except for L/D values of 1/4 and 1/2. Third, the B-K theory tends to underpredict the occasional high impulse values observed at smaller distances from charges of all geometries. This same effect is observed in the spherical charge data shown on Figure 2. Fourth, the B-K theory does not appear to predict the angular dependence of impulse as well as it does the radial dependence. The experimental impulse measurements do not vary as much with the angle of observation as the peak pressure measurements of Wisotski and Snyer. Moreover, the impulse does not appear to vary as systematically with angle as the peak pressure does. This may simply reflect the greater experimental uncertainty in the measurement of impulse, as noted by Wisotski and Snyer in their report. However, the less satisfactory performance of the B-K theory here is probably due mostly to the fact that the B-K theory assumes a simple pressure-time profile, whereas Wisotski and Snyer showed that cylindrical charges generate complex pressure waves at some angles. This is discussed in more detail later in this report. Finally, as in the case of the spherical charge calculations, the B-K equation sometimes predicts that impulse increases with distance at large R (see for example Table 2 at $\phi = 90°$, and Table 8). This is again attributable to the improper asymptotic behavior of the empirical pressure-distance curve, equation (5).

Figures 4 to 7 show plots of measured vs predicted impulse (I vs I_p) for each of the charge L/D ratios studied here, These figures illustrate some of the points discussed above: the general good performance of the B-K equation for impulse at $\phi = 90°$ from long charges, and

the increased scatter in the correlations for those cases where the angular variation of impulse is the primary feature.

A more detailed look at the relative differences between predicted and measured impulse in Tables 1 to 8 shows two consistent angle-dependent trends. First, the predicted impulses off the ends of long charges (L/D of 6/1 at $\phi = 0^{\circ}$ and L/D of 4/1 at $\phi = 0^{\circ}$ and 180°), and off the sides of disk-shaped charges (L/D of 1/4 at $\phi = 90^{\circ}$), are much lower than the measured values. On the other hand, predicted impulses along rays which pass near the corners of such charges (L/D of 1/4 at $\phi = 60^{\circ}$, 75°, 105°, and 120°, L/D of 4/1 at $\phi = 45^{\circ}$ and 135°, and L/D of 6/1 at $\phi = 30^{\circ}$) are substantially higher than the measured values. Wisotski and Snyer described the behavior of the pressure-time curves for both types of cases. For the first type, consider a long rod-shaped charge. Since the area of an end surface of such a charge is a small fraction of the total surface area of the charge, the shock wave generated there carries a small fraction of the total detonation energy, and thus decays rapidly with distance. However, at later times there is a second pressure pulse caused by energy from the stronger wave off the side of the charge feeding "around the corner". The B-K equation, as used here, computes the impulse using only the peak pressure of the first, weaker wave in most cases, and thus underestimates the impulse. The geometry is reversed, but the effect is the same, for waves off the sides of disk-shaped charges. At angles passing near the corners of the charges, on the other hand, Wisotski and Snyer showed that the end and side waves interact to form "bridge waves", by Mach reflection off each other. The pressure-time history in the vicinity of these bridge waves may be complex, making a simple correlation of impulse with the peak pressure-distance curve difficult. Since the B-K theory is explicitly derived on the assumption of a simple blast wave profile, it should not be surprising that it does not give accurate impulse predictions in regions where simple pressure-time profiles are not observed. Initially, it was hoped here that passing a smooth curve through the peak pressure-distance data would "smooth out" the effects of these pressure irregularities and give a reasonable impulse estimate via the B-K equation. The results given here show that this did not occur. However, the fact that the discrepancies between predicted and measured impulses follow a regular pattern suggests that an empirical correction factor could be applied to the B-K predictions to give useful impulse estimates.

SUMMARY AND RECOMMENDATIONS

The Brinkley-Kirkwood equation relating positive impulse to peak pressure-distance data has been shown to work quite satisfactorily for blast waves of the simple "classical" shape: a leading shock front followed by a steady decay of pressure to or below the ambient value. It gives good impulse estimates for blast waves from spherical charges, from the sides of long cylinders of explosive, and from the ends of flat charges. Insofar as this present study is concerned, i.e., a general characterization of the impulse from cylindrical charges, it is not completely successful because of the more complex pressure waves generated by these charges in some directions. The B-K equation was shown to be sensitive to the slope of the peak pressure-distance curve at large distances where the peak pressures are small. This is a problem which should be easily remedied, by using an empirical peak pressure-distance equation which has the correct asymptotic behavior at large distances.

To our knowledge, this is the first time that the Brinkley-Kirkwood theory (or any other theory, for that matter) has been used to obtain quantitative estimates of impulse using only peak pressure data. That it works as well as it does is certainly a tribute to the physical insight of its authors. It should be a powerful tool in areas beyond the scope of this study.

The application of this theory to the estimates of the impulse from cylindrical charges has shown where it works well and where further study is required. A major problem in this study, however, has been the lack of an adequate set of experimental impulse data for comparison with the theory. The data set of Wisotski and Snyer does not have the angular and distance resolution nor the measurement accuracy either to characterize the spatial distribution of the impulse or to adequately test the theoretical approach.

Three specific recommendations for future work arise from this study:

1. An empirical equation for peak pressure vs distance that has the correct asymptotic behavior at large distances should be used to provide the input data for the use of the B-K equation.

2. An attempt should be made to find an empirical way to account for the effects of multiple shock waves, as are observed off the corners of cylindrical charges, for example, in the use of the B-K theory. This could involve nothing more complicated than a geometry-dependent correction factor to be applied to results of the form reported here.

3. Most importantly, a better experimental characterization of the impulse from cylindrical charges should be carried out. There simply is not enough information available at the present time to estimate the spatial distribution of the impulse for non-spherical charges over a wide range of angles and distances.

BIBLIOGRAPHY

S. R. Brinkley and J. G. Kirkwood. "Theory of the Propagation of Shock Waves," *Phys. Rev.*, 71, 606-611, 1947.

H. J. Goodman. *Compiled Free-Air Blast Data on Bare Spherical Pentolite*, Aberdeen Proving Ground, MD, BRL REPORT NO. 1092, 1960.

M. N. Plooster, *Blast Front Pressure from Cylindrical Charges of High Explosive*, Final Report on Contract No. N00123-76-C-0166, Denver Research Institute, University of Denver, CO, 1978.

M. M. Swisdak Jr. *Explosion Effects and Properties; Part I-Explosion Effects in Air*, Naval Surface Weapons Center, White Oak Laboratory, Silver Springs, MD, TR 75-116, 1975.

J. Wisotski. *Blast Characterization of Astrolite A-15*, Denver Research Institute, University of Denver, CO, DRI REPORT NO. 2556, 1971.

J. Wisotski and W. H. Snyer. *Characteristics of Blast Waves Obtained from Cylindrical High Explosive Charges*, Denver Research Institute, University of Denver, CO, DRI REPORT NO. 2286, 1965.

TABLE 1. Impulse from Cylindrical Charge of Composition B, for Charge L/D Ratio of 1/4, Charge Weight W = 2.99 lb, at Angle ϕ from Charge Axis, and Distance R.

Legend: I measured impulse (psi-msec)
σ standard deviation of measured impulse
I_p impulse predicted from Brinkley-Kirkwood equation
I_s impulse from spherical charge of some weight

ϕ	0°	15°	30°	45°	60°	75°	90°	105°	120°	135°	150°	165°	180°
R=8.75'													
I	-	-	-	34.1	14.3	11.1	10.2	8.94	12.6	30.1	-	16.4	21.1
σ	-	-	-	-	1.90	1.63	1.79	2.22	3.63	12.0	-	-	-
I_p	-	-	-	18.99	18.10	15.3	6.47	16.00	20.49	14.92	12.40	14.80	19.69
I_s	7.97	7.97	7.97	7.97	7.97	7.97	7.97	7.97	7.97	7.97	7.97	7.97	7.97
R=14.4'													
I	10.9	8.38	10.2	14.5	8.32	7.23	8.37	7.13	8.68	11.2	9.12	9.39	19.6
σ	-	.81	1.52	2.49	.97	1.45	1.22	1.32	1.36	1.40	1.81	-	-
I_p	7.83	9.82	8.36	10.11	10.39	11.29	3.74	12.74	9.87	8.00	6.90	8.40	7.89
I_s	5.58	5.58	5.58	5.58	5.58	5.58	5.58	5.58	5.58	5.58	5.58	5.58	5.58

TABLE 2. As in TABLE 1, for L/D = 1/2, W = 1.59 lb.

ϕ	0°				90°				180°			
R	6'	10'	12'	16'	6'	10'	12'	16'	6'	10'	12'	16'
I	-	22.09	8.49	3.13	7.42	5.81	5.44	4.23	20.55	8.15	6.95	4.91
σ	-	4.93	.14	.48	.43	.29	.37	.29	4.08	.58	1.25	1.02
I_p		6.60	3.89	1.47	6.52	4.55	4.52	7.32	13.94	9.05	6.76	3.71
I_s	7.27	5.04	4.43	3.61	7.27	5.04	4.43	3.61	7.27	5.04	4.43	3.61

TABLE 3. As in TABLE 1, for L/D = 1, W = 3.05 lb.

ψ	0°	15°	30°	45°	60°	75°	90°	105°	120°	135°	150°	165°	180°
R=8.75'													
I	23.56	15.82	20.47	13.48	11.56	10.40	9.10	10.67	11.97	12.69	16.09	12.50	9.30
σ	4.25	4.38	3.42	2.30	.87	1.90	2.52	1.52	.85	2.20	4.87	3.68	2.49
I_p	9.21	12.63	18.22	11.66	16.94	8.99	8.71	8.88	13.33	13.75	11.31	9.95	8.86
I_s	8.05	8.05	8.05	8.05	8.05	8.05	8.05	8.05	8.05	8.05	8.05	8.05	8.05
R=14.4'													
I	5.09	6.35	16.13	8.09	7.56	6.26	6.36	6.60	8.67	7.82	7.52	7.53	5.83
σ	.89	1.94	1.02	1.21	1.34	.98	.62	.52	.64	.77	1.00	.49	1.47
I_p	3.63	4.52	8.78	11.93	11.30	5.76	5.12	6.49	8.73	9.15	8.91	4.19	3.83
I_s	5.65	5.65	5.65	5.65	5.65	5.65	5.65	5.65	5.65	5.65	5.65	5.65	5.65

TABLE 4. As in TABLE 1, for L/D = 2/1, W = 2.93 lb.

ϕ = 90°							
R	7.08'	8.86'	10.13'	13.44'	15.33'	17.44'	19.95'
I	14.18	8.79	8.02	6.13	5.76	5.45	4.55
σ	4.23	1.31	1.29	.52	.58	.73	.38
I_p	11.23	9.46	8.24	5.85	4.98	4.32	3.85
I_s	9.16	7.81	7.09	5.80	5.28	4.81	4.37

TABLE 5. As in TABLE 1, for L/D = 3/1, W = 4.38 lb.

ϕ = 90°						
R	7.09'	7.98'	8.98'	11.55'	15.33'	19.94'
I	18.66	12.30	10.66	9.44	7.03	5.87
σ	2.31	2.27	1.21	.77	.89	.33
I_p	13.42	12.66	11.74	9.43	7.05	5.82
I_s	11.52	10.58	9.73	8.13	6.64	5.50

TABLE 6. As in TABLE 1, for L/D = 4/1, W = 2.94 lb.

ϕ	0°		45°		90°		135°		180°	
I	5.62	4.82	11.85	8.01	10.56	5.25	12.80	7.59	11.66	2.94
σ	-	-	-	.41	1.07	.83	1.74	.57	-	.63
I_p	3.62	1.10	16.12	10.93	10.56	6.20	15.60	9.58	3.55	1.53
I_s	7.89	5.53	7.89	5.53	7.89	5.53	7.89	5.53	7.89	5.53

TABLE 7. As in TABLE 1, for L/D = 6/1, W = 4.42 lb.

ϕ	0°		30°		75°		90°	
R	10'	16.5'	10'	16.5'	10'	16.5'	10'	165'
I	7.26	3.16	9.61	7.91	8.42	7.00	10.30	6.80
σ	2.77	-	2.03	.98	.26	.04	-	.89
I_p	3.28	1.14	34.16	14.6	12.50	7.33	12.11	7.21
I_s	9.06	6.33	9.06	6.33	9.06	6.33	9.06	6.33

TABLE 8. As in TABLE 1, for L/D = 8/1, W = 5.72 lb.

ϕ=90°								
R	9.95	12.50'	15.25'	17.90'	20.70'	24.9'	30.5'	34.8'
I	10.55	9.74	7.39	7.41	6.66	5.81	4.08	3.62
σ	.70	1.12	.34	.55	.27	.18	.37	.37
I_p	13.68	11.12	8.79	7.15	5.97	4.92	4.36	4.40
I_s	10.53	8.94	7.76	6.92	6.24	5.46	4.73	4.30

INITIAL DISTRIBUTION

19 Naval Air Systems Command
- AIR-00D4 (2)
- AIR-03A (1)
- AIR-03E (1)
- AIR-03P2 (1)
- AIR-03P21 (1)
- AIR-310 (1)
- AIR-320 (1)
- AIR-330 (1)
- AIR-350 (3)
- AIR-350D (1)
- AIR-360 (1)
- AIR-526 (1)
- AIR-541 (1)
- AIR-5411 (1)
- AIR-5413 (1)
- PMA-242, Viars (1)

2 Chief of Naval Operations
- OP-506F (1)
- OP-982E (1)

2 Chief of Naval Material
- MAT-05 (1)
- MAT-08 (1)

7 Chief of Naval Research, Arlington
- ONR-102 (1)
- ONR-200 (1)
- ONR-429 (1)
- ONR-461 (1)
- ONR-472 (1)
- ONR-473 (1)
- ONR-474 (1)

11 Naval Sea Systems Command
- SEA-06A (1)
- SEA-62 (1)
- SEA-62R (5)
- SEA-62R31 (1)
- SEA-64E (1)
- SEA-99612 (2)

1 Deputy Assistant Secretary of the Navy (Research & Advanced Technology)
1 Commander in Chief, U.S. Pacific Fleet (Code 325)
1 Commandant of the Marine Corps (Weapons Branch, MC-DLMW)
1 Marine Corps Development and Education Command, Quantico (Landing Force Development Center)
1 Commander, Third Fleet, Pearl Harbor
1 Commander, Seventh Fleet, San Francisco
1 David W. Taylor Naval Ship Research and Development Center Detachment, Bethesda
1 Naval Air Engineering Center, Lakehurst
2 Naval Air Test Center, Patuxent River (CT-252, Bldg. 405) (Aeronautical Publications Library)
1 Naval Avionics Center, Indianapolis (Technical Library)
1 Naval Explosive Ordnance Disposal Technology Center, Indian Head
1 Naval Ocean Systems Center, San Diego (Code 1311)
1 Naval Ordnance Station, Indian Head (Technical Library)
2 Naval Postgraduate School, Monterey
- G. F. Kinney (1)
- Technical Library (1)

3 Naval Ship Weapon Systems Engineering Station, Port Hueneme
- Code 5711, Repository (2)
- Code 5712 (1)

13 Naval Surface Weapons Center, Dahlgren
- Code G-10
  - Oliver (1)
  - Williams (1)
- Code G-11, Goswick (1)
- Code G-13, Wasmund (1)
- Code G-205, Hales (1)
- Code G-25, Newquist (1)
- Code G-35, Waggener (1)
- Code R-10 (1)
- Code R-12
  - Filler (1)
  - Menz (1)
  - Short (1)
- Code R-13, Jacobs (1)
- Code R-15, Swisdak (1)

4 Naval Surface Weapons Center, White Oak Laboratory, Silver Spring
WR-13, R. Liddiard (1)
J. Erkman (1)
Dr. S. Jacobs (1)
Technical Library (1)
1 Naval War College, Newport
1 Office of Naval Research, Pasadena Branch Office
1 Office of Naval Technology, Arlington (MAT-07)
1 Operational Test and Evaluation Force, Atlantic
1 Pacific Missile Test Center, Point Mugu (Technical Library)
1 Army Armament Materiel Readiness Command, Rock Island (DRSAR-LEP-L, Technical Library)
4 Army Armament Research and Development Command, Dover
DRDAR-LCU-SS, J. Pentel (1)
Technical Library (3)
Aberdeen Proving Ground (Development and Proof Services)
7 Army Ballistic Research Laboratory, Aberdeen Proving Ground
DRDAR-BLT
Kinake (1)
Kitchens (1)
DRDAR-BLV, Johnson (1)
DRDAR-IBD, Watermier (1)
DRDAR-SEI-B (1)
DRDAR-T, Detonation Branch (1)
DRDAR-TSB-S (STINFO) (1)
1 Army Material Systems Analysis Activity, Aberdeen Proving Ground
1 Army Research Office, Research Triangle Park
1 Ballistic Missile Defense Advanced Technology Center, Huntsville
1 Harry Diamond Laboratories, Adelphi (Technical Library)
1 Redstone Arsenal (Rocket Development Laboratory, Test and Evaluation Branch)
1 White Sands Missile Range (STEWS-AD-L)
6 Air Force Armament Laboratory, Eglin Air Force Base
AFATL/DLD (1)
AFATL/DLJ (1)
AFATL/DLJW
Foster (1)
Posten (1)
AFATL/DLYD (1)
AFATL/DLYV (1)
1 Defense Nuclear Agency (Shock Physics Directorate)
12 Defense Technical Information Center
1 Department of Defense - Institute for Defense Analyses Management Office (DIMO), Alexandria
1 Lewis Research Center, NASA, Cleveland
1 California Institute of Technology, Jet Propulsion Laboratory, Pasadena, CA (Technical Library)
2 Johns Hopkins University, Applied Physics Laboratory, Laurel, MD (Document Library)
1 Princeton University, Forrestal Campus Library, Princeton, NJ
1 Stanford Research Institute, Poulter Laboratories, Menlo Park, CA
5 University of Denver, Denver Research Institute, Denver, CO (Myron N. Plooster)